ACOUSTIC-BASED TECHNOLOGIES COMBINED WITH ENZYMATIC AMPLIFICATION FOR THE ANALYSIS OF POINT MUTATIONS IN TISSUE AND LIQUID BIOPSY

Nikoletta Naoumi

PhD dissertation

Supervisor: Prof. Electra Gizeli

OCTOBER 15, 2021

UNIVERSITY OF CRETE
Biology department

Fortune favours the brave.

Terence 185/195 BC - 159 BC

Table of contents

Acknowledgments

I would like to give special thanks to my supervisor Prof. Electra Gizeli for her guidance, advice, and her trust in me. Working in her lab and collaborating with her was a great and exciting experience. I am really grateful for all the things she taught me and for helping me cultivate my skills. At this point, I would also like to deeply thank Dr. George Papadakis, who actually stood as my mentor during my first steps in the lab.

Next, I would like to thank Dr. Achilleas Tsortos, Dr. Pablo Mateos-Gil and Dr. Dimitra Chronaki for their advising during my thesis. Moreover, I would like to express my appreciation to Dr. Ilya Reiviakine who always was answering to my questions offering a piece from his broad knowledge on acoustic biosensors.

Many and special thanks to my colleague and friend Maria Megariti for the psychological support that offered to me all these years 😊. Moreover, many thanks to the rest lab members for being so kind and collaborative maintaining a pleasant environment in the lab.

Finally, I would like to thank the rest two members of my 3-member committee, Prof. Kriton Kalantidis and Dr. Stephanie Descroix for their useful and accurate advising during my thesis. Many thanks to all the members that participated at the CATCH-U-DNA project and happened to work with them.

Last but not least, I would like to thank Bodossaki Foundation for their scholarship during almost all the years of my PhD studies.

Oh! I forgot to thank myself for my passion and dedication to my goals and for being a racehorse during all these years making me feeling really proud of myself!

Abbreviations

ARMS-PCR	Amplification-refractory mutation system PCR
AS-PCR	Allele-Specific PCR
BAW	Bulk acoustic wave
bp	Base pairs
BSA/b-BSA	Bovine Serum albumin/biotinylated-BSA
C	Concentration
CAGR	compound annual growth rate
CBs	circulating biomarkers
cfDNA	Cell-free DNA
CRC	Colorectal Cancer
CTCs	circulating tumor cells
ctDNA	Circulating tumor DNA
D	Dissipation
ddPCR	Droplet digital PCR
DNA	deoxyribonucleic acid
dNTP	Deoxyribonucleotide triphosphate
DOPC	1,2-dioleoyl-sn-glycero-3-phosphocholine
dsDNA	Double strand DNA
FB	Fluidized bed
FFPE	Formalin fixed paraffin embedded
Fw	Forward
gDNA	Genomic DNA
HFF	High Fundamental Frequency
Hz/MHz	Hertz/Megahertz
IDT	interdigital transduces
K	Thousands
LCR	Ligase Chain Reaction
LDR	Ligase Detection Reaction
LNA	Locked Nucleic Acid
LM-SAW	Love mode -SAW
LOD	Limit of detection
MAF	mutant allele frequency
mL, µL	Milliliter, microliter
MRD	minimal residual disease
MRI	magnetic resonance imaging
mt	mutant
n	overtone
NAv	Neutravidin
NGS	Next generation sequencing
NSCL	non-small cell lung cancer
nt	nucleotides
NTC	Negative template control
OLA	Oligonucleotide Ligation Assay
PCB	printed circuit board
PCR	Polymerase Chain Reaction

PDMS	Polydimethylsiloxane
pM, aM, fM	Picomolar, attomolar, femtomolar
PNA	Peptide Nucleic Acid
POPC	1-palmitoyl-2-oleoyl-glycero-3-phosphocholine
QCM	Quartz Crystal Microbalance
QCM-D	Quartz Crystal Microbalance with Dissipation monitoring
qPCR	Quantitative PCR
RSAW	Rayleigh SAW
Rv	Reverse
SAW	Surface Acoustic Wave
SH-APM	Shear Horizontal Acoustic Plate Mode
SH-SAW	shear horizontal surface acoustic wave
SMPC	1-Stearoyl-2-myristoyl-sn-glycero-3-phosphocholine
SNVs	single nucleotide variants
ssDNA	Single strand DNA
TSM	Thickness shear mode
US	Ultrasound scans
wt	Wild type
δ	Decay length
ΔD	Dissipation changes
ΔF	Frequency changes
µM, nM	Micromolar, nanomolar

Abstract

Although biosensors hold their roots in the early nineteen-sixties, a great increase in the number of publications refer on this topic was recorded after the nineteen-eighties decade. Moreover, the increasing demand for inexpensive, simplified, sensitive and reliable sensors lead the biosensors market to a significant growth with a predicted compound annual growth rate (CAGR) of 7.3% for the years 2020 - 2027. Biosensors are applied in a wide range of fields including, healthcare and medical diagnostics and is expected to be positively affected by the new trend of precision medicine and the evenly huge market of Liquid biopsy.

Regular screening of cancerous point mutations is of great importance for efficient cancer management and treatment selection. Although excellent techniques like next-generation sequencing and the ultrasensitive droplet digital PCR have been developed, these techniques are lacking in fastness, simplicity and cost-effectiveness. The work presented here focuses on the development of new diagnostic approaches for the detection of ultralow concentrations of cancerous point mutations in human DNA utilizing acoustic biosensors combined with molecular amplification assays. Firstly, we present a universal acoustic methodology that involves the direct immobilization of biotinylated DNA targets on the sensor surface followed by liposome-based acoustic detection. Liposomes, are large nanoparticles (here 200nm) acting as acoustic energy-dissipation signal enhancers. For the DNA immobilization, we developed a surface chemistry composed of biotinylated-BSA and NAv; the substrate was reproducible and was successfully validated for its specificity and stability upon liposome and crude sample additions, respectively. While for the above we used a standard QCM-D device and a 5 MHz QCM sensor, a novel High Fundamental Frequency QCM (HFF-QCM) array of 24 miniaturized sensors operating at 150 MHz and a new acoustic device were also tested. The array permitted the faster and more cost-effective analysis of up to six different samples and the extraction of up to 24 measurements. The above-mentioned acoustic methodology, i.e., b-BSA/NAv and liposomes for immobilization and detection of DNA targets using the QCM-D device, was firstly combined with a PCR-free DNA amplification assay, the Ligase Chain Reaction (LCR). For the LCR we used probes modified with biotin and cholesterol to produce LCR products ready for immobilization on the NAv-coated sensor and acoustic detection. Following extended optimization, the detection of 3.3 $x10^3$ DNA molecules carrying the *BRAF* V600E point mutation was achieved. However, the overall assay suffered from some limitations concerning the target-independent ligated by-products that occurred during the LCR, leading to low sensitivity and decreased specificity. To overcome the problem of the low sensitivity and specificity Allele-Specific PCR (AS-PCR) was employed as an alternative method for DNA amplification. AS-PCR combined with acoustic detection improved the limit of detection down to 1 copy of mt target in an excess of 10^4 wt molecules, otherwise with a sensitivity of 0.01%, using genomic DNA carrying the *BRAF* V600E point mutation. For the amplification, we again used primers modified with biotin and cholesterol and for the acoustic detection, we employed the 150 MHz biochip array with great success. Since the initial protocol developed for the detection of the *BRAF* V600E mutation gave only qualitative results, the assay was further optimized and applied to the analysis of *KRAS* G12D mutation achieving both qualitative and quantitative results with a sensitivity of 0.05%. Finally, the assay was

validated for the detection of both point mutations in real FFPE-tissue and plasma samples obtained from melanoma, colorectal and lung and cancer patients. The obtained results were compared with those recorded from the standard methods used for tissue and liquid biopsy i.e., Sanger sequencing and droplet-digital PCR.

Περίληψη

Παρόλο που ο πρώτος βιοαισθητήρας ανακαλύφθηκε το 1962 από τον Leyland C. Clark, εκθετική άνοδος στις δημοσιεύσεις του αντίστοιχου τομέα καταγράφηκε μετά τα τέλη της δεκαετίας του 1980. Επιπλέον, η όλο και αυξανόμενη ζήτηση για οικονομικούς, εύχρηστους, ευαίσθητους και αξιόπιστους αισθητήρες έχει οδηγήσει σε μεγάλη ανάπτυξη της αγορά των βιοαισθητήρων, η οποία για το έτος 2020 υπολογίστηκε στα 26 δισεκατομμύρια δολάρια ενώ αναμένεται να ανέλθει στα 43,4 δισεκατομμύρια δολάρια το 2027 με προβλεπόμενο σύνθετο ετήσιο ρυθμό ανάπτυξης (CAGR) 7,3%. Ο κλάδος των βιοαισθητήρων βρίσκει εφαρμογή σε ένα ευρύ φάσμα τομέων, όπως αυτόν της ιατρικής διάγνωσης και αναμένεται να επηρεαστεί θετικά από τη νέες αναδυόμενες τάσεις της ιατρικής ακριβείας και της επίσης πολύ μεγάλης και ραγδαίας αναπτυσσόμενης αγοράς που αφορά την Υγρή βιοψία.

Σύμφωνα με τα δεδομένα, προκειμένου να επιτευχθεί η πλέον αποτελεσματική αντιμετώπιση του καρκίνου, απαραίτητη είναι η έγκαιρη και τακτική ταυτοποίηση τυχόν καρκινικών μεταλλάξεων τόσο για τη σωστότερη διάγνωση όσο και για την επιλογή καταλληλότερης θεραπείας και για έλεγχο της ανταπόκρισης του ασθενούς σε αυτήν. Αν και τα τελευταία χρόνια έχουν αναπτυχθεί εξαιρετικές τεχνικές για την αξιόπιστη ταυτοποίηση των καρκινικών μεταλλαγών, όπως η αλληλούχιση DNA νέας γενιάς (next-generation sequencing) και η ψηφιακή αλυσιδωτή αντίδραση πολυμεράσης τεχνολογίας σταγονιδίων (digital droplet PCR, ddPCR), αυτές οι τεχνικές εξακολουθούν να έχουν σημαντικά υψηλό κόστος και στερούνται απλότητας και ταχύτητας ως προς την έκδοση των αποτελεσμάτων. Η παρούσα εργασία επικεντρώνεται στην ανάπτυξη νέων διαγνωστικών μεθόδων για την ανίχνευση εξαιρετικά χαμηλών συγκεντρώσεων ανθρώπινου καρκινικού DNA και των φερόμενων σε αυτό σημειακών μεταλλαγών. Η ανίχνευση επιτυγχάνεται με τη χρήση ακουστικών βιοαισθητήρων σε συνδυασμό με μοριακές μεθόδους ενίσχυσης του DNA.

Σε πρώτη φάση, επικεντρωθήκαμε στην ανάπτυξη μία καθολικής μεθόδου για την ακουστική ανίχνευση του DNA, η οποία περιλαμβάνει την άμεση ακινητοποίηση μικρών συγκεντρώσεων (pM - nM) βιοτινυλιωμένου DNA στην επιφάνεια του αισθητήρα ακολουθούμενη από την ανίχνευσή του μέσω λιποσωμάτων. Τα λιποσώματα, είναι μεγάλα μόρια (για παράδειγμα εδώ γίνεται χρήση λιπωμάτων διαμέτρου 200 nm) που δρουν ως ενισχυτές του ακουστικού σήματος αυξάνοντας κατά πολύ τη διάχυση ενέργειας (energy dissipation). Για την ακινητοποίηση του DNA πάνω στη επιφάνεια του αισθητήρα, αναπτύξαμε ένα υπόστρωμα αποτελούμενο από βιοτινυλιωμένη-BSA και νιουτραβιδίνη (NAv); η NAv χρησιμεύει στην άμεση και αυθόρμητη ακινητοποίηση του βιοτινυλιωμένου DNA μέσω της πολύ ισχυρής συγγένειας που έχει η βιοτίνη για τη NAv. Το DNA είναι ειδικά σχεδιασμένο, έτσι ώστε εκτός από τη βιοτίνη στο ένα άκρο, να φέρει ένα μόριο χοληστερόλης στο άλλο άκρο του. Έτσι, η πρόσδεση των λιποσωμάτων στο DNA επιτυγχάνεται μέσω της χοληστερόλης η οποία αυθόρμητα εισέρχεται στη λιπιδική διπλοστοιβάδα τους. Το υπόστρωμα ελέγχθηκε ως προς (α) την επαναληψιμότητα στη σύνθεσή του, (β) την τυχόν μη ειδική πρόσδεση των λιποσωμάτων σε αυτό απουσίας DNA και (γ) την σταθερότητά του κατά την εισαγωγή μη προ-καθαρισμένων μοριακών αντιδράσεων. Ενώ για τα παραπάνω πειράματα χρησιμοποιήσαμε την τυπική QCM-D συσκευή και έναν QCM αισθητήρα των 5 MHz, δοκιμάσαμε, επίσης, αισθητήρες QCM υψηλής θεμελιώδους συχνότητας (HFF-QCM) σε συνδυασμό με μια νέα ακουστική συσκευή. Αναφορικά με αυτό, ήταν μία διάταξη 24 μικροσκοπικών αισθητήρων που

λειτουργούν στα 150 MHz. Η διάταξη αυτή, επέτρεπε την ταχύτερη και οικονομικότερη ανάλυση έως και έξι διαφορετικών δειγμάτων και την εξαγωγή έως και 24 μετρήσεων. Η προαναφερθείσα ακουστική μεθοδολογία, δηλαδή, βιοτινυλιωμένη-BSA/NAv σε συνδυασμό με τα λιποσώματα για την ακινητοποίηση και την ανίχνευση των DNA στόχων χρησιμοποιώντας τη συσκευή QCM-D, συνδυάστηκε αρχικά με μια μοριακή αντίδραση ενίσχυσης του DNA χωρίς PCR, την αλυσιδωτή αντίδραση λιγάσης (LCR). Για την LCR χρησιμοποιήσαμε ολιγονουκλεοτίδια (probes) τροποποιημένα με βιοτίνη και χοληστερόλη προκειμένου να παράγουμε τροποποιημένα προϊόντα LCR έτοιμα για ακινητοποίηση στον αισθητήρα και ακουστική ανίχνευση. Έπειτα από εκτεταμένη βελτιστοποίηση της όλης μεθοδολογίας, καταφέραμε να ανιχνεύσουμε 3,3 x10^3 μόρια DNA που φέρουν τη σημειακή μετάλλαξη *BRAF* V600E. Ωστόσο, η συνολική δοκιμασία έπασχε από ορισμένους περιορισμούς, όπως τα παραπροϊόντα που δημιουργούνταν κατά τη διάρκεια της αντίδρασης ανεξάρτητα από την παρουσία του DNA στόχου, οδηγώντας σε περιορισμένη ευαισθησία και μειωμένη ειδικότητα της αντίδρασης. Από την άλλη πλευρά, η αλληλοειδική PCR (AS-PCR) σε συνδυασμό με την προαναφερθείσα ακουστική μεθοδολογία βελτίωσε το όριο ανίχνευσης σημαντικά, επιτρέποντας την ανίχνευση 1 μορίου γενωμικού DNA στόχου που φέρει τη *BRAF* V600E μετάλλαξη σε περίσσεια 10^4 μορίων αγρίου τύπου, αλλιώς με ευαισθησία 0,01%. Για την ενίσχυση του μεταλλαγμένου DNA μέσω της PCR, χρησιμοποιήθηκαν και πάλι εκκινητές τροποποιημένοι με βιοτίνη και χοληστερόλη για την παραγωγή τροποποιημένων AS-PCR προϊόντων, ενώ για την ακουστική ανίχνευση, χρησιμοποιήθηκε το βιοτσίπ με τη διάταξη βιοαισθητήρων που λειτουργούν στα 150 MHz. Δεδομένου ότι το αρχικό πρωτόκολλο που αναπτύχθηκε για την ανίχνευση της μετάλλαξης BRAF V600E παρείχε μόνο ποιοτικά αποτελέσματα, η τεχνική βελτιστοποιήθηκε περαιτέρω και εφαρμόστηκε για την ανάλυση της μετάλλαξης *KRAS* G12D επιτυγχάνοντας τόσο ποιοτικά όσο και ποσοτικά αποτελέσματα με ευαισθησία 0,05%. Τέλος, η επιτυχής εφαρμογή και η αξιοπιστία της μεθόδου επικυρώθηκε με την ανίχνευση και των δύο σημειακών μεταλλάξεων σε πραγματικά δείγματα μονιμοποιημένου ιστού ενσωματωμένου σε παραφίνη (FFPE) και σε πραγματικά δείγματα πλάσματος προερχόμενα από ασθενείς με μελάνωμα, καρκίνο του παχέος εντέρου και καρκίνο του πνεύμονα. Τα λυφθέντα αποτελέσματα συγκρίθηκαν με αυτά που καταγράφηκαν από τις κλασσικές μεθόδους που χρησιμοποιούνται για βιοψία ιστού και υγρή βιοψία, δηλ. με την αλληλούχιση κατά Sanger και τη ddPCR.

Chapter 1

Introduction

Biosensors are compact analytical devices that convert a biological or chemical response into an electrical signal proportional to the concentration of the analyte. According to the International Union of Pure and Applied Chemistry (IUPAC) recommendations 1999, is a self-contained integrated device, capable to provide quantitative or semi-quantitative information using a biological recognition element, which is commonly called bioreceptor[1–4]. Their application embraces a variety of fields such as medicine through medical diagnostics, and drug discovery. Biosensors are also applicable in clinical and analytical chemistry food process and safety, water quality monitoring, environmental and industrial monitoring (fig. 1)[5–10]. Nowadays, the most considerable trend expected to impact biosensors is the emergence of precision medicine[10].

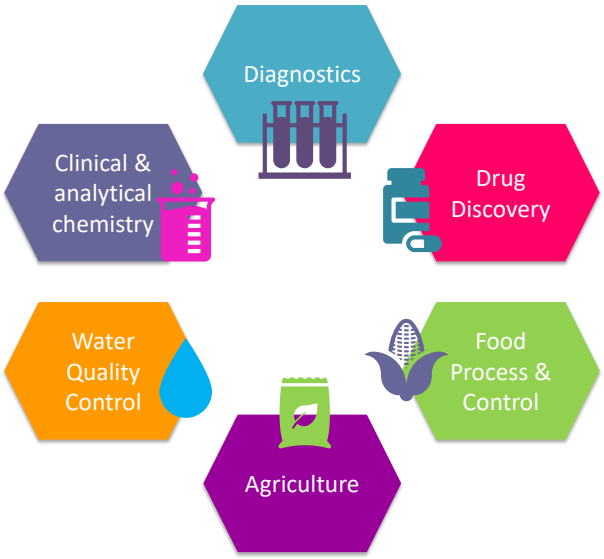

Figure 1. *Major fields biosensors find application.*

Biosensors hold their roots back to 1962 when Leyland C. Clark, based on his earlier invention known as the "Clark (oxygen) electrode", considered that electrochemical detection of oxygen or hydrogen peroxide could be used as the basis for a broad range of bioanalytical devices through the incorporation of appropriate immobilized enzymes. Therefore, he developed the first prototype glucose sensor for the monitoring of glucose through immobilized glucose oxidase in the oxygen electrode[10,11]. In 1975, Yellow Spring Instruments (YSI) commercialized the first biosensor applied for glucose detection[9]. Currently, the field of biosensors is a multidisciplinary area of research involving basic sciences (physics, chemistry and biology), micro/nano-technology, electronics, applied medicine and others. The increasing demand for inexpensive, simple, sensitive and reliable sensors has led the biosensors market to a significant growth; for instance, in 2020

biosensors market was calculated at $26 billion and is estimated to reach the $43.4 billion in 2027 with a predicted compound annual growth rate (CAGR) of 7.3%.

A biosensor consists of three main elements i.e., the bioreceptor, the transducer and the signal processing system, plus the analyte[1,9] (fig. 2):

- Analyte: The substance of examination during the analysis.
- Bioreceptor: The biological or biologically derived recognition system that specifically interacts with the analyte. The bioreceptor can be a biological material (protein such as enzyme, antibody, cell receptors or nucleic acid), a biomimetic material (peptide nucleic acid (PNA), locked nucleic acid (LNA), aptamers, recombinant antibody and receptors, lipid films), whole microorganisms or even nanoparticles functionalized with a biocomponent[1,12–14].
- Transducer: The role of the transducer is to convert the bio-recognition event into a measurable signal. Usually, the produced signal is optical or electrical and proportional to the amount of analyte-bioreceptor interaction.
- Signal processing system: The transduced signal is firstly converted from analogue to digital form and then to a graph displayed at the screen of a computer. This procedure is commonly consisted of a combination of hardware and software that converts results of the biosensor in a user-friendly manner. The output signal on the display can be numeric, graphic, tabular or an image, depending on the requirements of the end-user.

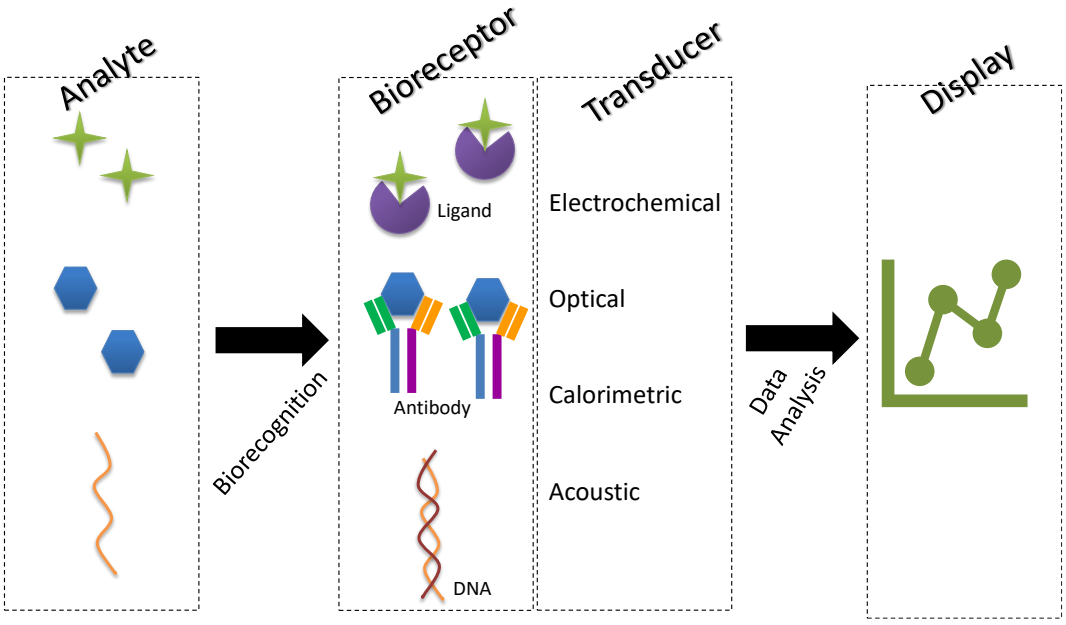

Figure 2. *Schematic representation of biosensor.*

As shown in Figure 3, biosensors are most often classified either based on their bioreceptor or based on their transduction principle. From the bioreceptor perspective, biosensors are divided into antibody-based (immunosensors), enzyme-based, DNA-based (genosensors), lipid film-based, whole-cell-based, aptamer-based (aptasensors), nanoparticle-based etc.

biosensors[1,12,13]. From the transducer perspective, biosensors are classified into piezoelectric/acoustic wave sensors, electrochemical, calorimetric and optical[1,15–17] (Fig. 3).

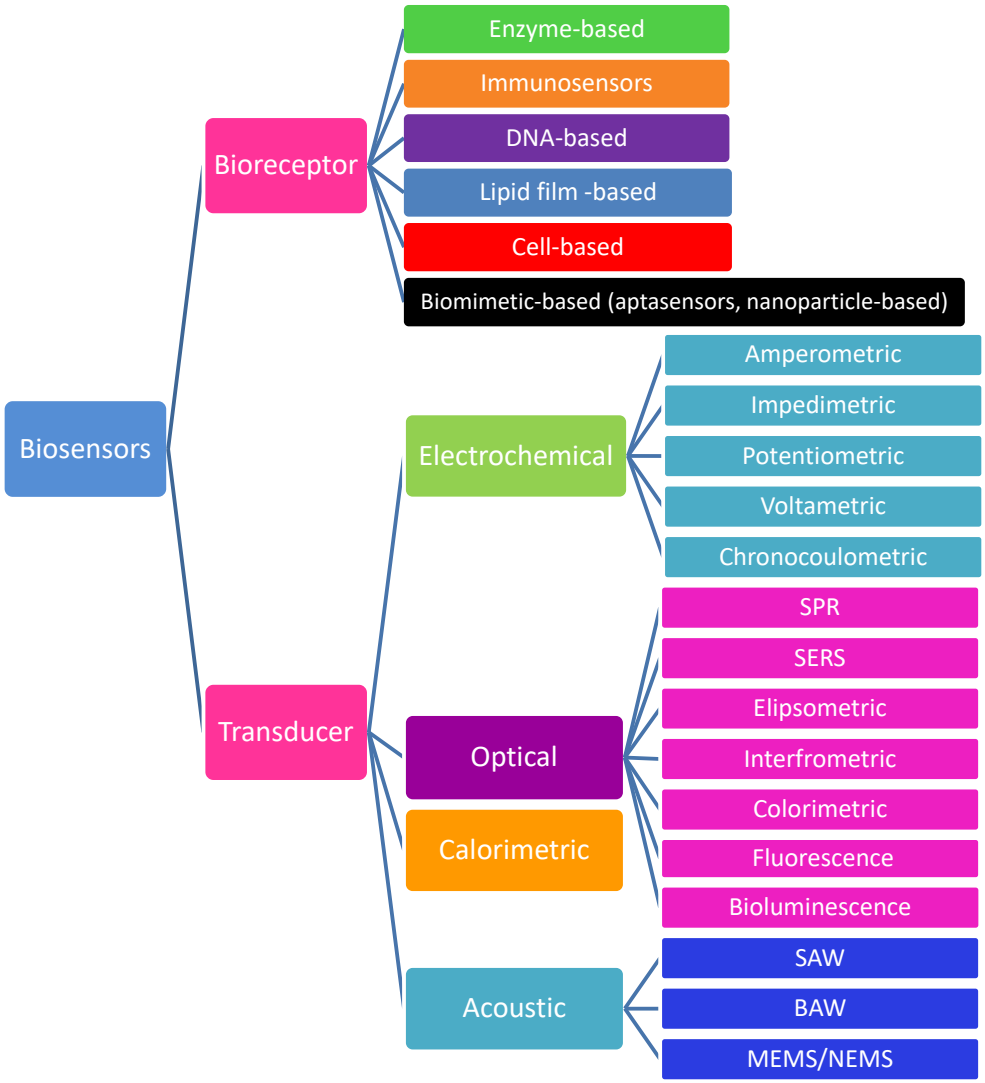

Figure 3. *Classification of biosensors, bioreceptors and transducers. LSPR-Localized Surface Plasmon Resonance; SPR – Surface Plasmon Resonance; SERS - Surface-enhanced Raman scattering; SAW – Surface Acoustic Wave; BAW – Bulk Acoustic Wave; MEMS/NEMS - micro/nano-electromechanical.*

In this work, acoustic wave sensors were utilized for the development of DNA biosensing assays in the field of molecular diagnostics.

Acoustic Wave Sensors

Acoustic wave sensors utilize acoustic waves (also referred as mechanical waves) as a sensing mechanism to monitor changes on the sensor surface. Briefly, the acoustic wave propagates through or on the surface of a substrate and any changes occurring at the

solid/sample interface affect its characteristics i.e., the amplitude and the velocity or frequency. Their generation is based on the piezoelectric phenomenon which was first discovered by Pierre and Paul-Jacques Curie in 1880. Curie brothers found that applying mechanical stress in certain materials -such as quartz- induces voltage generation and vice versa. Similarly, applying an electric field in an oscillatory manner result in oscillatory mechanical stress generating an acoustic wave, which propagates through the surface. The acoustic wave acts as a detection mechanism and afterwards is converted back to an electric field for measurement[16,18,19].

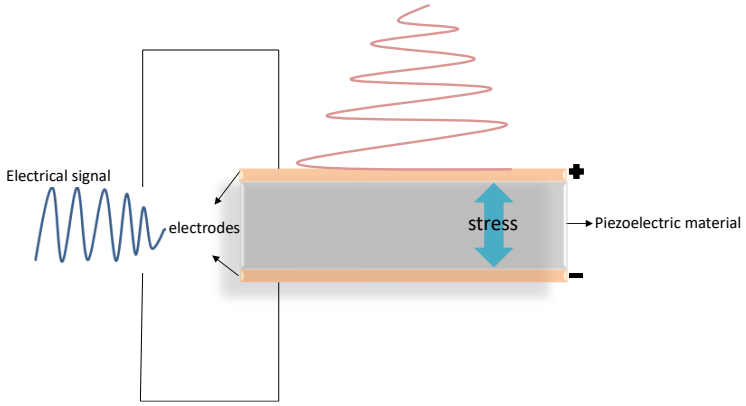

Figure 4. *Schematic representation of the piezoelectric phenomenon on oscillatory circuit.*

All acoustic sensors are using certain piezoelectric elements depending on their downstream application. The most commonly used are the quartz (SiO_2), lithium tantalate ($LiTaO_3$), and lithium niobate ($LiNbO_3$) since they are robust and environmentally stable. Among them, quartz is the most desirable as it is cost-effective, readily available in nature and easily synthesizable in high quantities. In addition, thin disks of quartz exhibit better temperature and chemical stability compared to other piezoelectric materials[16,18,19].

Acoustic wave sensors are divided into two main groups, depending on the acoustic waves that generate: Surface Acoustic Wave (SAW) and Bulk Acoustic Wave (BAW) sensors.

Surface Acoustic Wave (SAW) Sensors

SAW sensors usually consist of two photolithography produced interdigital transduces (IDT) (metal electrodes) patterned on a piezoelectric substrate or on a piezoelectric thin film derived from ST-cut quartz, $LiTaO_3$ or $LiNbO_3$[16,18,20]. In a typical approach, when an electric field is applied at a specific frequency, an acoustic wave is produced by the one IDT and travels across the sensing surface towards the other IDT. There, the wave is again converted into an electrical signal and in turn is transformed into a resulting signal of e.g., frequency change. In this kind of sensors, the acoustic wave is strongly confined on the piezoelectric substrate and propagates along the senor surface as shown in figure 4. Acoustic wave is thus very sensitive in changes occurring on the sensor surface, such as mass loading and viscosity changes which in turn are expressed as changes in the phase or amplitude, respectively[19,21].

Generally, SAW sensors operate at high frequencies ranging from 25 MHz – 1.5 GHz, and exhibit better sensitivity compared to BAW sensors which operate at a lower MHz range (5 MHz – 30 MHz). This stems from the fact that sensitivity is inversely proportional to the square of the resonance frequency. In theory, this means that the higher the operating frequency, the better the sensitivity. In addition, SAW sensors tend to have a lower penetration depth (δ) i.e., the sensing surface above the sensor, since δ is also inversely proportional to the square root of the resonance frequency[18,19,22].

The first SAW devices employed the so-called Rayleigh wave (RSAW) which moved vertically to the surface plane of the sensor (Fig. 4a). However, their application as chemical sensors was strongly limited to gas sensing, rather than biosensing assays which required buffer and thus liquid phase. The reason for this was that Rayleigh wave was highly attenuated into the liquid. Therefore, a different type of SAW sensor was developed where a different cut of crystal gave rise to horizontal instead of vertical wave. The new wave was named shear horizontal surface acoustic wave (SH-SAW) and propagated parallel to the surface plane minimizing energy losses upon use of the device in liquid media (Fig. 4b)[23]. This technology was further optimized by Gizeli E. and coworkers when they added a polymethylmethacrylate (PMMA) polymer film or novolac photoresist onto a quartz-based SH-SAW. Both materials acted as waveguides generating another type of waves known as "Love-waves" and additionally decreasing attenuation[20,21,24,25]. Overall, among SAW devices the Love-wave based had been mostly applied for biosensing assays in liquid.

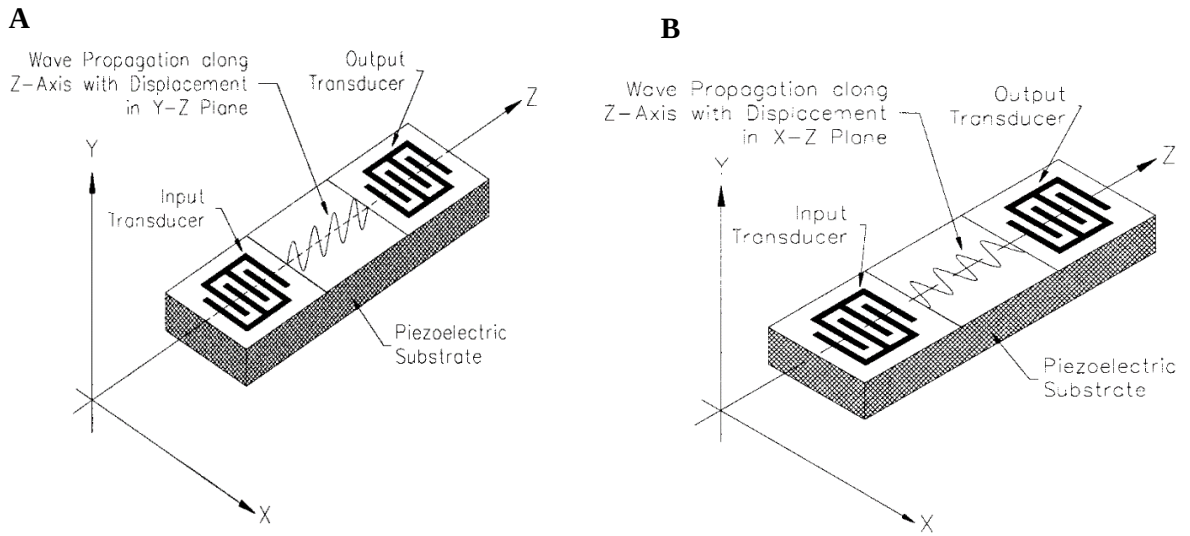

Figure 4. *A) RSAW; Rayleigh waves move vertically to the surface plane the sensor., B) SH-SAW; Changing the material orientation horizontal waves are generated parallel to the device's surface. Reprinted from Ref.*[19].

Bulk Acoustic Wave (BAW) Sensors – Quartz Crystal Microbalance (QCM)

BAW sensors constitute the oldest and simplest acoustic devices. They are categorized into Shear Horizontal Acoustic Plate Mode (SH-APM) and Thickness shear mode (TSM) resonators. The latter, also known as Quartz Crystal Microbalance (QCM), is the most widely used today applied to both gas and liquid environment[18,19]. A QCM sensor is composed of an

AT-cut quartz crystal sandwiched by two metal electrodes. Application of alternating current voltage to the two electrodes at the same frequency as the fundamental or the associated overtones -*n* (resonant frequencies), causes crystal deformation in an oscillatory manner with the two surfaces moving in an antiparallel fashion (Fig. 5). As a result of how the crystal deforms, a standing acoustic wave is generated. The wave travels across and beyond the crystal element, up to some hundred nm through the gas/liquid phase while is gradually decayed. As in the case of SAW sensors, the theoretical sensitivity of the sensor and the decay length -*δ*- of the acoustic wave depend on the resonant frequency of the crystal; both sensitivity and *δ* are decreased as the frequency increases[18,26]. The resonance frequency depends on a variety of factors such as the shear modulus, the density, and the material thickness[16,18,27].

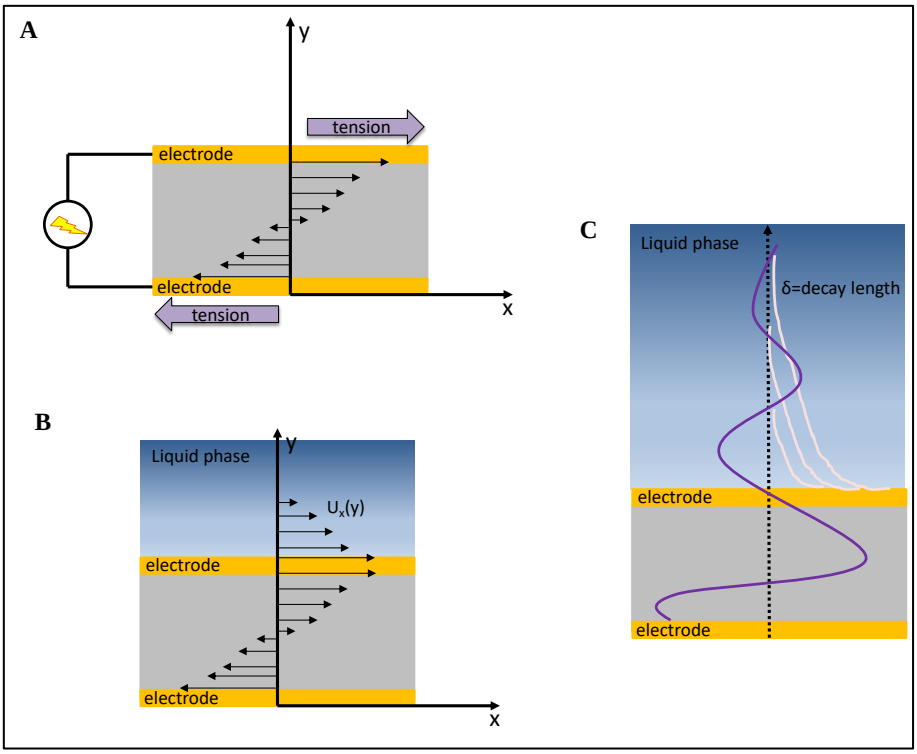

Figure 5. *Illustration of the side view of Quartz Crystal Microbalance sensor. (a) Application of oscillatory voltage results in a crystal tangential deformation, where the top and bottom surfaces move in antiparallel fashion generating an acoustic wave that propagates across the crystal material. (b) When the sensor is immersed in a fluid, the acoustic wave is transmitted into the fluid with the velocity (u_x) direction being parallel to the surface plane. (c) The acoustic wave is gradually decayed into the fluid, with a decay length δ and amplitude A (white lines). Both δ and A amplitude decrease with increasing sensor resonance frequency, or overtone (fn).*

➢ HFF-QCM

Generally, QCM exhibits lower mass sensitivity due to its lower operating frequencies of 5 MHz – 30 MHz. According to Sauerbrey´s equation, which correlates the recorded ΔF with the deposited mass on sensor surface[28], mass sensitivity is also proportionally dependent on the square of its resonance frequency *fn*. Additionally, in TSM resonators, the fundamental

resonance frequency is dependent on the thickness of the quartz. Hence, resonators operating at higher fundamental frequencies can actually be developed by thinning the quartz. However, reducing thickness beyond a certain point results in mechanically unstable, fragile and difficult to handle sensors. This problem has been addressed through the development of a new technology called "inverted-mesa". In this strategy, only a small circular area of the sensor is getting thinner while the surrounding parts remain in the typical thickness providing mechanical stability. By this method, High Fundamental Frequency (HFF) sensors of up to 200 MHz resonance frequency have been developed, exhibiting an improved sensitivity[29,30]. For example, a 100 MHz HFF-QCM immunosensor applied for the detection of carabyl pesticide achieved a similar detection limit as a 120 MHz Love Mode SAW sensor[31], and an improved by almost two orders of magnitude limit of detection compare to typical 9 MHz and 10 MHz QCM sensors[31–33]. Researchers from the same group also developed a HFF-QCM sensor operating at 150 MHz and claimed to exhibit an improved sensitivity since the combined frequency shift derived from Protein A followed by IgG capturing was calculated as -51000 Hz while in literature the corresponding shift for a 9 MHz QCM sensor was only -200 Hz[29]. Nevertheless, we would like to mention that higher frequency shifts do not necessarily mean lower detection limits and the sensor's sensitivity is affected by the signal/noise ratio, as well.

➢ QCM-D

Molecules addition on the QCM sensor surface results in a frequency shift, providing information about the mass of the deposited layer. When the sensor is immersed in liquid, the ΔF is affected not only by the adsorbed mass but also by the interaction of the molecules with the surrounding buffer, leading to energy losses. This led to the development of a new technique called Quartz Crystal Microbalance with Dissipation monitoring (QCM-D) which allows the simultaneous monitoring of frequency and energy losses (also known as dissipation) of the system at multiple overtones. As shown in Figure 6, when molecules adsorb onto the sensor's surface, resonance frequency decreases ($\Delta F = f_0 - f_i$, $f_i < f_0$) (fig. 6a) while the dissipation increases causing losses in the oscillation energy (fig. 6b). Dissipation is related to the viscoelastic properties of the adlayer (Voigt model) or surface-bound molecules. Dissipation is measured through the monitoring of the crystal's oscillation decay following a rapid switch-off of the driving voltage as follows (Fig. 6b):

$$D = \frac{E_{dissipated}}{2\pi E_{storred}}$$

with $E_{dissipated}$ being the energy dissipated during one oscillatory cycle and E_{stored} being the energy stored in the oscillating system[34,35]. Through the mathematical treatment reported by Voinova et al., 1999 which was based on Voigt viscoelastic model, the combined analysis of Δf and ΔD can provide information about the film thickness (d_f), effective density (ρ_f), shear viscosity (n_f) and elastic modulus (μ_f) of the adlayer[36].

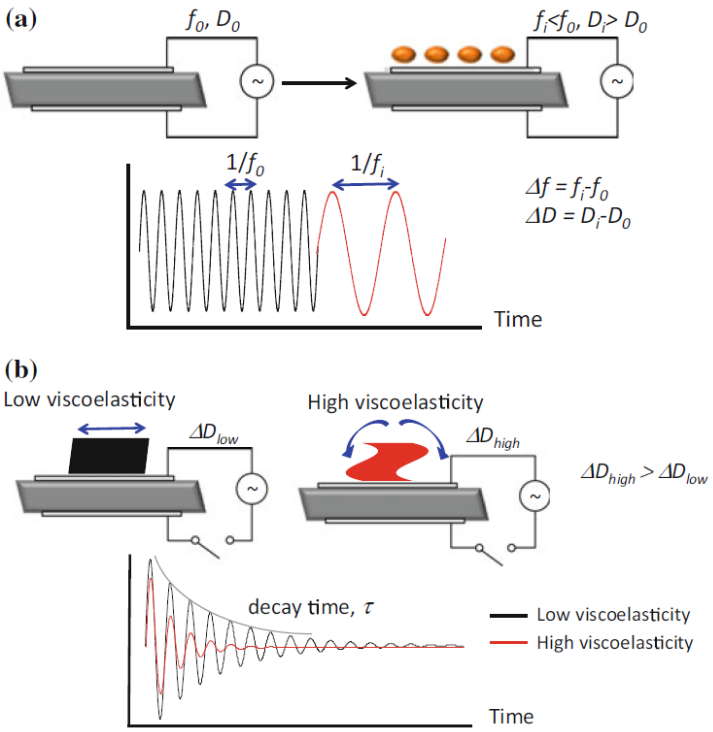

Figure 6. *Illustration of QCM-D measurement. a) Frequency change of the oscillating sensor upon mass addition. b) Difference in dissipation signals between layers of different viscosity; note that highly viscoelastic solution/films make oscillation energy decay faster vs time (red line) while less viscoelastic films maintain the oscillation energy hence is slowly decayed (black line). The illustration was obtained from Ref.*[35]

➢ Converting QCM data into mass change

When molecules adsorb on the sensor surface resonance frequency decreases linearly to the added mass. The relation of the frequency change (ΔF) to the adsorbed mass per unit area was demonstrated by Sauerbrey in 1959[28] as:

$$\Delta f = -\frac{n}{C}\Delta m,$$

where *n* is the overtone number and C is the mass sensitivity constant, i.e., how many ng of material per cm^2 of the sensor is needed to shift the resonance frequency 1 Hz. C is expressed as

$$C = \frac{t_q}{f_0}\rho_q$$

with t_q being the thickness of quartz, ρ_q being the density of quartz and equals to ~ –17.7 ng/(cm^2·Hz) for the typically used 5 MHz crystal. Clearly, lower C means higher mass sensitivity and since the C value depends purely on the fundamental resonant frequency of the crystal, higher f_0 leads to lower C and better mass sensitivity. There are three criteria that

must be fulfilled in order Sauerbrey equation to hold. First, the adsorbed mass must be small compared to the mass of the quartz; i.e., less than 2 %; second, the mass should be equally distributed on the surface of the sensor; and third, the mass should form a rigid film exhibiting very low or zero viscoelasticity (ΔD ~0). Sauerbrey equation is valid when sensing is performed in vacuum or gas phase, rather than liquid. In liquid phase, viscous and elastic contributions are present making the equation invalid. For better understanding, a sufficiently thin and rigid adsorbed film acts as a "dead" mass and follows perfectly the movement of the piezoelectric oscillator, while a viscoelastic or thicker film is not fully coupled to sensors oscillation (e.g., due to friction with the surrounding molecules) leading to overestimation or underestimation of the added mass, depending on the properties of the film[27,34,37]. In liquid phase, there are some cases where the film is considered "rigid" and the equation is still valid with acceptable error, such as when the $\Delta D << 1 \times 10^{-6}$ or $\Delta D/(\Delta F/n) << 4 \times 10^{-7}$ for a 5 MHz sensor. One should keep in mind that since the film is solvated, the calculated mass will reflect the masses of both the adsorbate and the solvent ($\Delta m = m_{absorbate} + m_{solvent}$), and not the dry mass. Another case where the Sauerbrey equation is still valid is when the ΔF and ΔD values at different harmonics do not result to significantly different values indicating a less viscoelastic film. In any other case, the equation becomes invalid[27,37]. To address this issue, a variety of models have been developed which are not discussed here as they are beyond the scope of this study.

Finally, similarly to the QCM, mass changes that occur in SAW sensors can also be calculated by the Sauerbrey equation utilizing the recorded changes in phase (Δph or ΔΦ) while viscoelastic properties are investigated through ΔA.

➢ Analysis and Interpretation of QCM data

Figure 7 presents a typical protein adsorption experiment, similar to those presented in this thesis. Adsorption of biotinylated Bovine Serum Albumin (b-BSA) on the gold surface results to both a frequency change (ΔF_1) which is proportionally related to the amount of the adsorbed mass and a change in the dissipation of the acoustic energy (ΔD_1) which is indicative of the protein-film structural and hydration properties. Similar changes are recorded during a follow-up step of Neutravidin (NAv) addition (ΔF_2 & ΔD_2). Significant information about the viscoelastic properties of the adsorbed protein film or the conformation of the surface-attached biomolecules can be derived by calculating the acoustic ratio ΔD/ΔF (see relevant section in page 21).

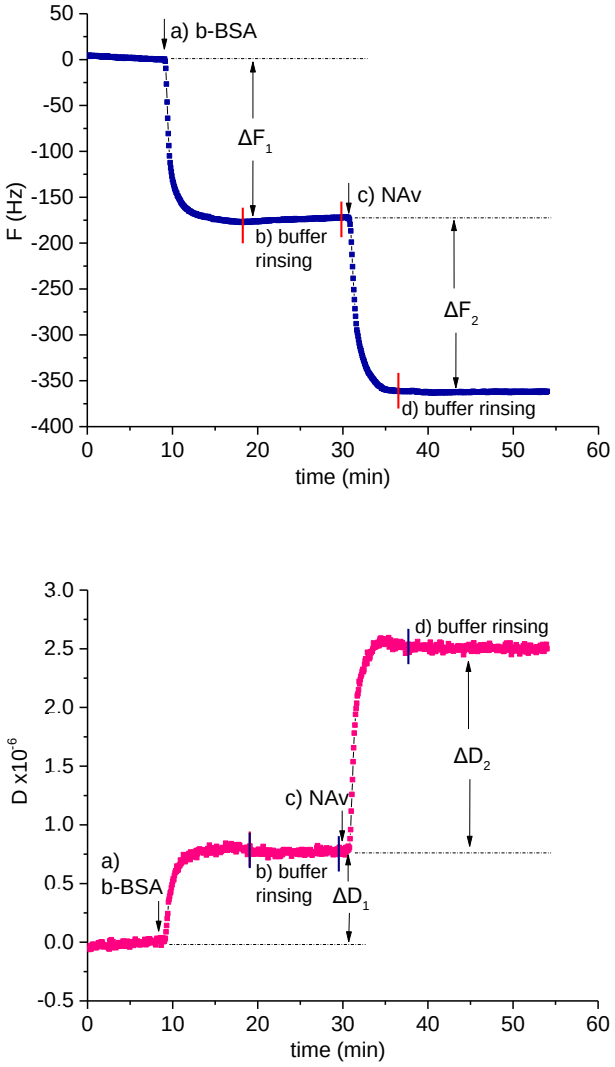

Figure 7. *Example of the real-time graphs obtained during a QCM-D experiment. a) Firstly, biotinylated Bovine Serum Albumin (b-BSA) is adsorbed on the sensor surface; upon adsorption, b-BSA forms a rigid film thus resulting to a high ΔF_1 (blue line) but low ΔD_1 change less than 0.8 x10^{-6} (pink line). c) Neutravidin (NAv) is then added and captured on b-BSA. NAv binding results to a high ΔF_2 change similar to that of b-BSA and a ΔD_2 quite higher compared to those of b-BSA. Steps b and d correspond to buffer rinsing.*

➢ Acoustic ratio; Uncovering ΔF and ΔD secrets

Generally speaking, as the size or the structural flexibility of the adsorbed molecules or the viscosity of the solution increases dissipation results to bigger values and its significance increases. Furthermore, by plotting Δ*f* versus Δ*D or* calculating the ratio *ΔD/ΔF* -also known as acoustic ratio- information about the conformation and the viscoelasticity of the adsorbed elements may be extracted. Briefly, the more viscoelastic protein-film will give a higher acoustic ratio.

While plenty of information can be extracted by the combined analysis of ΔF and ΔD through mathematical treatments based on the viscoelastic Voigt model, the latter assumes that the

deposited layer is a homogeneous viscoelastic film. In 2008, a new method of acoustic data interpretation was presented by Gizeli's research group by Tsortos A. et al.,[38]. According to this work, changes to the measured ratio ΔD/ΔF (also referred as acoustic ratio), parallel changes to the intrinsic viscosity *n* of various DNA molecules anchored to the device surface. The acoustic ratio reflects the energy dissipation per coupled unit mass. The authors treated the capture DNAs as "discrete molecules" rather than as a homogenous viscoelastic film. They hypothesized that since ΔD/ΔF correlates with the intrinsic viscosity *n* of the DNA molecule, then it should be independent of the DNA concentration or surface coverage, and being proportionally dependent on the shape, size and structure of the DNA[38].

$$\frac{\Delta D}{\Delta F} \propto n$$

The hypothesis was supported by mathematical treatment and following experimental tests they showed that a different acoustic ratio was obtained for dsDNA of different sizes but the same shape and for dsDNA of the same size but different shapes (straight, bent, triangle). They also confirmed that this characteristic acoustic ratio was not affected by the DNA concentration or surface coverage. Furthermore, they proved that for straight DNA (20 bp - 198 bp) a straight line was obtained when the acoustic ratio was plotted against DNA length, as they had predicted[38]. The new approach was successfully applied for the characterization of both ds and ss DNAs of various conformations[39–41], for the monitoring of structural changes such as the transition from the open to close form of Holiday Junction and vice versa[42] as well as the binding of the Hv1 histone on DNA[43]. The latter was investigated on a SAW device utilizing the ΔA/Δph ratio which is equivalent to ΔD/ΔF. Generally, similar experiments were also performed with a Love wave SAW device, providing the same results[40,43].

The development of this approach opens new possibilities in acoustic biosensors as research and diagnostic tools. For example, conformational changes derived from the interaction of DNA with DNA-binding proteins, such as transcription factors, can be investigated. Regarding the application into diagnostic tools, well-designed diagnostics can also be developed; molecular assays exploiting the acoustic ratio for the screening of cancerous point mutations and genetic variations have been already reported[44,45].

Biosensors in Cancer management

➢ Cancer

Cancer is the 2nd leading cause of death worldwide. According to World Health Organization, there were 10 million cancer-related deaths in 2020 (https://www.who.int/news-room/fact-sheets/detail/cancer), and this number is predicted

to rise by approximately 70% over the next two decades[46]. The best way to achieve effective and efficient management of cancer is the early diagnosis, the prognostication and the frequent monitoring of patient response to treatment.

Well-known techniques for cancer diagnosis involve imaging methods such as radiology, ultrasound scans (US) and magnetic resonance imaging (MRI) scans. Although these techniques are fast and easy-to-use, their application for monitoring of cancer patients is inappropriate and insufficient. For instance, radiology exposes patients to additional ionizing radiation which in turns can threaten patient's health, while US and MRI fail to reveal minimal residual disease (MRD), i.e. tumor components that remain after the therapeutic strategy. Moreover, none of these techniques provides genetic information which is often necessary for the selection of appropriate treatment and prognostication of patient response[47].

Genetic information about the tumor such as the existence of point mutations in cancer-related genes (e.g. in *KRAS* and *BRAF*) is essential for the selection of personalized treatment, significantly improving the overall survival (OS) of cancer patients[48–50]. Till now, for the screening of single nucleotide variants (SNVs), cancerous DNA is obtained through solid biopsy (also referred as tissue biopsy) which is commonly accepted as the gold standard of cancer diagnosis. During tissue biopsy, a small specimen is obtained directly from the tumor site and sometimes even a whole surgical procedure is required. Following tissue removal, the sample is usually fixed with formalin and embedded in a paraffin wax block for long term preservation and histological examination. Despite the overall benefits of tissue biopsy, it suffers from a variety of limitations: it is invasive and hazardous for patients' health; it is difficult to be obtained and sometimes not even possible; it is inappropriate for cancer monitoring; it is time-consuming and most importantly fails to reveal tumor heterogeneity[51–54] which is often linked to acquired treatment resistance and poor outcome[53,55].

Currently, the focus of oncologists on precision medicine turns them to Liquid biopsy approaches since they are not invasive and can be repeatedly performed facilitating effective disease and treatment monitoring. Liquid biopsy refers to the analysis of circulating biomarkers (CBs) released from tumor cells and are presented in body fluids such as blood, urine, saliva and cerebrospinal fluid. The most common CBs include circulating tumor DNA (ctDNA), cell-free RNAs (cfRNA, miRNAs), circulating tumor cells (CTCs) and extracellular vesicles (exosomes, apoptotic bodies). Isolation and analysis of CBs can provide a variety of information about genomic and epigenomic alterations as well as changes in the proteome and metabolome. Circulating tumor cells and circulating tumor DNA constitutes the most well studied and applied biomarkers in liquid biopsy. Although, both biomarkers can give information about genetic mutations, copy number alterations, changes in methylation etc., this information is easier to be obtained by ctDNA due to sample size while its analysis may be helpful for the estimation of tumor size as well[48,56].

➢ Circulating tumor DNA (ctDNA)

a. Characteristics

Circulating tumor DNA (ctDNA) is a fraction of cell-free DNA (cfDNA) which emanates from tumor cells and released into the circulation mainly through apoptosis and necrosis[57,58] (Fig. 8). ctDNA is double-stranded and according to sequencing-based analysis is highly fragmented ranging from 90 bp – 150 bp with a peak at ~140 bp[59,60]. Interestingly, it is more fragmented than cfDNA derived from healthy people which peaks at 167 bp and is equivalent to the DNA size wrapped around a nucleosome plus the linker DNA associated with Histone H1[58]. The total amount of ctDNA varies significantly among cancer patients, depending on the cancer stage and type. Generally, its quantity might be as low as 0.01% of the total cell-free and just a few copies per 5 mL of plasma. Its half-life is short, ranging from 16 minutes to 2.5 hours, due to its digestion from nucleases and filtration from the liver, spleen and kidney[57,58]. Overall, the highly fragmented nature of ctDNA as well as its ultralow amount makes its detection extremely challenging.

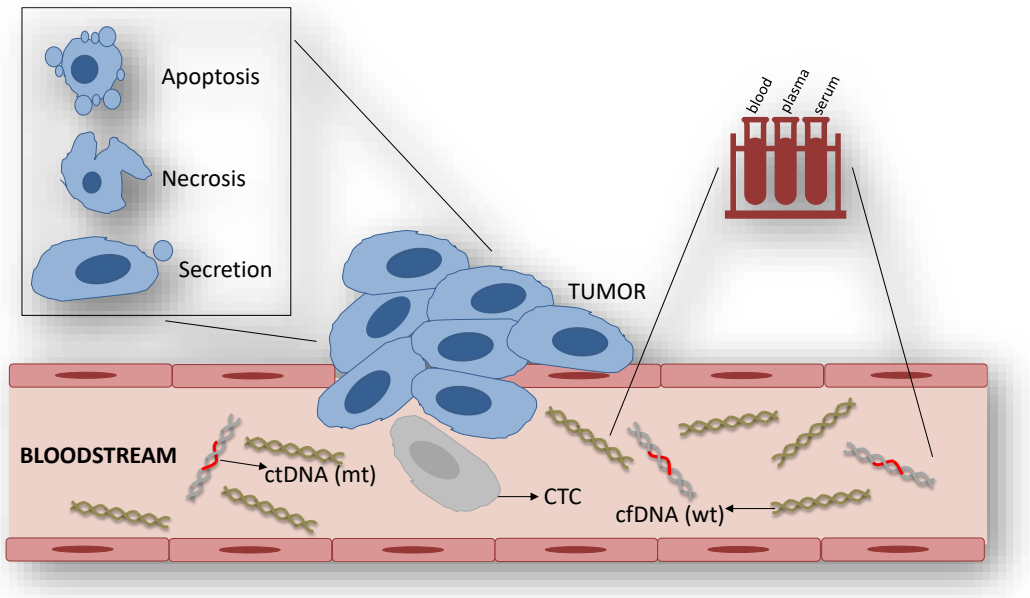

Figure 8. *Origins and extraction of cfDNA. Cells release DNA (cfDNA) in the bloodstream through a combination of cell death (apoptosis), necrosis and secretion with extracellular vesicles such as exosomes. The cfDNA that arise from cancerous cells is called circulating tumor DNA (ctDNA) and can carry genetic and epigenetic alterations like point mutations and methylation changes respectively. cfDNA can be extracted from a blood sample (plasma or serum). ctDNA -circulating tumor DNA; CTC – circulating tumor cell; cfDNA -cell free DNA; wt- wild type; mt – mutant.*

b. Clinical utility in cancer diagnosis and limitations

Circulating tumor DNA can carry various genetic and epigenetic changes, analysis of which may provide significant information about tumor dynamics[61]. Figure 9, summarizes the

potential applications of ctDNA in early detection, diagnosis, prognosis, treatment selection and treatment response. Regarding early detection, there are some cases where mutations in cancer driver genes like the *KRAS* and *TP53* have been detected to healthy people 2 years on average prior cancer[62]. However, generally the detection of point mutations in cfDNA prior cancer development becomes extremely difficult since there is no knowledge about which mutations to expect and the concentration of the mutations is much lower compared to early and late cancer stages. Apart from the technical issues, early detection in non-cancer patients may lead to false positives, since it is not feasible to distinguish between benign mutations that accumulate in non-cancerous areas or favorable tumors which remain small and do not cause any symptoms for many years[48,63,64]. Similarly, the application of ctDNA in diagnosis is very limited and is applied only when tumor location is known and sampling is unavailable. We could say that ctDNA is utilized mostly as a prognostic marker to monitor treatment response, relapse and resistance[58,61,63,64]. For example, high or low levels of ctDNA mutations are associated with poor outcome or positive response to treatment (radiotherapy, chemotherapy, surgical removal), respectively. Further, studies have demonstrated that ctDNA outperforms protein biomarkers like the cancer antigen 15-3 (CA 15-3) and carcinoembryonic antigen (CEA) which utilized for monitoring of breast and metastatic colorectal cancer (mCRC) in respect, indicating its value in MRD monitoring[61,64]. Finally, ctDNA analysis is of high clinical significance for the selection of appropriate treatment, since it can reveal tumor heterogeneity[51–54] which is often linked to acquired treatment resistance[53,55]. In any case, due to the non-invasive nature of this technique, ctDNA can be successfully used to track clonal evolution and resistance in the early stages giving the opportunity of readjustment to a better therapeutic procedure. Last but not least, ctDNA can be informative about the tumor size and stage through the mutant allele frequency which is correlated with the disease burden[48,58,63,64].

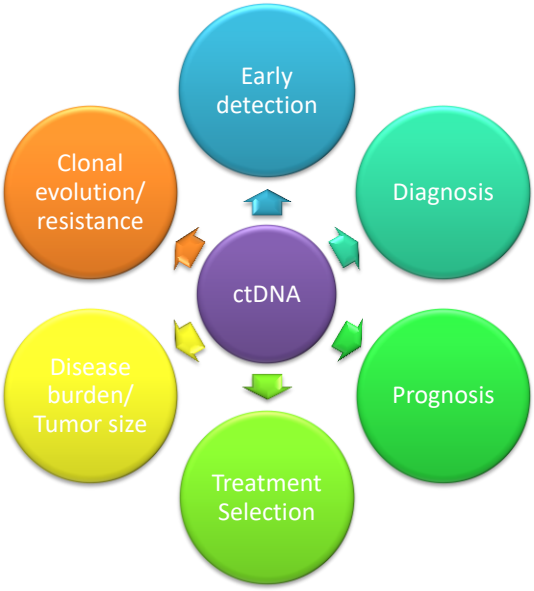

Figure 9. *The clinical value of circulating tumor DNA (ctDNA).*

It is worth mentioning, that the advancements in ctDNA analysis do not demonstrate that it can replace solid biopsies. The validity of ctDNA analysis is still under investigation and its application is limited due to lack of consistency between various detection and analytical methodologies[48]. Moreover, different point mutations are detected by solid and liquid biopsies, indicating that the two methods are complementary to each other[51].

c. Detection techniques

Analysis of point mutations in cancer-related genes (e.g. in *KRAS* and *BRAF*) is essential for the selection of personalized treatment improving the overall survival (OS) of cancer patients[48–50]. Despite the fact that many techniques have been developed for the screening of single nucleotide variants in tissue samples, Sanger sequencing and pyrosequencing remain the gold standard methods for cancer diagnosis. Both methods detect point mutations in a PCR-amplified region. However, they suffer from the low sensitivity of just 15-30% and 5-10%, respectively[65,66] (here sensitivity is referred to the mutant allele frequency which is defined as the % of mt/(mt+wt) copies). Targeted Next-generation sequencing (NGS) techniques like the Ion Torrent PGM platform combined with the Ion AmpliSeq Cancer Hotspot panel v2 and the MiSeq® system used with the TruSeq Amplicon Cancer Panel (Illumina) have been also applied, but their application is quite limited to research use only mainly due to the high cost, the complexity of data processing, the high error rate and the slow turnaround time (up to days)[67–69]. Contrary, there are plenty of PCR-based approaches that have been applied for the detection of certain point mutations in FFPE tissue samples exhibiting better detection limits and sensitivity. These are various real-time Taqman-based PCR methods, such as the FDA approved cobas® mutations tests, allele-specific PCR[66,70,71] and the ultrasensitive droplet-digital PCR (ddPCR) which can detect point mutations with a mutant allele frequency (MAF) of less than 0.01%[72]. Detection techniques applied for tissue biopsy are summarized in table 1 together with their detection limits.

Table 1. Techniques applied for the detection of point mutations in tissue biopsy samples.

Technique	Sensitivity	Method	Approach
Sanger[65,66]	15 - 30 %	Sequencing - based	Detection of multiple point mutations, Identification of new ones
Pyrosequencing[65,66]	5 -10 %		
Targeted NGS (Ion Torrent PGM, TruSeq technologies)[67–69]	1 -5 %		
Cobas® FDA approved test	5%	PCR - based	Detection of 1 or a few certain point mutations
AS-PCR/ARMS-PCR[66,70,71]	0.1 - 1 %		
ddPCR[72]	0.001 %		

NGS – Next Generation Sequencing; AS-PCR – Allele Specific PCR; ddPCR – droplet digital PCR

As earlier reported, ctDNA is highly fragmented and its total amount might be as low as 0.01% of the total cell-free (cf) DNA making its detection challenging[61,63]. To this end, a variety of highly sensitive ctDNA detection methods have been developed which are divided in two main categories depending on the number of mutations that can detect; Next-

generation sequencing (NGS) and PCR based techniques. Table 2 presents the most common ones reported in the bibliography. Among sequencing-based methods, conventional NGS technologies such as Whole Genome Sequencing, Whole Exome Sequencing and the Ion AmpliSeq are not suitable since they present a detection sensitivity higher than >1%[47,57]. Currently, new improved NGS approaches have been described such as the Tagged Amplicon Sequencing (TAm-Seq), Safe-Sequencing System (SafeSeqS) and CAncer Personalized Profiling by deep Sequencing (CAPP-seq) which exhibit a sensitivity of 0.2- 2%, 0.1 % and 0.01 %, respectively. These techniques, allow the analysis of multiple mutations in parallel in one or more genes[57,72,73]. However, their application to routine clinical diagnosis is strongly restricted due to the high error rate, the high cost, the complexity of data processing which requires extended bioinformatics analysis and specialized manpower, and the slow turnaround time. On the other hand, PCR-based assays are more cost-effective and allow the detection of single or low number of mutations. Since, typical Real-time PCR (RT-PCR) has low sensitivity (~10%)[56], various improved PCR-based methods such as the Peptide Nucleic Acid-Locked Nucleic Acid (PNA-LNA) PCR, co-amplification at lower denaturation temperature (COLD-PCR) and Allele-Specific amplification (AS-PCR) have been applied with their detection sensitivities estimated as 0.1 -1%, 0.1% and 0.1-2%, respectively[73,74]. However, like in the case of tissue biopsy, the higher sensitivities have been reported for digital PCR methods like the beads emulsion amplification magnetics PCR (BEAMing-PCR) [57] and the ddPCR[72,75], with the latter being the most frequently proposed technique for the detection of point mutations in ctDNA. Although the above methods are less cumbersome than sequencing, most of them still may be incapable for the detection of rare point mutations. Finally, while BEAMing-PCR[57] and ddPCR[72,75] have a detection sensitivity of 0.01% and 0.01- 0.001% in respect, they remain costly and complex for routine clinical use.

Table 2. ctDNA detection techniques for Liquid biopsy.

Approach	Method	Technology	Sensitivity	Advantages	Disadvantages
Deep Sequencing – multiple gene mutations	Targeted analysis	Ampliseq[57]	>2 %	> Prior knowledge for the expected mutations is not required, > Identification of new mutations	> Expensive, > Time - consuming, > Complex > Advanced Bioinformatic Analysis
		TAm-Seq	0.2 – 2%		
		SafeSeqS	0.1 %		
		CAPP-Seq	0.01 %		
Single or a few gene mutations	Quantitative PCR	COLD-PCR[73]	0.1 %	> Highly Sensitive > More cost and time effective compare to sequencing approaches	> Capable for monitoring known point mutations
		PNA-LNA-PCR[73]	0.1 – 1 %		
		AS-PCR[73,74]	0.1 – 2 %		
	Digital PCR (absolute quantification)	BEAMing-PCR[57]	0.01 %		
		ddPCR[72,75]	0.01 – 0.001 %		

Tam-Seq - Tagged Amplicon Sequencing (TAm-Seq); SafeSeqS - Safe-Sequencing System; CAPP-seq - CAncer Personalized Profiling by deep Sequencing; COLD-PCR - co-amplification at lower denaturation temperature;

PNA-LNA-PCR - Peptide Nucleic Acid-Locked Nucleic Acid; AS-PCR -Allele Specific PCR; BEAMing-PCR - beads, emulsion, amplification, magnetics PCR; ddPCR – droplet digital PCR

The past few years, there is extensive research in the field of DNA biosensors of all transduction principles (electrochemical, optical, acoustic) to develop novel techniques for the simplified, fast and inexpensive detection of single nucleotide variants (SNVs) and point mutations. Usually, the selective ability of these biosensing methods to the SNVs is based on the surface hybridization on DNA[76–78], peptide nucleic acid (PNA) or locked nucleic acid (LNA) probes, surface ligation[79], digestion[45], the use of molecular beacons[79] as well as a combination of two or more of the aforementioned approaches. Sensitivity is another important issue for identifying the point mutation. In order to improve the sensitivity of the DNA biosensors many methods have been introduced; enhancing steps through enzymatic amplification (e.g. polymerization[44,45,76,80], horse-peroxidase[81,82]), nanoparticle amplification (AuNPs, liposomes)[80,83–85] and other nanostructured-materials as recently reviewed by Bellassai & Spoto, 2016[86] have been described. Although the aforementioned techniques are able to detect single nucleotide mutations, the vast majority of them include a hybridization step of the DNA target with an immobilized capture probe. The above constitutes a major disadvantage when it comes to the detection of dsDNA like ctDNA and difficulties may arise: denaturation requires a heat source; hybridization is poorly controlled; and the prevention of reassociation of the denatured DNA becomes a significant issue. Dealing with these obstacles usually lead to methods with multiple processing steps, increasing the overall assay time. In addition, these methods have insufficient sensitivity, are of low technology readiness level and have not been validated with real samples. There are some excellent exceptions, though, such as the electrochemical DNA clutch method, where DNA clutch probes were utilized to prevent renaturation of the denatured DNA molecules, therefore facilitating efficient hybridization analysis[87]. Other methods are the nanoparticle enhanced surface plasmon resonance imaging (NESPRI)[88] and the piezoelectric plate sensor (PEPS)/fluorescent reporter microspheres (FRMs) techniques[89]. All the above techniques were applied for the detection of ctDNA in serum, plasma and urine samples respectively, achieving good sensitivity but not the required limit of detection (minimum number of mt molecules that can be detected). Overall, while the above works present elegant examples of biosensors and nano-biotechnology in clinical diagnostics only the electrochemical DNA clutch assay reached the require sensitivity similar to those of ddPCR[87]. Potential drawbacks of the above methods include the (a) use of expensive peptide nucleic acid (PNA) or locked nucleic acid (LNA) probes for the specific capturing of the mt target; (b) requirement for hybridization steps and temperature control; (c) laborious surface-activation and washing steps as well as nanoparticles synthesis and functionalization; and (d) low sensitivity and detection limit. Regarding the latter, even their relative low detection limit may be not enough when it comes to low copy number real samples with just a few mt copies (~2-10) in an excess of some thousand wt molecules.

Development of acoustic biosensing techniques for the detection of cancerous point mutations in BRAF and KRAS genes

RAS proteins (KRAS, HRAS, NRAS) are members of the small GTPase protein family and serve as GDP/GTP-regulated switches controlling various signaling pathways important for the regulation of cell proliferation and survival. RAS proteins are induced from growth factor receptors including the (a) epidermal growth factor receptors (EGFRs), (b) MET tyrosine kinase receptors for Hepatocyte growth factor (HGF) and (c) KIT tyrosine kinase receptors for Stem Cell Factor (SCF)[90]. In the RAS-RAF-MEK-ERK signaling pathway, also known as mitogen activated protein kinase (MAPK) pathway, following an external signal, which activates the tyrosine kinase receptor, RAS is activated through the adaptor molecules Grb2 and SOS which are located to the inner part of the cell membrane[91,92]. Activated Ras recruits the RAF serine-threonine kinases (BRAF, CRAF, ARAF) to the cell membrane where they are phosphorylated at threonine 599 and serine 602[91]. Activated (phosphorylated) BRAF can form BRAF-CRAF heterodimers and phosphorylate and activate the MEK1/MEK2. Finally, activated MEK1/2 phosphorylates the extracellular signal regulated kinases 1 and 2 (ERK1 and ERK2) which are then translocated from the cytoplasm into the nucleus and phosphorylate a variety of transcription factors (Fos, Myc, Elk and others) or targets other intracellular signaling molecules (RSK) [91,92]. Activating mutations within the RAS (e.g. KRAS) or RAF (e.g. BRAF) genes permit constitutive MAPK pathway activation, thereby causing deregulation in cellular growth and survival and help to potentiate oncogenesis[92–94]. Attempts to inhibit the MAPK pathway in order to block proliferation signaling, generates cross-talk between different pathways and the activation of compensatory pathways such as the PI3K-AKTmTORC1 signaling[94]. Note that RAS GTPases proteins can also activate independently the PI3K as well as the RalGDS proteins that are also activate effectors and have been shown to be important in some types of cancer[92].

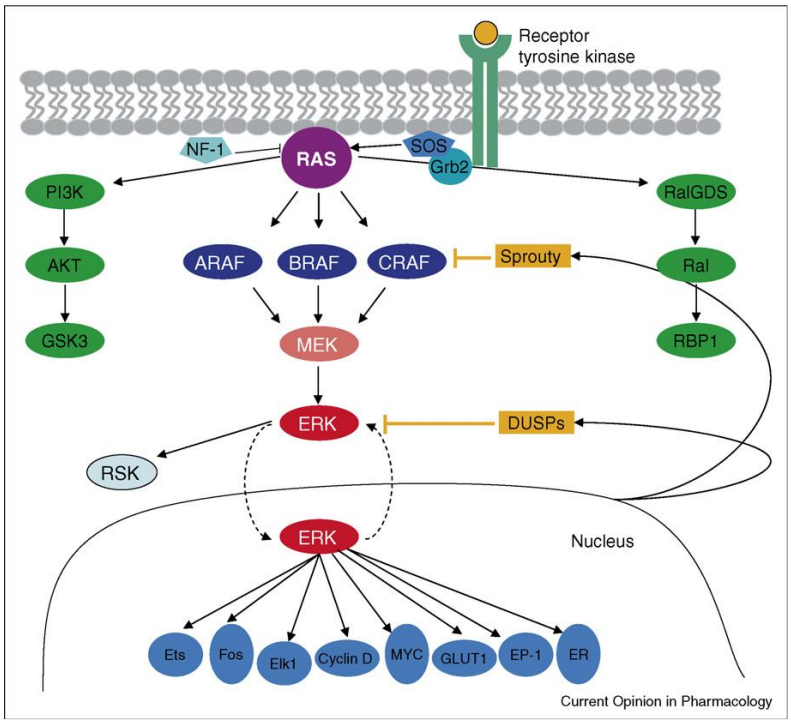

Figure 3. *The RAS-RAF-MEK-ERK pathway. The BRAF serine-threonine kinase functions downstream of RAS in the RAS-RAF-MEK-ERK mitogen activated protein kinase (MAPK) pathway. Activating mutations within the KRAS or BRAF gene permit constitutive MAPK pathway activation, thus causing deregulation in cellular growth and survival. Note that RAS proteins can independently activate other pathways playing important role in cancer progression through the PI3K and the RalGDS molecules. Schematic illustration was obtained by Ref.* [92].

Mutations in the *KRAS* gene occur early in the development of many cancers and are identified in more than 90% of pancreatic adenocarcinomas, 40% of colorectal cancers (CRC), 33% of non-small cell lung cancer (NSCLC) and ~15% of ovarian and endometrial cancers[90,95]. *KRAS* mutations are usually located in exon 2 at codons 12 and 13, with the G12D and G13D being the most frequently observed, respectively, both characterized by a C -> T transition[90,96]. *BRAF* mutations occur in approximately 8% of all human cancers, with high mutation frequency in malignant melanoma (50-70%), classic papillary carcinoma of the thyroid (40-70%), colorectal cancer (CRC, 5-15%)[92,97], non-small cell lung cancer (1% -7%)[98,99], ovarian cancer (13.8%)[100] and hairy cell leukemia (~97-100%)[91,101]. The most common mutation within the *BRAF* gene is the T1799A transversion that results in valine-to-glutamate substitution at codon 600 (V600E) and accounts for over 80% of all BRAF mutations[102].

In this work, new methods for the direct, ultrasensitive and specific detection of point-mutations in the *BRAF* and *KRAS* genes utilizing acoustic biosensing devices are presented. We focus on the detection of *BRAF* V600E or *KRAS* G12D mutations since they are the most frequently observed in the corresponding genes[96,102]. Moreover, their analysis is strongly recommended prior to treatment initiation. For instance, in melanoma, molecular testing for *BRAF* V600E mutation can provide valuable information for treatment selection; its inhibitors vemurafenib and dabrafenib are commonly used for the targeted therapy of melanoma patients providing significant benefits in terms of overall survival compared to

chemotherapy[49,104]. Regarding other cancer types, vemurafenib has been also shown to improve the survival of NSCL cancer patients[98,105]. In CRC, *BRAF* and *KRAS* mutational status identification is required since patients with activating mutations in these genes do not respond to Panitumumab or Cetuximab anti-EGFR monoclonal antibody (MoAb) therapy[50,106,107] and other treatment like bevacizumab should be applied[108]. In the proposed methods, acoustic detection is coupled either with pre-enrichment or with pre-amplification of the point mutations through Ligase Chain Reaction or Allele-Specific PCR, respectively. In both cases, we used modified pair of LCR probes or PCR primers that permits the direct immobilization of the dsDNA products on the sensor surface, obviating the need for a hybridization step. Furthermore, in order to enhance the detection capabilities of the assays, liposomes of 200 nm are employed to detect the DNA. Liposomes are highly dissipative molecules and act as acoustic dissipation signal enhancers. For this reason, in the following chapters we will mainly focus on the recording of the dissipation changes.

The current PhD is part of the CATCH-U-DNA Horizon2020 FET-OPEN project titled as "Detection of non-Amplified circulating tumor DNA with Ultrasound Hydrodynamics" (https://catch-u-dna.com/). Briefly, CATCH-U-DNA focuses on the development of a novel diagnostic technique for the detection of ctDNA targets without using the labor-intensive and occasionally biased PCR. Instead, the high amplification efficiency and specificity will be investigated initially through ligation-based techniques such as the Ligase Chain Reaction (LCR) together with an acoustic biosensor to probe the hydrodynamic shape and size of surface-attached molecules. About the latter, LCR products will be acoustically detected through the use of "soft" acoustic probes (e.g. liposomes) the binding of which greatly enhances the acoustic signal. Following LCR, allele-specific PCR will also be investigated as an alternative and more efficient method for the detection of the ctDNA targets. In order to further improve the detection limit of the method, High Fundamental Frequency sensors are employed as well. While the method focuses on the detection of ctDNA targets in the context of Liquid biopsy, the method will also be applied for tissue biopsy through the detection of point mutations in genomic DNA. Finally, a new extraction method that permits the specific isolation of only the targets of interest (e.g., *BRAF*) using a new version of the microfluidic fluidized bed[109,110] is going to be tested.

Objectives

The main goal of the current work is the development of an approach for the acoustic detection of the point mutations *BRAF* V600E and *KRAS* G12D in tissue and plasma samples in the context of tissue and liquid biopsy, respectively. The detection of point mutations in plasma samples automatically set the thresholds about the sensitivity and the limit of detection that the method should reach, i.e. 0.01% mutant allele frequency (MAF% - mt/(mt+wt) *100) and few mt copies, respectively. To achieve the main goal the work has been split in separate parts regarding the amplification of the DNA targets carrying the mutations followed by their immobilization and enhanced detection on the sensor surface. Below, a detailed step-by-step demonstration of the objectives of the current work is presented:

1. Development of a universal acoustic protocol for the direct capturing and immobilization on the sensor surface of DNA targets from unpurified molecular amplification reactions (Chapter 2).

2. Detection of the immobilized DNA targets through “soft” liposomes. Liposomes significantly enhance the dissipation of the acoustic signal improving the DNA limit of detection of the acoustic sensor (Chapter 2).

3. Replacement of the typical 35 MHz sensors and QCM device with a novel 150 MHz array of 24 miniaturized sensors and a platform. The array permits a more sensitive, fast and cost-effective multi-sample analysis (Chapter 2).

4. Enrichment of the DNA targets carrying the point mutation with a non-PCR based approach the Ligase Chain Reaction (LCR). LCR is a DNA amplification technique able to discriminate mismatches and to exponentially amplify the DNA target of interest. In contrast with the standard amplification technique PCR, LCR neither utilizes a DNA polymerase nor introduces errors and biased amplification (Chapter 3).

5. Application of a new DNA extraction technique based on the microfluidic magnetic fluidized bed for the capturing and enrichment only of the DNA targets of interest followed by LCR amplification and acoustic detection (Chapter 3).

6. If LCR does not achieve the required detection limit and sensitivity a highly specific Allele-specific PCR approach will be developed (Chapter 4).

7. Evaluation of the final method in real tissue and plasma samples (Chapter 5).

Chapter 2

Development of a universal acoustic detection protocol for DNA through Liposomes for amplification

Introduction

The study presented in this chapter aims to develop an acoustic methodology for the detection of surface-immobilized dsDNA targets at very low concentrations of DNA and in a simple manner (Fig. 1). Currently, the limit of detection is [DNA]≈5 nM. To achieve better sensitivity a signal amplification step was introduced consisted of the binding of liposomes to the surface-immobilized DNA[111]. Thus, liposomes were employed as dissipation signal enhancers. Regarding simplicity, we wanted the assay to be capable to capture the DNA targets on the sensor surface directly, obviating denaturation of the target and hybridization to immobilized capture probes. Finally, the assay should be adaptable to the analysis of crude samples, like molecular amplification reactions, thus overcoming the need for a purification/clean-up step.

As it will be shown in the next chapters (No 3 and 4), through DNA amplification assays, double labelled with biotin and cholesterol dsDNA products can be created (Fig. 1 suggested procedure). Biotinylated dsDNAs could be bound directly to a neutravidin (NAv) coated sensor, through the NAv-biotin interaction. This methodology, i.e., direct binding of dsDNA instead of initial hybridization to a complementary probe (Fig. 1 common procedure), has been shown in several works in *Biosensors Lab* to produce robust and stable dsDNA molecules bound on the sensor surface[44,45]. DNA immobilization is then followed by the subsequent capturing of a highly dissipative liposome via the cholesterol in a spontaneous process without the need of liposome functionalization (Fig. 1 suggested procedure). Liposomes greatly enhance the change in the acoustic signal leading to the detection of the immobilized DNA and significantly improving the detection limit to 2pM[111]. Nanoparticle (NP)-based signal enhancement is quite common, usually through the application of (oligonucleotide) functionalized gold nanoparticles (AuNPs)[84,112,113], (oligonucleotide) functionalized lipid vesicles[114,115] or the creation of dendritic-type structures with liposomes[116,116] or AuNPs[117]. These strategies have been shown by our group as well as others to be suitable for the acoustic detection of Recombinase Polymerase Amplification (RPA) products[118] and single-base mismatches[85,111,114,115,119]. However, in the majority of these studies frequency was monitored rather than dissipation. Here we take advantage of the highly dissipative liposomes that affect more the ΔD change. Overall, the proposed assay is advantageous because it eliminates the need for temperature and buffer controlling of several hybridization steps and the use of functionalized NPs or dendritic structures. Instead, here we use a one-step bioaffinity assay for the immobilization of the DNA target, while for the signal amplification non-functionalized liposomes are employed.

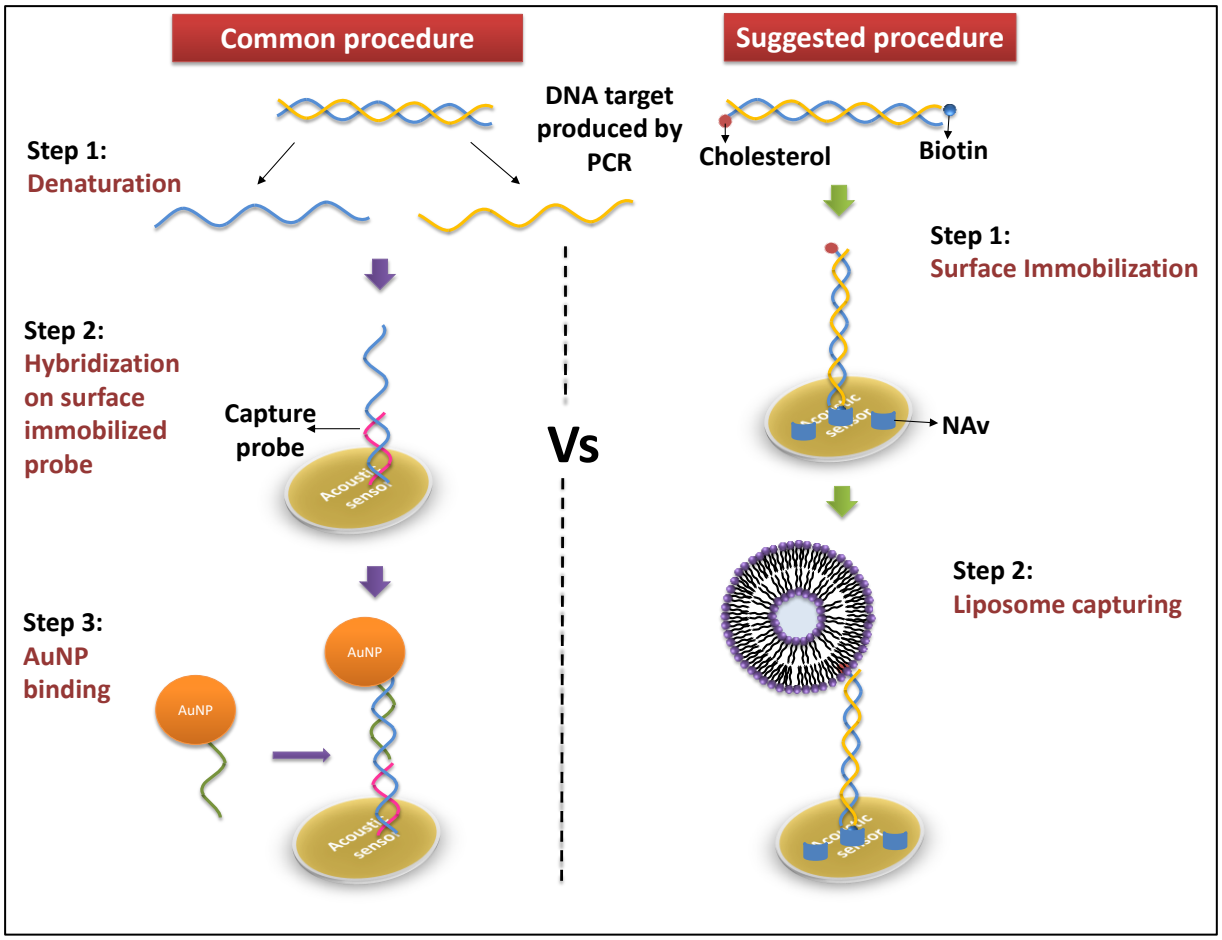

Figure 1. *Schematic illustration of the common acoustic detection technique Vs the one presented in this study. In the common procedure, a denaturation step is required for the dsDNA target to hybridized on the surface-immobilized capture probe. Following immobilization, a 2nd hybridization step is taking place where functionalized with oligonucleotide probes AuNPs are captured on the DNA target. Regarding the suggested procedure, firstly the ds and double-labelled with biotin and cholesterol DNA targets are immobilized on a Neutravidin (NAv)-coated sensor followed by the addition of 200nm liposomes which are spontaneously captured on the DNA by the cholesterol. Disadvantages of the common strategy are the need of two denaturation steps, the loss of DNA targets because some DNA strands will reassociate, and the increased number of steps (including the denaturation and the particles functionalization).*

For this study, two different Quartz Crystal Microbalance (QCM) devices were used and tested; the conventional QCM-D device (E4 QSense) combined with the typical 5 MHz gold sensor and a new High Fundamental Frequency QCM (HFF-QCM) array of 24 miniaturized sensors.

PART 1:

DEVELOPMENT OF NAV-BASED SUBSTRATES FOR CAPTURING OF BIOTINYLATED DNA TARGETS FOLLOWED BY LIPOSOME DETECTION: A QCM-D STUDY

Introduction

A key advancement in the successful acoustic detection of DNA targets is their direct immobilization on a neutravidin-coated gold sensor followed by the addition of liposomes. To achieve that, two main substrate chemistries were investigated; Neautravidin (NAv) adsorbed on the gold surface and high and low concentration of NAv bound to biotinylated-BSA (b-BSA) pre-adsorbed on Au. The surfaces were tested for the immobilization of biotinylated DNA, for their specificity during liposome injection as well as for their stability upon crude sample addition. All acoustic experiments were performed with 5 MHz sensors and the E4 QSense analyzer operating at 35 MHz (7^{th} overtone).

In our lab, liposomes of various diameters (30 nm – 200 nm) and lipid composition have been used including DOPC, POPC, DPPC, SMPC and PMPC. All the above were tested for their ability to dissipate acoustic energy. Overall, the larger liposome was identified as more dissipative[111]. Regarding the lipid composition, SMPC and PMPC liposomes had a higher dissipation capacity, however, these two liposomes were characterized by lower stability. On the other hand, POPC liposomes were pretty stable for more than 1 week. Moreover, in a work published by our group in May 2020, Milioni et al., showed that the LOD of dsDNA was improved by 3 orders of magnitude using the 200 nm POPC liposomes, reaching the 2 pM[111]. The same LOD was also achieved by the SMPC liposomes, indicating that despite the fact that were identified as more dissipative, the LOD wasn't improved. For these reasons, for the acoustic detection experiments, the POPC liposomes of 200 nm were mainly employed for the detection of DNA targets.

Materials & Methods

Materials	
QCM Cr-Au sensors 5 MHz	Advanced Wave Sensors (AWS) S.L., Paterna, Spain
Phosphate buffer Saline (PBS) tablet	Sigma-Aldrich, Miss., US
Avidin, NeutrAvidin™ Biotin-binding Protein	Invitrogen, US
BSA lyophilized powder, crystallized, ≥98.0% (GE)	Sigma-Aldrich, Miss., US
Biotin-$(AC_5)_2$-Sulfo-Osu	Dojindo, Japan
Microcon-30kDa Centrifugal Filter Unit with Ultracel-30 membrane	Merck KGaA, Darmstadt, Germany
F50chol3	Metabion International AG, Germany
1,2-dioleoyl-sn-glycero-3-phosphocholine (DOPC)	Avanti Polar Lipids Inc., Alabaster, USA
Nuclepore polycarbonate hydrophilic	Whatman plc, UK

membranes 0.2 μm

DNA Sequence (5’ -> 3’)	
F50chol3 ssDNA	**biotin-**AATTCAGAGAGGAGGAGAGAGCGGTGCGGTAGGAG AGAGAGAGGAGGATC**-cholesterol**

Quartz crystal microbalance with dissipation monitoring (QCM-D) acoustic device. A QSense Analyzer (E4 instrument) (Biolin Scientific, Sweden) was used for the simultaneous monitoring of frequency and dissipation. The QSense device was connected to an IPC4 peristaltic pump (Ismatec, Cole-Parmer GmbH, Germany) to adjust the flow rate at 50 μL/min and inject the samples into the system. Measurements were performed in continuous flow of PBS buffer pH=7.4, at 25 °C and all samples were diluted in the PBS. Following each sample addition, buffer rinsing was taken place and then frequency and dissipation changes were obtained. For the experiments Au-coated 5 MHz AT-cut quartz crystals were used. The reported values of frequency and dissipation changes were obtained at 35 MHz (7^{th} overtone); ΔF was not normalized by the overtone number. Prior use, the gold-coated sensors were rinsed with mili-Q water and 70 % EtOH, dried under N_2 flow and then subjected to 3 min plasma cleaning using a Harrick plasma cleaner PDC-002 (“Hi” setting) (Harrick Plasma, NY, USA).

Biotinylation of BSA. The biotin-$(AC_5)_2$-Sulfo-Osu was diluted in DMSO at 14.9 mM. BSA dissolved in PBS was incubated with the biotin-$(AC_5)_2$-Sulfo-Osu linker in PBS, in a molar ration of 1:10, for 1 h and 30 min at RT. After incubation BSA was purified using the Microcon-30kDa Centrifugal Filter Unit with Ultracel-30 membrane (Merck) following manufacturer instructions.

Liposome preparation. Lyophilized 1,2-dioleoyl-sn-glycero-3-phosphocholine (DOPC) lipids were dissolved in chloroform at final concentration of 10 mg/mL. 100 – 200 μL of the 10 mg/mL lipids were added in round bottom glass flask and dried homogenously under N_2 flow. The lipid film was then left for 30 min under N_2 gas followed by resuspension in PBS at a final concentration of 2 mg/mL by gentle vortexing. The resulting suspension was passed through polycarbonate membranes (Whatman NucleoporeTM) with a nominal pore diameter of 200 nm, using the Avanti Mini-Extruder. Stock solutions were stored at 4 °C for up to 6 days.

Acoustic detection of NAv and biotinylated-BSA/NAv. Neutravidin (NAv) (200 μL x 0.2 mg/mL) or biotinylated-BSA (b-BSA) (250 μL x 0.2 mg/mL) followed by the addition of NAv (200 μL x 0.2 mg/mL or 0.05 mg/mL) were physically adsorbed on the gold surface.

Acoustic detection of ssDNA target through liposomes. For the experiments a 50 nt ssDNA (F50chol3) target modified with a biotin at the 5’ end and cholesterol at the 3’ end was used. The target was diluted in 200 μL PBS in various concentrations ranging from 0.05 – 5 nM

(otherwise, 10 fmol – 1 pmol of ssDNA in 200 µL) and loaded on NAv or b-BSA/NAv coated sensors followed by the injection of 500 µL x 0.2 mg/mL DOPC liposomes.

Results & Discuccion

1. Evaluation of protein adsorption on sensor surface

Figure 2 shows the real-time monitoring of the NAv and of the b-BSA followed by NAv addition. Note that, the physisorption of b-BSA gave acoustic signal values, i.e., change in frequency (ΔF), dissipation (ΔD) and acoustic ratio (ΔD/ΔF) accounted for 183.4 ± 12 Hz, 0.75 ± 0.09 x10^{-6} and 0.0041 ± 0.00042 10^{-6}/Hz, respectively. These results were in agreement with previously reported values indicating saturation of the surface and a good formation of BSA layer.

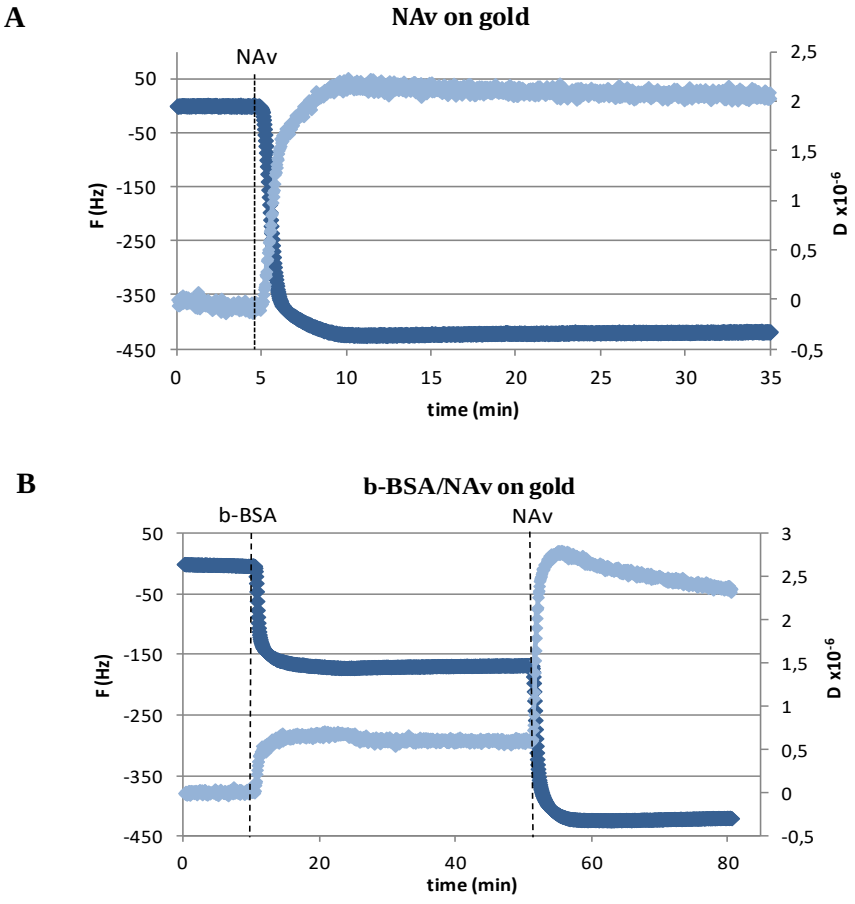

Figure 2. *Real time frequency and dissipation monitoring of (A) NAv & (B) b-BSA/NAv absorption on gold sensor surface.*

In Figure 3, the frequency and dissipation changes as well as the acoustic ratio measured during the adsorption of NAv on gold or binding to the b-BSA-modified surface are presented. The lower ΔF and ΔD signals obtained from the NAv binding on the b-BSA surface (-225 ± 21 Hz, 1.8 ± 0.37 x10^{-6} for high NAv concentration and 215 ± 22 Hz, 1.8 ± 0.21 x10^{-6} for low NAv concentration upon b-BSA) are characterized by a better reproducibility

compare to NAv directly on gold (-424 ± 50 Hz, 2.88 ± 0.62 x10^{-6}). The better reproducibility of the b-BSA/NAv substrate is most likely due to the specific binding of the NAv molecules on the BSA through the biotin-NAv interaction, which may lead to a smaller degree of NAv aggregation on the surface. Regarding the acoustic ratio (0.0064 ± 0.0013 for NAv on gold, 0.008 ± 0.0012 and 0.0084 ± 0.0008 for high and low [NAv] on b-BSA, respectively), the higher numbers measured on the b-BSA probably are due to the presentation of NAv in a more suspended way. Finally, while the two different concentrations of NAv did not significantly differ in their ΔF, ΔD and ΔF/ΔD values (Fig. 3), as reflected in the error bars of figure 3 and in the real time-graphs of figure 4 the signal of NAv had better reproducibility and stability in the case of low[NAv].

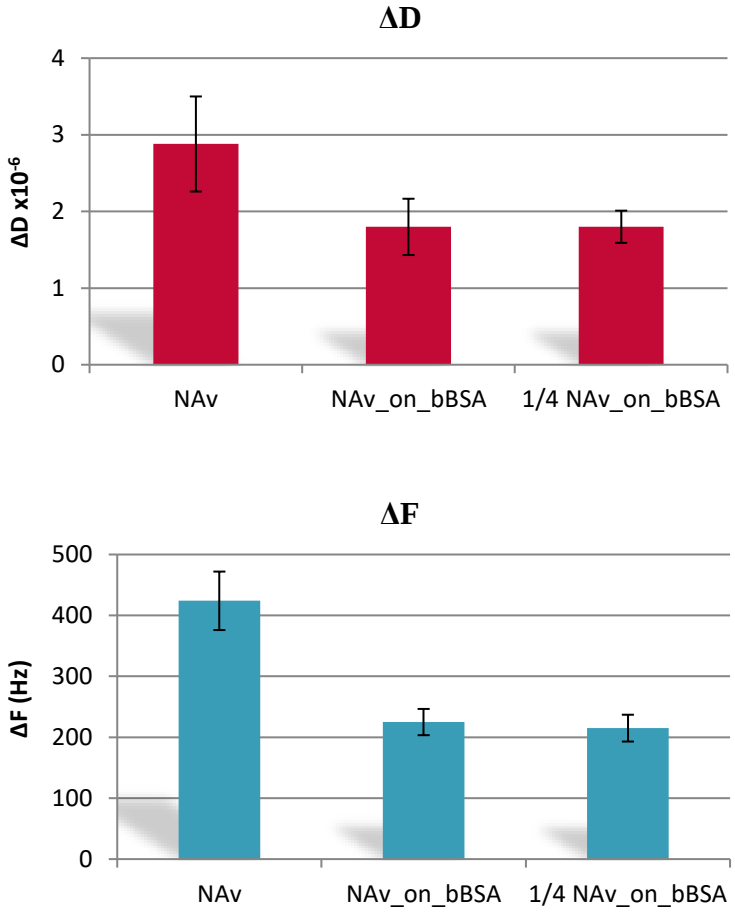

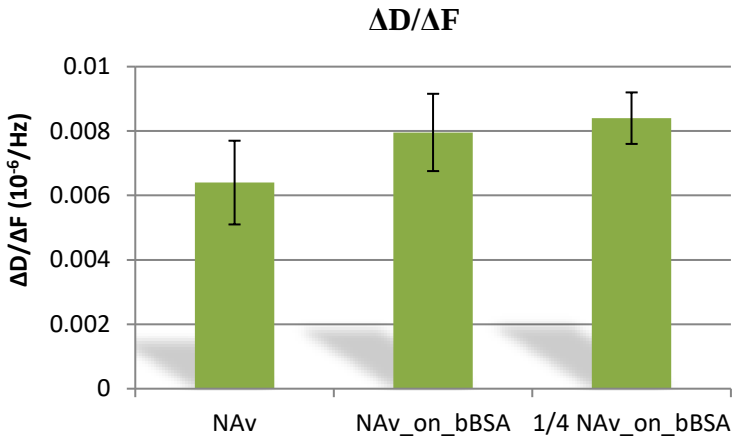

Figure 3. *Comparison of ΔF, ΔD and ΔD/ΔF average values of NAv when added directly on gold or a b-BSA pre-coated QCM surface.*

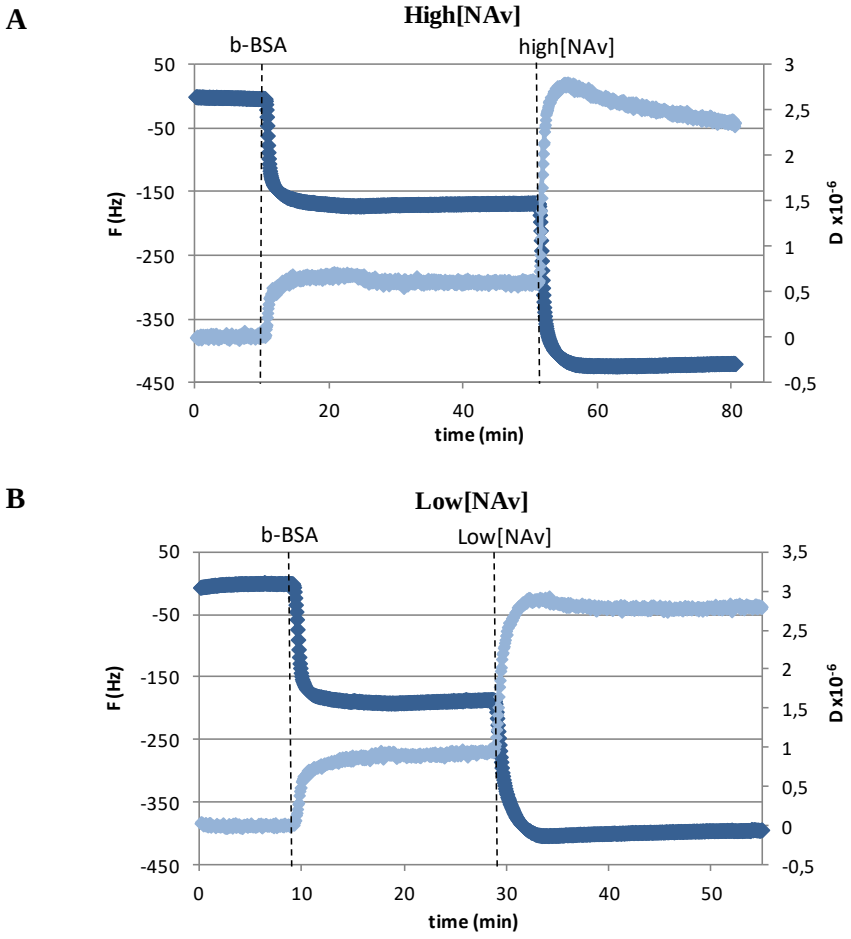

Figure 4. *Comparison of the real time curves of high[NAv] (A) and low[NAv] (B) when added on b-BSA pre-coated QCM surface.*

2. Detection of ssDNA through liposomes

The detection of DNA through highly dissipative liposomes (here DOPC liposomes of 200 nm) was monitored on both surfaces (Fig. 5). For the experiments, a synthetic ssDNA of 50 nt length modified by a biotin at the 5' end and cholesterol at the 3' end was used. Note that,

the addition of the DNA on the NAv-coated sensor result in no dissipation or frequency changes, since the DNA concentration was below the threshold for acoustic detection which for the acoustic sensor used here is [DNA] ≥5 nM of dsDNA**.**

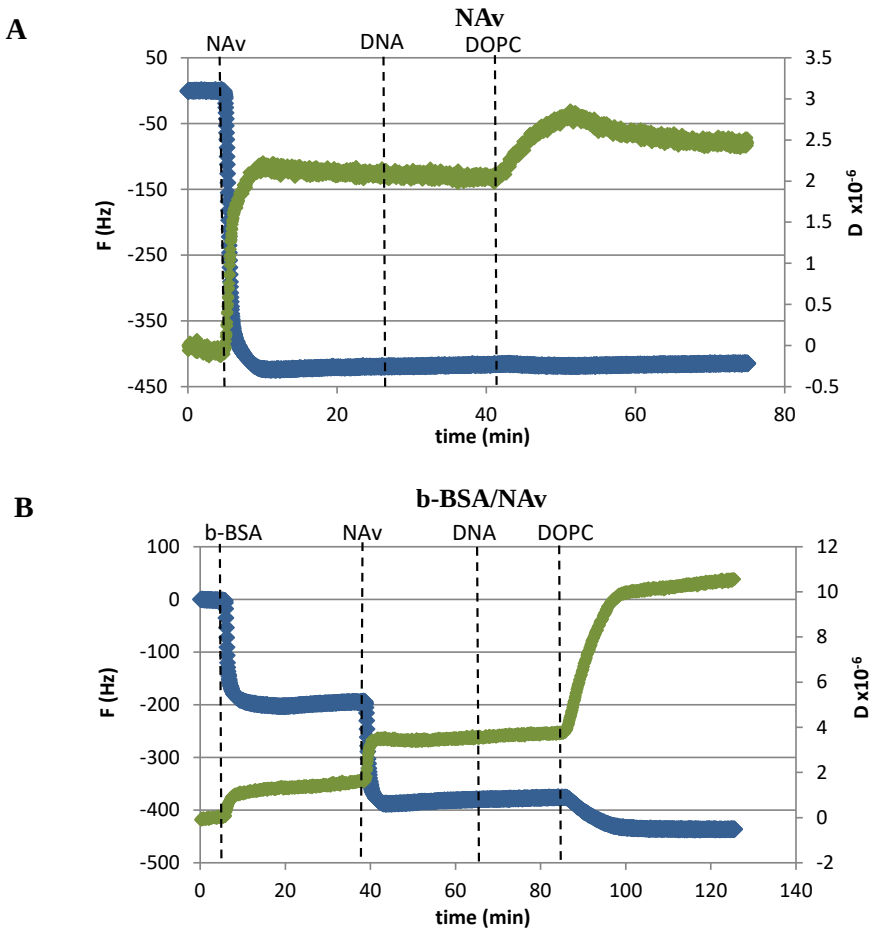

Figure 5. *Real time acoustic curves of frequency and dissipation response monitored upon the addition of 5 nM 50nt bio-DNA and 200 nm DOPC liposomes on (A) NAv or (B) b-BSA/[NAv] pre-coated surface.*

Figure 6A shows the changes in dissipation during liposomes binding as a function of the DNA concentration for the two NAv surfaces. Interestingly, while the response on the b-BSA is higher for [DNA]> 0.5 nM, the detection limit in both cases is the same and equal to 50 pM. The difference in the dissipation response is possibly attributed to the presence of the biotin linker in the BSA which may lead to the formation of a floating NAv layer above the BSA. Regarding frequency response, was proved to be less sensitive than the dissipation for [DNA]≤ 0.5 nM (Figure 6B).

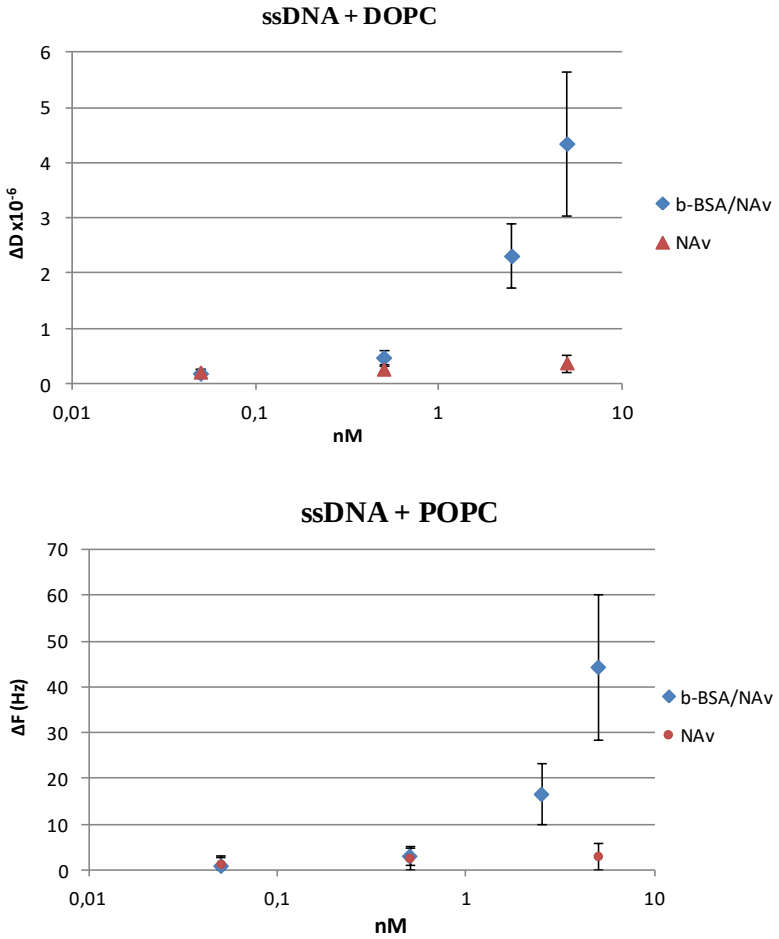

Figure 6. *Comparison of (A) dissipation and (B) frequency changes observed upon addition of 200nm DOPC liposomes on various concentrations of 50nt ssDNA pre-absorbed on NAv and b-BSA/NAv coated surfaces. Control experiments, i.e. protein coated surface followed by the addition of liposomes without DNA, gave 0.15* ± 0.08 x10^{-6} and *0.11* ± 0.01 x10^{-6} ΔD for NAv and b-BSA/NAv, *respectively. Both control values were lower than the ΔD values (0.214 ± 0.05 x10^{-6} and 0.19 ± 0.07 x10^{-6}) obtained in each case from the 50 pM detections.*

3. Investigation of the non-specific binding of the liposomes to Au surface

Finally, the specificity of the two surface chemistries was tested. For the experiments POPC liposomes instead of DOPC were used; these two liposomes had similar physicochemical characteristics and as was referred, POPC liposomes were employed for the rest experiments in the following chapters. POPC liposomes were added on NAv and b-BSA/NAv modified sensors without the addition of DNA. As presented in Figure 7A, the non-specific binding of the POPC liposomes was lower in the case of the b-BSA/NAv functionalized sensors. Even though the above control experiments on the two surfaces gave a similar and rather small non-specific response, i.e. ΔD= 0.15 ± 0.08 x10^{-6} and 0.11 ± 0.01 x10^{-6} for NAv and b-BSA/NAv respectively (Fig. 6), NAv gives a good specificity only when the gold sensors are new; otherwise non-specific interaction of liposomes on NAv-modified sensor could reach a ΔD value of 0.5 x 10^{-6}.

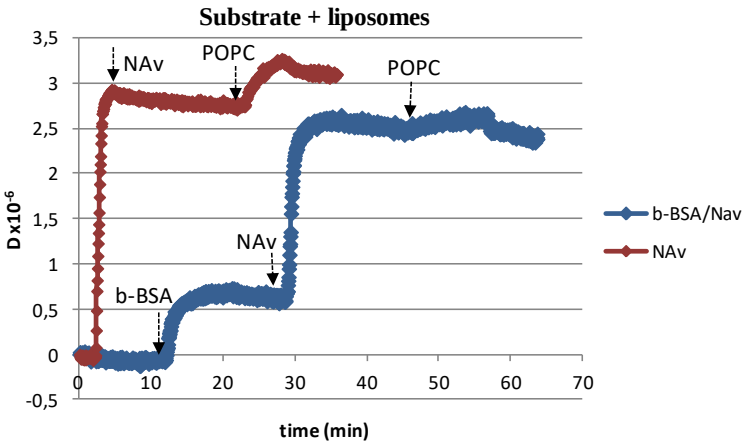

Figure 7. *Investigation of the non-specific binding of the liposmes on sensor surface. Addition of 200 nm POPC liposomes on NAv and b-BSA/NAv coated senor.*

Moreover, since the final goal is the development of a surface for the analysis of non-purified amplified products the substrates were tested upon the addition of a Ligase Chain Reaction mixture (without DNA target). As shown in figure 8, b-BSA/NAv substrate was proved to be more stable and reproducible, upon the addition of the amplification reaction; the addition of the reaction on the NAv-coated surface resulted in partial remove of the NAv, thus enhancing the non-specific interaction of the liposomes with the surface (Fig. 8B).

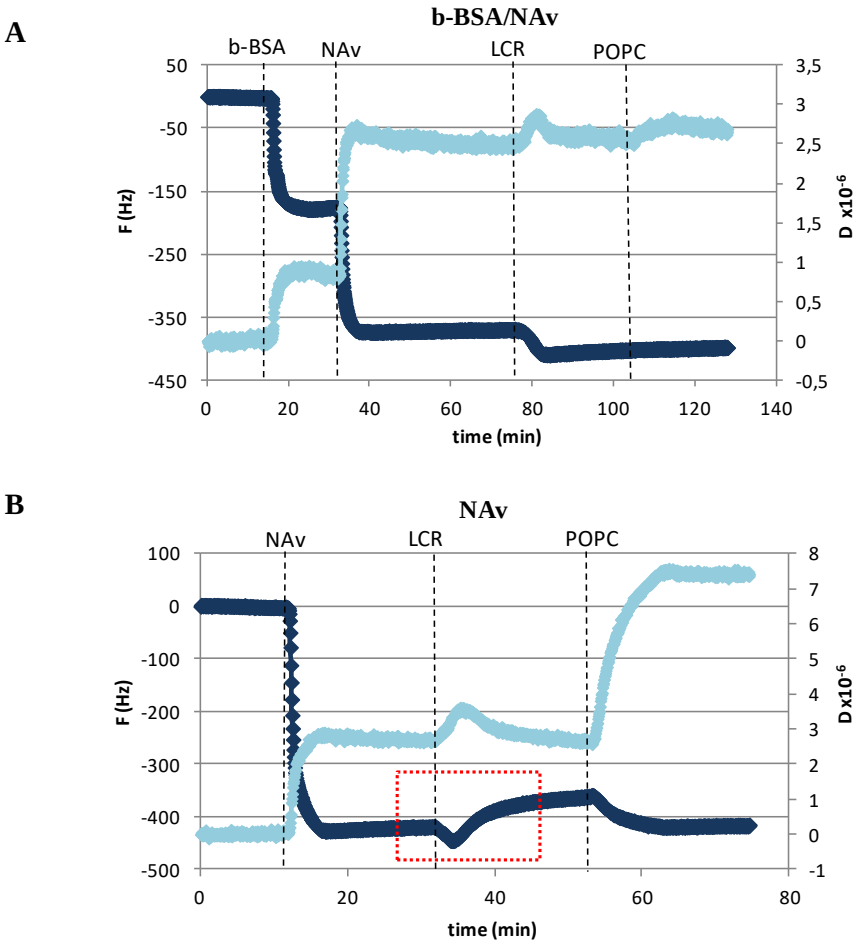

Figure 8. *Investigation of the non-specific binding of the liposomes on sensor surface upon LCR addition on (A) b-BSA/NAv and (B) NAv modified surface. The wash away of the Nav (red box) following addition of the amplification reaction caused non-specific binding of liposomes.*

Conclusions

Concluding, two NAv-modified substrates were evaluated i.e., NAv directly on gold and NAv bound on pre-absorbed b-BSA. The surfaces were tested for their ability to immobilize a 50 nt bio-ssDNA as well as for their specificity. Regarding the 50 nt DNA, while b-BSA/NAv gave higher ΔD values for DNA concentrations ≥ 0.5 nM (~ 168 % for the 5 nM), both surfaces exhibited the same limit of detection as low as 50 pM. Nevertheless, b-BSA/NAv was characterized by significantly better reproducibility and stability.

Moreover, in terms of specificity, b-BSA/NAv coated sensors resulted in lower non-specific values upon liposome addition. Finally, since the protocol was developed for the analysis of molecular amplification assays, the stability of the attached protein layer was checked upon the addition of an LCR mix; when NAv was absorbed directly on Au, the loading of the mix caused NAv to washed off. Overall, NAv layer was proved to be more stable upon b-BSA and suitable for the subsequent biological applications.

PART 2:

VALIDATION OF THE HFF-QCM PLATFORM AND BIOCHIP ARRAY TO BIOSENSING ASSAYS

Introduction

As already stated, High Fundamental Frequency (HFF) QCM sensors have been shown to exhibit better sensitivity by approximately two orders of magnitude compared to the conventional sensors operating at the low MHz range (≤ 10 MHz)[31–33]. This improvement is attributed to the fact that the frequency shift obtained by mass addition scales with the square of the resonance frequency according to the Sauerbrey relationship[28]. Here, the performance of a new High Fundamental Frequency QCMD (HFF-QCMD) device developed by *AWSensors* (AWS, S.L. Paterna, Spain) will be investigated. The device consists of 24 miniaturized QCM resonators integrated in an array configuration in the same quartz substrate, based on Monolithic QCM (MQCM) technology. The array was fabricated by a combination of photolithography and wet etching processes which have been reported to produce high quality, cost-effective and robust inverted MESA-based HFF-QCM resonators[120] (more information about the HFF-QCM sensors is provided in pages 17 - 18).

Basic advantages of the array, apart from the theoretical improved sensitivity, include the multiple sample analysis, the lower cost per sensor unit and the less sample/reagent consumption, hence, decreasing the cost of the assay, too. Moreover, due to the overall design of the acoustic chamber (flow cell + array), a faster sensing response and a reduced time of the overall assay are a given. Finally, since the physical and electrical properties of the array have been already characterized, here the array will be tested in liquid phase for various biosensing assays including protein detection, DNA detection, and DNA detection through liposomes. Part of the following results currently are under submission by Naoumi N. et al.[121].

Materials & Methods

Materials	
QCM 24-sensors array	Advanced Wave Sensors (AWS) S.L., Paterna, Spain
Phosphate buffer Saline (PBS) tablet	Sigma-Aldrich, Miss., US
NeutrAvidiv Protein	Thermo Fischer Scientific, Mass., USA
BSA lyophilized powder, crystallized, ≥98.0% (GE)	Sigma-Aldrich, Miss., US
Biotin-$(AC_5)_2$-Sulfo-Osu	Dojindo, Japan
Microcon-30kDa Centrifugal Filter Unit with Ultracel-30 membrane	Merck KGaA, Darmstadt, Germany
1-palmitoyl-2-oleoyl-glycero-3-phosphocholine (POPC)	Avanti Polar Lipids Inc., Alabaster, AL, USA
Whatman Nuclepore polycarbonate	Whatman plc, UK

hydrophilic membranes 0.2 µm	
NucleoSpin® Gel and PCR Clean-up	Macherey Nagel, GmbH & Co. KG
KAPA2G Fast HotStart ReadyMix	Kapa Biosystems, Inc., US
Human Genomic DNA 100 ng/µL	
High-performance liquid chromatography (HPLC)-grade oligonucleotides	Metabion International AG, Germany

DNA Sequences (5' -> 3')	
F50chol3 ssDNA	**biotin-**AATTCAGAGAGGAGGAGAGAGCGGTGCGGTAGGAG AGAGAGAGGAGGATC**-cholesterol**
R50	GATCCTCCTCTCTCTCTCCTACCGCACCGCTCTCTCCTCCTCTCTGAATT
F75chol	**biotin-**CCACCAAACGTTTCGGCGAGAAGCAGCCCATTATCGCCGGCA TGGCGGCCGACGCGCTGGGCTACGTCTTGCTGG-**cholesterol**
R75	CCAGCAAGACGTAGCCCAGCGCGTCGGCCGCCATGCCGGCGATAATGGCCTG CTTCTCGCCGAAACGTTTGGTGG
F21chol	**biotin-**TAGAGCTCCCTTCAATCCAAA**-cholesterol**
R21	TTTGGATTGAAGGGTGCTCTA
b-157Fw	**biotin**-TCCTGATGGGTTGTGTTTGG
157Rv	TGGTGGGGTGAGATTTTTGTC

Quartz crystal microbalance (QCM) with dissipation monitoring acoustic devices. For the experiments two QCM devices were used; the newly developed High Fundamental Frequency – QCM (HFF) (AWS S.L., Paterna, Spain) operating at 150 MHz and the commercial QSense Analyzer E4 instrument (QSense, Sweden). The HFF-QCM platform monitored a HFF-QCM array (AWS, S.L. Paterna, Spain) mounted on a custom Printed Circuit Board (PCB). Cleaning of the PCB and array included treatment with Hellmanex 2% for 30 min, rinsing with mili-Q water and 70 % EtOH and drying under N_2. Then, the array was cleaned by 30 min UV/Ozone (Ossila Ltd, Sheffield) followed by treatment with absolute EtOH for 30 min. The flow cell employed a PMMA gasket and a PDMS cell (AWS, S.L. Paterna, Spain), both cleaned with Hellmanex 2 % for 30 min, incubated with mili-Q water in a sonicator for 15 min and dried at 65 ^{o}C. The flow-cell was connected to a syringe pump of 50 µL or 250 µL installed in the platform. About the QSense Analyzer, the operating frequency for the results reported here is the 35 MHz (7 th overtone) (ΔF was not normalized by the overtone number). Before use, the Au-coated 5 MHz sensors were cleaned with Hellmanex 2 % for 15 min, rinsed with mili-Q water, dried under N2 and treated for 30 min with UV/Ozone (Ossila Ltd, Sheffield). Acoustic experiments were carried out under a continuous flow of 20 µL/min for the AWS device and at 50 µL/min for the QSense at 25 ^{o}C. All samples were diluted in PBS pH=7.4, which was the running buffer. Following each sample addition, buffer rinsing was taken place and then frequency and dissipation changes were obtained.

Acoustic detection of b-BSA and NAv. Protein samples were diluted in PBS pH=7.4. Neutravidin at a concentration of 0.2 mg/mL or 0.2 mg/mL of biotinylated-BSA (b-BSA) followed by the addition of 0.05 mg/mL NAv were applied on the device surface. In all cases the working volumes were V_{150MHz}=60 µL and V_{35MHz}=200 µL. Following each addition, buffer

rinsing was taken place and then frequency and dissipation changes (ΔF and ΔD respectively) were obtained. b-BSA was prepared after incubation of BSA lyophilized powder with biotin-$(AC_5)_2$-Sulfo-Osu linker in PBS, in a molar ratio of 1:10, for 1 h and 30 min at RT; after incubation, BSA was purified using the Microcon-30kDa Centrifugal Filter Unit with Ultracel-30 membrane following manufacturer instructions.

Preparation of dsDNA targets. To produce the 21, 50 and 75 bp dsDNA fragments, the biotin and cholesterol modified forward strand (F50chol3, F75chol, F21chol) was mixed with the complementary strand (R50, R75, R21 respectively) in a molar ratio of 10:1 x 10μM:1μM and total volume of 100μL PBS buffer. The solution was subjected to denaturation at 95 ^oC for 5 min followed by hybridization at room temperature for 1 h. For the production of the biotinylated-157 bp a 20 μL PCR consisted of 10 pmol biotin-157Fw (b-257Fw) primer, 15 pmol 157Rv primer, 10 μL of KAPA2G Fast HotStart ReadyMix and 10 ng Human Genomic DNA (template) was subjected to 30 cycles of 10 sec at 95 ^oC followed by 10 sec at 62.5 ^oC and 10 sec at 72 ^oC. An initial denaturation step for 5 min at 95 ^oC and final extension step at 72 ^oC for 1 min were included in the amplification protocol. Following PCR, PCR clean-up was performed according to the manufacturer's (NucleoSpin® Gel and PCR Clean-up - Macherey Nagel) instructions. Stock solutions of dsDNA fragments were stored at -20 ^oC and used within 1 month.

Liposome preparation. Lyophilized 1-palmitoyl-2-oleoyl-glycero-3-phosphocholine (POPC) lipids were dissolved in chloroform at final concentration of 10 mg/mL. 100 – 200 μL of the 10 mg/mL lipids were added in round bottom glass flask and dried homogenously under N_2 flow. The lipid film was then left for 30 min under N_2 gas followed by resuspension in PBS at a final concentration of 2 mg/mL by gentle vortexing. The resulting suspension was passed through polycarbonate membranes (Whatman NucleoporeTM) with a nominal pore diameter of 200 nm, using the Avanti Mini-Extruder. Stock solutions were stored at 4 °C for up to 6 days.

Acoustic detection of dsDNA. Various concentrations of dsDNA diluted in PBS pH=7.4 (83 nM to 500 nM for the 21 bp, 50 bp and 75 bp and 15 nM to 42 nM for the 157 bp) were loaded in NAv coated sensors and subjected to acoustic detection at 150 MHz. For the 35 MHz sensor, concentrations of 25 nM – 100 nM and 2.25 nM – 19.56 nM for the 50 bp and 157 bp DNA targets, respectively were used. In all cases the working volumes were V_{150MHz}=60 μL and V_{35MHz}=200 μL, unless otherwise stated.

Acoustic detection of dsDNA through liposomes at 150 MHz. dsDNA fragments of 21 bp and 50 bp were diluted in PBS buffer at 83 nM and 500 nM and loaded on the NAv coated 150 MHz array followed by the addition of 100 μL x 0.2 mg/mL solution of 200 nm POPC liposomes prepared through extrusion as described before.

Results & Discussion

1. Description of the High Fundamental Frequency QCM (HFF-QCM) acoustic array biochip for multiple samples analysis

The HFF resonator array used in this work includes 24 miniaturized crystals integrated monolithically to a single substrate, in a layout of six rows with four resonators/row (Fig. 9A). This array chip is ideal for high-throughput analysis[122] and low-volume biosensing applications. Because the array is very small and fragile for direct handling during experiments, it was mounted on a PCB (Fig. 9B); the latter also provides mechanical, electrical and thermal interface between the acoustic wave device and the recording instrument. A gasket and a cell have been developed and integrated with the PCB + array assembly (Fig. 9C and D). The flow cell device seals the microsensors individually, so that it is possible to flow liquid in the desired direction over the sensor top surface without affecting the array electrical connections placed on the bottom surface or interfere with the different lines of sensors. During experimental conditions the liquid moves sequentially on each one of the four sensors in the same row (Fig. 2E), running from the input to output. Each crystal has 0.2581 mm^2 active surface and holds 1.5 µL sample-volume above the sensor. For the sake of comparison, the corresponding values for the 5 MHz sensor are 19.635 mm^2 and 40 µL, respectively. More information on the array can be found in Fernandez R. et al., 2020[120].

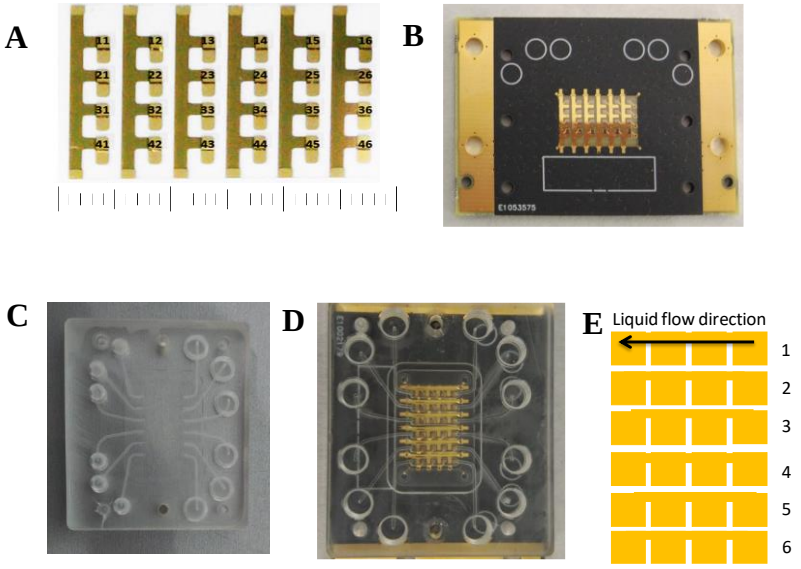

Figure 9. *(A) Acoustic array consisting of 24 HFF-QCM sensors arranged in 6 lines of 4 sensors per line; (B) Photograph of the array mounted on a custom Printed Circuit Board; (C) The PDMS flow cell alone and (D) after integration with the array/PCB board. (E) Schematic representation of the liquid flow along the 6 lines and over the 4 sensors per line.*

2. Performance evaluation of the HFF biochip array

While the electrical properties of the acoustic array have been extensively investigated[120], its performance during biosensing experiments has not been analyzed in depth and reported yet. For this reason, we firstly studied the device response to the absorption of proteins as

well as the detection of dsDNA through the subsequent binding of liposomes. Specifically, the physisorption of 2 proteins directly on gold, i.e., NAv and b-BSA, and the binding of NAv on a pre-adsorbed layer of b-BSA, are monitored. The observed acoustic signal changes were compared to results obtained with the standard 35 MHz QCM device (5 MHz sensor, 7th overtone). Due to the specific characteristics of the two systems in terms of resonator size and fluidics, the added amount of each protein slightly differed (Table 1); however, in each case surface saturation was achieved. After each addition step, buffer rinsing was performed and the ΔF and DΔ changes were measured at equilibrium. Figure 10 shows that the relative signal responses of all three proteins upon absorption/binding to the surface exhibits the same trend.

Table 1. *Amounts and concentrations of NAv and b-BSA proteins added to each sensor surface.*

QCM Sensor	NAv	NAv on b-BSA	b-BSA
150 MHz	60 µL x 0.2 mg/mL	60 µL x 0.05 mg/mL	60 µL x 0.2 mg/mL
5 MHz	200 µL x 0.2 mg/mL	200 µL x 0.05 mg/mL	250 µL x 0.2 mg/mL

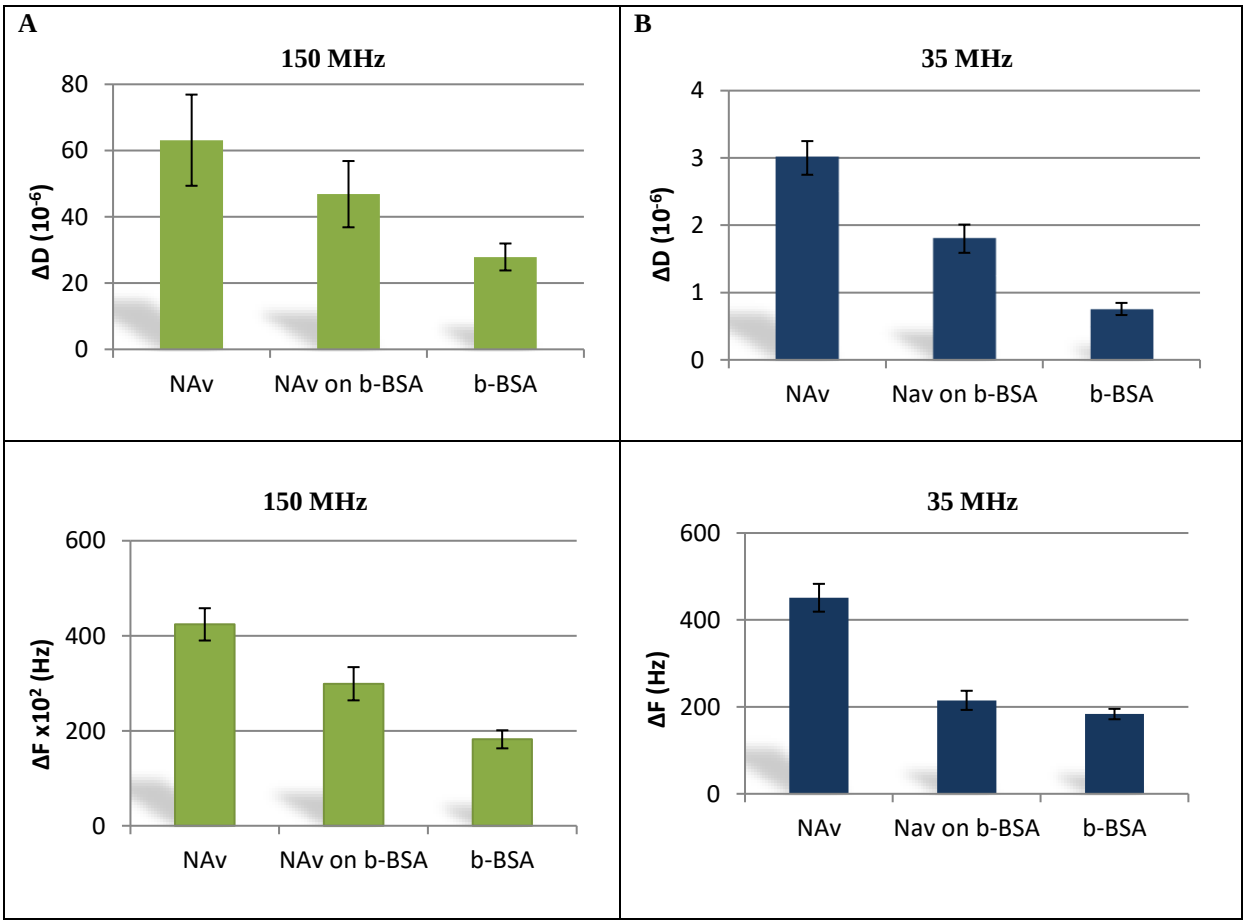

Figure 10. *(A) Comparison of ΔF and ΔD average values of NAv and b-BSA absorption on the 150 MHz HFF-QCM sensors as well as NAv binding to pre-absorbed b-BSA; (B) The same as in (A) on the 35 MHz QCM sensor.*

As a follow-up experiment, we investigated the immobilization of various concentrations of biotinylated double-strand (ds) DNA of 50 bp and 157 bp on NAv. Table 2 summarizes the Limit of detection (LOD) regarding the applied concentrations (nM) and the DNA amount (pmol) of the two DNAs on the 35 MHz and 150 MHz sensors. Concerning the total amount

of DNA in pmol, the LOD was the same for both sensors and equal to 5 pmol for the 50 bp DNA and 0.45 pmol for the 157 bp DNA. In terms of concentration the 150 MHz was proved to be less sensitive compared to the 35 MHz sensor (83 nM Vs 25 nM for the 50 bp and 15 nM Vs 2.25 nM for the 157 bp, respectively). To better understand the above when the 0.45 pmol of the 157 bp were diluted in 60 µL (7.5 nM) and injected into the 150 MHz sensor no signal response was measured. However, when the same DNA amount i.e., 0.45 pmol, was diluted in the less total volume of 30 µL (15 nM), a high acoustic response was obtained (Fig. 11). The difference in the sensitivity may reflect differences in the kinetics of the two systems due to the different flow cell assembly.

Table 2. *LOD obtained from the immobilization of b-50 bp and b-157 bp DNA on 35 MHz and 150 MHz Nav-coated sensors.*

Frequency (MHz)	35		150	
DNA (bp)	pmols	nM	pmols	nM
50	5	25	5	83
157	0.45	2.25	0.45	15

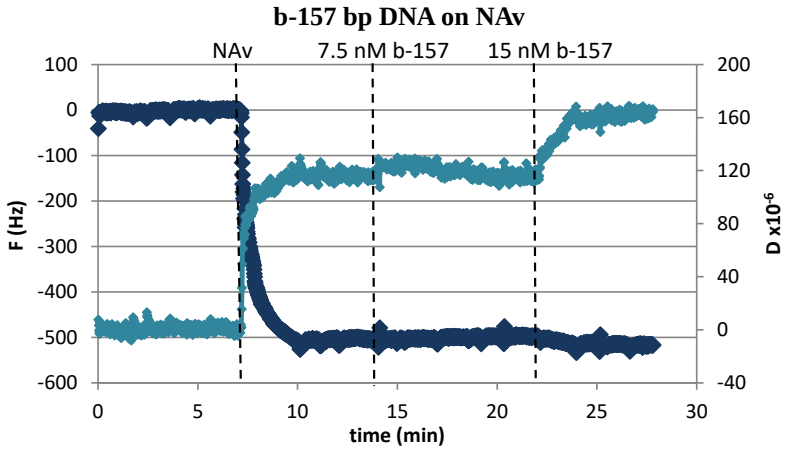

Figure 11. *Binding of b-157 bp DNA on NAv-coated sensors at 150 MHz. As shown in the graph, 7.5 nM DNA (0.45 pmol in 60 µL) were loaded on NAv, followed by buffer, where the DNA was washed off. Then 15 nM DNA (0.45 pmol in 30 µL) were loaded, causing a high change in the ΔF and ΔD of the acoustic signal.*

Figure 12 shows that the 24-array biochip essentially operates in the same fashion as the single QCM device; loading of various lengths of biotinylated ds DNA on NAv follows a linear relationship between the acoustic ratio (ΔD/ΔF) versus the DNA length[38,43].

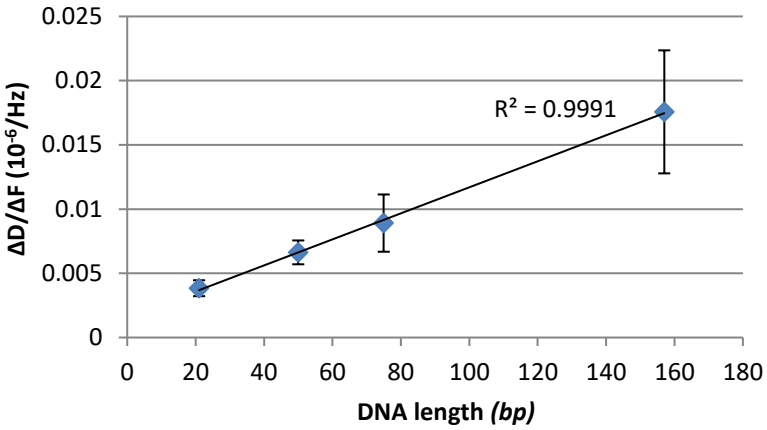

Figure 12. *Acoustic ratio expressed as ΔD/ΔF as a function of the length of b-DNA, attached on a NAv modified surface.*

Finally, since we aimed to develop a protocol for the detection of dsDNA in crude samples using a step of amplification through liposomes, we further monitored the binding of 200 nm diameter POPC liposomes on dsDNA in buffer at 150 MHz. We tested two concentrations (500 nM and 83 nM) of 2 different lengths of DNA i.e., 21 bp and 50 bp, carrying a biotin at their 5' end for immobilization to the surface and a cholesterol at their 3' end for the binding of liposomes (see Fig. 1A, page 32). ΔF and ΔD, measured for both the DNA and POPC binding steps, are presented in Table 3. For the same concentration, the binding of the two DNAs (21 and 50 bp) gives a similar frequency change (6.5±0.9 and 5.7±1.3 x10^3 Hz corresponding to a larger dissipation signal change in the case of the longer DNA. The subsequent binding of 200 nm liposomes also results in higher dissipation in the case of the longer DNA anchor. The above results are in good agreement with previous findings[111]. It is noted that there is a rather large variant (~15%) in both acoustic signals; the source of the high error bars is probably related to differences in surface coverage or in the acoustic response of each individual resonator within the array.

Table 3. *Table of the recorded ΔD and ΔF values during the binding of two concentrations of DNA followed by the addition of liposomes (200 nm); the DNA is double labelled, with a biotin at the 5' end for surface attachment and a cholesterol at the 3' end for liposomes binding.*

DNA (nM)	DNA (bp)	ΔD_{DNA} (10^{-6})	ΔF_{DNA} (10^{3}) (Hz)	ΔD_{POPC} (10^{-6})	ΔF_{POPC} (10^{3}) (Hz)
83	21	23.5±2.9	6.5±0.9	324±53.0	15.4±4.3
	50	39.4±8.6	5.7±1.3	346±70.0	8.9±0.7
500	21	83.3±4.8	21.2±1.9	375±31.6	18.0±3.1
	50	147±34.0	21.4±1.8	439±39.0	15.0±1.8

Conclusions

In this work, the application of a novel HFF biochip array is reported. The array operates at 150 MHz and allows the analysis of up to 6 samples providing up to 24 measurements (4 measurements/sample).

The application of the new array to common biological assays was tested; standard proteins, i.e., b-BSA and NAv, dsDNA of various lengths, and liposomes on dsDNA were successfully detected. The results were compared with those obtained from the conventional QCM device and 5 MHz gold sensors operating at 35 MHz. In all cases, results were in good agreement. However, the sensitivity of the new array was estimated to be slightly lower for dsDNA detection compared to the sensitivity of the 35 MHz system. Even though these results were not expected according to the theory about the HFF sensors, they were in agreement with results reported from a member of the manufacturer's lab.

Overall, the successful detection of proteins, dsDNA and liposomes with the 150 MHz acoustic array demonstrate the suitability of the new system for subsequent application on molecular biology detection assays. Furthermore, the need for lower samples volumes (e.g., 60 vs 200 μL), the faster analysis time, and the ability for multi-sample analysis, make the 24-acoustic array a promising diagnostic tool.

Chapter 3

Detection of the *BRAF* V600E point mutation in ctDNA utilizing a QCMD device combined with Ligase Chain Reaction

Introduction

Ligase-based amplification or detection techniques have been extensively utilized for the discrimination of single nucleotide polymorphisms and point mutations. They are considered as a promising and powerful tool for genotyping assays since they can provide high specificity, sensitivity as well as multiplexing ability in a cost-effective and simple way[123]. In these techniques, a DNA ligase is employed to favor the amplification or detection of one target versus the target which carries a mismatch. Ligation-based amplification techniques can be roughly divided into two main categories: those that use a ligase for the mismatch discrimination and a polymerase with strong strand displacement activity for the amplification and the detection of the "ligated" target like the Rolling cycle amplification and the Strand Displacement Amplification reactions. The other category includes methods mainly based on the ligation for the detection such as the Oligonucleotide Detection Assay (OLA), the Ligase Detection Reaction (LDR), the Ligase Chain Reaction (LCR) and LCR variants (Gap-LCR, Nested-LCR). OLA reaction is based on the covalent joining of two adjacent oligonucleotides by a DNA ligase when they are hybridized with full complementarity to the DNA target usually combined with a PCR pre-amplification step[124]. On the other hand, the ligase detection reaction (LDR) achieves linear target amplification by repeated ligation of one pair of complementary to the target probes through a cycling protocol of denaturation followed by annealing and ligation. LDR is also known as linear LCR. Finally, LCR or exponential LCR leads to target amplification through a cycling protocol as well, however in this case two pair of probes are added to the reaction leading to exponential amplification[123].

LCR principle

LCR is a DNA template-dependent technique performed by a thermostable DNA ligase lacking blunt-end ligation activity in the presence of 2 pairs of oligonucleotide probes, each pair complementary to the corresponding strand of the target. Upon hybridization of the probes with the target, the ligase connects the two adjacent oligos only when perfect complementation occurs. This procedure requires the cycling of two temperatures for denaturation and annealing/ligation and lead to the formation of dsDNA products. The formed ligated products serve as templates in subsequent cycles as in PCR leading to exponential amplification. In the presence of a single base mismatch at the junction site probes will not hybridize perfectly and hence no further ligation and amplification will occur (Fig. 1)[123]. LCR has been reported to hold better specificity than the typical PCR[125]. Moreover, in contrast with PCR, LCR does not introduce any uncontrolled amplification bias, i.e. the preferential amplification of some DNA templates over the others within the same reaction, and errors[126–128]. Nevertheless, despite the specificity reported for LCR, target-independent ligation especially in the absence of template DNA remains one of the main disadvantages of LCR[123]. LCR has been broadly applied to the detection of pathogens[125,129–

[135], genetic diseases[123,136,137] and on a smaller scale for point mutations[138–140]. Moreover, commercialized FDA-approved products based on LCR have also appeared[125,129,132,133].

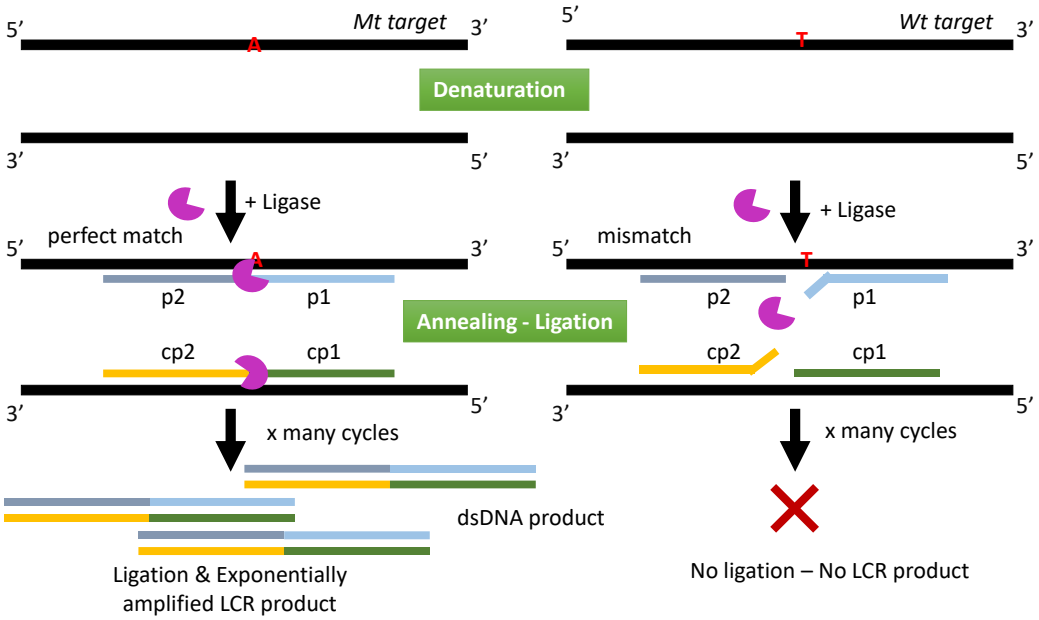

Figure 1. *Exponential Ligase Chain Reaction (LCR): DNA Ligase connects the two adjacent oligos only when they are fully complementary to the target (Mt target).* The formed ligated products serve as templates in subsequent cycles as in PCR. *Performing many cycles of denaturation and annealing/ligation, the target will be exponentially amplified due to the use of two pair of probes. Contrary, if there is a mismatch in the ligation site (Wt target) ligation will not occur and therefore neither amplification.*

As stated above, LCR can also be performed using one pair of complementary to the target probes, e.g. either the p1/p2 probes or the cp1/cp2 probes illustrated in Figure 1. However, this approach will lead to linear amplification.

Ligase-based detection combined with biosensors

DNA Ligases have been commonly applied for the detection of point mutations in acoustic as well as electrochemical biosensing applications. In the vast majority of these assays, a DNA target hybridize to a surface-immobilized capture probe followed by the loading of a 2nd probe which is hybridized to the captured target. DNA ligase is then loaded and connects the two adjacent oligos, i.e., the capture probe and the second probe using the target DNA as template. Ligation takes place only when perfect complementation occurs. Following ligation, the non-ligated DNA are dehybridized and washed away through thermal[82,141,142] or chemical treatment[81,83]. To achieve efficient detection often a signal amplification step is included in the biosensing assay, through the binding of gold or other nanoparticles[83], enzymatic catalysis[81,82,142] and molecular beacons[141]. Although there are numerous of the aforementioned techniques, to the best of our knowledge, publications reporting biosensing detection of LCR are minimal, and all of them regarded electrochemical sensors[137,143,144].

A modified Ligase Chain Reaction combined with acoustic detection

Here, we present an alternative LCR assay couple for the first time with an acoustic detection approach for the analysis of point mutations presented in circulating tumor DNA. In this approach, firstly LCR is carried out using oligonucleotide probes modified with biotin and cholesterol, hence producing double-labelled dsDNA products modified at the 5' end with a biotin and at the 3' end with cholesterol (Fig. 2). These biotinylated LCR products are then detected with the acoustic approach presented in Chapter 2/Figure 1 suggested procedure; biotinylated-dsDNA will be bound directly to a b-BSA + Neutravidin (NAv) coated sensor through the biotin-NAv interaction followed by the subsequent capturing of 200 nm POPC liposomes via the cholesterol. Advantages of our method compared to others employing a surface ligation step on sensor surface, is the direct immobilization of the target-derived products on the substrate, obviating a difficult to control hybridization step, thermal or chemical release of the un-captured target and problems with the reassociation of the DNA target. Also, we take advantage of the exponential amplification via the LCR which can help us achieve a significantly improved detection limit combined with excellent specificity. Overall, our assay consists of two "amplification" steps; the first is the enzymatic enrichment of the mt target through LCR and the 2nd is the signal enhancement through nanoentities, i.e., liposomes.

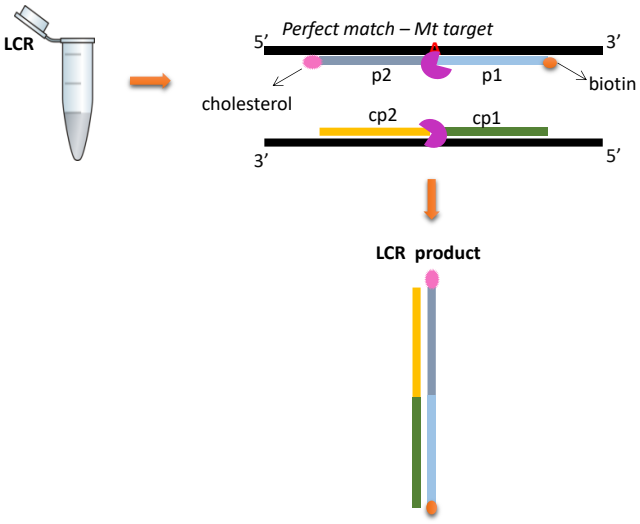

Figure 2. *LCR is carried out using oligonucleotide probes modified in their one end with biotin or cholesterol, producing dsDNA products modified at the 5' end with a biotin and at the 3' end with cholesterol. This will favor the direct immobilization on acoustic sensor surface.*

For the development of the LCR protocol we chose the *BRAF* V600E point mutation. The clinical value of *BRAF* identification status as a diagnostic, prognostic and treatment selection marker has already been described in Chapter 1/pages 30-31.

PART 1:

INVESTIGATING THE LIGATION PERFORMANCE OF AMP-LIGASE USING A SIMPLIFIED SSDNA TARGET

Introduction

As previously described, during LCR, modified with biotin and cholesterol probes will be used, therefore creating LCR products carrying a biotin and a cholesterol to each end of the produced DNA. These modifications are required for the direct immobilization of the LCR products on the NAv-modified sensor surface and the capturing of liposomes, respectively. However, the presence of biotin and cholesterol could affect or even completely inhibit the reaction. To this end, here the ligation performance of the AmpLigase Thermostable DNA ligase was investigated in the presence of modified and un-modified probes. For the experiments, we used a simplified strategy, i.e., ssDNA as a target and linear LCR amplification (otherwise Ligase Detection Reaction – LDR).

Materials & Methods

Materials	
High-performance liquid chromatography (HPLC)-grade oligonucleotides	Metabion International AG, Germany
Ampligase® DNA Ligase (5 U/µL)	Epicentre (Lucigen), Middleton, US
Ampligase® 10X DNA Ligase Reaction Buffer	Epicentre (Lucigen), Middleton, US
BSA, Molecular Biology Grade 20 mg/mL	New England Biolabs, Mass., US
T4 Polynucleotide Kinase (PNK) (3' phosphatase minus) Enzyme & Buffer 10x	New England Biolabs, Mass., US
Adenosine 5'-Triphosphate (ATP) 10 mM	New England Biolabs, Mass., US
GelRed® Nucleic Acid Gel Stain	Biotium, California, US

DNA Sequences of probes (5' -> 3')	
miR21-1-chol	CTGATAAGCTAACTGCATCGTGGAG-**cholesterol**
miR21-2-biotin	**biotin**-AGATCCCGCTAAGCTCAACATCAG**T**
miR21-1c	CTCCACGATGCAGTTAGCTTATCAG
miR21-2c	**A**CTGATGTTGAGCTTAGCGCGATCT

** The red bold nucleotide corresponds to the mismatch discrimination nucleotide.*

DNA Sequences of targets (5' -> 3')	
miR21 wt	TAGCTTATCAG**A**CTGATGTTGA
miR21 mt	TAGCTTATCAG**C**CTGATGTTGA
miR21 wt-c	TCA ACA TCA G**T**C TGA TAA GCT A

** The red bold nucleotide corresponds to the mismatch site.*

Design of the LCR probes: For the screening of the miR21 wt from the miR21 mt which differed in a single nucleotide 2 oligonucleotide pairs of probes were designed. Each probe was 25 nt in length. The 1st pair of probes –miR21-1-chol & miR21-2-biotin - was complementary to the miR21 wt and the 2nd pair –miR21-1c & miR21-2c - to the miR21 mt

targets, while the two pairs were complementary to each other, too. The last nucleotide of the 3' end of the miR21-2-biotin and the last nucleotide of the 5' end of the miR21-2c probes carried the mismatch discrimination nucleotide and complementary to miR21 wt target. Furthermore, the miR21-2-biotin was modified by a biotin at 5'end and the miR21-1-chol probe by a cholesterol at 3'end.

Linear Ligase Chain Reaction (LCR) amplification protocol. All reactions were performed in the thermal cycler peqSTAR 2X Gradient with high ramping rate (max heating and cooling rate of 5 °C/sec). LCR was carried out in 25 µL reactions containing 10 pmol of each of the two probes, 1x AmpLigase DNA Ligase Reaction buffer, 0.1 µg/µL BSA, 2.5 U of the thermostable AmpLigase DNA Ligase enzyme and the appropriate amount of target. For the miR21 wt-c target the miR21-1c & miR21-2c probes were used, while for the miR21 wt or mt targets the modified with biotin and cholesterol miR21-2-biotin & miR21-1-chol probes were added. The reaction mixture was firstly heated at 94 °C for 5 min, followed by 40 cycles of denaturation at 92 °C for 30 sec and annealing/ligation at 62.5 °C for 60 sec. LCR products were electrophoresed on 2.0 % (w/v) agarose gel stained with GelRed Nucleic Acid Gel Stain and visualized, under UV light. A no template control (NTC) was included in every run.

Phosphorylation of the LCR probes. 300 pmol of the miR21-2c or miR21-1-chol were mixed with 1x T4 PNK reaction buffer, 1 mM ATP, 0.1 µg/µL BSA and 10 U T4 PNK Enzyme in a final volume of 50 µL. The mixture was incubated at 37 °C for 60 min followed by heat inactivation at 65 °C for 20 min. The reactions were stored at -20 °C till use.

Exponential Ligase Chain Reaction (LCR) amplification protocol. All reactions were performed in the thermal cycler peqSTAR 2X Gradient with high ramping rate (max heating and cooling rate of 5 °C/sec). LCRs were carried out with both the phoshorylated and non-phosphorylated miR21-2c or miR21-1-chol probes. In each case, LCR was performed in 25 µL reactions containing 5 pmol of each probe (miR21-1-chol, miR21-2-biotin, miR21-1c and miR21-2c), 1x AmpLigase DNA Ligase Reaction buffer, 0.1 µg/µL BSA, 2.5 U of the thermostable AmpLigase DNA Ligase enzyme and the appropriate amount of miR21 wt-c target. The reaction mixture was firstly heated at 94 °C for 5 min, followed by 40 cycles of denaturation at 92 °C for 30 sec and annealing/ligation at 62.5 °C for 60 sec. LCR products were electrophoresed on 2.0 % (w/v) agarose gel stained with GelRed Nucleic Acid Gel Stain and visualized, under UV light. A no template control (NTC) was included in every run.

Results & Discussion

1. Investigation of linear LCR for the amplification of DNA targets

During this first set of experiments, the ligation performance of the thermostable DNA ligase "AmpLigase" in carrying linear LCR was investigated. To simplify the assay, as target the single strand 22 nt DNA oligo mir21-wt-c was used as well as an unmodified pair of primers (miR21-1c & miR21-2c); 1 pmol of target was successfully amplified and detected with high

specificity after 40 cycles of linear LCR (30'' denaturation at 92 °C followed by 60'' ligation step at 62.5 °C). LCR products were analyzed on 2% agarose gel (Fig. 3A). Following these results, the same protocol was tested using the LCR probes miR21-1-chol and miR21-2-biotin modified with a cholesterol at the 3' end and with a biotin at the 5' end, respectively. Probes were mixed with 1 pmol miR21 target wt or carrying a mismatch at the middle of the sequence (mt) and subjected to amplification. Only the wt target was detected indicating the good mismatch discrimination ability of the enzyme (Fig. 3B). However, the efficiency of the reaction was proved to be very low since the detection of less than 1 pmol of target was not achieved in the above conditions.

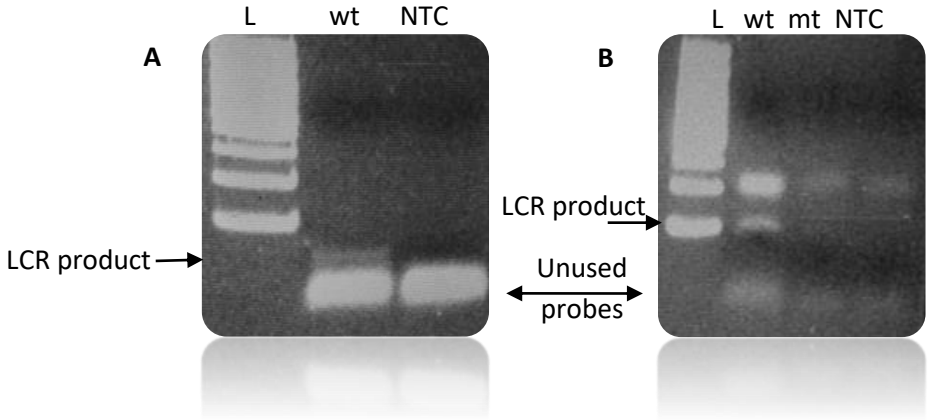

Figure 3. *Detection of 1 pmol miR21 target by 40 cycles of linear LCR. A) 1 pmol of the miR21-wt-c or no template (no template control –NTC) were mixed with 10 pmol of probes, 25 bases each (w/o biotin or cholesterol). B) 1 pmol of miR21-wt, 1 pmol of miR21-mt (carrying a mismatch in the middle of its sequence) and a NTC were mixed with 10 pmol of biotin & cholesterol probes. In both cases only the 1 pmol of wt created visualized products of 50 bases proving the high specificity of the method. A 100 bp DNA ladder (L) was used.*

2. Investigation of exponential Ligase Chain Reaction (LCR) for the amplification of DNA targets

In order to increase the efficiency of the assay, exponential LCR was applied for the detection of lower DNA amounts; 0.1 pmol of miR21-wt target or NTC were mixed with 5 pmol of each of the 4 LCR probes miR21-1c, miR21-2c, miR21-1-chol and miR21-2-biotin and subjected to 40 amplification cycles (30'' at 92 °C followed by 60'' at 62.5 °C). As shown in figure 4A, exactly the same products were visualized in the two reactions consisted of two bands at high (~1000 bp) and low (<100 bp). These bands were most probably either some by-product formation derived from the primers in a target-independent way or due to cholesterol modified probe which form aggregations counterparting the other probes. Moreover, ligated products were visualized in different molecular weight-size than the expected due to the existense of cholesterol (Fig 4B).

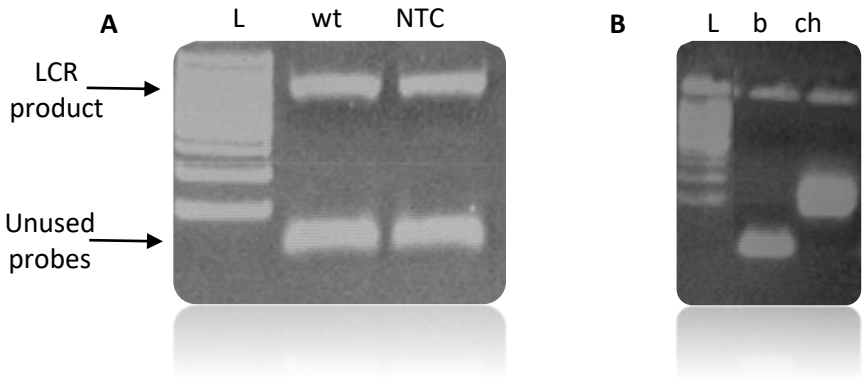

Figure 4. *A) Detection of 0.1 pmol miR21-wt target by 40 cycles exponential LCR; miR21-wt-c or no template (no template control –NTC) were mixed with 5 pmol of probes (*miR21-1c, miR21-2c, miR21-1-chol and miR21-2-biotin*), 25 bases each. B) Electrophoresis of 1 μL stock solution of miR21-1-bio (lane 2) and miR21-2-chol (lane 3) primers (100 pmol/μL). Note that the cholesterol-modified prime was visualized at higher molecular weight (~100-200 bp) despite its size (25 bases). A 100 bp DNA ladder (L) was used.*

Assuming that the phosphorylation of the probes might increase the ligation efficiency of the assay, the detection of 0.1 pmol miR21-wt target was repeated with the new conditions but the result remained the same (Fig. 5A). Finally, as a control experiment, NTC LCRs were performed with and without thermal cycling. Regarding the latter, since LCR was prepared and directly electrophoresed, theoretically negligible ligation would have occurred. As shown in Figure 5B, the same pattern was observed between the two NTCs. We therefore conclude that for the optimization of the exponential LCR un-modified pair of probes should be designed and tested. Nevertheless, since we aimed at the development of a protocol for ctDNA detection, for the rest experiments we decided to focus on the analysis of more complex targets closer to the characteristics of the ctDNA, like dsDNA of >200 bp.

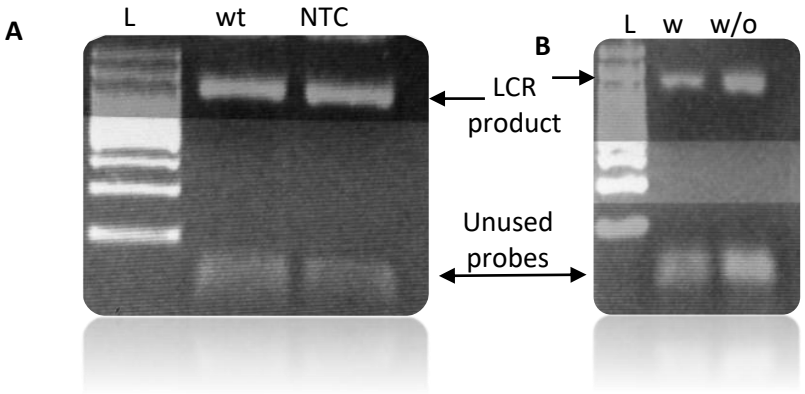

Figure 5. *A) Detection of 0.1 pmol miR21-wt target by 40 cycles exponential LCR; miR21-wt-c or no template (no template control –NTC) were mixed with 5 pmol of probes (miR21-1c, miR21-2c, miR21-1-chol & miR21-2-biotin), 25 bases each. Prior LCR miR21-2c & miR21-1-chol were phospholylated. B) NTC LCRs with (w) and without (w/o) cycling. For the LCRs the non-phosphorylated probes were added to the reaction. A 100 bp DNA ladder (L) was used.*

Conclusions

Briefly, an LCR protocol was developed for the linear amplification of the ssDNA miR21-wt target. While the assay had a good specificity amplifying only the wt and not the target with the mismatch (mt), the efficiency was very low; only 1 pmol of target (otherwise 6 x10^{11}

molecules) was successfully detected. For this reason, we tried to apply an exponential LCR for the amplification of lower DNA amounts. Subjecting the LCR mixtures to gel analysis, we concluded that the cholesterol primer aggregated affecting the electrophoresis of the rest probes and products as well as the molecular weight. Finally, we failed to come up with a specific conclusion concerning the amplification through exponential LCR and the protocol should be further optimized using an unmodified pair of probes. Moreover, no acoustic experiments were performed as we decided to continue with the development of an exponential LCR protocol on dsDNA targets carrying or not a cancer-related point mutation of interest mimicking the ctDNA.

PART 2 – 1ST APPROACH:

DEVELOPMENT OF AN LCR – ACOUSTIC ANALYSIS PROTOCOL FOR THE DETECTION OF THE *BRAF* V600E CANCEROUS MUTATION

Introduction

In this part, we focused on the development of an LCR protocol applicable to dsDNA fragments mimicking the ctDNA and carrying or not the *BRAF* V600E mutation. In the previous section, we proved that AmpLigase remained functional upon the addition of modified probes. For this reason, the initially proposed assay was employed here as well. We note that, since the purpose is the detection of point mutations in ctDNA, an extremely low detection limit of <10 copies is required.

Principle of LCR/acoustic detection assay

Schematic representation of the assay method is shown in Fig. 6. According to the illustration, LCR is performed by two pair of probes -p2/p1 & cp2/cp1- 50 nt each. The 1st pair of probes -p2/p1- is complementary to the "+" strand of the *BRAF* gene and the 2nd pair -cp1/cp2- to the "–" strand, while the two pairs are complementary to each other, too. The 3' end of the p1 and the 5' end of the cp1 probes are complementary to the T->A single nucleotide variant (SNV), corresponding to the *BRAF* V600E point mutation. Regarding the 1st pair of probes, the p1 is biotinylated at the 5' end, while the p2 probe is modified by a cholesterol at the 3' end. During LCR of several repeats, DNA fragments of 100 bp employing both a biotin and a cholesterol molecule are exponentially produced only in the case of the mt target where fully complementarity occurs. In contrast, in the case of wt target no amplified products are generated due to the presence of the mismatch on the ligation site. Ligation products are then loaded directly on a b-BSA/NAv-modified sensor, without prior purification or sample heating. b-BSA/NAv substrate was chosen based on previous results proving the stability of NAv in the presence of the LCR mix only when NAv is captured on b-BSA (chapter 2, part 1, Fig. 8). The presence of NAv allows the capturing of the biotin/cholesterol-modified amplicons in the case of the mt target and the unused biotinylated probe with its complementary strand in the case of wt. In order to achieve an ultralow detection limit of just a few copies of mt target, a second amplification step is employed where POPC liposomes of 200 nm are injected and captured by the immobilized mt products via the cholesterol-end. The later, causes high changes in the acoustic signal leading to the detection of immobilized DNA.

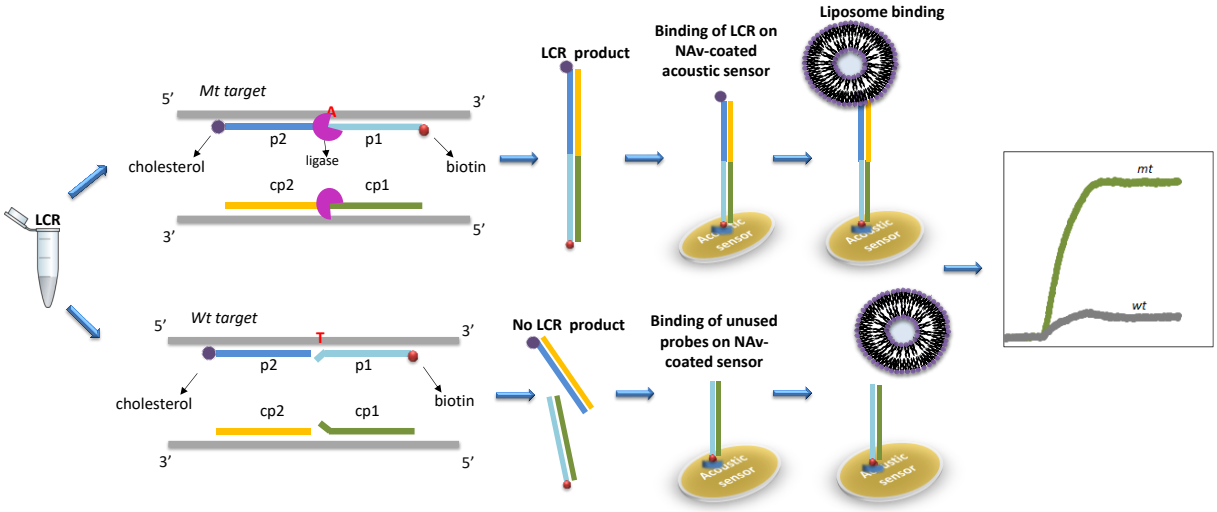

Figure 6. *Schematic representation of the concept of the acoustic assay for the detection of the BRAF V600E point-mutation. Firstly, LCR is carried out, with a modified set of probes which amplifies selectively the mt target producing ds double labeled (biotin and cholesterol) amplicons. The biotinylated mt products, are directly immobilized on the b-BSA/NAv modified sensor surface. Regarding the case of the wt target the biotinylated-probe and its complementary strand are hybridized and immobilized through the NAv as well. Finally, in the case of the mt-derived dsDNA amplicons, the cholesterol-end further triggers the binding of liposomes which produce a distinct acoustic signal change (dissipation) discriminating samples containing low copies of mt targets against those containing wt.*

Materials & Methods

Materials	
High-performance liquid chromatography (HPLC)-grade oligonucleotides	Metabion International AG, Germany
BRAF V600E reference standard, 50 %	Horizon Discovery Ltd, UK
BRAF wt reference standard	Horizon Discovery Ltd, UK
KAPA2G Fast HotStart ReadyMix	Kapa Biosystems, Inc., US
NucleoSpin® Gel and PCR Clean-up	Macherey Nagel, GmbH & Co. KG
T4 Polynucleotide Kinase (3' phosphatase minus) Enzyme & Buffer 10x	New England Biolabs, Mass., US
Adenosine 5'-Triphosphate (ATP) 10 mM	New England Biolabs, Mass., US
BSA, Molecular Biology Grade 20 mg/mL	New England Biolabs, Mass., US
Ampligase® DNA Ligase (5 U/μL)	Epicentre (Lucigen), Middleton, US
Ampligase® 10X DNA Ligase Reaction Buffer	Epicentre (Lucigen), Middleton, US
GelRed® Nucleic Acid Gel Stain	Biotium, California, US
Phosphate buffer Saline (PBS) tablet	Sigma-Aldrich, Miss., US
Avidin, NeutrAvidin™ Biotin-binding Protein	Invitrogen, US
BSA lyophilized powder, crystallized, ≥98.0% (GE)	Sigma-Aldrich, Miss., US
Biotin-$(AC_5)_2$-Sulfo-Osu	Dojindo Molecular Technologies Inc.
Microcon-30kDa Centrifugal Filter Unit with Ultracel-30 membrane	Merck KGaA, Darmstadt, Germany
1-palmitoyl-2-oleoyl-glycero-3-phosphocholine (POPC)	Avanti Polar Lipids, Inc. (Alabaster, AL, USA)
Nuclepore polycarbonate hydrophilic	Whatman plc, UK

membranes 0.2 μm	

DNA Sequences (5’ -> 3’)	
***BRAF*-gen-Fw**	ACC TAAACTCTTCATAATGCTTGC
***BRAF*-gen-Rv**	TGAGACCTTCAATGACTTTCTAGT
***BRAF*-p1**	GGATCCAGACAACTGTTCAAACTGATGGGACCCACTCCA T CGAGATTTC**T**
***BRAF*-p1-biotin**	**biotin**-GGATCCAGACAACTGTTCAAACTGATGGGACCCACT CCATCGAGATTTC**T**
***BRAF*-p2-chol**	CTGTAGCTAGACCAAAATCACCTATTTTTACTGTGAGGT CT TCATGAAGA-**cholesterol**
***BRAF*-p2**	CTGTAGCTAGACCAAAATCACCTATTTTTACTGTGAGGTCT TCATGAAGA
***BRAF*-cp1**	**A**GAAATCTCGATGGAGTGGGTCCCATCAGTTTGAACAGTT GTCTGGATCC
***BRAF*-cp2**	TCTTCATGAAGACCTCACAGTAAAAATAGGTGATTTTGGT CTAGCTACAG

** The red bold nucleotide corresponds to the mismatch discrimination nucleotide.*

PCR for the creation of the *BRAF* mt/wt dsDNA template. The ligase chain reaction described here was done exclusively on PCR products as template. The PCR products were mimicking a 277bp DNA region of the BRAF gene carrying or not the *BRAF* V600E mutation. For the reaction, 10 μL of the KAPA2G Fast HotStart ReadyMix were mixed with 10 pmol of *BRAF*-gen-Fw and 10 pmol of *BRAF*-gen-Rv primers in a total volume of 20 uL. As template, 10 ng genomic DNA BRAF V600E 50 % or *BRAF* wt reference standard were added. The reaction was subjected to 30 - 35 cycles of 10 sec at 95 ^{o}C followed by 10 sec at 57 ^{o}C and 10 sec at 72 ^{o}C. An initial denaturation step for 5 min at 95 ^{o}C and final extension step at 72 ^{o}C for 1 min were included in the amplification protocol. A no template control (NTC) was included in every run. Following amplification, PCR products were purified with the Nucleospin Gel and PCR clean-up kit according to manufacturer’s instructions. The presence of specific amplification products was checked by gel electrophoresis on 2.0 % (w/v) agarose gel stained with GelRed Nucleic Acid Gel Stain and visualized under UV light.

Design of the LCR probes: For the screening of the *BRAF* V600E point mutation versus the wt 2 oligonucleotide pairs of probes were designed. Each probe was 50 nt in length. The 1st pair of probes -*BRAF*-p1 & *BRAF*-p2- was complementary to the “+” strand of the *BRAF* gene and the 2nd pair -*BRAF*-cp1 & *BRAF*-cp2- to “–“ strand, while the two pairs were complementary to each other, too. The last nucleotide of the 3’ end of the *BRAF*-p1 and the last nucleotide of the 5’ end of the *BRAF*-cp1 probes carried the mismatch discrimination nucleotide complementary to the mt target. Furthermore, the *BRAF*-p1 probe was modified by a biotin at 5΄end (*BRA*F-p1-biotin) and the *BRAF*-p2 probe by a cholesterol at 3΄end (*BRAF*-p2-chol) favoring the subsequent immobilization of the LCR products on the sensor surface.

Phosphorylation of the LCR probes. 300 pmol of the *BRAF*-cp1 or *BRAF*-p2-chol or *BRAF*-p2 were mixed with 1x T4 PNK reaction buffer, 1 mM ATP, 0.1 μg/μL BSA and 10 U T4 PNK Enzyme in a total reaction volume of 50 μL. The mixture was incubated at 37 °C for 60 min followed by heat inactivation at 65 °C for 20 min. The reactions were stored at -20 °C till use.

Exponential LCR for the specific amplification of the *BRAF* V600E mutation. All reactions were performed in the thermal cycler peqSTAR 2X Gradient with high ramping rate (max heating and cooling rate of 5 °C/sec). LCRs were carried out with both the unmodified pair of probes *BRAF*-p1 and *BRAF*-p2 as well as their modified with biotin and cholesterol version. In each case, LCR was performed in 25 μL reactions containing 5 pmol of each probe (*BRAF*-p1, *BRAF*-p2, *BRAF*-cp1 and *BRAF*-cp2), 1x AmpLigase DNA Ligase Reaction buffer, 0.1 μg/μL BSA, 2.5 U of the thermostable AmpLigase DNA Ligase enzyme and the appropriate amount of the *BRAF* V600E 50% or *BRAF* wt PCR-derived target. The reaction was heated at 94 °C for 3 min followed by 99 cycles of denaturation at 92 °C for 5 sec and annealing/ligation at 75 °C for 10 sec, unless otherwise stated. When the unmodified probes were used, the products were analyzed by gel electrophoresis on 2.0 % (w/v) agarose gel stained with GelRed Nucleic Acid Gel Stain and visualized, under UV light. When the modified with biotin and cholesterol probes *BRAF*-p1-biotin and *BRAF*-p2-chol were used the reaction was subjected to 99 cycles of amplification protocol followed by acoustic analysis as described below. A no template control (NTC) was included in every run.

Liposome preparation. Lyophilized 1-palmitoyl-2-oleoyl-glycero-3-phosphocholine (POPC) lipids were dissolved in chloroform at final concentration of 10 mg/mL. 100 – 200 μL of the 10 mg/mL lipids were added in round bottom glass flask and dried homogenously under N_2 flow. The lipid film was then left for 30 min under N_2 gas followed by resuspension in PBS at a final concentration of 2 mg/mL by gentle vortexing. The resulting suspension was passed through polycarbonate membranes with a nominal pore diameter of 200 nm, using the Avanti Mini-Extruder. Stock solutions were stored at 4 °C for up to 6 days.

Acoustic device. The QSense Analyzer (E4 instrument) (Biolin Scientific, Sweden) was used for the simultaneous recording of frequency and dissipation changes. The QSense device was connected with the peristaltic pump IPC4 (Ismatec, Cole-Parmer GmbH, Germany) to adjust the flow rate at 50 μL/min and inject the samples into the system. Measurements were performed in continuous flow of PBS buffer pH=7.4, at 25 °C. For the experiments Au-coated 5 MHz sensors were used. The reported values of frequency and dissipation changes were obtained at 35 MHz (7^{th} overtone); ΔF was not normalized by the overtone number. Prior use, the gold-coated sensors were rinsed with mili-Q water and 70 % EtOH, dried under N_2 flow and then subjected to 3 min plasma cleaning using a Harrick plasma cleaner PDC-002 ("Hi" setting) (Harrick Plasma, NY, USA). All samples were diluted in the running buffer, PBS pH=7.4. Following each addition, buffer rinsing was taken place and then frequency and dissipation changes were obtained.

Acoustic analysis of LCR with Neutravidin (NAv) -coated sensor. Prior to the addition of the LCR products for the acoustic analysis, the gold sensor surface was functionalized with 200 µL x 0.2 mg/mL NAv. All the 25 µL of the LCR were diluted in PBS at a final volume of 200 µL and loaded at the sensor surface. Following LCR addition a suspension of 0.2 mg/mL of 200 nm POPC liposomes was added at a volume of 500 µL.

Acoustic analysis of LCR on biotinylated-BSA/NAv (b-BSA/NAv) coated sensor. Prior to the addition of the LCR products for the acoustic analysis, the gold sensor surface was modified with 250 µL x 0.2 mg/mL b-BSA followed by the addition of 200 µL x 0.2 mg/mL or 0.05 mg/mL NAv. b-BSA was prepared after incubation of BSA lyophilized powder with biotin-$(AC_5)_2$-Sulfo-Osu linker in PBS, in a molar ratio of 1:10, for 1 h and 30 min at RT; after incubation, BSA was purified using the Microcon-30kDa Centrifugal Filter Unit with Ultracel-30 membrane following manufacturer instructions. The 25 µL LCRs were diluted in PBS at a final volume of 200 µL or 125 µL; the 200 µL LCR solution was loaded on the high NAv-coated surface at the flow rate of 50µL/min, while the 125 µL LCR dilution was added on the low NAv-coated sensor at 25 µL/min. In both cases, a suspension of 500 µL x 0.2 mg/mL 200 nm POPC liposomes was added.

Results & Discussion

1. Creation of a dsDNA target mimicking the BRAF gene sequence

As stated above, the main goal is the development of an assay for the detection of the BRAF V600E point mutation, a T->A transversion, in ctDNA fragments. For this reason, to set the protocol, a dsDNA of 277 bp mimicking the BRAF sequence and carrying (mt) or not (wt) the V600E mutation was used. The 277 bp dsDNA was produced by PCR from wt or heterozygous mt genomic DNA from cell lines, thus mt always consisted of 50 % mt and 50 % wt (Fig. 7). The primers were designed in such way in order the V600E mutation to be almost in the middle of the sequence.

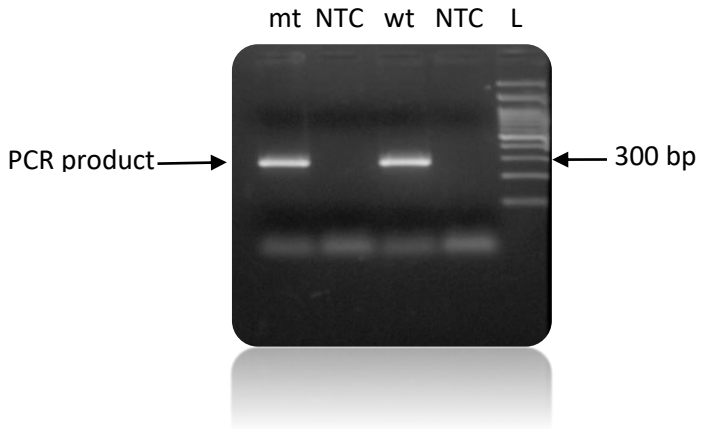

Figure 7. *PCR-derived 277 bp target carrying (mt) or not (wt) the V600E point mutation. A 100 bp DNA ladder (L) was used.*

2. Optimization of an exponential LCR protocol for the amplification of BRAF-V600E mutation

Since linear LCR was proved to have low efficiency, the exponential LCR was employed for the amplification of the *BRAF* V600E target using AmpLigase enzyme. Although, for the acoustic detection modified with biotin and cholesterol probes are required, taking into account the results reported in Chapter 3/part 1, the LCR protocol was firstly optimized using unmodified oligonucleotides. The protocol was tested for the amplification of low number of DNA molecules as well as for its specificity i.e., selective amplification of only the mt target vs the wt. The optimization of experimental parameters, including the concentration of probes and ligation temperature and time, were investigated for the proposed LCR assay. Finally, 10 ng of mt *BRAF* 277 bp sequence (which was consisted of 50 % mt and 50 % of wt) and 5 ng of wt were successfully detected with high specificity using an exponential LCR protocol of 50 cycles of 10'' denaturation and 5'' ligation, at 92 ^{o}C and 75 ^{o}C respectively (Fig. 8A). Using the same protocol and increasing only the number of cycles a limit of detection assay was performed. Finally, 100 fg of mt *BRAF* sequence, corresponding to 1.67 x10^5 molecules of mt target, gave rise to visualized products on 2 % agarose gel after 99 cycles of exponential LCR. As controls, 100 fg wt target (otherwise 3.34 x 10^5 copies) or no template (NTC) were also subjected to the same protocol where no LCR product was observed (Fig. 8B).

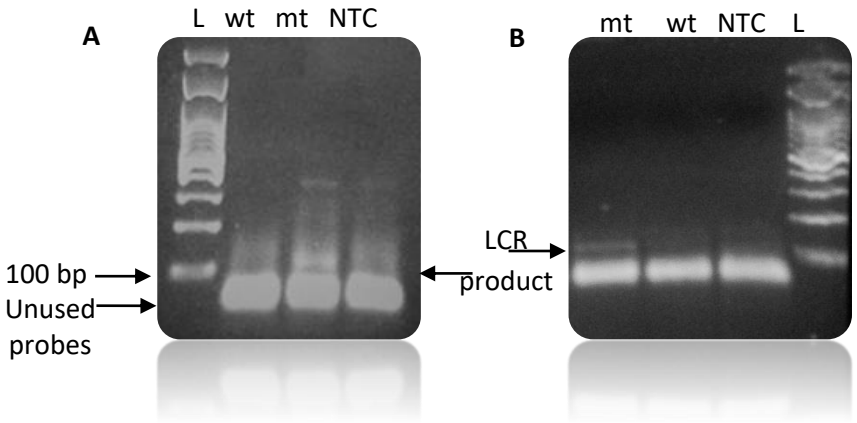

Figure 8. *Detection of BRAF V600E point mutation with high specificity by exponential LCR: a) 5 ng of wt BRAF sequence, 10 ng of 50% wt & 50 % mt BRAF sequence and no template were mixed with 5 pmol of each of all 4 probes and subjected into exponential LCR of 50 cycles. b) No template control (NTC), 100 fg BRAF wt (3.34 x10^5 copies) & 100 fg BRAF V600E in 1:1 ratio (50%) with wt (1.67 x10^5 mt copies) were mixed with 5 pmol of each of all 4 probes and subjected to exponential LCR of 99 cycles. A 100 bp DNA ladder (L) was used.*

As a follow-up experiment, LCR was performed using the modified version of probes *BRAF*-p1-biotin & *BRAF*-p2-chol. As presented in Figure 9, when 10 pg of mt in 1:1 ratio with wt & 5 pg of wt *BRAF* target of 277 bp were mixed with the two pair of probes and the products were visualized on 2% agarose gel, there was no difference between the mt and wt. Moreover, ligated products are visualized in different molecular weight-size than the expected. These results were in agreement with those presented in Chapter 3/part 1 and attributed to the presence of the cholesterol probe.

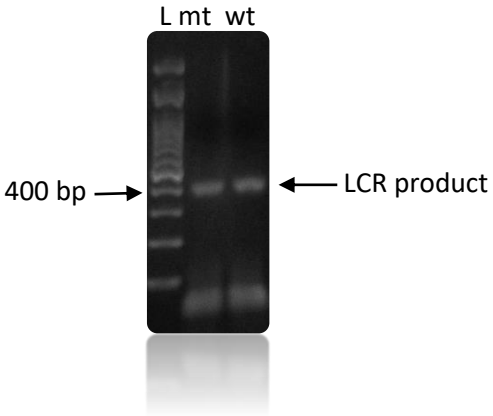

Figure 9. *Exponential LCR: 10 pg of mt (50 % mt & 50 % wt, corresponding to 1.67 x10^7 mt copies) & 5 pg (1.67 x10^7) wt BRAF target of 277 bp were mixed with 5 pmol of each probe BRAF-p1-biotin, BRAF-p2-chol, BRAF-cp1 & BRAF-cp2 and incubated for 50 cycles. No difference between mt and wt was observed probably due to the aggregations that cholesterol forms. A 100 bp DNA ladder (L) was used.*

3. Analytical performance of LCR followed by acoustic detection of BRAF V600E mutation

Eventually, the detection of LCR products through a common acoustic device (QCM-D) operating at 35 MHz (7th overtone) was investigated. To evaluate the overall performance and the limit of detection (LOD) of the LCR when combined with analysis on the acoustic sensor, exponential LCRs of 99 cycles were performed for several amounts (i.e., 1.67 x10^8 - 1.67 x10^5 number of mt molecules, 1.67 x10^8 wt copies, as wt control and no template) of the initial *BRAF* dsDNA template of 277 bp. Note that, although, the mt *BRAF* dsDNA of 277 bp consisted of 50 % V600E (mt) sequence and 50 % wt, here only the mt number of molecules are mentioned. For the reactions the modified *BRAF*-p1-biotin & *BRAF*-p2-chol probes were used, favoring the subsequent immobilization assay of the dsDNA product on the resonator. Regarding the above, amplification was followed by loading of the LCR mixtures on the sensor surface pre-functionalized with b-BSA and NAv. We chose the b-BSA/NAv substate vs only NAv, since the direct adsorption of NAv on the sensor was unstable upon the addition of a LCR mix (see Chapter 2, page 42). Specifically, the b-BSA/high[NAv] substrate described in *Chapter 2, pages 38-40* was selected; recall that, b-BSA/high[NAv] substrate had slightly worse reproducibility and stability compare to b-BSA/low[NAv], which was used in the next step of LCR detection (see below).

Firstly, we investigated if the frequency and dissipation changes (ΔF and ΔD) or the resulted acoustic ratio (ΔD/ΔF) caused by the direct immobilization of the 100 bp LCR product on the b-BSA/NAv coated surface could differentiate between the mt and wt reactions. Following a washing step with buffer, we concluded that the recorded acoustic signal changes could not discriminate between the mt and wt LCR reactions as well from the NTC (Fig. 10). The recorded changes were related to the non-specific adsorption of the LCR cocktail components (i.e., BSA, Ligase, biotinylated probe and its complementary strand) rather than the biotinylated LCR amplicons. Considering the low starting amount of mt DNA template in

the reaction, the general low efficiency of the LCR and the 10 times dilution for injecting the mix on the device, even after the amplification the product would be in the sub nM range; the latter is below the LOD of DNA which for the QCM-D device used in this work is around 5nM.

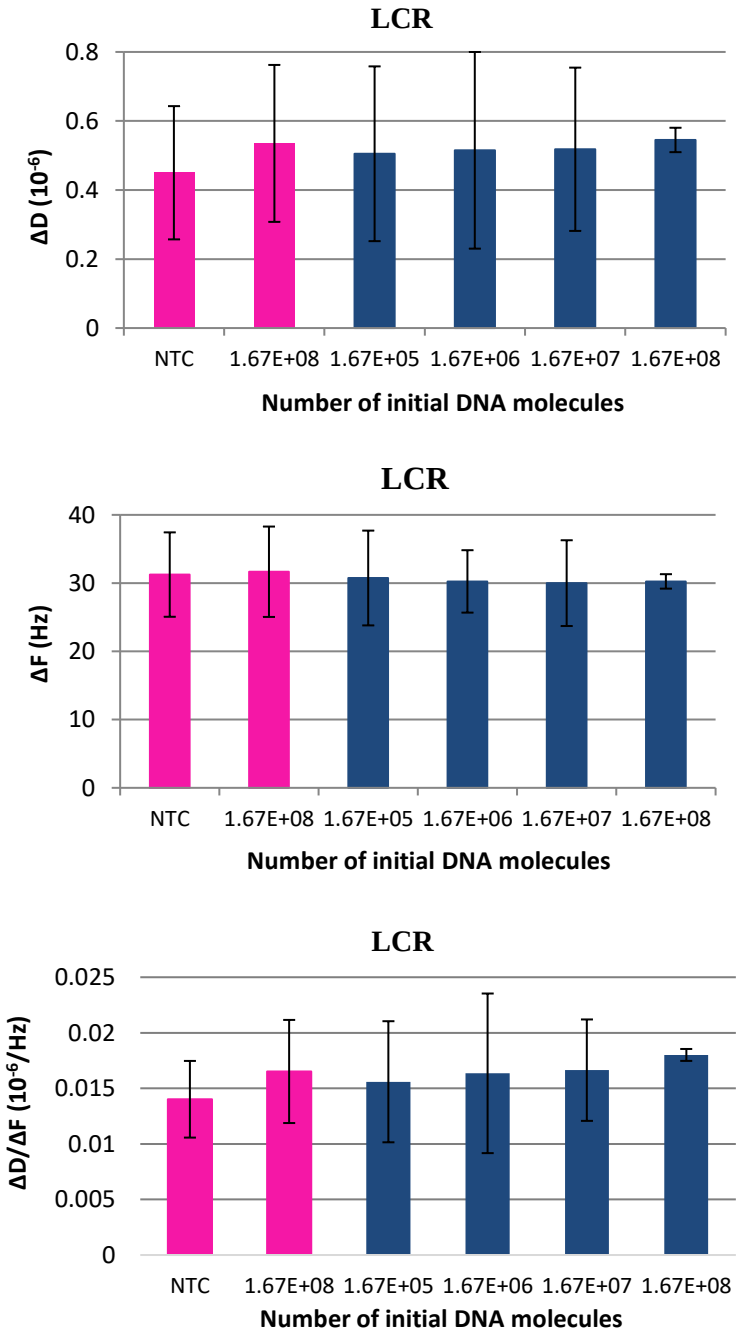

Figure 10. *ΔD, ΔF & ΔD/ΔF values obtained from the addition of various BRAF V600E LCR reactions on b-BSA/high[NAv]. DeepPink columns corresponds to the NTC and wt controls (1.67E+08).*

To achieve the acoustic detection a last step of liposome addition of 200 nm was employed (Fig. 11A). ΔD values were measured and presented in Figure 12A. While the reactions containing 1.67 x10^8 -1.67 x10^6 mt DNA were distinguished from the wt (ΔD: 1.48 ± 0.62) the LCR of 1.67 x 10^5 mt copies failed to give significant ΔD change (ΔD_{mt}=1.12 ± 0.66 x10^{-6} < ΔD_{wt}=1.48 ± 0.6 x10^{-6}). The latter, was not in agreement with the gel electrophoresis results,

where the LOD was estimated at 1.67 x 10^5 mt copies -however- when compared to just 3.34 x10^5 wt molecules. About the ΔF and the acoustic ratio, the first gave the same pattern as the ΔD (Fig. 12B) while the second resulted to similar values between all the mt samples and between the mt and the wt (Fig. 12C). Note that, the specific capturing of the LCR product on the sensor surface was also investigated; LCRs of 1.67 x10^8 copies were prepared with both the biotinylated and the non-biotinylated *BRAF*-p1 probe. As shown in Figure 11B, when the non-biotinylated probe was used no significant changes in the acoustic signal were recorded in contrast with the biotin-modified LCR product.

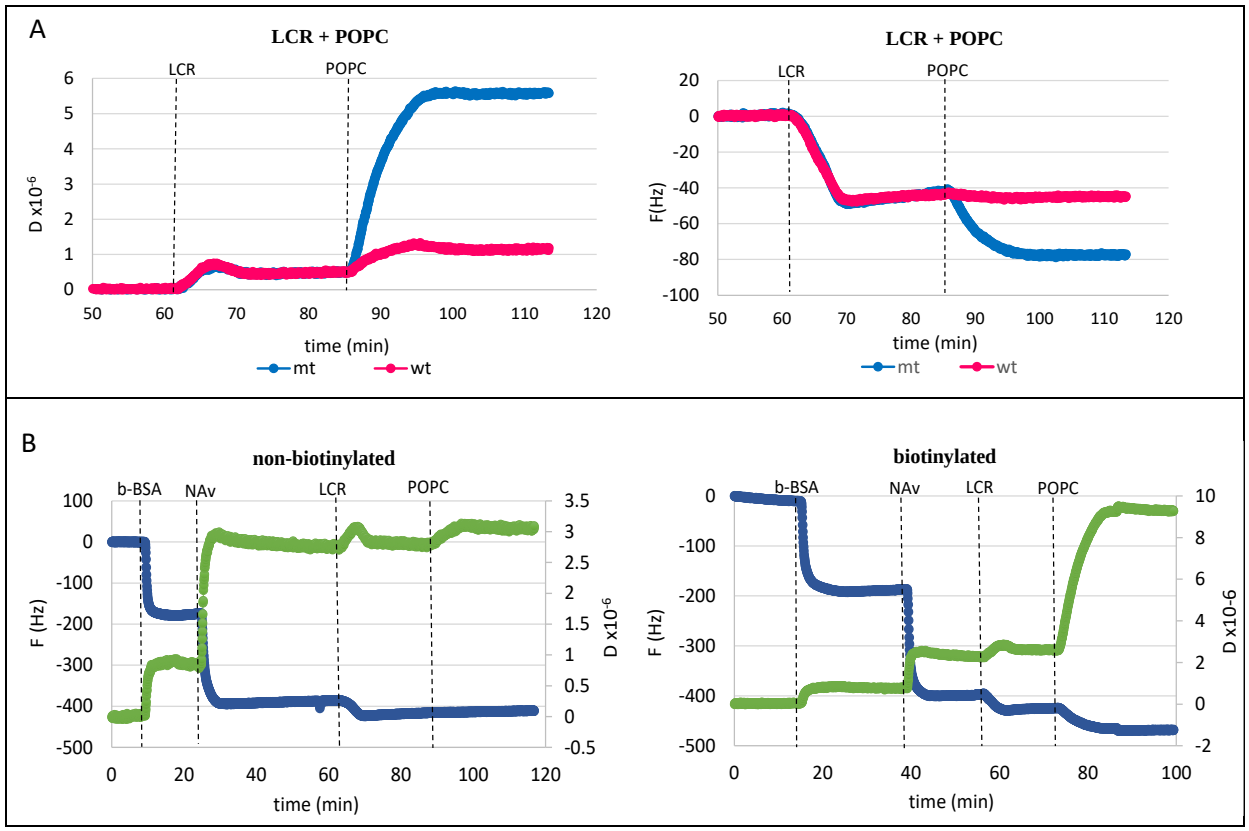

Figure 11. *A) Representation of the real time detection of a mt (starting template; 1.67E+07 BRAF V600E molecules) vs a wt LCR through POPC liposomes of 200 nm. The LCR products were immobilized on the b-BSA/high[NAv] substrate. Note that, the addition of the liposomes caused a high change in the dissipation (left panel) and frequency (right panel) only when the target was presented. B) Real time curves of frequency and dissipation monitored during the addition of LCR reactions carried out without (left panel) or with (right panel) the biotinylated version of BRAF-p1 probe. Only when the modified with biotin probe was used a significant acoustic signal was recorded, indicating the specific capturing of the LCR products.*

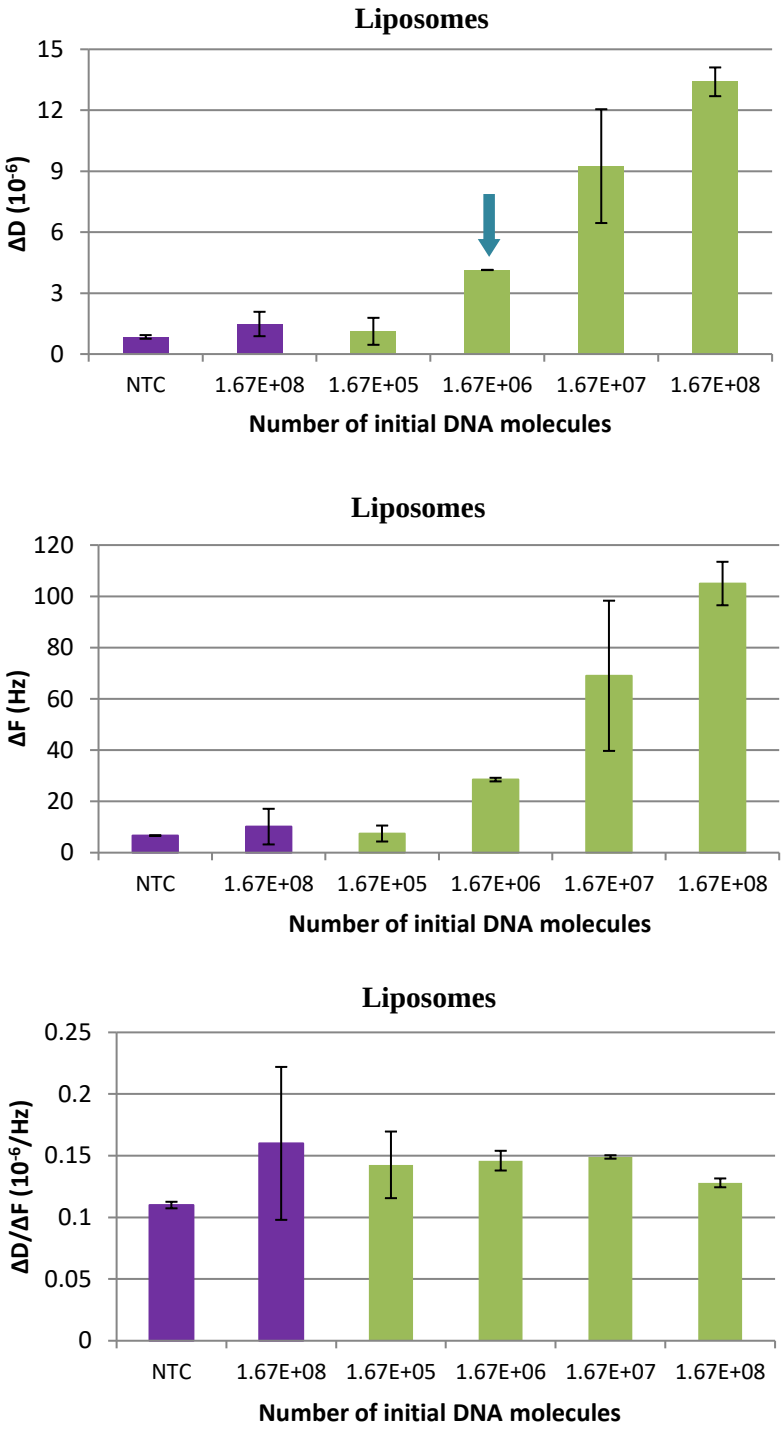

Figure 12. *Comparison of ΔD, ΔF and ΔD/ΔF values obtained from LCR of various amounts of the BRAF V600E DNA (1.67E+08 – 1.67E +05) detection through 200 nm POPC liposomes. LCR products were bound on the b-BSA/high[NAv] substrate. Purple columns correspond to the NTC and wt controls (1.67E+08).*

Assuming that the high NAv concentration may partially caused the non-specific values obtained for the wt, the same experiment was carried out, but this time LCR products were immobilized on the b-BSA/low[NAv] substrate. Similarly to the high[NAv], 1.00 x10^5-1.67 x10^7mt copies were subjected to LCR amplification. LCRs were then loaded on the sensor surface precoated with b-BSA/low[NAv]. The detection was achieved after the addition of 200 nm liposomes which caused high changes in the acoustic signal. As controls, LCRs

containing 1.67 x10^6 wt copies or no template were subjected to the same amplification and acoustic analysis protocol. We reduced the number of wt copies since in real ctDNA samples the amount of the wt target is usually between 10^4 – 10^5 molecules. Figure 13, presents the obtained acoustic values; based on this figure the LOD was improved by an order of magnitude, to the 1.00 x10^5 mt copies which resulted in ΔD =1.24 ± 0.36 x10^{-6} - 1.55 ± 0.36 x10^{-6} respectively, compared to the 1.67 x10^6 wt copies accounted for ΔD=0.5 ± 0.3x10^{-6} at the low[NAv] substrate. Note that the new LOD was in agreement with the gel electrophoresis results described above.

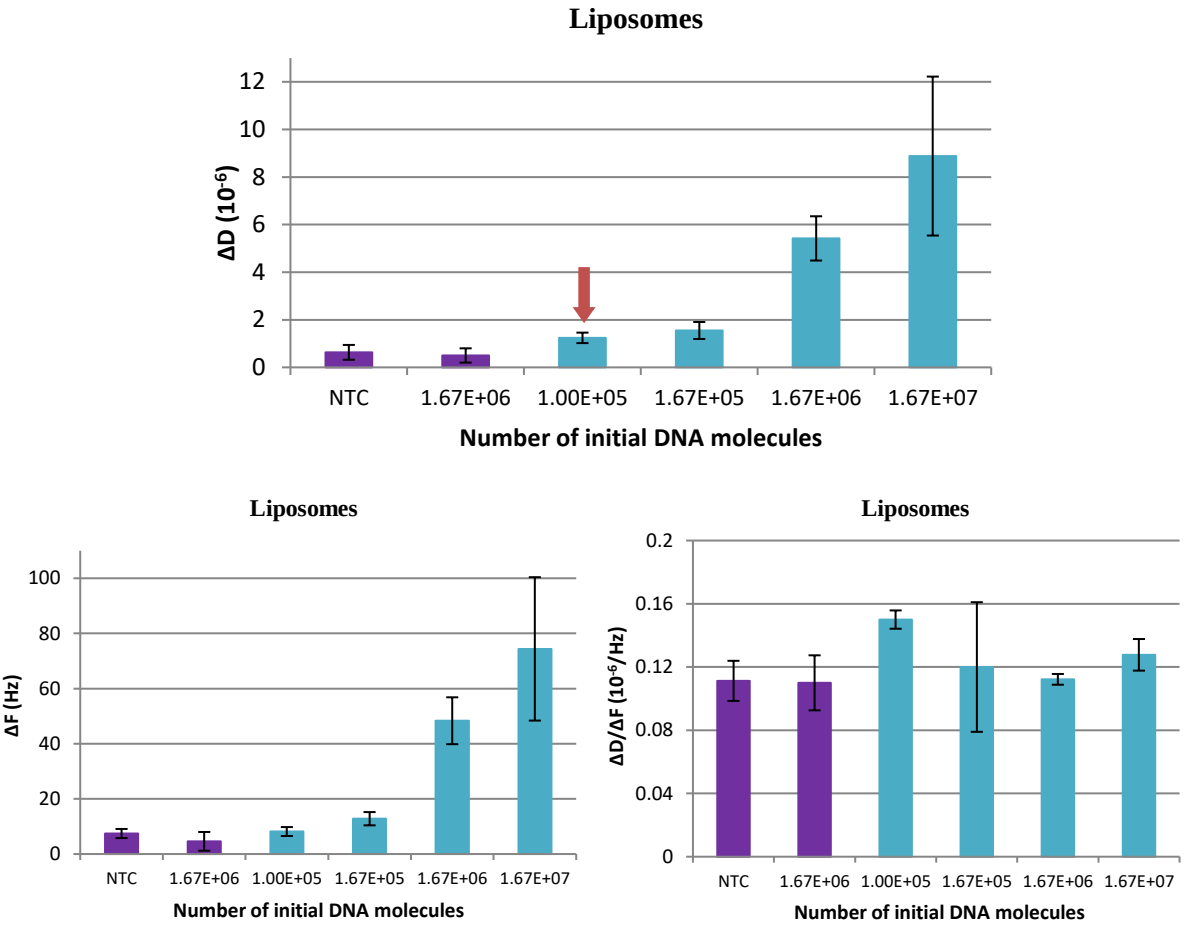

Figure 13. *Acoustic detection of LCR of various amounts of the BRAF V600E DNA (1.67E+08 – 1.67E +05) through 200 nm POPC liposomes. LCR products were bound on the b-BSA/low[NAv] substrate. Wt (1.67E+06) and no template control (NTC) reactions were run and plotted as well, here presented as purple columns. Note that the large error bars represent variability within different LCRs.*

4. Attempts for further optimization of the LCR protocol

Although, the LOD was decreased to the 10^5 mt copies, the overall efficiency of the assay remained low. In real cell-free DNA samples, the amount of the DNA target carrying the mutation might be as low as 1-10 copies, orders of magnitude lower than our achieved LOD. For this reason, many attempts for further optimization of the proposed LCR assay took place, some of them described in the following paragraphs.

Firstly, LCR reactions were run for 149 cycles instead of 99. In these experiments, 3.3 x 10^4 dsDNA molecules of the 277 bp *BRAF* target carrying the V600E mutation, 3.3 x 10^4 wt *BRAF* and no template were subjected to amplification and the amplified products were analyzed by gel electrophoresis. As shown in figure 14, a background signal of the same molecular weight and intensity as this of the expected LCR product was observed both in the wt and NTC samples. This background signal was most probably caused due to target-independent blunt-end ligation of the *BRAF*-p1/*BRAF*-cp1 and *BRAF*-p2/*BRAF*-cp2 duplexes rather than contamination; during LCR, there are three ways that the ligase can lead in a product, a. through target specific ligation b. through non-specific ligation in the mismatch site and c. via target-independent ligation of the probes (Fig. 15). Fewer number of cycles, i.e., 125 were also tested and compared to 99 cycles; background signal was again obtained but only when 125 cycles were performed. We concluded that this non-specific signal became predominant when LCRs of more than 99 cycles were run, although (according to the manufacturer) the AmpLigase enzyme used here had no detectable activity on blunt-ends. However, our results were in agreement with previous studies evaluating LCR and AmpLigase[145–147]. In these studies, the enzyme was tested for the detection of a point mutation in a PCR-amplified template of 370 bp mimicking the Ha-*ras* gene[146] or in a synthetic ssDNA carrying or not a point mutation[147]. In the first case, a background signal was observed for LCR of more than 40 amplification cycles[146], while in the second study a limit of 30 LCR cycles was estimated.

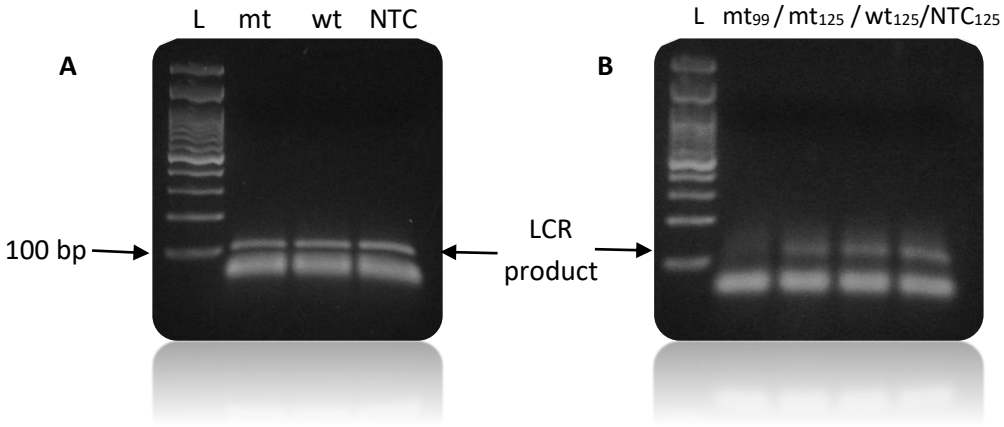

Figure 14. *Detection of 3 x10^4 copies of BRAF V600E point mutation by exponential LCR of A)149 and B)125 amplification cycles. A) 3 x10^4 mt (50 %), 3 x10^4 wt molecules of BRAF sequence and no template (NTC) were subjected to LCR of 149 cycles. B) 3 x10^4 mt (50 %) (mt$_{99}$ and mt$_{125}$), 3 x10^4 wt molecules of BRAF sequence or no template (NTC) were subjected to LCR of 99 (lane 1) or 125 cycles (lanes 2-4). A 100 bp DNA ladder (L) was used.*

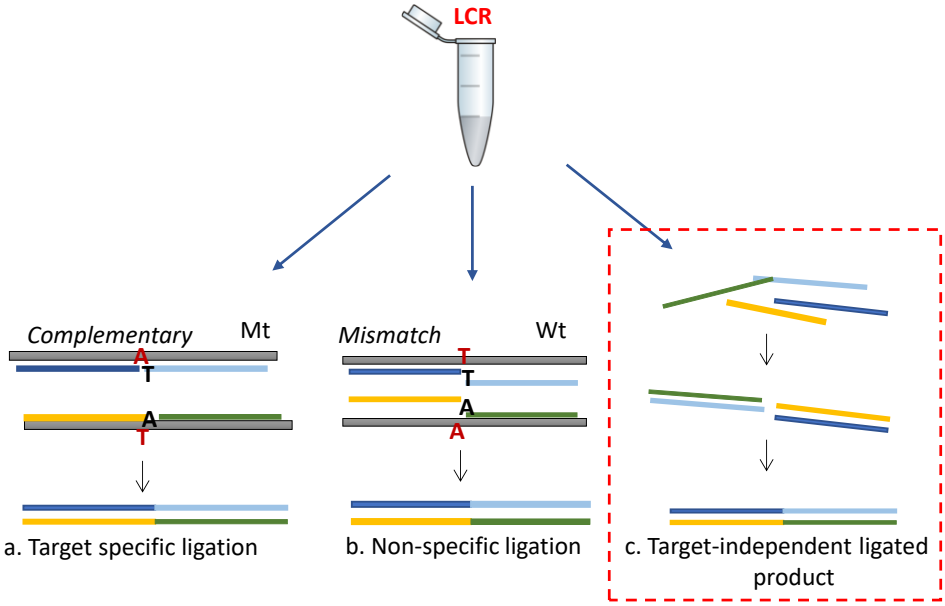

Figure 15. *Schematic representation of a LCR reaction (by-) products: a. target specific ligation b. non-specific ligation in the mismatch site and c. target-independent ligation of the probes of the reaction*.

To avoid the blunt-end ligation, other approaches including the performance of LCR assays using the non-phosphorylated *BRAF*-cp1 & *BRAF*-p2 probes were assessed. The assays contained 1.67 x10^5 - 1.67 x10^7 molecules *BRAF* V600E 50% or 1.67 x10^7 – 1.67 x10^5 *BRAF* wt 277 bp template and subjected to 149 amplification cycles. Following gel electrophoresis of the LCR mixtures and visualization under UV light, no ligated products were observed (Fig. 16).

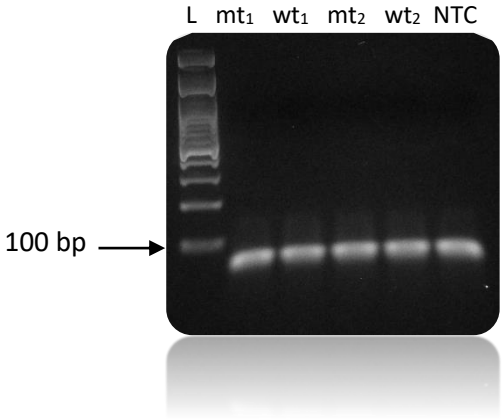

Figure 16. *Gel analysis of 99 cycles exponential LCR with non-phosphorylated BRAF-p2 & BRAF-cp1 probes. Lane 1 (mt_1) 1.67 x10^7 copies of 50% V600E 277 bp, Lane 2 (wt_1) 1.67 x10^7 wt copies 277 bp, lane 3 (mt_2) 1.67 x10 copies 50% V600E 277 bp, Lane 4 (wt_2) 1.67 x10^5 wt copies 277 bp, lane 5 no template control (NTC). A 100 bp DNA ladder (L) was used.*

Then, we tried to examine the performance of the following back-to-back LCR assays described in Figure 17: A. 1.5 µL derived from an exponential LCR of 99 cycles was subjected to 2nd 99 cycles amplification protocol and D. 1µL of linear LCR of 99 cycles using only the one pair of probes was added to an exponential LCR mix for other 99 cycles of amplification.

In both cases, as initial template, 1.67 x 10^5 of 50 % mt 277 bp or 1.67 x10^5 wt molecules were added. Products were analyzed in 2% agarose gel and visualized under UV light; both approaches gave rise to template-independent blunt-end ligation amplicons (figure 17A & D). Moreover, back-to-back LCRs with a PCR-clean up step between the two amplification protocols were tested. Specifically, exponential LCR of 99 cycles was cleaned-up and the eluted product was mixed with new LCR cocktail but without adding probes (we hypothesized that since probes are complementary to each other, they formed duplexes which are eluted during clean-up, too) (Fig. 17B). The final mix was subjected to 99 cycles of exponential amplification. The 2nd approach involved the performance of a 99-cycles linear LCR followed by clean-up and 99 cycles exponential LCR amplification (Figure 17C). The two approaches resulted to blunt-end (B) and no ligation (C), respectively.

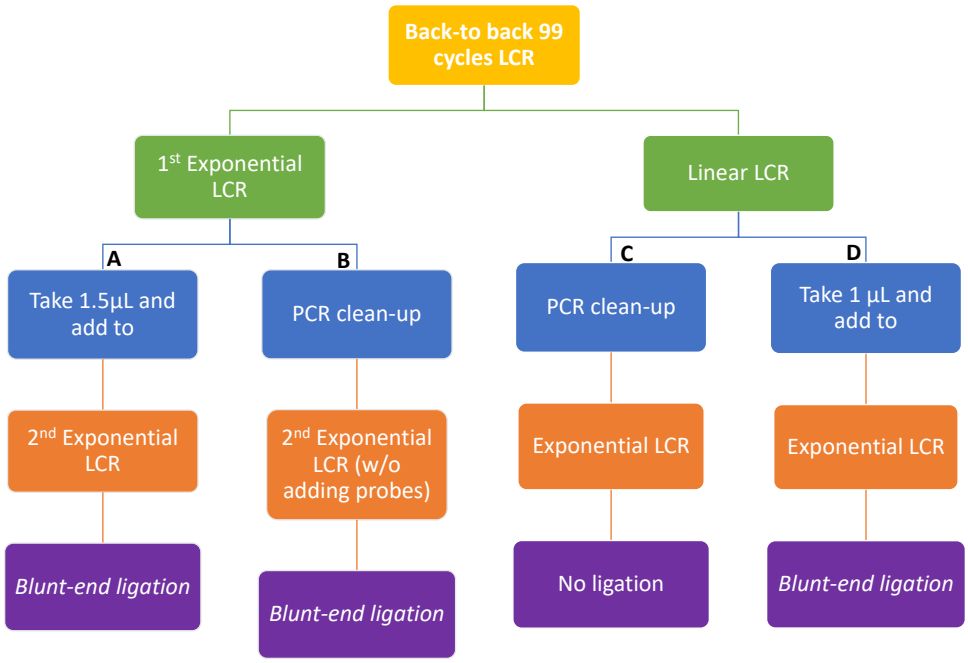

Figure 17. *Illustration of the examined back-to back LCRs and the obtained results.*

Conclusions

To summarize, we established an exponential 99-cycles LCR protocol for the specific amplification of dsDNA targets carrying the *BRAF* V600E point mutation followed by acoustic detection through highly dissipative liposomes. While the binding of the LCR amplicons on the NAv-coated sensor surface did not produce distinguishable changes between the control reactions (NTC + wt) and the LCRs containing the mt target, the addition of the 200 nm liposomes enhanced the acoustic signal leading to the detection of 1.67 x 10^5 initial mt molecules.

The above reported LOD was still far from the clinically relevant regarding ctDNA detection in real samples. Since LCR's efficiency is closely related to the number of thermal cycles, LCR of more cycles was investigated; nevertheless, the LOD not only was not improved but also

target-independent blunt-end ligation was observed when LCR exceeded the 99 cycles. Closer research could take place through a real-time LCR, to estimate the exact cycle where template-independent or non-specific ligation was generated.

Modified LCR assays have been developed in order to overcome the blunt-end ligation like gap-LCR (or PLCR)[138,145] and nested-LCR[123,148]. During Gap-LCR a DNA polymerase lacking 3' - 5' proofreading exonuclease and 5'- 3' nick-translation exonuclease activities is utilized to fill in a gap between the annealed allele-specific primers, which are subsequently joined by DNA ligase[123]. Regarding nested LCR, a primary LCR amplification step is carried out to generate separately the two pairs of probes which then are applied to a second LCR amplification to form the final product. However, both methods suffer from significant drawbacks preventing their use. For instance, Gap-LCR uses a polymerase for the specific amplification of the mt target which is by default out of the main goal of the project. Regarding nested-LCR, this assay is characterized by great complexity since three different LCR reactions are necessitated for the analysis of one sample.

On the other hand, there are some suggestions for the elimination of blunt-end ligation during typical LCR, including the addition of some μg salmon or herring sperm carrier DNA[146,148], the presence of noncomplementary tails on the outside of oligonucleotides and the use of single-base 3' overhangs on discriminating oligonucleotides[148]. Since there are preliminary data showing that the addition of some hundred ng of human genomic DNA (~125) completely inhibited the ligation (data not shown) and also blunt-end template-independent ligation has been observed even when carrier DNA is used[146], the 2nd and 3rd approaches are going to be used as presented in part 2 - 2nd approach (page 76).

PART 2 – 2ND APPROACH:

OPTIMIZED LCR – ACOUSTIC ANALYSIS PROTOCOL FOR THE DETECTION OF THE *BRAF* V600E POINT MUTATION

Introduction

As described in the 1st approach, single base 3' overhangs at the discrimination probes and the presence of non-complementary tails are common strategies to eliminate the blunt-end ligation and reduce the target-independent ligated by-products. Moreover, according to manufacturer instructions, ligation selectivity increases when the mismatch discrimination nucleotide is at the 3' end. For these reasons, new LCR probes were designed, where the mismatch discrimination nucleotide remained at the 3' end of the p1 probe while in 2nd pair of probes it was transferred from the 5' end of cp1 probe to the 3' end of cp2 probe. Moreover, 18 nt non-complementary to the target or the probes DNA tail was added at the 3' end of the p2 probe (Fig. 18).

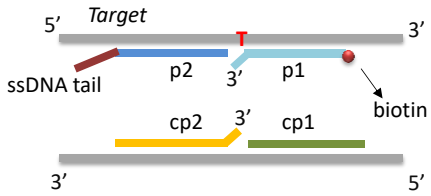

Figure 18. *Illustration of the new probe design. In both pair of probes (p1-p2 & cp1-cp2) the mismatch discrimination nucleotide is located at the 3' end. In addition, p2 probe was modified by a ssDNA tail non-complementary to the target.*

Moreover, assuming that the cholesterol in the p2-probe may affect the overall efficiency of the assay since cholesterol tends to aggregates, we developed a new acoustic detection protocol. In this approach, cholesterol is added downstream in the assay through a 20 nt cholesterol-modified DNA probe as shown below (Fig. 19).

Concept of the improved LCR/acoustic biosensing assay

The schematic of the proposed strategy for the detection of *BRAF* V600E mutation is illustrated in figure 19. Firstly, the two pair of probes are hybridized with the template at the region flanking the point mutation. This time, the probes are designed in such way, where the 3' end of the p1 and cp2 probes recognized the SNV. Moreover, the p1 probe is modified with a biotin at the 5' end, while the p2 probe carries a non-complementary to the target DNA region of 18 nt at the 3' end. Following LCR of several cycles, a biotinylated dsDNA product of 100 bp, with an extra ssDNA region of 18 nt is formed. LCR is directly injected on a b-BSA/NAv modified sensor obviating any purification or denaturation step, and the products are captured on the surface through the NAv-biotin interaction. Then, a ssDNA probe modified by a cholesterol is loaded and hybridized to the ssDNA region of the LCR product triggering the binding of 200nm POPC liposomes.

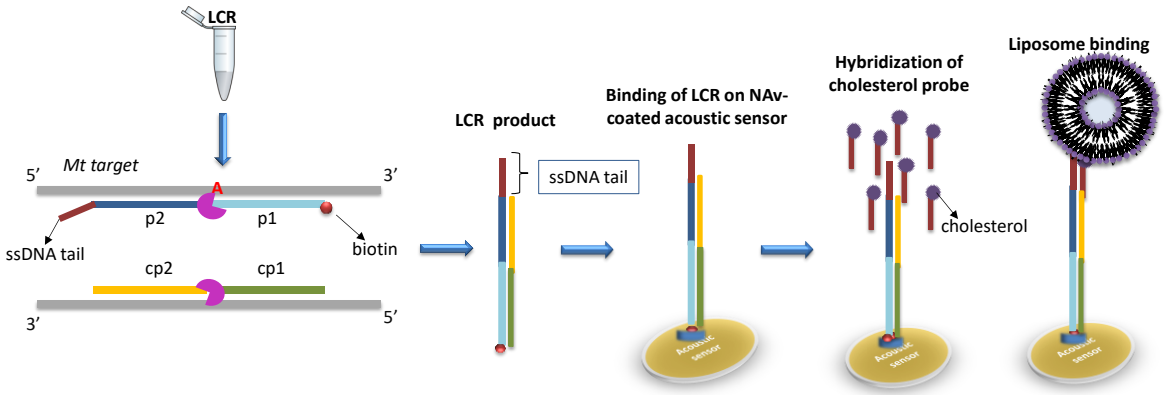

Figure 19. *Schematic representation of the new experimental approach for the acoustic detection of LCR products using the new LCR protocol: firstly, a dsDNA product with a 20nt ssDNA region is generated during LCR, followed by surface immobilization on b-BSA/NAv coated sensor. Following immobilization, a cholesterol-modified 20 nt DNA probe is hybridized to the ssDNA region triggering the capturing of POPC 200 nm liposomes.*

Materials & Methods

Materials	
High-performance liquid chromatography (HPLC)-grade oligonucleotides	Metabion International AG, Germany
T4 Polynucleotide Kinase (3' phosphatase minus) Enzyme & Buffer 10X	New England Biolabs, Mass., US
Adenosine 5'-Triphosphate (ATP) 10 mM	New England Biolabs, Mass., US
BSA, Molecular Biology Grade 20 mg/mL	New England Biolabs, Mass., US
Ampligase® DNA Ligase (5 U/µL)	Epicentre (Lucigen), Middleton, US
Ampligase® 10X DNA Ligase Reaction Buffer	Epicentre (Lucigen), Middleton, US
HiFi *Taq* DNA Ligase Enzyme & Reaction Buffer 10X	New England Biolabs, Mass., US
GelRed Nucleic Acid Gel Stain	Biotium, California, US
Phosphate buffer Saline (PBS) tablet	Sigma-Aldrich, Miss., US
NeutrAvidiv Protein	Thermo Fischer Scientific, Mass., USA
BSA lyophilized powder, crystallized, ≥98.0% (GE)	Sigma-Aldrich, Miss., US
Biotin-$(AC_5)_2$-Sulfo-Osu	Dojindo, Japan
Microcon-30kDa Centrifugal Filter Unit with Ultracel-30 membrane	Merck KGaA, Darmstadt, Germany
1-palmitoyl-2-oleoyl-glycero-3-phosphocholine (POPC)	Avanti Polar Lipids Inc., Alabaster, AL, USA
Nuclepore polycarbonate hydrophilic membranes 0.2 µm	Whatman plc, UK

DNA Sequences (5' -> 3')	
***BRAF*-p1-biotin**	**biotin**-GGATCCAGACAACTGTTCAAACTGATGGGACCCACT CCATCGAGATTTCT
***BRAF*-p2-ext20**	CTGTAGCTAGACCAAAATCACCTATTTTTACTGTGAGGTCT TCATGAAGAGGGGGTAGGAGTGTCGTT
***BRAF*-cp1-new**	GAAATCTCGATGGAGTGGGTCCCATCAGTTTGAACAGTTG

	TCTGGATCC
***BRAF*-cp2-new**	TCTTCATGAAGACCTCACAGTAAAAATAGGTGATTTTGGT CTAGCTACAG**A**
***BRAF*-p1-bio-15**	**biotin**-CT CCA TCG AGA TTT C**T**
***BRAF*-p2-35**	CTG TAG CTA GAC CAA GGG GGT AGG AGT GTC GTT
***BRAF*-cp1-15**	GA AAT CTC GAT GGA G
***BRAF*-cp2-15**	TGG TCT AGC TAC AG**A**
20nt-DNAchol	**cholesterol**-GATGAACGACACTCCTACCCCC

** The red bold nucleotide corresponds to the mismatch discrimination nucleotide.*

Design of the LCR probes: For the screening of the *BRAF* V600E point mutation versus the wt 2 new oligonucleotide pairs of probes were designed. The three of the four probes were 50 nt each in length (*BRAF*-p1-biotin, *BRAF*-cp1-new, *BRAF*-cp2-new). The fourth probe (*BRAF*-p2-ext20) was 68 nt in length, with the 3' end complementary to the 20nt-DNA-chol. The 1st pair of probes -*BRAF*-p1-biotin & *BRAF*-p2-ext20- had the same sequence like the *BRAF*-p1-biotin & *BRAF*-p2 which were reported in *Part 2 – 1st approach*, with extra 18 bases at the 5' end of the p2 probe. Again, the *BRAF*-p1 probe was modified with a biotin at its 5' end, favoring the immobilization of the LCR product on the acoustic sensor surface. Regarding the 2nd pair of probes -*BRAF*-cp1-new & *BRAF*-cp2-new – they had the same sequence like the *BRAF*-cp1 and cp2 reported in the *1st approach*, with 1 nucleotide different at the 3' end of *BRAF*-cp2 and the 5' end of BRAF-cp1. With the new design, the last nucleotide of the 3' end of the *BRAF*-cp2-new recognizes the mismatch (instead of the 5' end of *BRAF*-cp1) improving the specificity of the assay.

Design of 15 nt LCR probes: Two new oligonucleotide pairs of probes were design for the exponential amplification of the *BRAF* V600E point mutation versus the wt. The three of the four probes were 15 nt each in length (*BRAF*-p1-bio-15, *BRAF*-cp1-15, *BRAF*-cp2-15) while the fourth probe (*BRAF*-p2-35) was 33 nt in length. Regarding the *BRAF*-p1-bio-15 and the *BRAF*-cp2-15 the last nucleotide of their 3' end recognized the point mutation. Moreover, the BRAF-p1-bio-15 probe was modified with a biotin at the 5' end, and the 3' end of the *BRAF*-p2-35 was complementary to the 20 nt DNA chol.

Phosphorylation of the LCR probes. 300 pmol of the *BRAF*-cp1-new, *BRAF*-p2-ext20, *BRAF*-cp1-15 or *BRAF*-p2-35 were mixed with 1x T4 PNK reaction buffer, 1 mM ATP, 0.1 μg/μL BSA and 10 U T4 PNK Enzyme in a total reaction volume of 50 μL. The mixture was incubated at 37 °C for 60 min followed by heat inactivation at 65 °C for 20 min. The reactions were stored at -20 °C till use.

Exponential LCR amplification of the *BRAF* V600E mutation using the AmpLigase DNA Ligase and 50 nt LCR probes. All reactions were performed in the thermal cycler FastGene® Ultra Cycler Gradient - thermal cycler with 96 wells (NIPPON Genetics Europe). Various LCR protocols were tested with differences in the amount of the enzyme (1 U form 2.5 U), the annealing temperature (65 °C form 75 °C) and time (5sec from 10 sec), the number of cycles (30 cycles instead of 50 cycles) and the amount of probes (2 pmol each instead of 5 pmol).

The final optimized LCR protocol consisted of 2 pmol of each probe (*BRAF*-p1-biotin, *BRAF*-p2-ext20, *BRAF*-cp1-new and *BRAF*-cp2-new), 1x AmpLigase DNA Ligase Reaction buffer, 0.1 μg/μL BSA, 1 U of the thermostable AmpLigase DNA Ligase enzyme and the desired amount of the 277 bp *BRAF* V600E 50% or *BRAF* wt purified PCR target (see: *Part 2 – 1st approach*) in total volume of 25 μL. The final conditions of the amplification protocol included 94 °C for 3 min followed by 30 cycles of denaturation at 92 °C for 5 sec and annealing/ligation at 65 °C for 5 sec. LCR products were then analyzed either by gel electrophoresis on 2.0 % (w/v) agarose gel stained with GelRed Nucleic Acid Gel Stain or with acoustic experiment as described below. A no template control (NTC) was included in every run.

Exponential LCR amplification of the *BRAF* V600E mutation using the HiFi *Taq* DNA Ligase. All reactions were of 25 μL and performed in the thermal cycler FastGene® Ultra Cycler Gradient - thermal cycler with 96 wells (NIPPON Genetics Europe). Two LCR protocols were tested; the 1st protocol consisted of 0.5 μL HiFi Taq DNA ligase mixed with 5 pmol of each probe (*BRAF*-p1-biotin, *BRAF*-p2-ext20, *BRAF*-cp1-new and *BRAF*-cp2-new) in 1x HiFi Taq reaction buffer. The 2nd protocol contained 1x reaction buffer, 1 μL of HiFi Taq DNA ligase and 2 pmol of each probe. In both cases the reaction cocktails were mixed with the desired amount of the 277 bp PCR-derived mt or wt target (see: *Part 2 – 1st approach)* and subjected to amplification. The cycling protocol consisted of an initial denaturation step at 95 °C for 3 min, followed by cycling at 92 °C (5 sec) and at 75 °C (10 sec) for 50 times in the 1st case and at 92 °C (5 sec) and at 75 °C (10 sec) for 35 or 40 times in the 2nd approach.

Exponential LCR amplification of the *BRAF* V600E mutation utilizing 15 nt LCR probes . All reactions were performed in the thermal cycler FastGene® Ultra Cycler Gradient - thermal cycler with 96 wells (NIPPON Genetics Europe). LCR mixtures of 25 μL were prepared containing 5 pmol of each probe (*BRAF*-p1-15, *BRAF*-p2-35, *BRAF*-cp1-15 and *BRAF*-cp2-15), 1x AmpLigase DNA Ligase Reaction buffer, 0.1 μg/μL BSA and 1 U of the thermostable AmpLigase DNA Ligase enzyme. As template the 277 bp *BRAF* V600E 50% or *BRAF* wt purified PCR target (see: *Part 2 – 1st approach*) was used. The mixtures were heated at 94 °C for 3 min followed by 30 cycles of denaturation at 92 °C for 5 sec and annealing/ligation at 55 °C for 5 sec. LCR products were then acoustically analyzed as described below.

Acoustic device. The QSense Analyzer (E4 instrument) (Biolin Scientific, Sweden) was used for the simultaneous recording of frequency and dissipation changes at the 35 MHz (7th overtone); ΔF was not normalized by the overtone number. The QSense device was connected with the MINIPLUS Evolution peristaltic pump (GILSON, USA) to adjust the flow rate at 50 μL/min, unless otherwise stated. Measurements were performed in continuous flow of PBS buffer pH=7.4, at 25 °C. All samples were diluted in the running buffer, PBS pH=7.4 and following each addition, buffer rinsing was taken place. Prior to the experiment, the used Au-coated 5 MHz sensors were cleaned with Helmanex 2% for 15 min, rinsed with mili-Q water and 70 % EtOH and dried under N_2 flow. Then the sensors were subjected to 30 min UV/Ozone cleaning (Ossila Ltd, Sheffield).

Acoustic analysis of LCR. For the analysis of the LCR products, the gold sensor surface was firstly modified with 250 µL x 0.2 mg/mL b-BSA followed by the addition of 200 µL x 0.05 mg/mL NAv. b-BSA was prepared after incubation of BSA lyophilized powder with biotin-$(AC_5)_2$-Sulfo-Osu linker in PBS as described in part 2 (1st approach). Then, 20 µL of LCR mix was diluted in PBS at a final volume 125 µL and injected into the system at the flow rate of 25 µL/min. Following LCR addition, 200 µL x 500 nM 20nt-DNA-chol were loaded followed by the addition of 500 µL x 0.2 mg/mL solution of 200 nm POPC liposomes, prepared through extrusion as described before in part 2 (1st approach).

Results & Discussion

1. Development and optimization of a new LCR protocol for the detection of BRAF V600E mutation

For the exponential LCR reactions described in this approach, a different thermocycler (FastGene® Ultra Cycler Gradient) was used. Although the new cycler supposed to be capable of an average ramp rate of 5 °C/s like the previous one (peqSTAR 2X Gradient), finally was proven to operate with a slower ramp rate. The above, completely altered how LCR worked. For this reason, LCR conditions were optimized incrementally by altering the AmpLigase concentration, the quantity of the new probes, the ligation temperature and the cycle numbers. The products were analyzed by gel electrophoresis and visualized under UV light (expected band at ~120 bp). Firstly, 2.5 units (U), 1.5 U and 1.25 U of AmpLigase were mixed with 5 pmol of each probe and subjected to a 50-cycle protocol with the annealing temperature at 75 °C for 10 sec. As template, 1.67 $x10^{10}$ V600E molecules (consisted of 50 % mt & 50 % wt, but here only the number of mt molecules are referred), 3.34 $x10^{10}$ copies of wt *BRAF* 277 bp or no template (NTC) were used. According to the results, the best enzyme quantity which resulted to a clean NTC and less non-specific LCR product at the wt control compare to the mt, was the 1.25 U (Fig. 20). However, the efficiency of the assay was significantly low for this high input of DNA target (1.67 $x10^{10}$ mt copies).

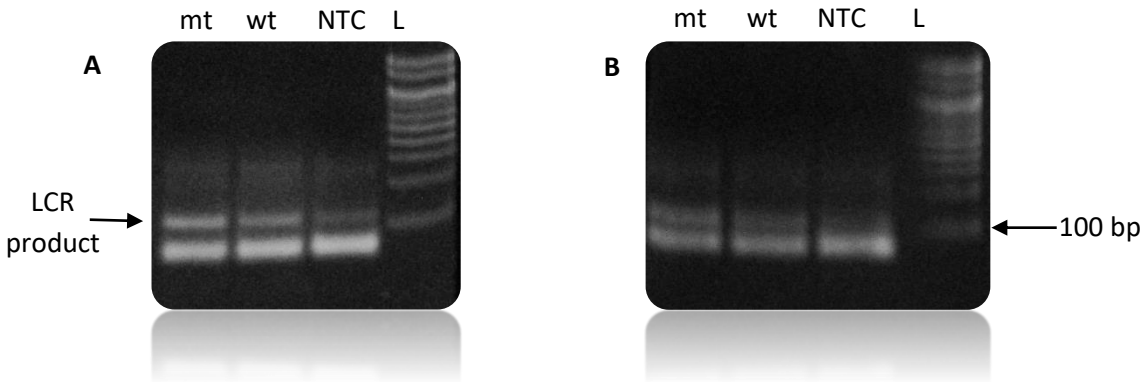

Figure 20. *LCR of 50 cycles with A) 1.5 U and B) 1.25 U AmpLigase. In both cases, 3.34 $x10^{10}$ mt (50 % mt & 50 % wt), 3.34 $x10^{10}$ wt molecules 277 bp target or no template (NTC) were mixed with 5 pmol of each of the four probes and subjected to 50 cycles of denaturation at 92 °C for 5'' followed by annealing/ligation at 75 °C for 10''. A 100 bp DNA ladder (L) was used.*

Considering that the optimum temperature for AmpLigase enzyme is the 65 ^{o}C, the same LCRs were prepared and run at the aforementioned temperature for 5-10 seconds ligation time. As shown in figure 21, in both cases no template-independent ligation was observed at the NTC, while the wt control produced non-specific ligated products following 25 amplification cycles. The latter was not of concern, since the 1.67 x10^{10} wt molecules were an excessive amount, far more than the clinically relevant which is maximum 10^5 copies. Clearly the "5'' ligation protocol" carried a better discrimination ability between the mt and the wt samples (Fig. 21B). For this reason, the protocol was further refined by decreasing the quantity of probes from 5 pmol to 2 pmol each. This time 1.67 x10^7 of mt or 3.34 x10^7 of wt *BRAF* 277 bp copies were amplified with high-specificity following 25 cycles of LCR (Fig. 22). Finally, in order to achieve the detection of lower DNA concentrations 5 additional amplification cycles were added to the protocol. Overall, the protocol consisted of 30 repeats of denaturation at 92 ^{o}C for 5 sec and 5 sec ligation at 65 ^{o}C. By this protocol, 1.67 x10^5 mt molecules were successfully detected when compared with 3.34 x10^5 wt copies; visualized products were observed exclusively in the case of mt target, indicating the high specificity of the assay. Interestingly, despite the improvements in the ligation protocol, i.e., the design of 3' single base overhangs and the non-complementary DNA region at the *BRAF*-p2-ext20 probe, template-independent ligation again appeared when >30 cycles were performed (Fig. 23). It is worth mentioning, that as increasing the number of cycles from 25 – 35, LCR by-products were also observed at higher molecular weights (~300 bp).

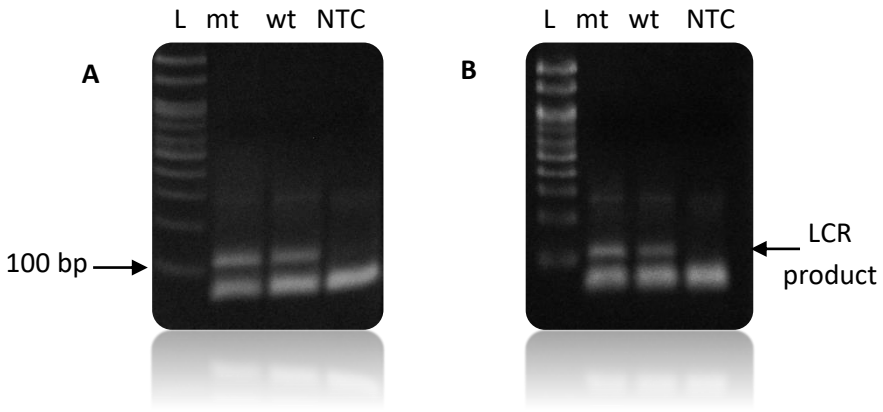

Figure 21. *LCR of 25 amplification cycles of denaturation at 92 ^{o}C for 5'' followed by annealing/ligation at 65 ^{o}C for A) 10''or B) 5''. In both cases, 1.67 x10^{10} mt, 3.34 x10^{10} wt copies 277 bp target or no template (NTC) were mixed with 5 pmol of each of the four probes and subjected to the above LCR protocol. A 100 bp DNA ladder (L) was used.*

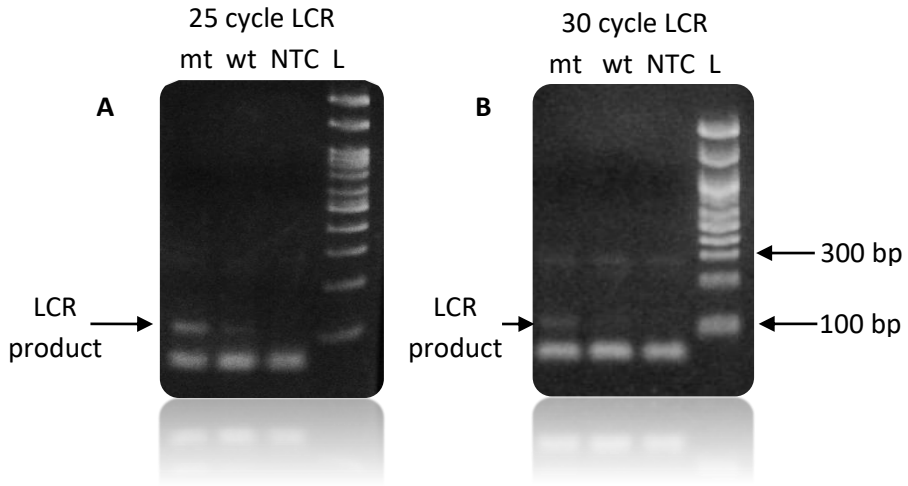

Figure 22. *Final optimized LCR protocol containing 2 pmol of each probe. The protocol consisted of 25-30 cycles of 5'' at 92 °C and 65 °C, respectively. A) 1.67 x10^7 mt, 3.34 x10^7 wt BRAF 277 bp copies and no template were successfully detected following 25 amplification cycles. B) 1.67 x10^5 mt, 3.34 x10^5 wt BRAF 277 bp copies and no template were amplified with high specificity following 30 cycles of LCR. A 100 bp DNA ladder (L) was used.*

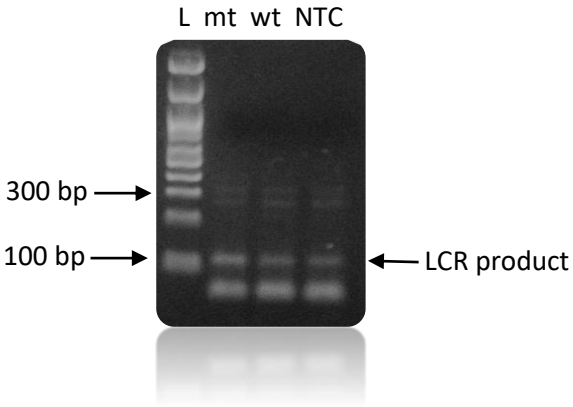

Figure 23. *Target-independent ligation following a reaction of 35 amplification cycles. 1.67 x10^5 BRAF V600E in 1:1 ratio (50%) with wt, 3.34 x10^5 BRAF wt molecules & no template were mixed with 2 pmol of each of all 4 probes and subjected to exponential LCR of 35 cycles. Wt and negative reactions generated by-products visualized in 2% agarose gel through target-independent ligation.*

The current LCR protocol compared to the first reported method created for the amplification of the *BRAF* V600E point mutation (1st app), was significantly improved in terms of efficiency since the same detection limit was achieved after 30 cycles instead of 99. Note that, despite the increased efficiency no improvement in the sensitivity was recorded when LCR products analyzed by gel electrophoresis.

2. Evaluation of the detection sensitivity of the 30-cycles LCR protocol combined with acoustic detection

Following the setting up of the LCR protocol, its combination with the newly proposed acoustic method was evaluated. As described above, for the capturing of the liposomes a 20nt cholesterol-modified probe (20nt chol-probe) was firstly added in high concentration (500 nM). To verify the specificity of the new detection approach, we flowed the 20 nt chol-

probe through the b-BSA/NAv coated sensing surface followed by the addition of POPC liposomes. As expected, no significant ΔD or ΔF changes (0.25 x10^{-6} and 2.3 Hz, respectively) were caused, confirming the specificity of the acoustic approach (Fig. 24).

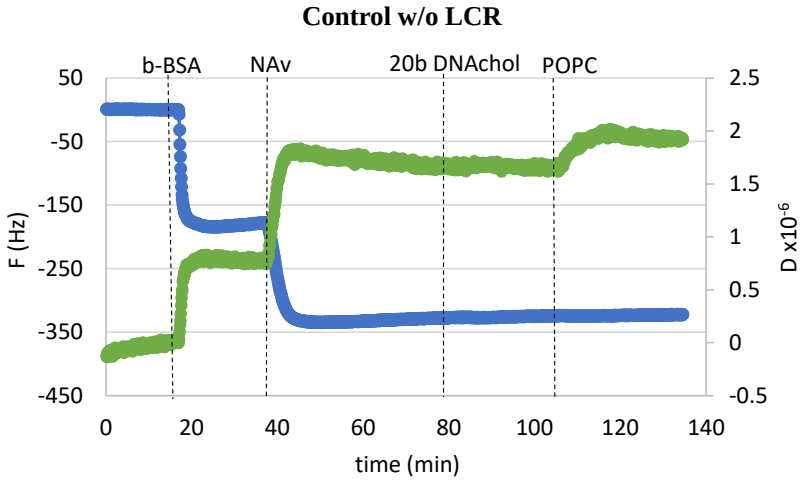

Figure 24. *Specificity assay; the addition of the 20nt chol-probe produced negligible changes in the acoustic signal.*

LCRs were performed for several concentrations of initial *BRAF* 277 bp template, i.e., 3.30 x10^3, 1.67 x10^4, 1.67 x10^5 & 8.35 x10^5 number of mt (V600E) molecules (C_{mt}) employing also the wt in a ratio 1:1. As a control, samples containing only the wt target in a concentration of C_{wt}=2 xC_{mt} were used. Analysis of the LCR products on functionalized with b-BSA/NAv acoustic sensors, without the addition of liposomes, resulted to no considerable changes in the generated acoustic values (ΔD, ΔF and ΔD/ΔF) between the mt samples and their corresponding wt controls (Fig. 25).

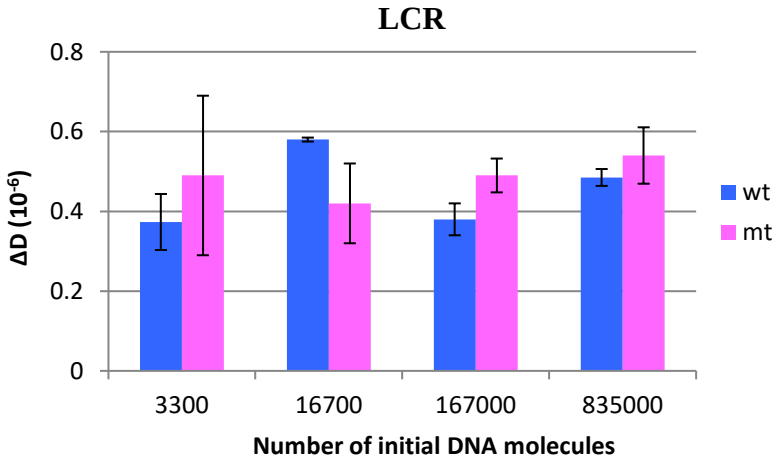

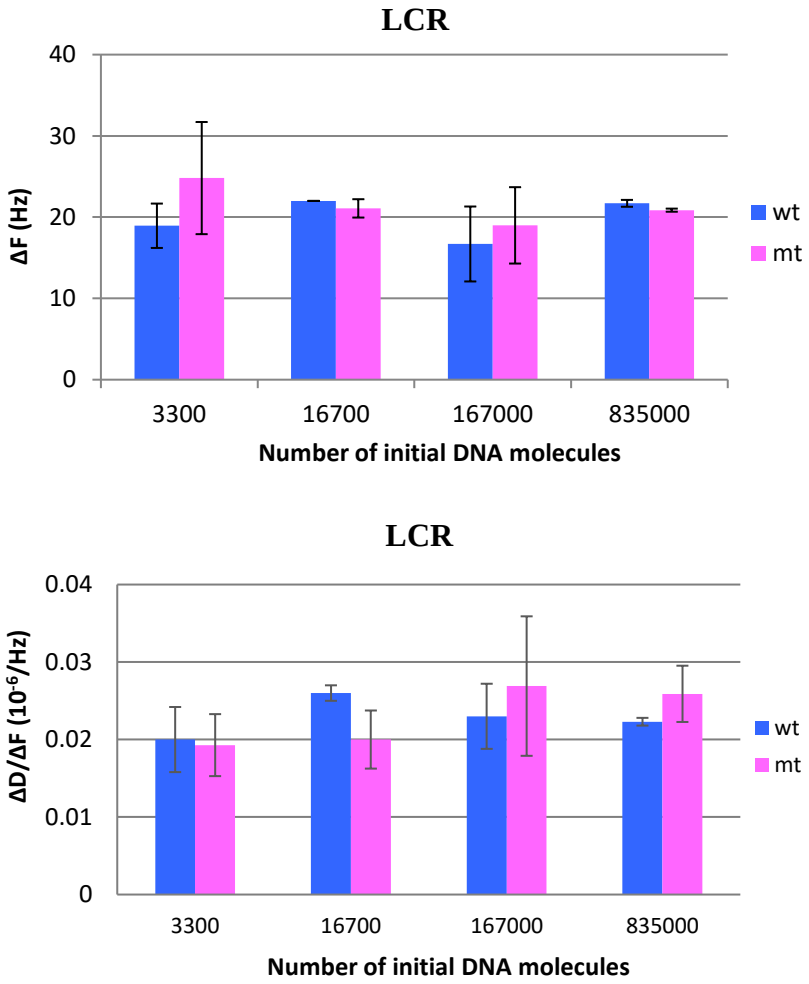

Figure 25. *ΔD, ΔF & ΔD/ΔF values obtained from the addition of various BRAF V600E LCR reactions on b-BSA/NAv.*

Adding the cholesterol-modified probe and the 200 nm POPC liposomes the changes in dissipation (ΔD), in frequency (ΔF) and the acoustic ratio (ΔD/ΔF) were measured and presented in figure 19A, C & E. Note that, although the wt control gave a background signal and while it is not completely clear in the graph, for the same LCR preparation and the same acoustic experiment the method's detection limit was the 3.30 x10^3 copies of mutant target (N=6) when the ΔD was compared (Fig. 26A & F). In addition, as expected for a higher amount of starting mt template a greater ΔD signal was measured. Regarding frequency response, the ΔF was proved to be less sensitive and with large error bars, while the ΔD/ΔF gave no differences between the mt and the wt reactions (Fig. 26C & E). For better representation of the above results, the % difference ($\frac{x1-x2}{(\frac{x1+x2}{2})} * 100$) of the ΔD and ΔF between the same set of mt/wt samples was calculated and plotted, as well (Fig. 26B & D).

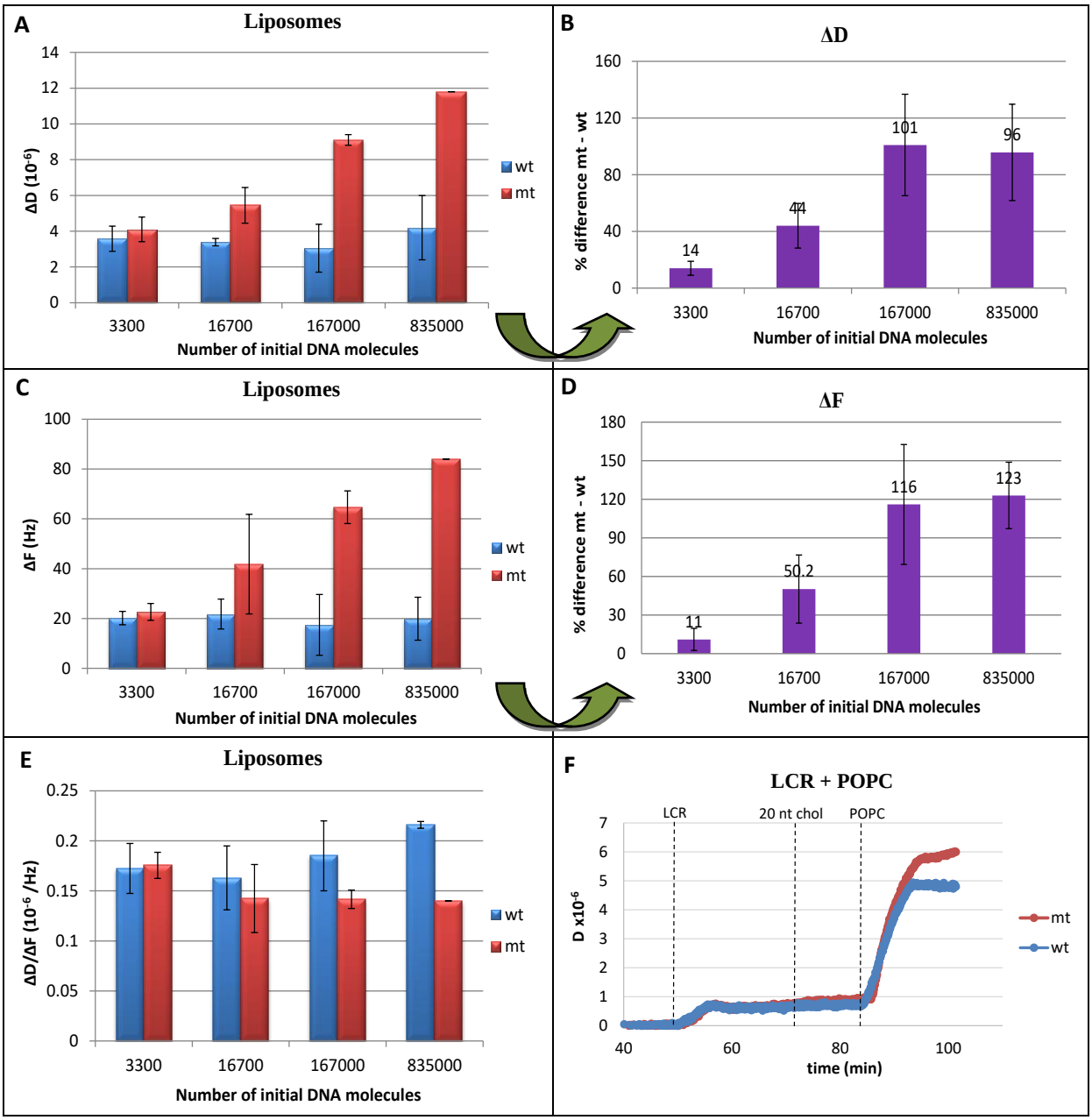

Figure 26. *Acoustic signal changes obtained by the capturing of POPC liposomes on various BRAF V600E LCR reactions and their corresponding wt controls. A) Comparison of ΔD changes observed between the mt/wt reactions. B) % difference between mt and wt reactions of the same LCR preparation and acoustic experiment. C) Same as A but for the ΔF. D) same B but for the ΔF changes. E) Same as A but for the ΔD/ΔF values. F) Real-time monitoring of the dissipation changes during the acoustic detection of LCR through liposomes starting from C_{mt}=3.3 x10^3 molecules BRAF V600E target. Note that, in all cases, the wt control contains wt molecules in a concentration of 2 x C_{mt}.*

It is worth mentioning, that the background signal produced from the wt samples remained constant regardless of the initial amount of the wt DNA target used. The constant background suggested that a significant amount of the LCR products was produced through non-specific and template-independent ligation following mechanisms b & c described above (Fig. 15). For example, the acoustic analysis of NTC LCRs created a ΔD of 3.05 ± 0.77 (N=4).

Finally, compared to the previous mentioned acoustic LOD (1st app.), the current detection limit was improved by two orders of magnitude, at 3.3 x10^3 mt copies prior to LCR. Furthermore, compared to the gel electrophoresis results the LOD was also decreased by two orders of magnitude, demonstrating the higher sensitivity of the acoustic device.

3. Attempts for further optimization of the LCR – acoustic detection method

Aiming to improve the LOD by at least two orders of magnitude at the 10 mt copies and to decrease the non-specific ligation, more attempts for LCR optimization took place. These attempts involved: a. the increase in the number of cycles; b. the change of annealing temperature & the ligation time; c. the use of more dissipative liposomes; d. the use of a different thermostable ligation enzyme, the HiFi *Taq* DNA Ligase instead of the AmpLigase Thermostable DNA Ligase; e. the use of shorter LCR probes.

a. Performance of 35 cycles LCR

As presented above, LCR of more than 30 cycles ended up in the creation of target-independent by-products. To assess the effect of these by-products on the acoustic detection, LCRs containing ~170 mt copies in 1:1 ratio with wt or 340 wt copies were subjected to 35 amplification cycles followed by acoustic analysis. As shown in figure 27, noticeably higher ΔD changes were recorded in both the mt and the wt reactions (12.5 x10^{-6} and 11.5 x10^{-6}, respectively) compared to the changes obtained from a 30-cycle LCR which for the wt accounted for 3.58 x10^{-6} Vs 11.5 x10^{-6}.

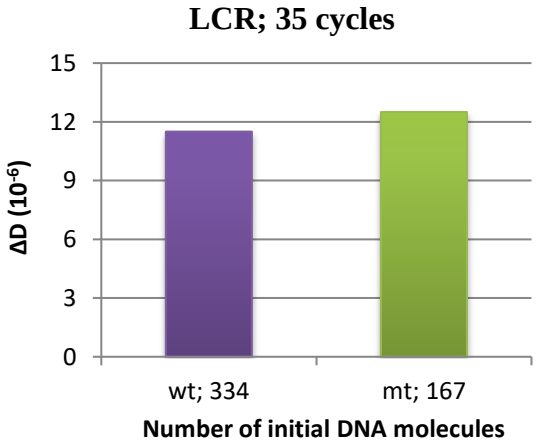

Figure 27. *Comparison of ΔD changes obtained at the POPC liposome step following the addition of mt/wt LCRs of 35 amplification cycles.*

b. Change of annealing temperature and ligation time

LCRs containing 3.3 x10^3 mt copies in 1:1 ratio with wt were carried out for 30 repeats of 92 ^oC and 60 ^oC for 2 sec instead of 92 ^oC and 65 ^oC for 5 sec. As a control, reactions with C_{wt}=2 x C_{mt} were performed. As shown in figure 28A, no improvement was achieved; contrariwise,

mt reactions did not always distinguish from the wt (% difference [mt-wt] 26 ± 20). Increasing the number of cycles target-independent ligation was generated (Fig. 28B).

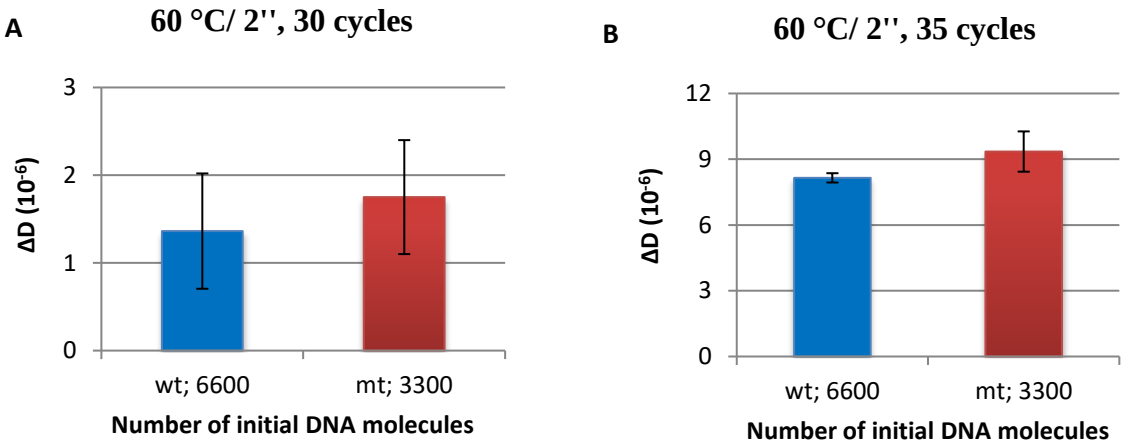

Figure 28. *Comparison of ΔD changes obtained by the capturing of POPC liposomes following the addition of mt/wt LCR reactions of A) 30 and B) 35 cycles.*

c. Use of more dissipative liposomes

In Chapter 2, part 1, the reasons according to POPC liposomes of 200 nm were chosen as acoustic probes are described. Briefly, extended research on the ability of liposomes to dissipate acoustic energy depending on their size and lipid composition has been accomplished. According to the results, the larger liposome dissipated higher acoustic energy. Regarding the lipid composition, SMPC liposomes were characterized as the more dissipative. Nevertheless, when SMPC and POPC liposomes of 200 nm tested in LOD assays, the same LOD was measured. The latter, was also confirmed in the following experiment, where SMPC liposomes were employed for the detection of 3.3 x10^3 mt molecules when compared with a wt control (Fig. 29). Notably, in the case of SMPC experiments, there was a general decrease in the acoustic signal which was probably attributed to the lower yield of LCR products -possibly due to the used enzyme's aliquot- rather than to the acoustic assay. More repeats are required to validate this result. In any case, taking into consideration the overall advantages of the POPC liposomes related to their stability (>1 week vs 4 hours for the SMPC) and their easy preparation (RT and 40 °C for the POPC and SMPC, respectively), POPC continued to constitute the best option.

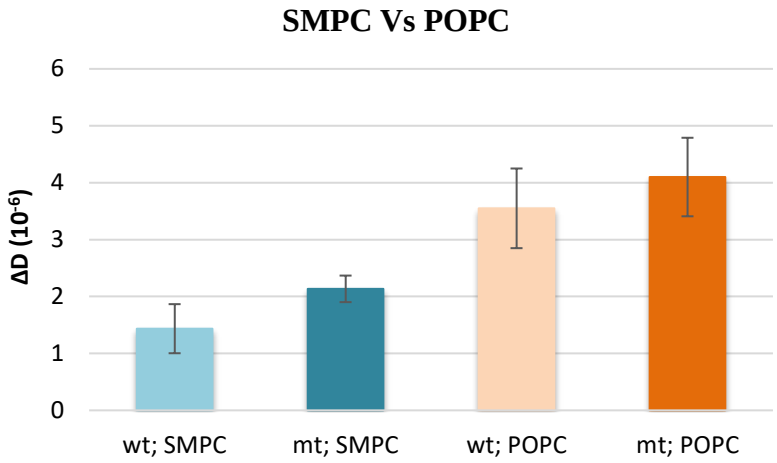

Figure 29. *Comparison of ΔD changes measured after the capturing of 200 nm SMPC or POPC liposomes on the amplicons derived from mt/wt LCR reactions. Note that, while the LCR reactions and the experiments run with each kind of liposome were performed in completely different time periods, are plotted together for the sake of comparison.*

d. Investigation of the ligation performance of HiFi *Taq* DNA ligase

In these experiments, the ligation performance of the HiFi *Taq* thermostable DNA ligase was investigated. Following extended optimization of the probes' amount and the cycling parameters, the optimum LCR conditions were determined. Finally, 1.67 x 10^5 molecules of *BRAF* V600E 277 bp target in 1:1 ratio with wt, were mixed with 2 pmol of each probe and subjected to 35 amplification cycles of 92 °C and 70 °C for 5 sec, respectively. The assay was performed for two enzyme concentrations, i.e., 0.5 μL and 1 μL, and the products were analyzed by gel electrophoresis. As controls, reactions containing 3.3 x10^5 *BRAF* wt molecules or no template (NTC) were added to the same amplification protocol. According to figure 30A, target-independent ligation was observed for the higher enzyme input. Moreover, when LCRs containing one order of magnitude less template (1.67 x10^4 mt and 3.3 x10^4 wt copies) were run for more than 35 amplification cycles (40) the background signal was significantly increased (Fig. 30B). Acoustic analysis of these reactions resulted to indistinguishable acoustic values (data not shown). Overall, the above results demonstrated that no progress was succeeded using the HiFi *Taq* DNA ligase.

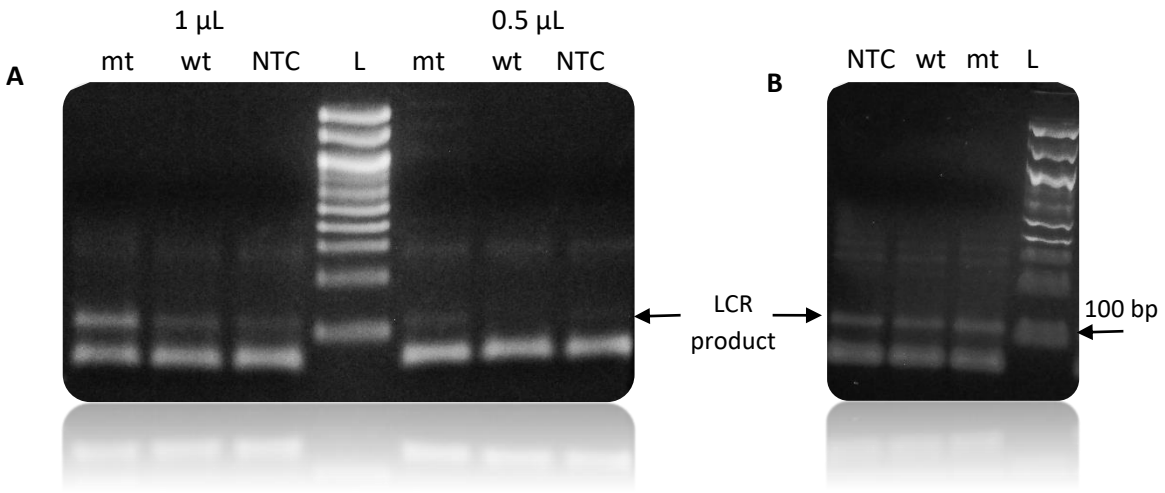

Figure 30. *Exponential LCR for the amplification of the BRAF V600E mutation utilizing the HiFi Taq DNA ligase. A) 1.67 x10^5 copies of mt 277 bp target in 1:1 ratio with wt, 3.34 x10^5 wt molecules and no template (NTC) were mixed with 1 µL or 0.5 µL ligase, 2 pmol of each of the four probes and subjected to 35 repeats of denaturation at 92 °C for 5'' followed by annealing/ligation at 70 °C for 5'. B) Target-independent ligation following a reaction of 40 amplification cycles. 1.67 x10^4 mt molecules in 1:1 ratio with wt, 3.34 x10^4 BRAF wt molecules & no template were mixed with 0.5 µL enzyme, 2 pmol of each of all 4 probes and subjected to the cycling protocol described above. Wt and negative reactions generated by-products visualized in 2% agarose gel through target-independent ligation. A 100 bp DNA ladder (L) was used.*

e. Application of *15 nt* LCR probes

Finally, we speculated that the use of shorter probes may reduce the target-independent ligation allowing us to increase the number of cycles and achieve a better detection limit. For this reason, new probes of just 15 nt were applied for LCR. The probes were designed in the same way as the 50 nt, i.e., the mismatch discrimination nucleotide was placed at the 3' end of each pair of probes (*BRAF*-p1-bio and -cp2), while the BRAF-p2 probe was modified with an extra 18 nt tail favoring the acoustic detection method.

Following optimization, several concentrations of initial template (i.e., 3.30 x10^3, 1.67 x10^4 & 1.67 x10^6 number of mt molecules employing also the wt in a ratio 1:1) were subjected to LCR of 30 cycles (5'' denaturation at 92 °C and 5'' ligation at 55 °C) and acoustic detection. As a control, a sample containing only wt target was used (C_{wt} = 2 xC_{mt}). Although target-independent ligation was minimized (average ΔD of all wt controls; 0.8 ± 0.26 x10^{-6} Vs 3.57 ± 0.51 x10^{-6} for the 15 nt and the 50 nt probes, respectively), the sensitivity of the assay was decreased, too. None of the low concentration samples i.e., 3.30 x10^3 & 1.67 x10^4 copies were detected (Fig. 31). By increasing the number of cycles -from 30 to 35-, high ΔD changes were produced from both mt/wt reactions of low concentrations (3.30 x10^3 & 1.67 x10^4). However, the increase was independently of the input target indicating that again the LCR by-products were preponderant of the target-dependent (data not shown).

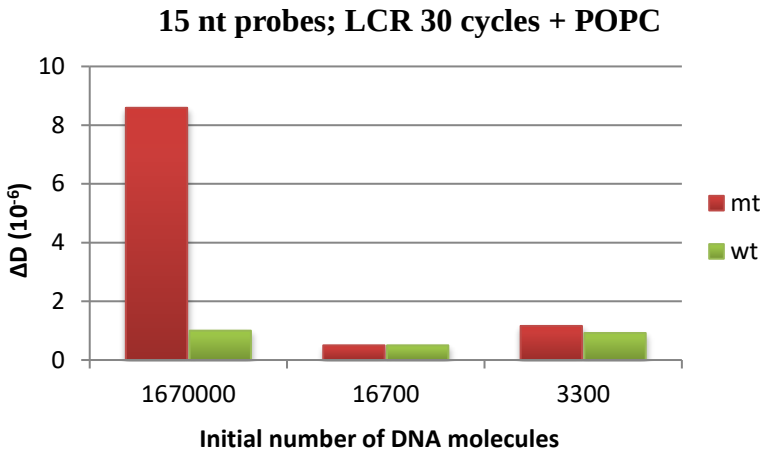

Figure 31. *Acoustic detection of BRAF V600E following an LCR of 30 cycles with the 15 nt probes. Comparison of dissipation changes observed after loading POPC liposomes of 200 nm on LCR amplicons captured on b-BSA/NAv modified sensors.*

4. Comparison of LCR/Acoustic method with other ligase-based single nucleotide variants (SNVs) detection techniques

As already mentioned, conventional LCR techniques, as well as its variants, have been widely applied for specific detection in a wide range of samples including genetic diseases, cancerous point mutations and pathogens. In table 1, our LCR/acoustic detection technique is compared with excellent paradigms of ligase-based methods. Among LCR approaches coupled or not with nano-biotechnology (Table 1; *1 -7*) we achieved a similar to the best-reported detection limits reaching the aM range within 30 cycles of LCR and a total duration of ~2.7 hours including the acoustic analysis. Our method carries a better detection efficiency even among improved variations of LCR, such as LCR coupled with Rolling Cycle Amplification (RCA) & fluorescence detection (220 aM Vs 1 fM)[147], Gap-LCR coupled with quantum dots detection (5.5 zmol Vs 170 zmol)[149], PCR followed by Ligase Detection Reaction (LDR) and Capillary gel electrophoresis (CGE) - Laser induced fluorescence (LIF) detection (220 aM Vs 0.1 nM)[140] and PCR followed by Oligonucleotide Ligation Assay (OLA) and electrochemilluminescnce (ECL) (5.5 zmol Vs 10 fmol)[150]. Finally, LCR and acoustic detection had a significantly improved detection limit compared to surface ligation biosensing approaches combined with an enhancing step like gold nanoparticles[151], silver deposition[142] or enzymatic amplification (horse peroxidase)[81] (220 aM Vs 0.9 pM, 80 fM and 1 pM, respectively). Note that, low abundance single nucleotide mutations of less than 100 copies are detected only through LCR coupled with a 2nd amplification molecular reaction like Hyperbranch-RCA or qPCR.

Last but not least, compared to other DNA array or biosensing platforms normally employed in DNA detection, the proposed acoustic technology allows the processing of non-purified samples and overcomes the issues arising during the detection of dsDNA targets, i.e., the need for sample heating and the prevention of DNA strands reassociation.

Table 1. *Comparison of various versions of Ligase Chain Reaction (LCR) and ligation-based amplification techniques. LCR-Ligase chain reaction; RCA – Rolling Cycle Amplification; LDR – Ligase detection reaction; OLA – Oligonucleotide ligation assay; LSAW – Leaky surface acoustic wave; fc –* ferrocene; *AuNPs - Gold nanoparticles; QDs - Quantum dots; SMS – Single molecule spectroscopy; CCD – Charge-coupled device; CGE- Capillary gel electrophoresis; LIF – Laser induced fluorescence; ECL – Electrochemilluminescnce; FRET - fluorescence resonance energy transfer; spFRET - single pair fluorescence resonance energy transfer; JEV – Japanese encephalitis virus.*

Amplification assay	Detection system	Enhancing step	Target	Cycles / approach duration	LOD/ Sensitivity	Reference
1. LCR/QCM	Acoustic	Liposomes	*BRAF* V600E (T->A)	30 / 2.75 hours	3300 copies **or** 5.5 zmol **or** 220 aM / 50%	Current study
2. LCR	Fluorescence	Microbeads	*β*-globin (A->T)	30 /-	10 fM	Meng et al., 2010[152]
3. Real-time LCR	Colorimetric	AuNPs	*KRAS*	30 / -	20 aM / 0.1 %	Shen et al., 2012[153]
4. Real-time LCR	FRET	-	C->T	160-200 / -	120 copies or 10 aM/0.1 %	Sun et al., 2015[154]
5. LCR	Electrochemi-cal	-	*EGFR* T790M C->T	30	10 aM / 0.1 %	Zhang et al., 2019[144]
6. eLCR	Electrochemi cal	Horse peroxidase	*CYP2C19*2* allele	30	0.5 fM / 0.01%	Liu et al., 2020[137]
7. fc-labeled LCR	Electrochemi cal	ferrocene (Fc)-labeled	*EGFR* T790M C->T	30	0.75 aM/ 0.01 %	Hu et al., 2020[143]
8. LCR + RCA	Fluorescence (SYBR I)	-	*β*-globin (A ->T)	30	1 fM / 1%	Cheng et al., 2013[147]
9. Gap-LCR + HRCA	Fluorescence (SYBR I)	-	*BRAF* V600E (T->A)	45	5 copies, 200 zM	Zhang et al., 2019[155]
10. Gap-LCR + qPCR	Taqman probe	-	*β*-globin (A ->T)	25 LCR + 25 qPCR	3 copies / 0.01%	Yi et al., 2012[138]
11. Gap-LCR	SMS	QDs	*KRAS* (G->A)	60	170 zmol	Song et al., 2013[149]
12. PCR + LDR	CCD camera	AuNPs + silver staining	*β*-globin IVS2 654 (C->T)	45 PCR + 20 LDR	0.1%	Yi et al., 2011[156]
13. PCR + LDR	CGE - LIF	-	*KRAS G12 (multiplex)*	-	0.1 nM / 1%	Hamada et al., 2014[140]
14. PCR + OLA	ECL	-	*TP53* codon 273 (G->A)	35	10 fmol	Zhou et al., 2003[150]
15. PCR + OLA	ELISA	-	*KRAS* G12/13 (multiplex)	30	10 %	Rothschild et al., 1997[124]
16. LDR	spFRET	-	*KRAS* G12	1 / 5 min	600 copies / 0.1%	Wabuyele et al., 2003[157]
17. Surface ligation	Electrochemi-cal	Enzymatic silver deposition	*KRAS G12* (C->A)	-	80 fM	Zhang et. Al., 2007[142]
18. Surface ligation	Electrochemi-cal	AuNPs	-	-	0.9 pM / 0.1%	Wang et al., 2011[151]

19. Surface ligation	Leaky SAW	Horse peroxidase	A2293G JEV *(A -> G)*	-	1 pM	Xu et al., 2011[81]

Conclusions

By further optimizing the LCR probes as well as the acoustic detection method, the overall efficiency of the assay was noteworthily improved; by the new protocol 3.3 $x10^3$ *BRAF* V600E molecules in 1:1 ratio with wt gave a higher ΔD change when compared with a wt control containing Wt_{copies}=2x $mt_{copies.}$ Note that, this LOD was achieved only through acoustic analysis. To be exact, the acoustic methodology was two orders of magnitude more sensitive than the typical analysis on gel stained with an ultrasensitive gel dye (Gelred). Interestingly, during the acoustic experiment, the wt control gave a background signal which remained constant regardless of the initial amount of the wt input molecules. Specifically, the average acoustic signal of all the wt reactions of 6.6 $x10^3$ – 1.67 $x10^6$ copies prior to LCR was calculated at ΔD= 3.57 ± 0.51 $x10^{-6}$, quite similar to those derived from negative LCRs (NTC) which was ΔD= 3.05 ± 0.77 $x10^{-6}$. The above result demonstrated that the main LCR by-products are formed through target-independent ligation.

Following these results, repeated efforts for lowering of the LOD and the specificity of the assay took place. Nevertheless, no significant improvement was observed; when the specificity was improved the LOD was either remained the same or decreased. In any case, increasing the number of cycles, LCR ended up in target-independent ligation. The above has been extensively described in the bibliography as one of the main drawbacks of the exponential LCR, besides its theoretical excellent specificity for mismatch discrimination[123].

Eventually, it should be pointed out that the main issues of the proposed approach are the detection limit and the specificity of the molecular assay rather than the acoustic detection method (including the amplification step through liposomes). LCR is by nature a low efficiency method when it comes to the detection of low abundance SNPs or cancerous point mutations. To our knowledge, the best-reported detection limit of ligase chain reaction is the 120 copies, where 160 – 200 LCR cycles are combined with FRET real-time detection[154]. Note that, in this approach non-specific signal is also detected in the wt and blank controls, however, in lower values compared to the mt target. Furthermore, in a large variety of publications, in order to achieve a better detection limit, LCR is either combined with other amplification techniques like typical PCR[123,135], allele-specific PCR (gap-LCR)[145], qPCR[138] and Rolling Cycle Amplification (RCA)[147,155] or is converted to ligase-based detection techniques consisted of a preamplification PCR step followed by Ligase Detection Reaction (LDR)[140,156,158], oligonucleotide ligation assay (OLA)[124,159] or gap-LCR[139]. Finally, despite the limitations of our method for application in ctDNA detection, the proposed technique could still be effective for the detection of other kinds of targets such as miRNAs, pathogens etc.

PART 3:

COMBINING LCR/ACOUSTIC DETECTION OF MUTATED *BRAF TARGET* WITH THE 2ND GENERATION MICROFLUIDIC FLUIDIZED BED SELECTIVE CTDNA EXTRACTION APPROACH

Introduction

Common ctDNA extraction techniques use commercial spin column kits usually containing silica membranes. Despite their wide application, significant variability in the capture efficiency and yield between the different extraction kits has been observed[160,161]. Moreover, the loss of small DNA fragments (<100 bp) is a crucial challenge. Their recovery is of great importance in ctDNA analysis, since ctDNA fragments range from 90 bp – 150 bp[59,60]. Optimized extraction kits with high affinity to all fragment sizes have been developed, however, still substantial amounts are lost at the purification stage[61]. In addition, these methods require quite manual handling and sample transfer to different tubes thus increasing both the overall process complexity as well as the risk of cross contamination[162].

In addition to the above, ctDNA detection becomes quite challenging due to the high fragmentation and the small ctDNA/cfDNA ratio (as low as 0.01 %), especially at the early cancer stages[61,163]. Another complication is its presence in an extremely heterogeneous DNA population. cfDNA purification kits are not capable of preferentially extracting specific DNA targets and a lot of unnecessary cfDNA sequences are extracted and injected to analysis potentially affecting the assay's efficiency.

In this section, a new technology for the selective extraction of specific ctDNA targets is presented. The method has been developed at the Macromolecules and Microsystems in Biology and Medicine (MMBM) Lab at the Institut Curie, Paris, France and utilizes the microfluidic fluidized bed (FB) technology. The new technology, referred as 2nd generation fluidized bed, is an improved version of the 1st generation microfluidic magnetic fluidized bed developed by the same team[109]; through the 2nd generation FB larger samples can be processed while DNA is extracted in less time and more efficiently due to the higher working flow rate (15 µL/min vs 5µL/min) and surface extraction (manuscript under preparation).

Briefly, serum or plasma samples containing cell-free DNA is perfused on a miniaturized microfluidic PDMS chip of 250µm height, filled with 500 µg of streptavidin-coated Dynabeads (magnetic) beads. The magnetic beads are functionalized with 80nt biotinylated probes complementary to the target of interest (here the *BRAF* gene). Using a permanent magnet, continuous flow mixing is achieved. Furthermore, good homogeneity of the beads during the extraction is created using magnetic beads of two different sizes mixed in 1:1 ratio and the addition of an external vibration force. Microfluidic FB technology could be especially advantageous for the capturing of DNA since is characterized by high surface to volume ratio, constant mixing, low flow resistance and continuous operation, therefore

potentially enhancing capture efficiency[109]. Here, its application will favor the specific capturing and the pre-enrichment of the BRAF target for the subsequent amplification through LCR and acoustic analysis. Part of these results are described at "Circulating tumor DNA extraction from biological samples on magnetic microfluidic fluidized bed at high throughput" (manuscript under preparation)

As shown in Figure 32, two main approaches for ctDNA extraction followed by LCR and acoustic analysis will be tested; target specific enrichment via hybridization on complementary capture probes followed by beads' collection and LCR either directly on beads or after release of the captured DNA. If the first approach works, i.e., on-beads LCR, then LCR directly on-chip could be investigated. Regarding the latter, successful on-chip molecular amplification reaction such as Rolling Cycle Amplification has previously been reported by Hernández-Neuta et al., 2018[110].

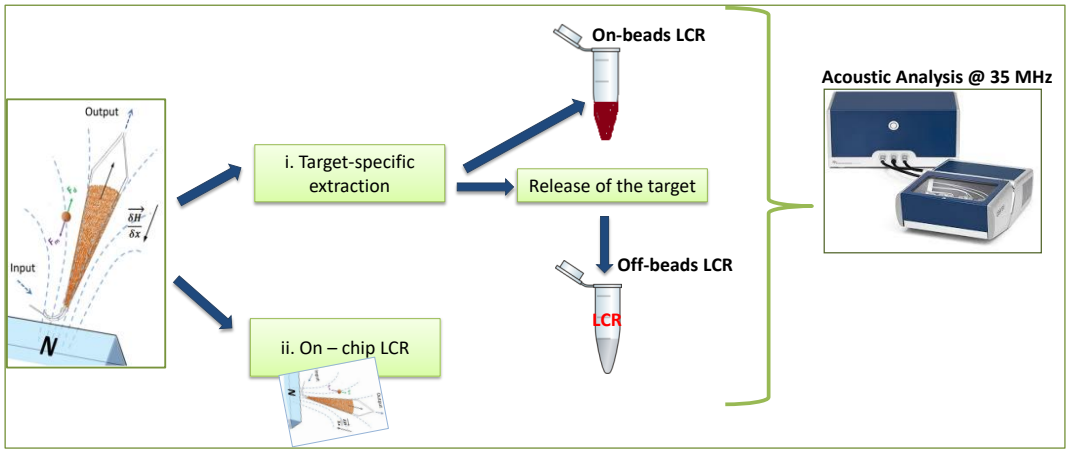

Figure 32. *Approaches of ctDNA extraction via the Fluidized bed followed by LCR and acoustic detection.*

Materials & Methods

Materials	
High-performance liquid chromatography (HPLC)-grade oligonucleotides	Metabion International AG, Germany or IDT Technologies, Leuven, Belgium
Dynabeads MyOne Streptavidin T1 of 1 µm	Invitrogen, US
Dynabeads M-270 Carboxylic Acid of 2.8 µm	Invitrogen, US
Adenosine 5'-Triphosphate (ATP) 10 mM	New England Biolabs, Mass., US
BSA, Molecular Biology Grade 20 mg/mL	New England Biolabs, Mass., US
Ampligase® DNA Ligase (5 U/µL)	Epicentre (Lucigen), Middleton, US
Ampligase® 10X DNA Ligase Reaction Buffer	Epicentre (Lucigen), Middleton, US
SYBR™ Safe DNA gel stain	Invitrogen, US
GelRed Nucleic Acid Gel Stain	Biotium, California, US
Proteinase K (20mg/mL)	Invitrogen, US
Biotin 20 mM in DMSO	
Phosphate buffer Saline (PBS) tablet	Sigma-Aldrich, Miss., US
Bovine Serum Albumin (BSA)	Sigma-Aldrich, Miss., US

Tris (hydroxymethyl) aminomethane hydrochloride (TRIS-HCL)	Sigma-Aldrich, Miss., US
Sodium chloride (NaCL)	Sigma-Aldrich, Miss., US
NeutrAvidiv Protein	Thermo Fischer Scientific, Mass., USA
BSA lyophilized powder, crystallized, ≥98.0% (GE)	Sigma-Aldrich, Miss., US
Biotin-$(AC_5)_2$-Sulfo-Osu	Dojindo, Japan
Microcon-30kDa Centrifugal Filter Unit with Ultracel-30 membrane	Merck KGaA, Darmstadt, Germany
1-palmitoyl-2-oleoyl-glycero-3-phosphocholine (POPC)	Avanti Polar Lipids Inc., Alabaster, AL, USA
Nuclepore polycarbonate hydrophilic membranes 0.2 µm	Whatman plc, UK

DNA Sequences of probes and primers (5' -> 3')	
bio-80nt BRAF MT	AAACTGATGGGACCCACTCCATCGAGATTTC**T**CTGTAGCTAGACC AAAATCACCTATTTTTACTGTGAGGTCTTCATGAA-**biotin**
bio-80nt BRAF WT	AAACTGATGGGACCCACTCCATCGAGATTTC**A**CTGTAGCTAGACC AAAATCACCTATTTTTACTGTGAGGTCTTCATGAA-**biotin**
BRAF-rev-80 bp	**biotin**-GAATTGAGGCTATTTTTCCACTGATTAAATTTT TGGCCCTGAGATGCTGCTGAGTTACTAGAAAGTCATTG AAGGTCT CA
BRAF–fw-80 bp	ATATATCTGAGGTGTAGTAAGTAAAGGAAAACAGTAGATCTCATT TTCCTATCAGAGCAAGCATTATGAAGAGTTTAGGT-**biotin**
BRAF-p1	**biotin**-GGATCCAGACAACTGTTCAAACTGATGGGACC CACTCCATCGAGATTTC**T**
BRAF-p2	CTGTAGCTAGACCAAAATCACCTATTTTTACTGTGAGGTCT TCATGAAGA
BRAF-cp1	**A**GAAATCTCGATGGAGTGGGTCCCATCAGTTTGAACAGTT GTCTGGATCC
BRAF-cp2	TCTTCATGAAGACCTCACAGTAAAAATAGGTGATTTTGGT CTAGCTACAG
BRAF-p2-ext20	CTGTAGCTAGACCAAAATCACCTATTTTTACTGTGAGGTCT TCATGAAGAGGGGGTAGGAGTGTCGTT
BRAF-cp1-new	GAAATCTCGATGGAGTGGGTCCCATCAGTTTGAACAGTTG TCTGGATCC
BRAF-cp2-new	TCTTCATGAAGACCTCACAGTAAAAATAGGTGATTTTGGT CTAGCTACAG**A**
20nt-DNAchol	**cholesterol**-GATGAACGACACTCCTACCCCC

** The red bold nucleotide corresponds to the mismatch discrimination nucleotide.*

DNA Sequences of targets (5' -> 3')		
AF488-80nt BRAF MT		**AF488**-TTCATGAAGACCTCACAGTAAAAATAGGTGATTTTG GTCTAGCTACAG**A**GAAATCTCGATGGAGTGGGTCCCATCA GTTT
AF488-80nt BRAF WT		**AF488**-TTCATGAAGACCTCACAGTAAAAATAGGTGATTTTG GTCTAGCTACAG**T**GAAATCTCGATGGAGTGGGTCCCATCA

	GTTT
BRAF-mt-277 bp	ACCTAAACTCTTCATAATGCTTGCTCTGATAGGAAAATGAGA TCTACTGTTTTCCTTTACTTACTACACCTCAGATATATTTCTT CATGAAGACCTCACAGTAAAAATAGGTGATTTTGGTCTAGCT ACAG**A**GAAATCTCGATGGAGTGGGTCCCATCAGTTTGAACA GTTGTCTGGATCCATTTTGTGGATGGTAAGAATTGAGGCTAT TTTTCCACTGATTAAATTTTTGGCCCTGAGATGCTGCTGAGTT ACTAGAAAGTCATTGAAGGTCTCA
BRAF-wt-277 bp	ACCTAAACTCTTCATAATGCTTGCTCTGATAGGAAAATGAGA TCTACTGTTTTCCTTTACTTACTACACCTCAGATATATTTCTT CATGAAGACCTCACAGTAAAAATAGGTGATTTTGGTCTAGCT ACAG**T**GAAATCTCGATGGAGTGGGTCCCATCAGTTTGAACA GTTGTCTGGATCCATTTTGTGGATGGTAAGAATTGAGGCTAT TTTTCCACTGATTAAATTTTTGGCCCTGAGATGCTGCTGAGTT ACTAGAAAGTCATTGAAGGTCTCA

** The red bold nucleotide corresponds to the mismatch site.*

Capturing of AF488-80nt *BRAF* MT/WT ssDNA targets spiked in PBS using the 2nd generation of Fluidized Bed (FB). For these experiments PDMS chips were used. The chips were of 250 μm high and had capacity for 500 μg magnetic beads. Pressure and flow rates required for the experiments were controlled with All-in-One (A-i-O) software (Fluigent, France). Prior to any experiment the streptavidin coated Dynabeads were functionalized with 100 pmol of the biotinylated bio-80nt *BRAF* MT or WT capture probes which were fully complementary to the *BRAF* sequences AF488-80nt *BRAF* MT or WT, respectively. To start the experiment, the system was initially filled with a solution of PBS-BSA 1%. Then, beads of 2 different diameters were introduced manually by using a pipette tip installed at the outlet of the chip and guided at the right position in the chip by moving a magnet. Specifically, the Dynabeads MyOne Streptavidin T1 of 1 μm & the Dynabeads M-270 Carboxylic Acid of 2.8 μm mixed in 1:1 ratio (250 μg each) were used. After the bead loading, the NdFeB12 permanent magnet of 1.47T was placed close to the chip inlet and aligned with the chamber axis at a 1.50 mm distance. Vibrating of the input tube was also applied to achieve a good homogeneity of the beads during the experiment. Following the set-up of the system, 10 nM (corresponding to 2.5 pmol of ssDNA) of the 5' fluorophore labeled AF488-80nt BRAF MT or AF488-80nt *BRAF* WT target (excitation maximum at 499 nm and emission maximum at 520 nm) diluted in buffer (Tris-HCl, 5mM EDTA, NaCl 1M, Tween 20 0.1%, pH=7.5) were loaded for 16 min with a flow rate of 15 μL/min at 49 ^{o}C. Intensity of the un-captured target was measured in the exit of the fluidized bed with inverted microscope and compared with the highest intensity derived from the 10 nM when loaded on the fluidized bed system without beads.

Beads collection and treatment prior to linear LCR. Following capturing, the beads were pushed out from the chip and collected into a 1.5 mL tube. The tube was placed in the magnetic rack for 3 min followed by removement of the supernatant and resuspension of the beads in 15 μL of mili-Q water. Then, the beads were heated at 95 °C for 10 min.

Following heating, the beads were immediately transferred in a magnetic rack placed into the ice, to prevent the rehybridization of the DNA target with the capture probes bio-80nt BRAF MT or bio-80nt BRAF WT. Finally, 14 μL of the supernatant were collected and mixed with the linear LCR cocktail as mentioned below.

Phosphorylation of the *BRAF*-cp1, *BRAF*-p2, *BRAF*-cp1-new and *BRAF*-p2-ext20 LCR probes. 300 pmol of each probe were mixed with 1x T4 PNK reaction buffer, 1 mM ATP, 0.1 μg/μL BSA and 10 U T4 PNK Enzyme in a total reaction volume of 50 μL. The mixture was incubated at 37 °C for 60 min followed by heat inactivation at 65 °C for 20 min. The reactions were stored at -20 °C till use.

Linear LCR on 80 nt DNA targets mimicking the *BRAF* sequence. All reactions were performed in the thermal cyclers Tprofessional Basic Gradient 96 or T-Personal Combi Thermocycler (Biometra, Analytik Jena GmbH) in total volume of 25 μL. Each mixture contained 1x AmpLigase DNA Ligase Reaction buffer, 0.1 μg/μL BSA, 2.5 U of the thermostable AmpLigase DNA Ligase enzyme and 1 pair of probes. Two different templates were used; the AF488-80nt *BRAF* MT / WT targets or their complementaries bio-80nt BRAF MT / WT. When the AF488-80nt *BRAF* MT / WT targets were used 10 pmol of each BRAF-cp1 and *BRAF*-cp2 probes were added in the reaction. Similarly, for the amplification of the bio-80nt *BRAF* MT / WT targets the *BRAF*-p1 and *BRAF*-p2 pair of probes was used. In each case the reaction was heated at 92 ^{o}C for 3 min followed by 5 sec denaturation at 92 ^{o}C and 10 sec ligation at 70 ^{o}C. A no template control (NTC) was included in every run. LCR products were then analyzed either by gel electrophoresis on 2.0 % (w/v) agarose gel and visualized, under UV light, after staining with SYBR Safe DNA gel stain to check the presence of specific amplification products. A no template control (NTC) was included in every run.

Capturing of dsDNA *BRAF* targets spiked in serum or plasma samples using the fluidized bed (FB). Plasma or serum samples (300 μL) pretreated with Proteinase K (2.5 mg/L) for 2h at 37 °C were mixed with the *BRAF*-mt-277 bp or *BRAF*-wt-277 bp targets at various concentrations ranging from 10 pM to 10 fM and with 0.4μM of each biotinylated capture probe *BRAF*-fw-80 bp and *BRAF*-rv-80 bp. Capture probes were complementary to the antisense and sense strand of the BRAF-mt/wt 277 bp target. After mixing, the sample was heated at 95°C to denature the dsDNA followed by cooled down allowing the capture probes to anneal at each strand of the DNA. To start the experiment, the FB was initially filled with PBS-BSA 1% and then, 500 μg of streptavidin (SAv)-coated magnetic beads Dynabeads MyOne Streptavidin T1 (1 μm) & the Dynabeads M-270 Carboxylic Acid (2.8 μm) mixed in 1:1 ratio (250 μg each) were introduced manually and guided at the right position in the chip by moving a magnet. After the bead loading, the magnet was aligned with the microfluidic chamber and positioned at a distance of 1.5 mm from the chip inlet. Then, 150 μL of the treated plasma or serum sample was injected in the chip at the flow rate of 5 μL/min. Following capturing of the complex “capture probe-DNA target” on the streptavidin-coated beads a last step of PBS injection was performed. Pressure and flow rates required for the

experiments were controlled with All-in-One (A-i-O) software (Fluigent, France). Vibrating of the input tube was also applied to achieve a good homogeneity of the beads during the experiment. dsDNA capturing on the beads was evaluated by LCR and acoustic analysis as described below.

Beads collection and treatment prior to exponential LCR. Following capturing, the beads were pushed out from the chip and collected into a 1.5 mL tube. Then, the tube was placed in the magnetic rack for 3 min, the supernatant was removed and the beads were mixed with 50 µL of 4 µM biotin diluted in mili-Q water for 10-15 minutes at RT. Following incubation, three washing steps with mili-Q water took place. After the last washing step, the beads were resuspended in 16 µL mili-Q water and heated at 95 °C for 5 min. Following heating, the beads were immediately transferred *in a magnetic rack placed into the ice,* to prevent the rehybridization of the DNA target with the capture probes BRAF-rev-80 bp & BRAF-fw-80 bp. Finally, 15 µL of the supernatant were collected and mixed with the exponential LCR cocktail as mentioned below.

Exponential LCR amplification on dsDNA targets mimicking the *BRAF* sequence. All reactions were performed in the thermal cycler FastGene® Ultra Cycler Gradient with 96 wells (NIPPON Genetics, Europe) or the QuantumStudio3-RealtTime PCR (Applied Biosystems, USA). Each reaction were of 25 µL containing 2 pmol of each probe (*BRAF*-p1-biotin, *BRAF*-p2-ext20, *BRAF*-cp1-new and *BRAF*-cp2-new), 1x AmpLigase DNA Ligase Reaction buffer, 0.1 µg/µL BSA and 1 U of the thermostable AmpLigase DNA Ligase enzyme. The template was either the 15 µL of the beads/released target described above, or 2.5 µL of the input or output serum and plasma samples. The amplification protocol consisted of an initial denaturation step at 94 °C for 3 min and 30 cycles of denaturation at 92 °C and annealing/ligation at 65 °C, each step for 5 sec. LCR products were then analyzed either by gel electrophoresis on 2.0 % (w/v) agarose gel stained with GelRed Nucleic Acid Gel Stain or with acoustic experiment as described below. A no template control (NTC) was included in every run.

Acoustic device. The QSense Analyzer (E4 instrument) (Biolin Scientific, Sweden) was used for the simultaneous recording of frequency and dissipation changes at the 35 MHz (7^{th} overtone); ΔF was not normalized by the overtone number. The QSense device was connected with the peristaltic pump MINIPLUS Evolution peristaltic pump (GILSON, USA) to adjust the flow rate at 50 µL/min, unless otherwise stated. Measurements were performed in continuous flow of PBS buffer pH=7.4, at 25 °C. All samples were diluted in the running buffer, PBS pH=7.4 and following each addition, buffer rinsing was taken place. Prior to the experiment, the used Au-coated 5 MHz sensors were cleaned with Helmanex 2% for 15 min, rinsed with mili-Q water and 70 % EtOH and dried under N_2 flow. Then the sensors were subjected to 30 min UV/Ozone cleaning (Ossila Ltd, Sheffield).

Liposome preparation. Lyophilized 1-palmitoyl-2-oleoyl-glycero-3-phosphocholine (POPC) lipids were dissolved in chloroform at final concentration of 10 mg/mL. 100 – 200 µL of the 10 mg/mL lipids were added in round bottom glass flask and dried homogenously under N_2 flow. The lipid film was then left for 30 min under N_2 gas followed by resuspension in PBS at a final concentration of 2 mg/mL by gentle vortex. The resulting suspension was passed through polycarbonate membranes with a nominal pore diameter of 200 nm, using the Avanti Mini-Extruder. Stock solutions were stored at 4 °C for up to 6 days.

Acoustic analysis of LCR. For the analysis of the LCR products, the gold sensor surface was firstly functionalized with 250 µL x 0.2 mg/mL b-BSA followed by the addition of 200 µL x 0.05 mg/mL NAv. Then, 20 µL of LCR mix was diluted in PBS at a final volume 125 µL and injected into the system at the flow rate of 25 µL/min. Following LCR addition, 200 µL x 500 nM 20nt-DNA-chol were loaded followed by the addition of 500 µL x 0.2 mg/mL solution of 200 nm POPC liposomes. b-BSA was prepared after incubation of BSA lyophilized powder with biotin-$(AC_5)_2$-Sulfo-Osu linker in PBS, in a molar ratio of 1:10, for 1 h and 30 min at RT; after incubation, BSA was purified using the Microcon-30kDa Centrifugal Filter Unit with Ultracel-30 membrane following manufacturer instructions.

Results & Discussion

1. Selective capturing of synthetic ssDNA BRAF target followed by LCR amplification

The experiments described in this section took place at the Macromolecules and Microsystems in Biology and Medicine (MMBM) Lab at the Institut Curie, Paris, France.

In this set of experiments, we focused on the capturing of synthetic oligonucleotide ssDNA target spiked in buffer. The target was of 80 nt length carrying (mt) or not (wt) the *BRAF* V600E point mutation in the middle of the sequence. Moreover, both the mt and the wt ssDNA BRAF targets were modified by the fluorophore Alexa-Fluor (AF) 488 at their 5'end to evaluate the capture efficiency by measuring the fluorescence intensity at the outlet of the channel chip (Fig. 33).

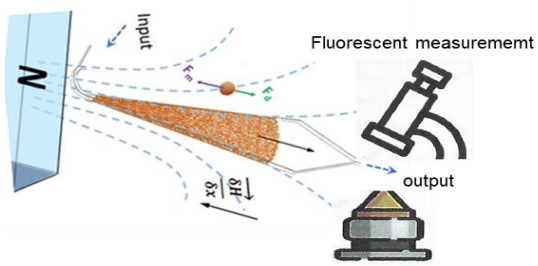

Figure 33. *Basic experimental set up of fluidized bed.*

a. Development of a linear LCR protocol for the amplification of AF488-80nt *BRAF target*

Prior to any experiment involving the combined application of the FB with the LCR, LCR performance was firstly verified with the detection of 1 pmol of AF488-80nt *BRAF* mt, wt (wt control) or no template control (NTC). Reaction mixtures containing 5 pmol of each probe (*BRAF*-p1, *BRAF*-p2, *BRAF*-cp1 and *BRAF*-cp2) were subjected to exponential amplification through 99 cycles of denaturation at 92 °C for 5 sec and ligation at 75 °C for 10 sec (LCR protocol described in part 2-1st app.). Gel electrophoresis analysis revealed blunt-end ligation to all three samples despite the use of an optimized protocol (data not shown). This result is likely ascribed to the employment of a different thermocycler. While different protocols with changed annealing temperature, time and fewer cycles were tested, none of them gave rise to specific amplification products. For this reason, a linear LCR (LCR with just the one pair of complementary probes) protocol was developed where the template was mixed with 10 pmol of each complementary probe -*BRAF*-cp1 and *BRAF*-cp2- and subjected into 56 cycles of linear LCR (5'' denaturation at 92 ^{o}C followed by 10'' ligation step at 70 ^{o}C). Figure 34 shows the specific amplification of 1 pmol mt, wt targets or NTC under optimized conditions. Note that, a slight background signal was observed in the case of wt, however, that was not of concern in this stage of experiments. Lower than 1 pmol DNA amounts were also tested, but no ligation products were observed. Thus, for the combined experiments with the fluidized bed we focused on high concentration inputs, i.e. 10 nM (otherwise 2.5 pmol diluted in 250 μL buffer).

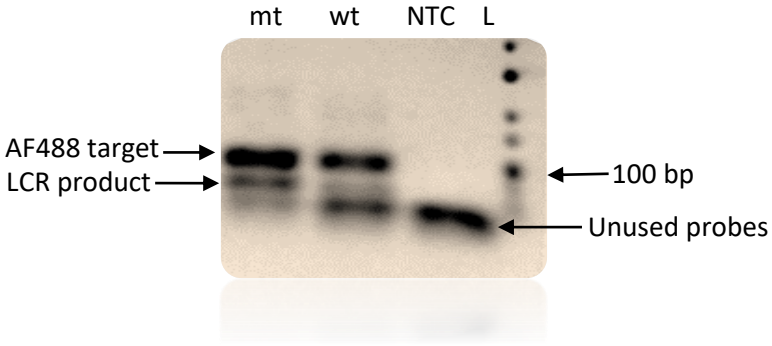

Figure 34. *Linear LCR for the amplification of 1 pmol mt, wt or no template (NTC) AF488-80nt BRAF target. In each case template was mixed with 10 pmol of the complementary probes BRAF-cp1 and BRAF-cp2 and subjected to 56 repeats of 5'' denaturation at 92 ^{o}C and 10'' ligation step at 70 ^{o}C. The GeneRuler Low Range DNA Ladder 25 bp (L) was used. Note that, LCR product is single strand of 100 bases and runs below the 100 bp molecular weight.*

b. Capturing of AF488-80nt *BRAF* target on fluidized bed followed by LCR

To evaluate the overall combined assay, 240 μL x10 nM (1.5 x10^{12} copies) of AF488-80nt *BRAF* target containing (mt) or not (wt) the V600E single nucleotide mutation was prepared in buffer and captured by hybridization on the Myone^{TM} streptavidin-coated magnetic beads. For the specific capturing, the beads were functionalized with the fully complementary to the target probes biotin-*BRAF*-80nt mt or wt. The experiments were performed using the 2nd generation fluidized bed and a microfluidic platform implemented

on an epifluorescence inverted microscope. The capture efficiency of the mt and wt target was estimated at approximately 75 %.

Following capturing, the mt and wt ssDNA targets were released from the beads via heat, collected to a different tube and amplified under optimized LCR conditions. As presented in Figure 35, visualized LCR products were generated only in the case of mt target, indicating the successful detection of the target following capturing and release from the fluidized bed with high specificity.

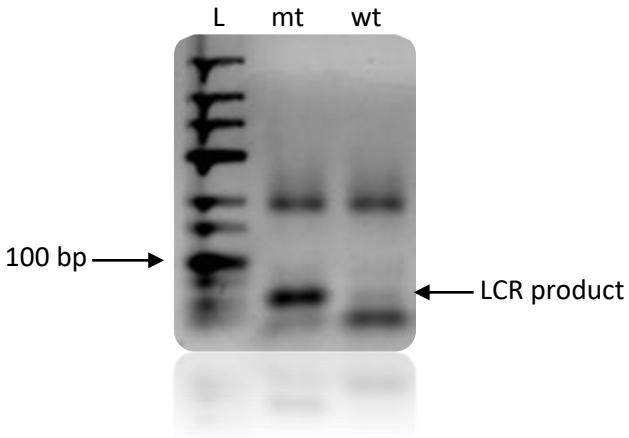

Figure 35. *Detection of 10 nM mt and wt AF488-80nt BRAF target by linear LCR following capturing on the fluidized bed (capture efficiency of 75%) and heat-release of the target. The GeneRuler Low Range DNA Ladder 25 bp (L) was used.*

Next, it was tested the detection of 240 μL x10 nM (1.5 x10^{12} copies) AF488-*BRAF* mt and wt targets following capturing on the fluidized bed and on-beads linear LCR. Specifically, after the experiment, the beads with the captured target were collected and subjected to two LCR assays differentiated in the added amount (normal and high concentration) of the LCR probes. The above aimed to overcome the competition of the LCR probes with the captured probes since they were complementary for the same region of the target. LCR products were analyzed in 2% agarose gel. As shown in figure 36, no LCR product was detected.

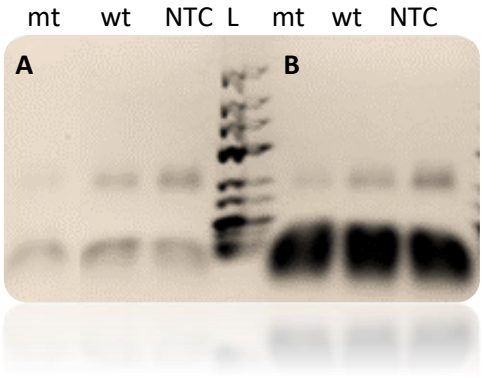

Figure 36. *On-beads LCR for the detection of mt/wt or no template (NTC) AF488-80 nt BRAF target after capturing on fluidized bed. 1/2 of beads (250 μg) with captured mt, wt or no target were mixed with a) 10 pmol or b) 40 pmol of probes and subjected into linear LCR. In both cases, no clearly visible ligated product was*

produced. This was partially expected since both the 50 pmol of capture probes with which were functionalized the streptavidin-coated beads and the LCR probes competed against the same region of the target.

To understand if LCR did not work due to the competition of the capture probes with the probes of LCR or due to the presence of the magnetic beads, linear LCR reaction was carried out for the detection of the bio-80nt or AF488-80nt BRAF mt/wt targets in the presence of a) magnetic beads which were functionalized with 20nt probes non-complementary to the BRAF sequence and b) non-functionalized magnetic beads. As presented in fig. 37, the mt target was successfully amplified in all cases. The above results indicated that the main limitation for the on-beads LCR was the competition between the LCR probes and the captured probes, which were complementary for the same region of the target.

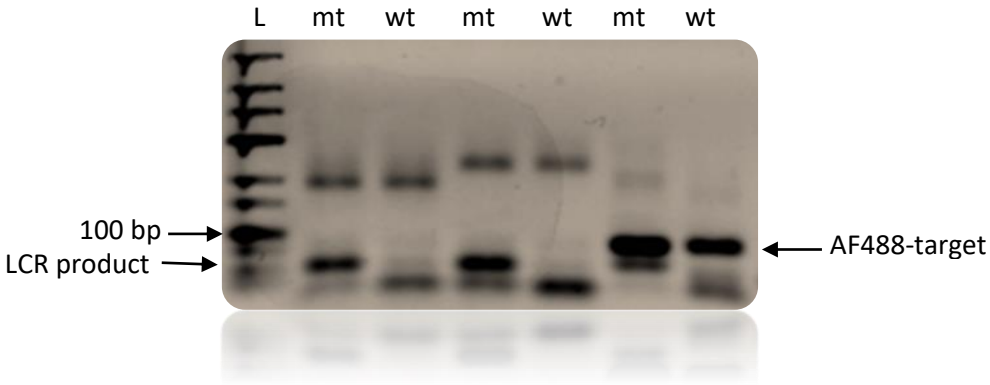

Figure 37. *Detection of 1 pmol BRAF target by linear LCR, in the presence of functionalized and non-functionalized streptavidin coated magnetic beads: left -> right: 25 bp ladder (L), 1 pmol mt, 1 pmol wt bio-80nt BRAF in the presence of magnetic beads functionalized with a 20nt probe non-complementary to the target, 1 pmol mt, 1 pmol wt bio-80nt BRAF in the presence of non-functionalized magnetic beads and 1 pmol mt, 1 pmol wt AF488-80nt BRAF in the presence of non-functionalized magnetic beads. Note that the 50 % of magnetic beads are streptavidin coated and probably interact with the template. In all cases mt target was successfully amplified with high specificity in the presence of magnetic beads.*

2. Detection of dsDNA targets in serum and plasma followed by LCR amplification and acoustic detection

Following the successful off-beads combination of the magnetic FB technology with the LCR for the detection of ssDNA *BRAF* target, the next step was the capturing of dsDNA BRAF targets spiked in human serum and plasma followed by amplification via exponential LCR (described in part 2-2nd app.) and acoustic detection. Concerning the DNA capturing, a second strategy was developed by MMBM lab in order to tackle the challenge of the dsDNA present in biological samples. In this approach, firstly 300 µL of plasma or serum samples were pretreated with Proteinase K to digest protein that can interfere in the ctDNA capture. Then, synthetic *BRAF* target of 277 bp carrying or not the V600E mutation was spiked in at various concentrations and mixed with the complementary biotinylated capture probes (CP) *BRAF*-fw-80 bp and *BRAF*-rv-80 bp (1). The mixture was heated at 95°C to denature dsDNA (2) and cooled down to allow the capture probes to anneal at each strand of DNA (3). Finally, 150 µl of the treated sample was injected through the FB (at 5 µL/min) containing Myone^{TM}

streptavidin-coated magnetic beads which bound the bio-CP-target complex (4). Detection of the ctDNA captured on the beads was evaluated by LCR and acoustic detection (5) (Fig. 37).

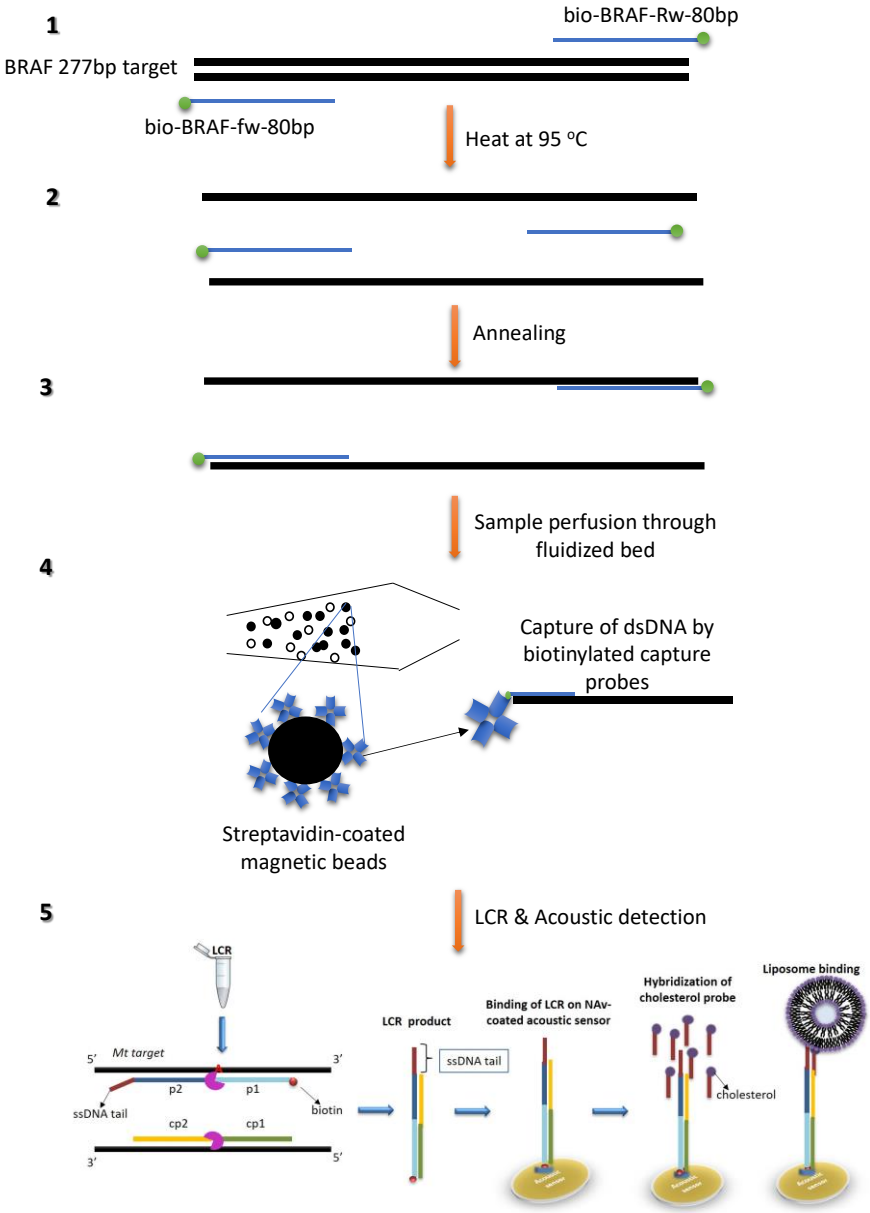

Figure 37. *Methodology of dsDNA capturing in human serum or plasma applying the fluidized bed.*

A first series of experiments were performed on human serum with the collaboration of biosensors lab at the Institute of Molecular Biology and Biotechnology (IMBB) (Heraklion, Greece). For these experiments, a compact and portative FB platform was developed by MMBM group and installed at biosensors lab. This automated prototype was developed by integrating different fluidic modules and fully controlled by a PC interface to allow an automated DNA extraction (Fig. 38).

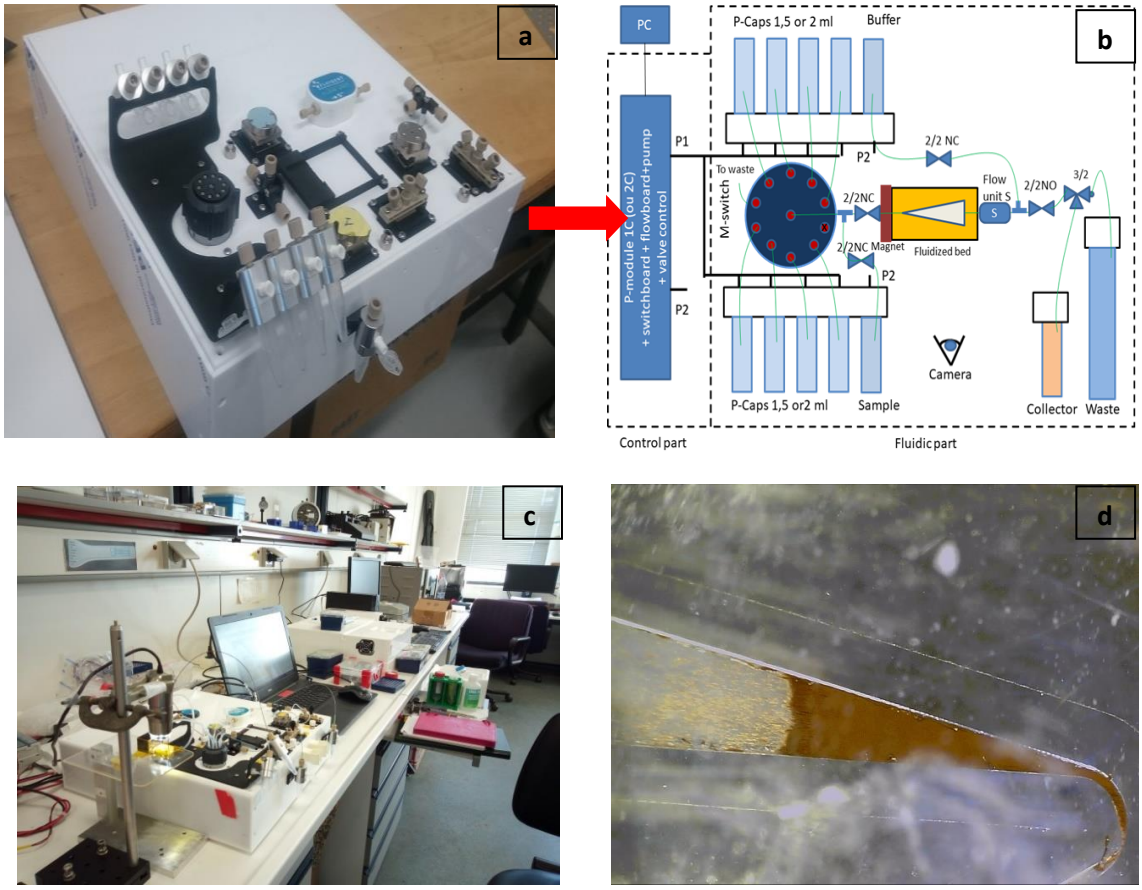

Figure 38. *(a) Picture of the fluidized bed microfluidic platform, (b) schematic illustration of microfluidic system from Fluigent Microfluidic Inc, (c) FB platform installed at IBMM-Forth (Heraklion, Greece) and (d) FB microchip filled with magnetic beads.*

a. Capturing of dsDNA 277 bp *BRAF* target in serum samples followed by LCR and acoustic analysis

Serum samples obtained from healthy donors were spiked in with the mutant dsDNA 277 bp *BRAF* sequence. Following the capturing on magnetic beads, the serum samples and the beads were collected and analyzed. As previously mentioned, LCR was carried out either directly on-beads or after the release of the target from the beads (Fig. 39). Prior to LCR, beads were treated with biotin to block the free streptavidin pockets. This step was necessary in order to prevent the binding of the biotinylated LCR probes and the biotinylated LCR product to the streptavidin-coated beads.

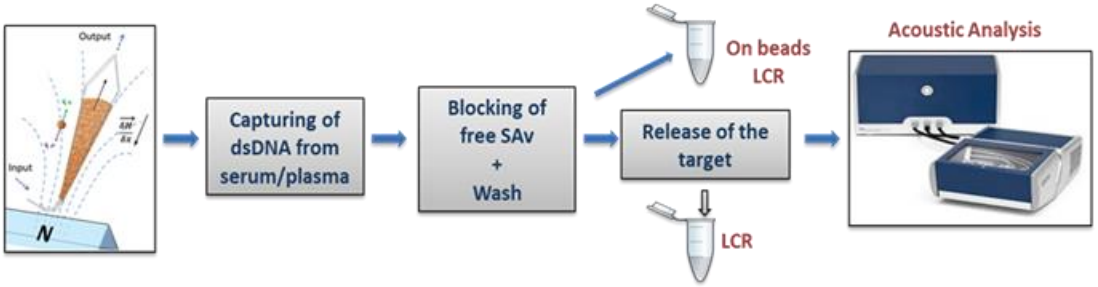

Figure 39. *Schematic representation of the capturing of dsDNA mt target from plasma and serum samples followed by LCR and acoustic analysis.*

Initially, the extraction and the acoustic detection of 150 µL x1 pM (9 x10^7 copies) dsDNA mt target spiked in serum was investigated. As stated above, following extraction and before the LCR, beads were treated with 4 µM biotin to block the free streptavidin pockets, followed by 3 washing steps with dH_2O. Figure 40, presents the real-time graphs obtained by the acoustic analysis of both LCR reactions i.e., from LCR directly on-beads and LCR with only the released target. The ΔD and ΔF values obtained at the liposome step accounted for ΔD=2.1 x10^{-6} / ΔF=-10 Hz and ΔD=16.24 x10^{-6} / ΔF=-140 Hz for on beads-LCR and beads-free LCR, respectively. The outcome was also confirmed by gel electrophoresis (Fig. 41). A Positive control LCR derived from 2.5 µL (15 x10^5 copies) of the initial sample (1 pM of dsDNA 277 bp *BRAF* target spiked in human serum) was also included in the gel analysis. Overall, the above results indicated that LCR was significantly more efficient following release of the target. Hence, for the rest of the experiments, we focused on the target-release approach.

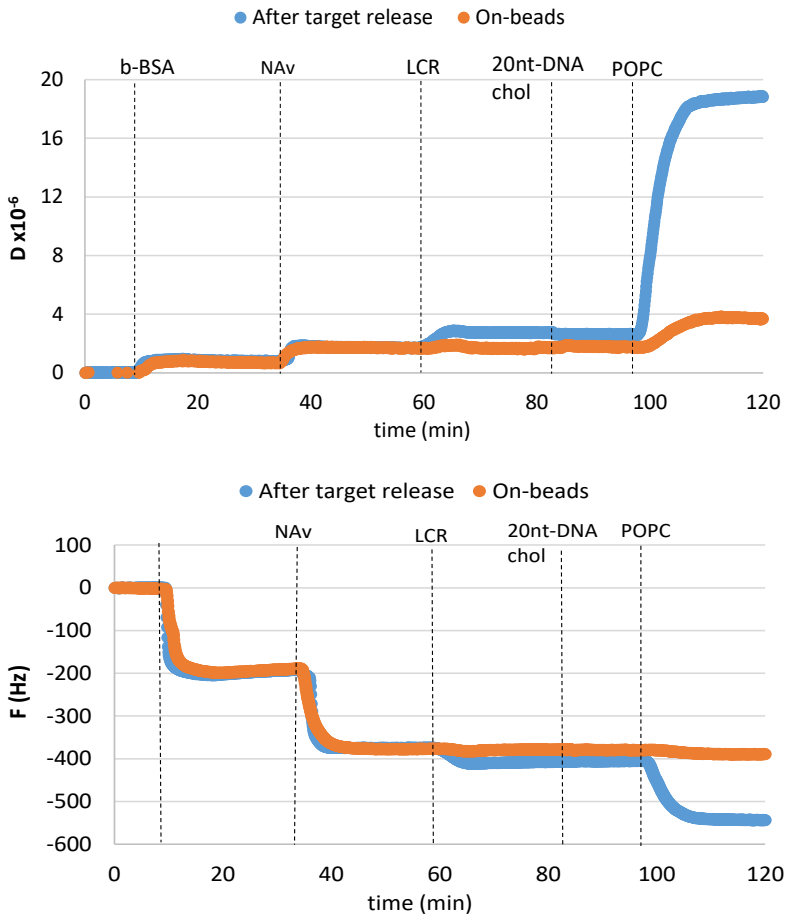

Figure 40. *Comparison of the ΔD (left) and ΔF (right) real-time curves obtained by the acoustic analysis of the LCR reactions of 1 pM of ds277 bp BRAF mt target after capturing in serum samples by the fluidized bed.*

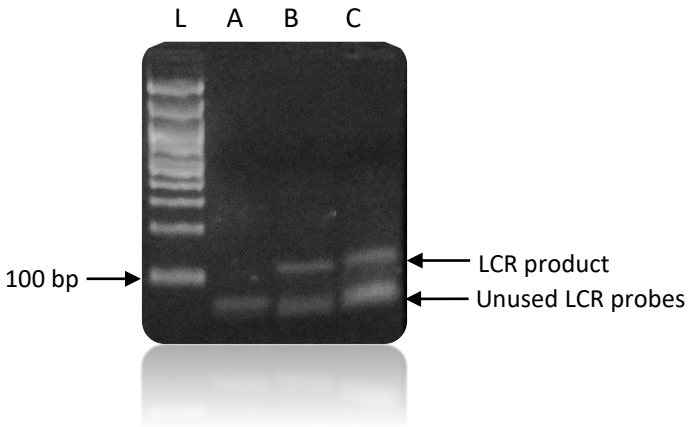

Figure 41. *Detection of 1 pM (*9 x10^7 copies) *dsDNA 277 bp mt BRAF target by gel electrophoresis (2 % agarose gel) of LCR products after capturing in serum samples by fluidized bed. Left -> Right; 100 bp Ladder (L), LCR on-beads (A), LCR off-beads (B), LCR form initial serum sample (C). The expected LCR product size is 120 bp.*

Lower DNA concentrations such as 100 fM (9 x10^6 copies) were also analyzed. In this case, LCR was successfully carried out only after release of the target and the products were analyzed exclusively by gel electrophoresis as presented in Figure 42.

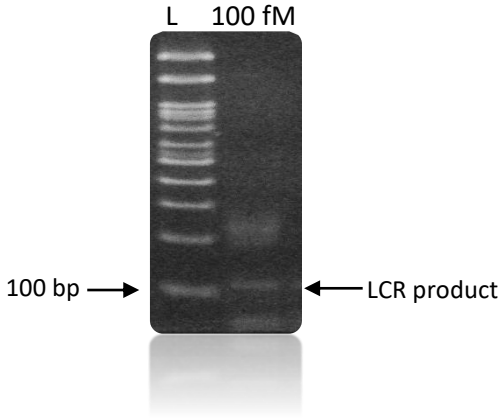

Figure 42. *Detection of 100 fM dsDNA 277 bp mt BRAF target following capturing in human serum by the fluidized bed and heat-release. LCR products were visualized on 2 % agarose gel. Left -> right: 100 bp Ladder (L), off-beads LCR. The expected LCR product size is 120 bp.*

Since the carrying of the LCR was not taking place in the presence of the beads, blocking of free streptavidin pockets was not necessary. Moreover, taking into account that the washing steps with the dH_2O could destabilize and partially release the captured target due to low salt concentration, the beads were washed 3 times with PBS and re-suspended in dH_2O. By this protocol, 100 fM (9 x10^6 copies) and 1 fM (9 x10^4 copies) of mt target were captured on FB and analyzed by LCR and acoustic detection. However, no or very low detection occurred (data not shown). Regarding the 1 fM, this was expected because of the low capture efficiency of the FB for this concentration (approximately 40 % according to calculations from previous experiments at the MMBM lab) which led to low template input for the final LCR reaction. On the other hand, we waited for a better result concerning the 100 fM concentration. We thus suspected that the changes in the protocol may negatively affected

the assay. For this reason, the rest experiments were performed by the initially described protocol and the capturing of 1 pM was successfully repeated.

b. Capturing of dsDNA 277 bp *BRAF* target in plasma samples followed by LCR and acoustic analysis

To continue the extraction experiments plasma was selected due to its validity and wide application for ctDNA analysis in clinical practice compared to serum[61,163,164]. In this set of experiments, 150 µL of 10 pM (9 x10^8 copies) – 10 fM (9 x10^5 copies) *BRAF* target carrying (mt) the V600E point mutation were spiked in human plasma and captured through the FB. In all cases the capture efficiency was expected to be at ~70% ± 10% according to experiments performed at the MMBM lab. To verify the specificity of the technique, as control samples containing 10 pM (9 x10^8 copies) – 10 fM (9 x10^5 copies) of dsDNA 277 bp wt target were prepared and analyzed as well. Except from the wt control, negative controls, including plasma samples without any DNA template, passed from FB as well. Following capturing all samples were subjected to LCR amplification and acoustic experiment. ΔD and ΔF values were measured at the liposome step and presented in figure 43. According to the plot, a detection limit of 1 pM (9 x10^7 copies) mt target was recorded when compared to the corresponding wt control. As a control, we also analyzed LCRs derived from 2.5 uL initial sample i.e., plasma spiked in with mt or wt dsDNA 277 bp at a concentration of 10 fM – 10 pM. Keep in mind that LCR's detection limit was set at 3.3 x10^3 copies when target was spiked in buffer. As shown in Fig. 44, clearly, the overall efficiency of the assay was negatively affected by the sample source, since only the 1.5x10^6 – 1.5x10^7 (otherwise 2.5 µL x 1 pM – 2.5 µL x 10 pM) were detected.

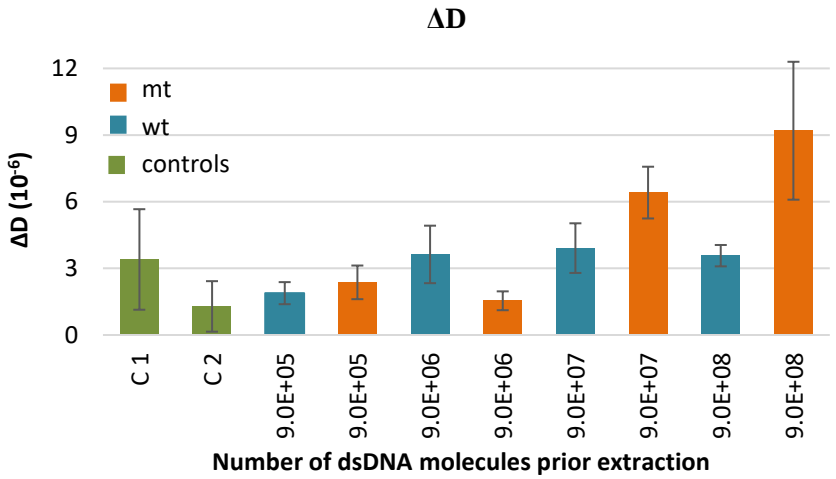

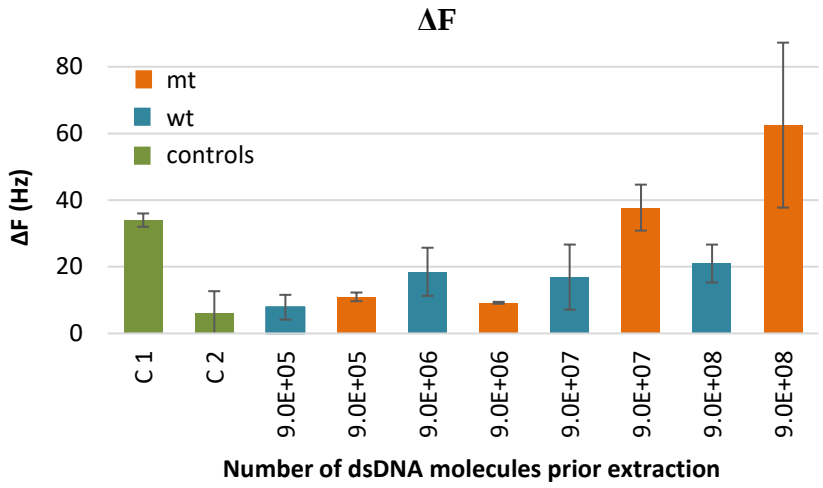

Figure 43. *Comparison of ΔD and ΔF changes recorded at the 200 nm POPC liposome step during the acoustic analysis of LCR derived from dsDNA 277 bp BRAF mt/wt targets spiked in human plasma samples following capturing on FB. C1 and C2 correspond to negative control plasma samples with and without capture probes, while NTC correspond to typical no template LCR (LCR + water). Note that, capture efficiency was about 70% ± 10%.*

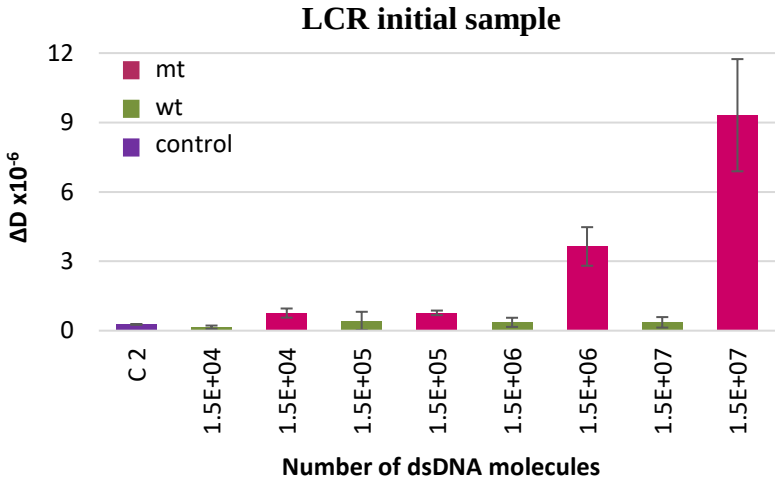

Figure 44. *Comparison of ΔD changes recorded at the 200 nm POPC liposome step during the acoustic analysis of LCR derived from 2.5 μL human plasma samples spiked in with dsDNA 277 bp BRAF mt/wt targets at various concentrations ranging from 10 fM – 10 pM (otherwise 1.5 x10^4- 1.5 x10^{7}copies). C2 corresponds to negative LCR control, plasma sample without DNA.*

Conclusions

Concluding, during the first set of experiments an initial protocol was established for the capturing on the fluidized bed of the ssDNA carrying or not the *BRAF* V600E point mutation spiked in buffer. Capturing was followed by linear LCR for the specific enrichment of the mt target. Two methods were explored: LCR directly on beads or LCR after the release of the target. LCR reactions were analyzed on 2 % agarose gel. By this protocol, 10 nM (1.5 x10^{12} copies) of 80 nt mt targets were successfully detected with high specificity, when compared with a wt control and when the target was released from the beads. Then, the capturing of mt dsDNA target spiked in human serum or plasma samples was investigated this time using a portable and automated FB device. Capturing was followed by exponential LCR and

acoustic detection. This time, the detection of the dsDNA sequence of interest was possible at a concentration of 100 fM (9 x10^6 copies) - 1 pM (9 x10^7 copies) in human serum and 1 pM (9 x10^7 copies) – 10 pM (9 x10^8 copies) in human plasma samples, respectively. However, the release of the target from the beads was proved once again to be critical for the LCR to achieve efficient amplification of the mt target.

Regarding the high detection limit of the assay, this could be attributed to various parameters such as the source of the sample, the capture and the release efficiency of the target. While, more research is required for the application of the overall method, i.e., FB combined with LCR, to blood samples for ctDNA extraction, the proposed technique may has potential for the extraction and detection of other kinds of targets as well. These targets can be miRNAs presented in plasma or serum, DNA from pathogens or human genomic DNA for the determination of single nucleotide polymorphisms linked with genetic diseases. Regarding FB, notable advancements of this technology are the ability to extract in a fast and simple manner only the DNA targets of interest from a heterogonous DNA population; work with crude samples like serum, plasma etc; and enrich and concentrate specific areas of the DNA target. All the above could significantly favor the downstream analysis.

Chapter 4

Detection of cancerous point mutations with an acoustic array biochip combined with Allele-Specific PCR

Introduction

As summarized in the main introduction, PCR-based techniques are the most well studied and applied for the detection of point mutations in both genomic and cell-free DNA. Among them, ddPCR constitutes the most reliable choice due to its high sensitivity (<0.01% MAF), specificity and absolute quantification ability. However, ddPCR is costly and remain complex for routine clinical analysis. The immediate next option which can provide an acceptable sensitivity with low cost are the various Allele-Specific PCR-based approaches. During Allele-Specific PCR the 3' terminal nucleotide of the sense, antisense or both primers is complementary to the point mutation/single nucleotide variant site. The primer which holds the discrimination activity is called allele-specific primer. In the presence of a mismatch, the last nucleotide of the 3' end of the allele-specific primer does not match with the template DNA thus obstructing the subsequent polymerization when the DNA polymerase lacks 3' -> 5' exonuclease proofreading activity (Fig. 1). To further enhance primer specificity artificial mismatched nucleotides can be introduced at the penultimate (second to the terminal) or the antepenultimate (third to the terminal) position at the 3'-end of the allele-specific primer[71,165]. The best reported detection sensitivity for AS-PCR techniques is 0.1 % - 1%[66,70,71] and 0.1% - 2%[73,74] for genomic and ctDNA, respectively. Despite the acceptability of these detection limits, more research for the achievement of better ones closer to those of ddPCR is performed. The above would lead to a low-cost and equally reliable to ddPCR assay.

In this work, Allele-Specific PCR (AS-PCR) is combined with the novel High Fundamental Frequency Quartz Crystal Microbalance (HFF-QCM) biochip array operating at 150 MHz for the direct detection of point-mutations in the *BRAF* and *KRAS* genes. Details about the design, operation and validation of the HFF-QCM acoustic biosensor and the biochip array have been already described in Chapter 2, part 2. Briefly, the new biochip array allows the fast and cost-effective analysis of up to 6 samples and the extraction of up to 24 measurements (4 measurements/sample). Acoustic detection is coupled with an ultrasensitive AS-PCR for the specific amplification of just 1-10^3 mt DNA targets carrying the *BRAF* V600E or *KRAS* G12D point mutation in a background of 10^4 wt molecules, otherwise with a sensitivity of 0.01 – 10 %. We chose these mutations as the most frequently observed in the corresponding genes[96,103]. The clinical value of *BRAF* and *KRAS* identification status as a diagnostic, prognostic and treatment selection marker has been already described in Chapter 1. For their selective amplification we use a pair of primers modified in their 5' ends with biotin and cholesterol, therefore permitting the direct immobilization of the AS-PCR dsDNA products on the sensor surface, obviating the need for a hybridization step (Fig. 1). Furthermore, in order to enhance the detection capabilities of the assay, POPC liposomes of 200 nm are employed as acoustic signal enhancers. Moreover, for the experiments, the standard QCM-D device (QSense analyzer) and the sensor operating at 35 MHz (7^{th} overtone) were used as a reference.

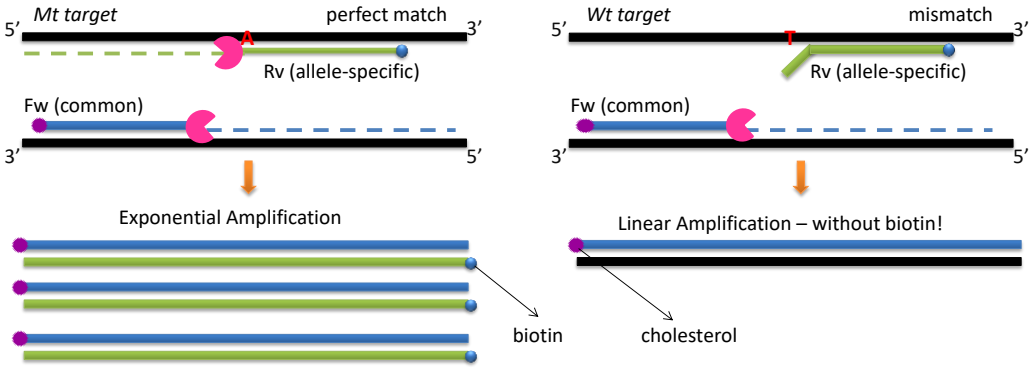

Figure 1. *Detailed representation of Allele-specific PCR. Here, the Fw primer is common and amplifies both the mt and wt sequence, the latter in a linear way. Upon hybridization of the Rv allele- specific primer, exponential amplification will occur only when the 3' end of the primer is complementary to the target (mt). Note that the primers are modified with the biotin being at the allele-specific primer. This means that only the products derived from the favourable target (here the Mt) would be immobilized on a potential acoustic experiment with NAv-substrate. Dashed lines represent the primer extension from the polymerase (pink).*

Materials & Methods

Materials	
High-performance liquid chromatography (HPLC)-grade oligonucleotides	Metabion International AG, Germany or Eurofins Genomics Ebersberg, Germany
gblock *BRAF* V600E/wt	Integrated DNA Technologies, Inc., BVBA, Belgium
***BRAF* V600E reference standard, 50 %**	Horizon Discovery Ltd, UK
***BRAF* wt reference standard**	Horizon Discovery Ltd, UK
***KRAS* G12D reference standard, 50%**	Horizon Discovery Ltd, UK
***KRAS* wt reference standard**	Horizon Discovery Ltd, UK
KAPA2G Fast HotStart ReadyMix	Kapa Biosystems, Inc., US
GelRed Nucleic Acid Gel Stain	Biotium, California, US
Phosphate buffer Saline (PBS) tablet	Sigma-Aldrich, Miss., US
NeutrAvidiv Protein	Thermo Fischer Scientific, Mass., USA
BSA lyophilized powder, crystallized, ≥98.0% (GE)	Sigma-Aldrich, Miss., US
Biotin-$(AC_5)_2$-Sulfo-Osu	Dojindo, Japan
Microcon-30kDa Centrifugal Filter Unit with Ultracel-30 membrane	Merck KGaA, Darmstadt, Germany
1-palmitoyl-2-oleoyl-glycero-3-phosphocholine (POPC)	Avanti Polar Lipids, Inc., Alabaster, AL, USA
Nuclepore polycarbonate hydrophilic membranes 0.2 µm	Whatman plc, UK

DNA Sequences of probes/primers (5' -> 3')		**Product size (bp)**
***BRAF*-p1**	GGATCCAGACAACTGTTCAAACTGATGGGACCCACT CCATCGAGATTTCT	181
***BRAF*-gen-Fw**	ACC TAAACTCTTCATAATGCTTGC	
***BRAF*-cp2-new**	TCTTCATGAAGACCTCACAGTAAAAATAGGTGATTTTG	184

	GT CTAGCTACAG**A**	
***BRAF*-gen-Rv**	TGAGACCTTCAATGACTTTCTAGT	
***BRAF*-V600EF**	**chol-**ACTACACCTCAGATATATTTCTTCATG	89
***BRAF*-V600ER**	**biotin-**CCCACTCCATCGAGATTGC**T**	
***KRAS*-G12DF**	**biotin-**CTTGTGGTAGTTGAAGCGG**A**	85
***KRAS*-G12DR**	**chol-**CATATTCGTCCACAAAATGATTCTG	
***BRAF*-17nm**	**(chol-)** CCTTTACTTACTACACC	98
***BRAF*-V600ER**	**biotin-**CCCACTCCATCGAGATTGC**T**	

** The red bold nucleotide corresponds to the mismatch discrimination nucleotide.*

DNA Sequences of targets (5' -> 3')	
***BRAF*-V600E target**	CCTTTACTTACTACACCTCAGATATATTTCTTCATGAAGACCT CACAGTAAAAATAGGTGATTTTGGTCTAGCTACAG**A**GAAAT CTCGATGGAGTGGGTCCCATCAGTTTGAACAGTTGTCTGGA TCCATTTTGTGGATGG
***BRAF*-wt target**	CCTTTACTTACTACACCTCAGATATATTTCTTCATGAAGACCT CACAGTAAAAATAGGTGATTTTGGTCTAGCTACAG**T**GAAAT CTCGATGGAGTGGGTCCCATCAGTTTGAACAGTTGTCTGGA TCCATTTTGTGGATGG

** The red bold nucleotide corresponds to the mismatch site.*

Allele Specific-PCR (AS-PCR) for the detection of the *BRAF* V600E in the 277 bp target using the LCR probes. *Creation of the 277 bp PCR-derived template:* These experiments were exclusively performed on PCR products mimicking a 277bp DNA region of the *BRAF* gene carrying or not the *BRAF* V600E mutation; 10 µL of the KAPA2G Fast HotStart ReadyMix 2X were mixed with 10 pmol of *BRAF*-gen-Fw and 10 pmol of *BRAF*-gen-Rv primers in a total volume of 20 uL. As template, 10 ng genomic DNA *BRAF* V600E 50 % or BRAF wt reference standard or no template (NTC) were added. The reaction was subjected to 30 cycles of 10 sec at 95 ^{o}C followed by 10 sec at 57 ^{o}C and 10 sec at 72 ^{o}C. An initial denaturation step for 5 min at 95 ^{o}C and final extension step at 72 ^{o}C for 1 min were included in the amplification protocol. Following amplification, PCR products were purified with the Nucleospin Gel and PCR clean-up kit and the specific 277 bp product was verified by agarose gel electrophoresis on 2.0 % (w/v) gel stained with GelRed Nucleic Acid Gel Stain. *AS-PCR using the LCR probes:* AS-PCR reactions of 20 µL were prepared containing 10 µL of KAPA2G Fast HotStart ReadyMix 2X, 5 pmol forward (Fw) and 5pmol reverse (rv) primer. Two sets of fw-rv primers were tested; the *BRAF*-gen-Fw with the *BRAF*-p1-biotin and the *BRAF*-cp2-new with the *BRAF*-gen-Rv. In each case the desired amount of mt, wt or no template (NTC) was added. All reactions were subjected to a two-step amplification protocol consisted of an initial denaturation step at 95 ^{o}C for 3 min, followed by a two-step cycling protocol of 95 ^{o}C for 2 sec and 60 ^{o}C for 5''. After amplification reaction products were electrophoresed and visualized under UV light as described above.

Allele Specific –PCR (AS-PCR) for the detection of the *BRAF* V600E in genomic DNA. 5 µL KAPA2G Fast HotStart ReadyMix 2X were mixed with 5 pmol of the allele-specific

biotinylated reverse primer *BRAF*-V600ER and with 5 pmol of the cholesterol modified forward primer *BRAF*-V600EF in a total volume of 10 uL. These primers were optimized for the BRAF-V600E mutation detection by Z. Yang et al.[71] As template, 50 ng genomic DNA *BRAF* V600E 50% serially diluted with BRAF wt reference standard in ratios ranging from 0.01% to 10% was used. The cycling protocol consisted of an initial denaturation step for 3 min at 95 ^{o}C followed by 55 cycles of 10 sec at 94 ^{o}C, 10 sec at 60 ^{o}C and 10 sec at 72 ^{o}C. AS-PCR products were then analyzed by gel electrophoresis on 2.0 % (w/v) agarose gel stained with GelRed Nucleic Acid Gel Stain and by acoustic analysis as well (see below). A no template control (NTC) was included in every run.

Detection of the *BRAF* V600E via Allele Specific-PCR (AS-PCR) in 141 bp gblock target. The same amplification protocol as described above *(AS-PCR for the detection of the BRAF V600E in genomic DNA)* was applied. Briefly, 5 µL of KAPA2G Fast HotStart ReadyMix 2X were mixed with 5 pmol of the allele-specific biotinylated reverse primer *BRAF*-V600ER and with 5 pmol of the cholesterol modified forward primer *BRAF*-V600EF in a 10µL reaction. As template a 141 bp gblock mimicking the *BRAF* sequence carrying (mt) or not (wt) the V600E mutation was used. The mt gblock was mixed with the wt in various ratios ranging from 0.01% - 10%. The reactions were subjected to 50-55 cycles of 10 sec at 94 ^{o}C, 10 sec at 60 ^{o}C and 10 sec at 72 ^{o}C, followed by gel electrophoresis on 2.0 % (w/v) agarose gel.

Detection of the *KRAS* G12D via real-time Allele Specific-PCR (AS-PCR). For the *KRAS* G12D mutation analysis 10 pmol of the mutation-specific biotinylated forward primer (*KRAS*-G12DF), 10 pmol of the cholesterol-modified reverse primer (*KRAS*-G12DR) and 1µL 20X SYBR® Green I Nucleic Acid Stain were mixed with 10 µL KAPA2G Fast HotStart ReadyMix 2X in a total volume of 20 µL. As template, 50 ng genomic DNA *KRAS* G12D 50% serially diluted with *KRAS* wt reference standard in ratios ranging from 0.05% to 10% was used. PCR reactions mixtures were carried out at CFX Real-Time PCR Detection Systems (Bio-Rad). The cycling protocol consisted of an initial denaturation step for 5 min at 95 ^{o}C followed by 45 cycles of 10 sec at 94 ^{o}C, 10 sec at 62 ^{o}C and 2 sec at 72 ^{o}C). A NTC reaction was included in every run.

Quartz crystal microbalance (QCM) with dissipation monitoring acoustic devices. For the experiments two QCM devices were used; the High Fundamental Frequency – QCM (HFF-QCM) (AWS S.L., Paterna, Spain) operating at 150 MHz and the commercial QSense Analyzer E4 instrument (QSense, Sweden). The HFF-QCM platform monitored a HFF-QCM array (AWS, S.L. Paterna, Spain) mounted on a custom Printed Circuit Board (PCB). Cleaning of the PCB and array included treatment with Hellmanex 2% for 30 min, rinsing with mili-Q water and 70 % EtOH and drying under N_2. Then, the array was cleaned by 30 min UV/Ozone (Ossila Ltd, Sheffield) followed by treatment with absolute EtOH for 30 min. The flow cell employed a PMMA gasket and a PDMS cell (AWS, S.L. Paterna, Spain), both cleaned with Hellmanex 2 % for 30 min, incubated with mili-Q water in a sonicator for 15 min and dried at 65 ^{o}C. The flow-cell was connected to a syringe pump of 50 µL or 250 µL installed in the platform.

About the QSense Analyzer, the operating frequency for the results reported here is the 35 MHz (7 th overtone); ΔF was not normalized by the overtone number. Before use, the Au-coated 5 MHz sensors were cleaned with Hellmanex 2 % for 15 min, rinsed with mili-Q water, dried under N2 and treated for 30 min with UV/Ozone (Ossila Ltd, Sheffield). Acoustic experiments were carried out under a continuous flow of 20 µL/min for the AWS device and at 50 µL/min for the QSense at 25 ^{o}C. All samples were diluted in PBS pH=7.4, which was the running buffer. Following each sample addition, buffer rinsing was taken place and then frequency and dissipation changes were obtained.

Liposome preparation. Lyophilized 1-palmitoyl-2-oleoyl-glycero-3-phosphocholine (POPC) lipids were dissolved in chloroform at final concentration of 10 mg/mL. 100 – 200 µL of the 10 mg/mL lipids were added in round bottom glass flask and dried homogenously under N_2 flow. The lipid film was then left for 30 min under N_2 gas followed by resuspension in PBS at a final concentration of 2 mg/mL by gentle vortexing. The resulting suspension was passed through polycarbonate membranes with a nominal pore diameter of 200 nm, using the Avanti Mini-Extruder. Stock solutions were stored at 4 °C for up to 6 days.

Acoustic analysis of AS-PCR. Prior to the analysis of the AS-PCR reaction described on the gold sensor surface was modified with b-BSA injected at a concentration of 0.2 mg/mL followed by the addition 0.05 mg/mL of NAv. In all cases the working volumes were V_{150MHz}=60 µL and V_{35MHz}=200 µL. b-BSA was prepared after incubation of BSA lyophilized powder (Sigma-Aldrich) with biotin-$(AC_5)_2$-Sulfo-Osu linker in PBS, in a molar ratio of 1:10, for 1 h and 30 min at RT; after incubation, BSA was purified using the Microcon-30kDa Centrifugal Filter Unit with Ultracel-30 membrane following manufacturer instructions. Following the creation of the substrate, a sample of 2.5 µL or 8 µL of the *BRAF* or *KRAS* AS-PCR reactions respectively, diluted in a total volume of 20 µL, was loaded on the 150 MHz sensors (flow rate: 14 µL/min). Similarly, 2.5 µL or 10 uL of the *BRAF* or *KRAS* AS-PCR, diluted in a total volume of 125 µL, was applied to the 35 MHz QCM device surface at a flow rate of 25 µL/min. In both cases, a suspension of 0.2 mg/mL of 200 nm POPC liposomes was added at a volume of 100 µL (150 MHz) or 500 µL (35 MHz).

Results & discussion

1. Preliminary results of AS-PCR performance for the detection of BRAF V600E mutation

AS-PCR reactions completed in this phase performed exclusively using PCR-products as template, which mimicked the *BRAF* gene. These products had length of 277 bp and derived from wt or heterozygous mt genomic DNA carried the V600E single nucleotide mutation. Due to the primer design, the V600E mutation was almost in the middle of the sequence.

Preliminary results indicating the excellent amplification efficiency of the AS-PCR were obtained using 2 set of Fw-Rv primers, initially design for the performance of Ligase Chain

Reaction. The 1st set of primers involved the BRAF-p1 LCR probe and the BRAF-gen-Fw primer, while the 2nd set included the BRAF-cp2 LCR probe and the BRAF-gen-Rv primer. BRAF-gen-Fw and BRAF-gen-Rv primers amplified both the mt and the wt sequence, while BRAF-p1 and BRAF-cp2 probes only the mt target; this is due to the design of the probes which have the allele-specific (AS) nucleotide for the mt target in the last position of the 3' end (Fig. 1). Both sets were mixed with 1670 copies of mt target containing in 1:1 ratio wt and with 3300 copies of wt template. The mixtures were subjected to 30 2-step (denaturation & annealing-extension) PCR cycles (2'' at 95 ^{o}C followed by 5'' at 60 ^{o}C). PCR products were visualized on 2 % agarose gel, according to the 1st set of primers, i.e., BRAF-p1/BRAF-gen-Fw, gave rise to better amplification results (Fig. 2). Note that, by this set of primers a slight band generated from the wt reaction was also observed.

Then, to demonstrate the LOD of the assay 167 – 1.67 mt copies in 1:1 ratio with wt were mixed with the 1st set of primers followed by AS-PCR. As control, 167 – 1.67 wt copies were also subjected to the same amplification protocol. As a shown in figure 3, the sensitivity was estimated at the 16.7 mt copies which gave rise to visualized products of greater intensity compared to the wt controls.

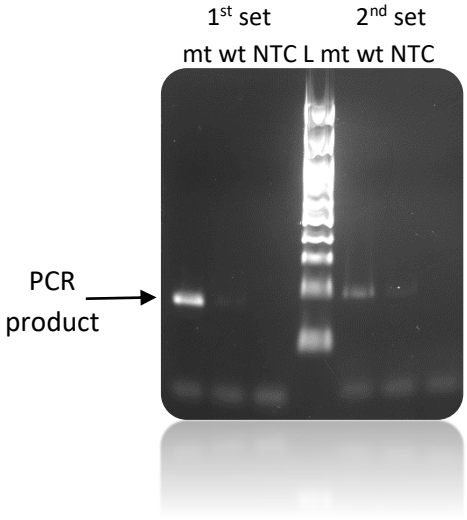

Figure 2. *AS-PCR for the amplification of BRAF V600E mutation applying the LCR probes. Lanes 1-3; AS-PCRs derived from 1670 mt copies in 1:1 ratio with wt, 3300 wt molecules and NTC mixed with the 1st set of primers. Lane 4; 100 bp Ladder, Lane 5- 7; same as the lanes 1-3 but with the 2nd set of primers. The expected PCR products are of 181 bp – 184 bp, respectively.*

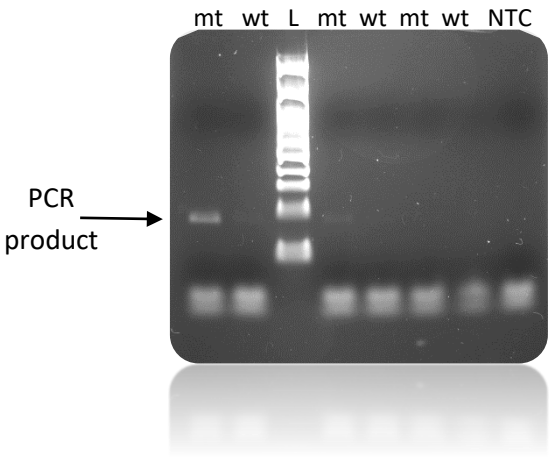

Figure 3. *AS-PCR for the amplification of BRAF V600E mutation applying the 1st set of primers. Lanes 1-2; AS-PCRs derived from 167 mt and 330 wt molecules. Lane 4; 100 bp Ladder, Lanes 5-8; AS-PCR containing 16.7 mt, 33 wt, 1.67 mt, 3.3 wt molecules as well as an NTC reaction. Note that, mt is always mixed with wt in 1:1 ratio. The expected PCR products are of 181 bp – 184 bp, respectively in 1:1 ratio with wt.*

Finally, for the rest experiments, optimized primers for the detection of the V600E mutation were designed and tested; these experiments included the detection of just 1 copy of mt target in various mixing ratios with wt. Additionally, the primers were properly modified for the subsequent immobilization on acoustic sensor, too.

2. Development of an optimized AS-PCR combined iwth acoustic detection

As stated above, one of the main objectives of this work was to design an assay that could combine the high sensitivity of ddPCR with a less cumbersome and more cost-effective method. The final protocol we developed involved the specific amplification of the point mutation via AS-PCR, followed by a two-step acoustic assay.

For the AS-PCR, a set of primers[71] was used of which the forward (Fw) amplifies both the mutant (mt) and wild type (wt) sequences while the reverse (Rv) only the mt target; this is due to the Rv design which has the allele-specific (AS) nucleotide for the mt target in the last position of the 3' end. To further enhance Rv primer's specificity, an artificial mismatched nucleotide was introduced at the antepenultimate (third to the terminal) position at the 3'-end. For the sake of the downstream acoustic analysis, the Fw primer is modified with a cholesterol in its 5' end, and the Rv primer by a biotin. Following amplification, DNA fragments of 89 bp employing both a biotin and a cholesterol molecule in the case of the mt target or only a cholesterol molecule in the case of the wt target are produced. The AS-PCR reaction is then loaded directly on the NAv-modified HFF acoustic biochip without prior purification. The presence of NAv allows the immobilization of only the mt DNA-amplicons which carry a biotin molecule, through the NAv-biotin interaction. In order to achieve the clinically relevant detection limits of few copies of mt target in the presence of larger amounts of the wt, ultrasensitive detection is necessary, even after AS-PCR. This becomes

even more significant if detection occurs directly inside the crude AS-PCR cocktail where issues of non-specific binding become of concern. For this reason, a solution of POPC liposomes is injected and captured by the immobilized products via the cholesterol-end of the mt amplified products. Liposomes act as signal enhancers causing high changes in the acoustic signal leading to the detection of immobilized DNA. This strategy has been shown by our group as well as others to be suitable for the acoustic detection of Recombinase Polymerase Amplification (RPA) products[118] and single-base mismatches[111,115,119]. The basic principle of the AS-PCR/acoustic methodology used for the detection of *BRAF* V600E mutation is presented diagrammatically in Fig. 4.

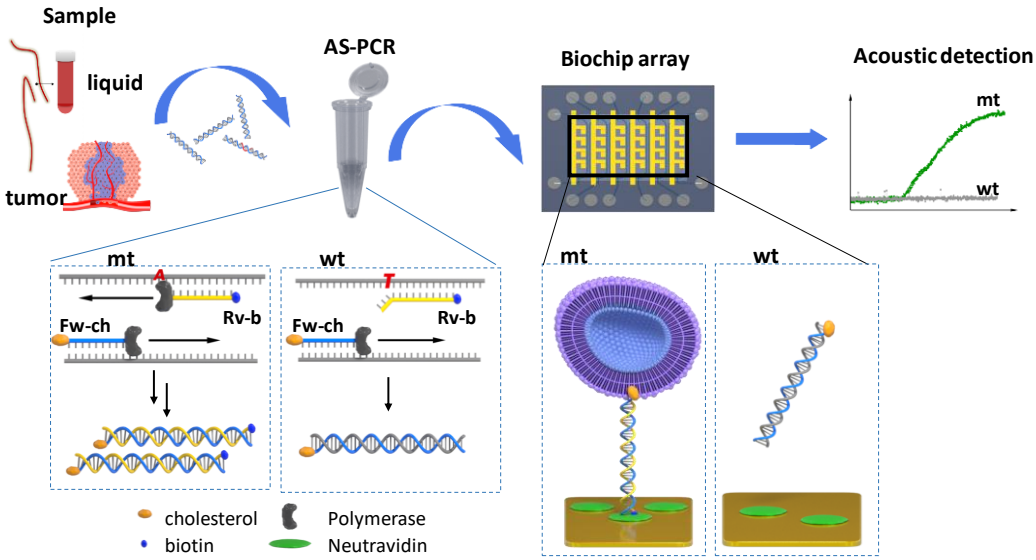

Figure 4. *Schematic representation of the concept of the acoustic assay for the detection of the BRAF V600E point-mutation. Starting from a tumor sample, allele-specific (AS) PCR is carried out with a modified set of primers which amplifies selectively the mt target producing ds double labeled (biotin and cholesterol) amplicons, as well as only cholesterol-modified wt products. The biotinylated mt products are directly immobilized on the NAv modified sensor surface of the biochip array, which can further trigger the binding of liposomes via the cholesterol-end. Cholesterol binding produces a distinct acoustic signal change (dissipation), discriminating a single mt target even in the presence of a background of wt products (10^4).*

3. Analytical performance of the AS-PCR – HFF-QCM acoustic array for the detection of point mutations

a. *BRAF* V600E

To determine the LOD and the sensitivity of the assay, mt genomic DNA carrying the *BRAF* V600E point-mutation was diluted with wt DNA in a range from 0.01% to 10% (i.e., 1:10^4 to 1:10 mt:wt ratio or 1-2 and 10^4 copies of mt DNA, respectively). The mt:wt dilutions, as well as 100% (10^4 copies) wt genomic DNA (control), were subjected to AS-PCR of 55 cycles (1h 40 min) followed by acoustic detection on the biochip array. For the immobilization of the biotinylated mt target, we used a surface modified with b-BSA/NAv; this is based on previous findings in our lab showing a higher stability of the NAv protein in the presence of a crude

sample when immobilized via b-BSA rather than direct adsorption on the gold layer (chapter 1, part 1, Fig. 8).

Firstly, it was investigated if the ΔF and ΔD changes caused by the direct immobilization of the AS-PCR products on the b-BSA/NAv coated surface could differentiate between the mt and wt reactions. Following a washing step, it was concluded that recorded acoustic signal changes could not discriminate between the mt and wt AS-PCR products (Fig. 5). The changes recorded in both signals and for all tested mt:wt reactions were attributed primarily to the non-specific adsorption of the PCR cocktail components (i.e., DNA polymerase, biotinylated primer) and by-products (i.e. primer dimmers), both of which resulted in a significant background signal overshadowing the response from the specific binding of the biotinylated amplicons. This is not surprising since the initial amount of the mt DNA template in the reaction (1-10^3 copies, i.e., from 160 zM – 160 aM) is very low and after enzymatic amplification the produce amplicons would be in the sub nM range; this is below the threshold limit of detection of DNA which for the 150 MHz HFF QCM device used in this work is >10nM (chapter 1, part 1, table 2).

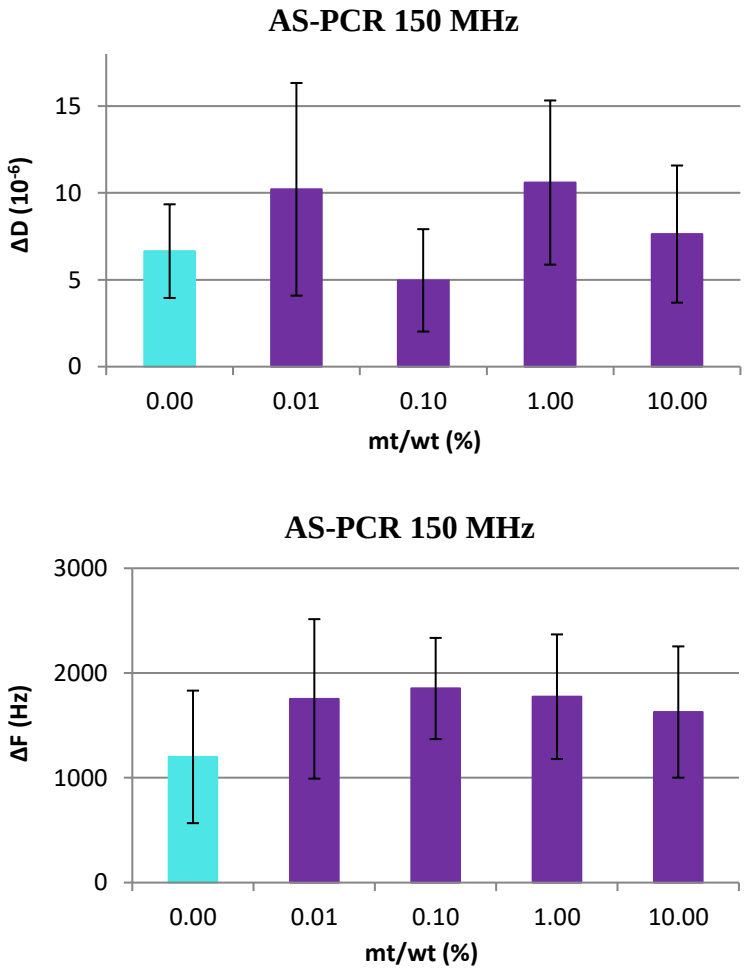

Figure 5. *ΔD &, ΔF values obtained from the addition of various mt:wt ratios of BRAF V600E AS-PCR reactions on b-BSA/NAv coated surface at 150 MHz. 0.00 % corresponds to AS-PCR containing 0 mt and 10^4 wt molecules (control).*

For this reason, we employed a second step, where liposomes were used as signal amplifiers during their binding at the 5' cholesterol present at the mt amplicon. The real-time binding of the liposomes to the AS-PCR modified surface was very specific since, in the absence of the mt target, nearly zero dissipation change was recorded (Fig. 6). Figure 6 summarizes the average dissipation values recorded at the liposome step for all the mt:wt dilutions which were $110\pm50\times10^{-6}$, $136\pm47\times10^{-6}$, $131\pm31\times10^{-6}$ and $90\pm21\times10^{-6}$ for the 0.01%, 0.1%, 1%, 10%, respectively. A sensitivity and a LOD of 0.01% and 1-2 copies respectively were recorded using the dissipation response. For the above concentration range of the DNA target, the frequency response was not as sensitive as the dissipation (Fig. 7). This is in agreement with previous works, where dissipation signal was proven to be more sensitive compared to frequency when low DNA concentrations (fmol) were detected via liposomes as signal amplifiers[111,118]. Finally, as expected, no different ΔD/ΔF values were observed between the mt and the wt reactions as well (data not shown).

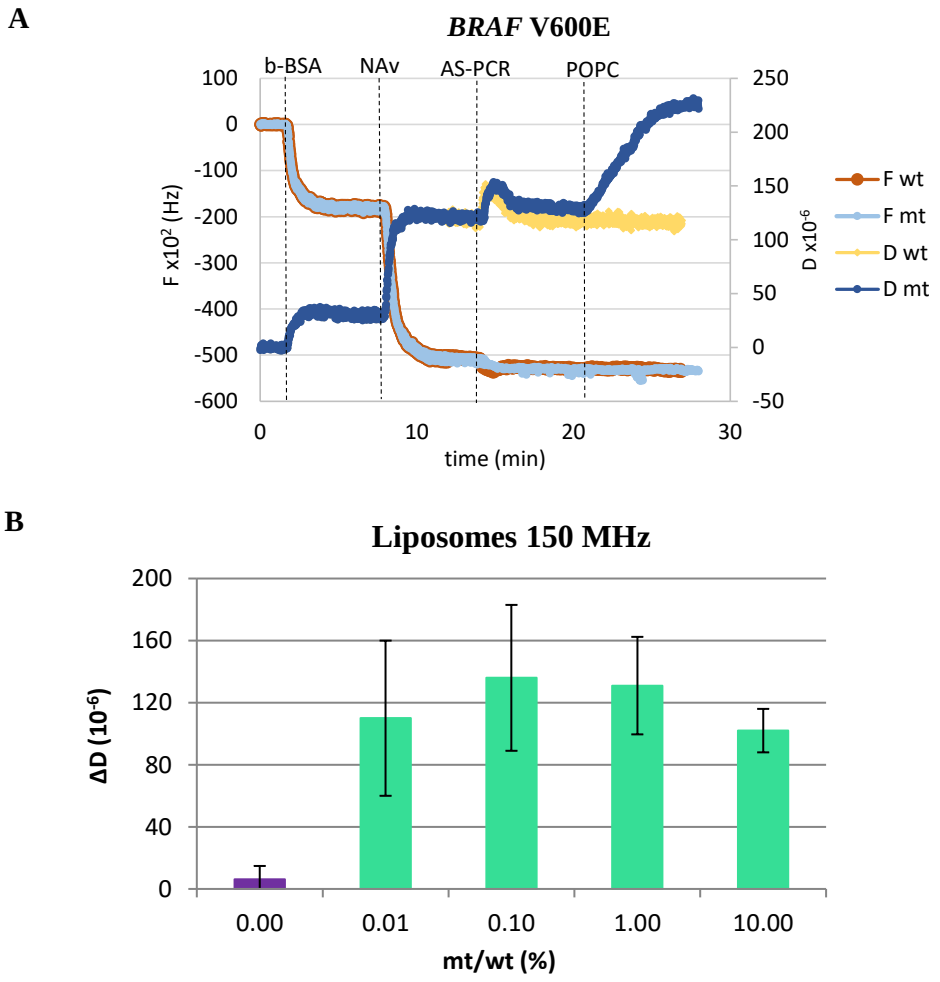

Figure 6. *A) Real time acoustic detection of the KRAS G12D mutation together with a control sample (reaction containing 10^4 wt DNAs) with the 150 MHz acoustic biochip array. B) Acoustic detection with the 150 MHz acoustic biochip array of the BRAF V600E DNA in the presence of wt DNA (0.01%, 0.1%, 1%, 10% and 0% mt:wt) after AS-PCR and addition of 200 nm POPC liposomes. 0.00% corresponds to AS-PCR containing 0 mt and 10^4 wt molecules (control).*

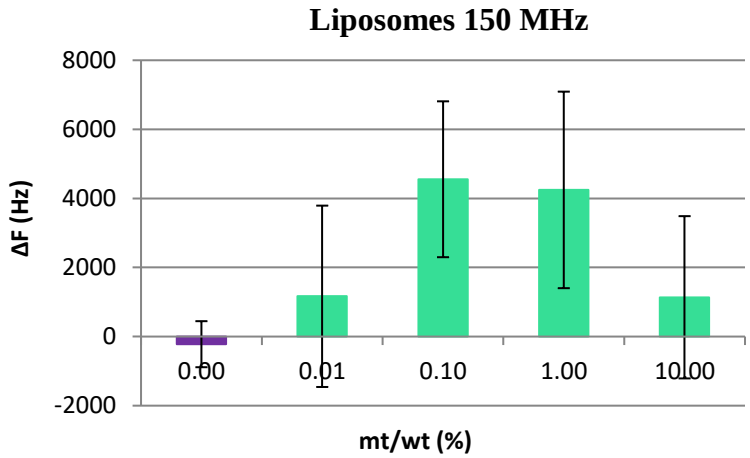

Figure 7. *Comparison of frequency changes observed after loading of BRAF V600E AS-PCR (0.01%, 0.1%, 1%, 10% and 0% mt:wt ratios) on b-BSA/NAv modified sensors followed by the addition of 200 nm POPC liposomes at 150 MHz. 0.00% corresponds to AS-PCR containing 0 mt and 10^4 wt molecules (control).*

Based on Fig. 6, we note that the assay provides only qualitative results since it can differentiate between the presence or absence of the mutation but cannot distinguish between the various mt:wt ratios. This is attributed to the fact that As-PCR had reached a plateau following the 55 cycles employed in this assay. Further optimization of the AS-PCR conditions during real-time PCR and/or surface bio-architecture is necessary to achieve quantitative results.

b. KRAS G12D

The AS-PCR/acoustic detection method was further optimized during real-time PCR. This time, the method was applied for the detection of the *KRAS* G12D mutation, a G→A transition[96]. For this assay, a slightly modified version of Figure 4 was employed: of the pair of primers used, the Rv was modified by a cholesterol and was designed to amplify both the mt and wt targets, while the Fw was biotinylated and was specific for the mutant allele. As before, an artificial mismatched nucleotide was introduced at the antepenultimate (third to the terminal) position at the 3'-end of the Fw primer. As in the case of *BRAF*, the analytical performance of the assay was examined; mt genomic DNA carrying the *KRAS* G12D mutation was mixed with wt DNA at gradually decreasing ratios ranging from 0.05% to 10% (otherwise, from 5 – 1000 mt copies diluted in 10^4 wt molecules). The mt:wt dilutions, 100% (10^4 copies) wt genomic DNA, as well as no template control (NTC) were subjected to real-time AS-PCR; this was in order to determine the number of cycles needed for all the samples to be at the range of the exponential-to-early-plateau phase of the PCR relatively to their initial mt DNA input. As shown in Fig. 8, the obtained Cq values were estimated at 36.8±0.3, 39.9±0.3, 41±0.3 and 43.6±0.3 for the 10%, 1%, 0.5% and 0.1%, respectively. The 0.05% dilution failed to give a Cq value, however, a slight increase in the signal was observed at 44.5 cycles. Regarding the wt and the NTC reactions, no increase in the signal was recorded. Therefore, an AS-PCR of 45 cycles (1h) was established and used for the rest of the experiments followed by acoustic analysis.

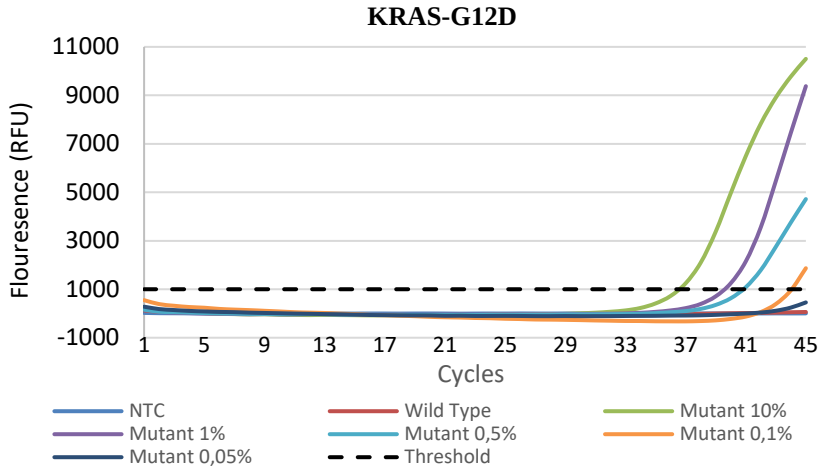

Figure 8. *Schematic representation of the PCR curves obtained by Real-Time AS-PCR of the KRAS G12D mt:wt dilutions (0.05%, 0.1%, 0.5%, 1%, 10% and 0% mt:wt ratios). The threshold was set at 1000 RFU (dashed line). In all cases the Real Time PCR assays included a wt reference control which contained 10^4 wt DNAs (red line) as well as a NTC reaction (blue).*

A notable difference to the *BRAF* analysis was that the ΔD measurement obtained from the direct binding of the AS-PCR products on the b-BSA/NAv coated surface could discriminate to some extent the mt:wt ratios from the wt, although the error bars were very large (Fig. 10). This response can be attributed to the higher volume used, first, for the *KRAS* AS-PCR reaction as opposed to the *BRAF* one (20 μl vs 10 μl) and secondly, during loading on the HFF QCM sensor surface (8 μl vs 2.5 μl). Moreover, the reduction of the No of AS-PCR cycles to 45 may have also resulted in fewer by-products and lower non-specific binding. As expected, applying the liposomes all the mt:wt dilutions were distinguished from the wt control which gave zero dissipation change (Fig. 11). Note that the obtained ΔD values were analogous to their initial mt:wt ratio and when plotted against the number of mt molecules the curve relationship was turned into linear with R^2= 0.95 (Fig. 11B inset). Nevertheless, if only the 0.05%-1% was plotted, the R^2 was improved at 0.99; this is due to the fact that 10% is at the early plateau phase at 45 cycles of AS-PCR. Overall, the above results indicate that upon optimization of the assay conditions, ultra-sensitive, specific and quantitative information can be provided through acoustic measurement of the dissipation signal. Regarding frequency, the response was not as sensitive as the dissipation giving a reliable discrimination only at the level of the 10% mt:wt (Fig. 12).

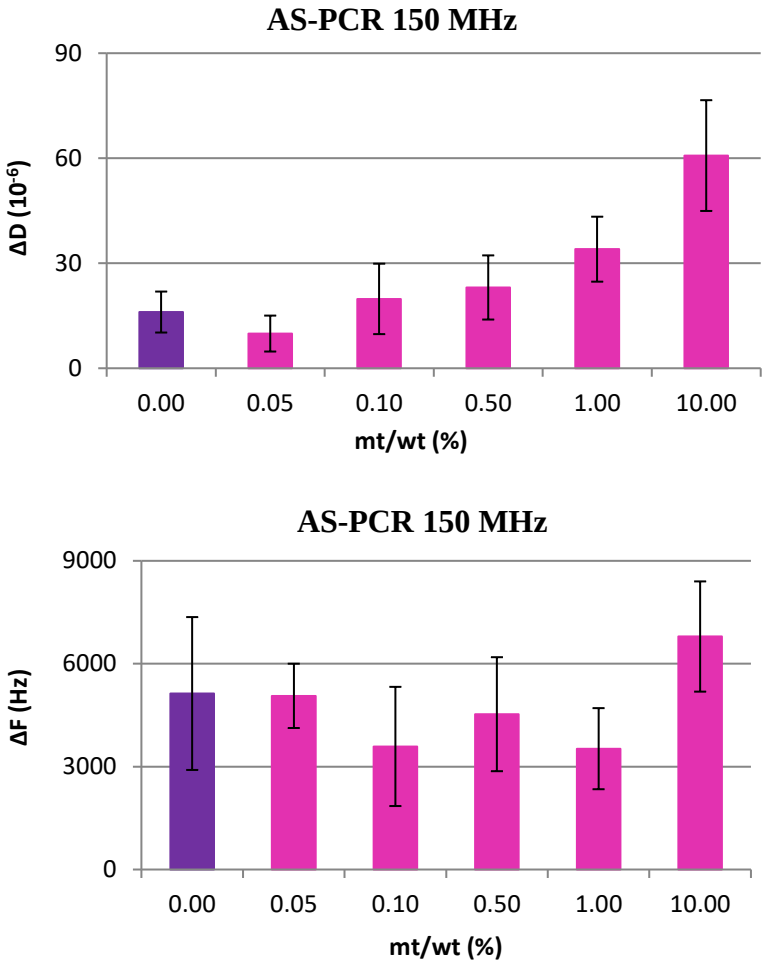

Figure 10. *ΔD & ΔF values obtained from the addition of various mt:wt ratios of KRAS G12D As-PCR reactions on b-BSA/NAv coated surface at 150 MHz. 0.00% corresponds to AS-PCR containing 0 mt and 10^4 wt molecules (control).*

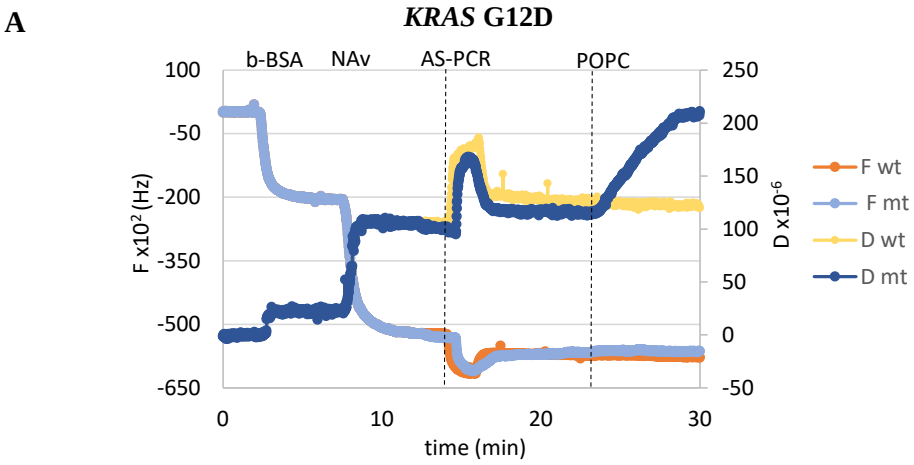

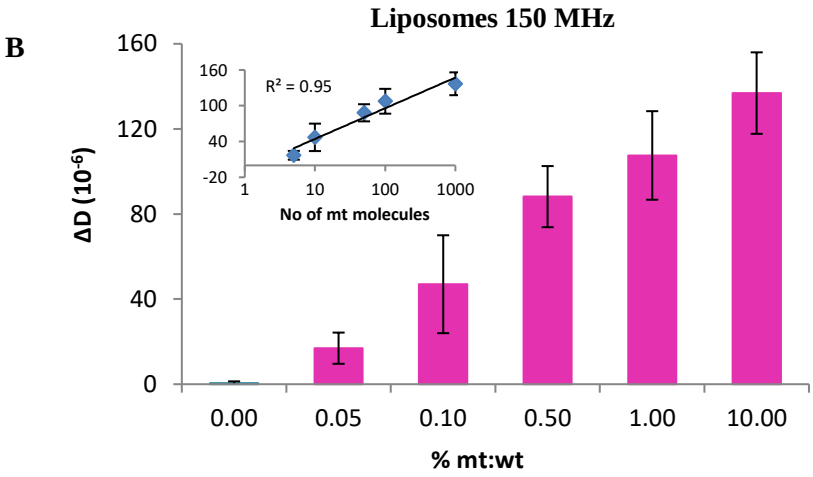

Figure 11. *A) Real time acoustic detection of the KRAS G12D mutation together with a control sample (reaction containing 10^4 wt DNAs) with the 150 MHz acoustic biochip array. B) Acoustic detection with the 150 MHz acoustic biochip array of the KRAS G12D DNA in the presence of wt DNA (0.05%, 0.1%, 0.5%, 1%, 10% and 0% mt:wt) following AS-PCR and addition of 200 nm POPC liposomes. The inset shows the linear curve relationship (R^2= 0.95) of the obtained ΔD values when plotted vs number of mt molecules in logarithmic scale. 0.00% corresponds to control reaction containing 0 mt and 10^4wt DNAs.*

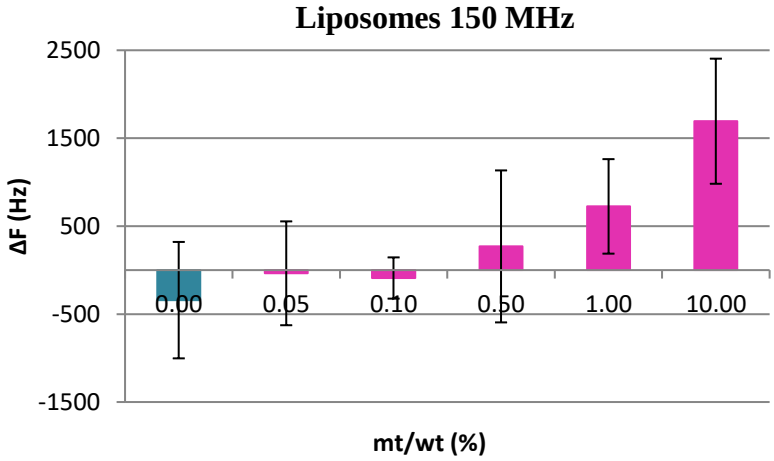

Figure 12. *Comparison of frequency changes observed after loading of the KRAS G12D AS-PCR (0.05%, 0.1%, 0.5%, 1%, 10% and 0% mt:wt ratios) on b-BSA/NAv modified sensors followed by the addition of 200 nm POPC liposomes at 150 MHz. 0.00% corresponds to control reaction containing 0 mt and 10^4wt DNAs.*

4. Effect of the operating frequency

To evaluate the efficiency of the 150 MHz acoustic biochip array towards the analysis of cancer point mutations we used the established 35 MHz QCM sensor to perform the same assays and compare results. Differences between the two devices would include the penetration depth inside the sensing solution (43 nm for the 150 MHz and 90 nm for the 35 MHz) and the sensitivity of frequency to the adsorbed mass; the latter according to the Sauerbrey equation scales up with the square of the fundamental resonator frequency f_o. In addition, differences in the size of the two QCM-devices, geometry of the flow cell and applied flow rate can affect the amount of immobilized target.

Results were in good agreement with those obtained with the HFF-QCM array biochip. Specifically, in both *BRAF* and *KRAS* mutation analysis the 35 MHz device failed to detect the *BRAF* and *KRAS* AS-PCR samples upon their direct loading on the b-BSA/NAv coated sensor (Fig. 13).

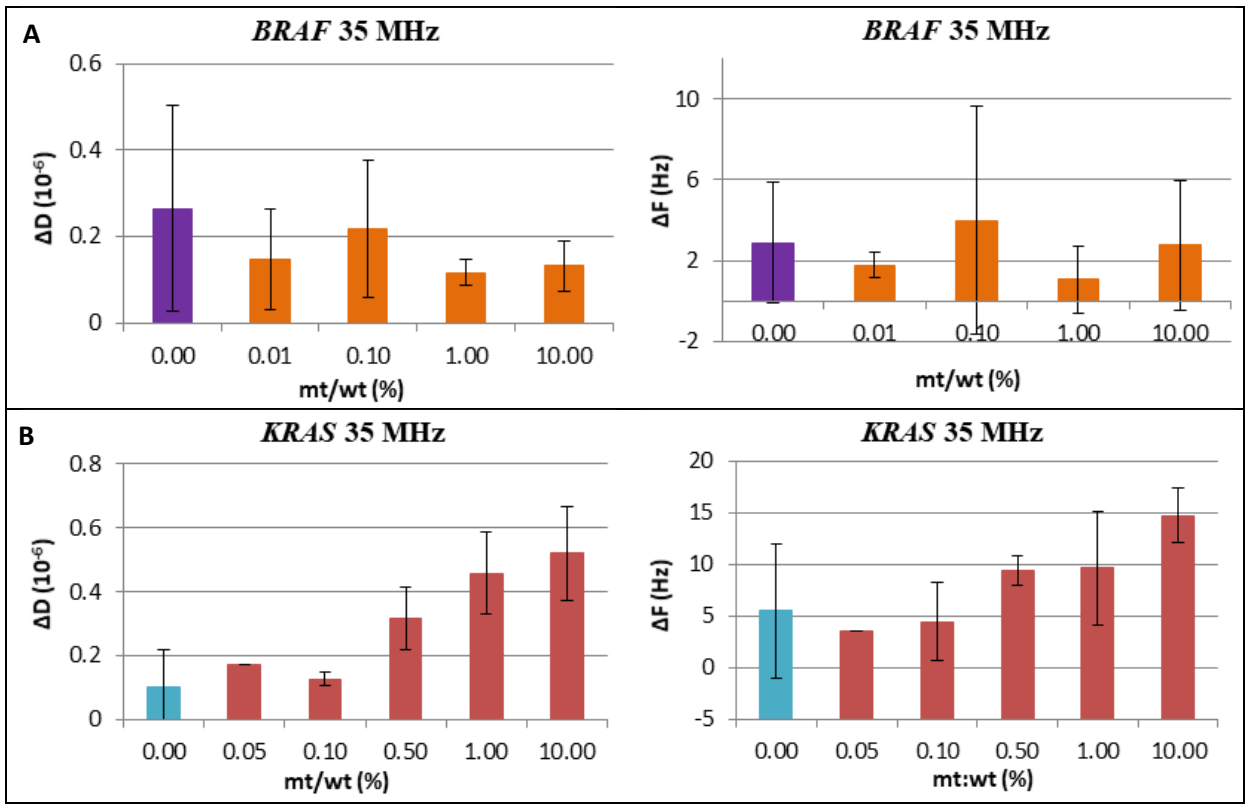

Figure 13. *A) ΔD & ΔF values obatined from the addition of various mt:wt ratios of BRAF V600E AS-PCR reactions on b-BSA/NAv coated surface at 35 MHz. B) Same as (A) but for the KRAS G12D mutation. 0.00 % corresponds to control reaction containing 0 mt and 10^4wt DNAs.*

Moreover, based on Fig. 14, we conclude that following the addition of liposomes the two devices gave the same dissipation response and LOD towards the detection of all tested mt:wt AS-PCR samples. As for the frequency, clear ΔF changes were obtained for all the mt samples in contrast to the 150 MHz array (Fig. 15).

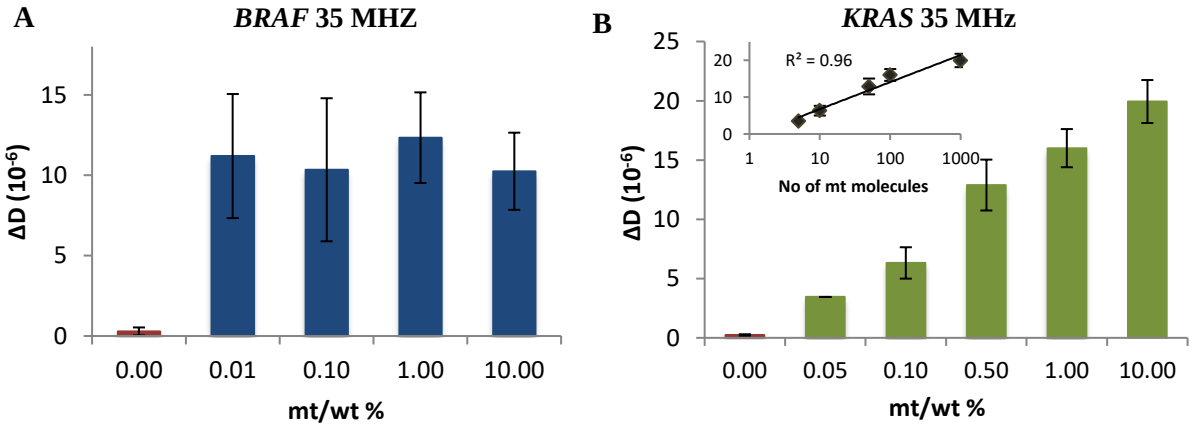

Figure 14. *A) Acoustic detection of the BRAF V600E DNA in the presence of wt (0.01%, 0.1%, 1%, 10% and 0%*

mt:wt) after AS-PCR and binding of 200 nm POPC lipsomes at 35 MHz. B) Same as (A) but for the KRAS G12D point mutation in the presence of wt DNA (0.05%, 0.1%, 0.5%, 1%, 10% and 0% mt:wt). The inset shows the linear curve relationship (R^2= 0.95) of the obtained ΔD values when plotted vs number of mt molecules in logarithmic scale. 0.00% corresponds to control reaction containing 0 mt and 10^4wt DNAs.

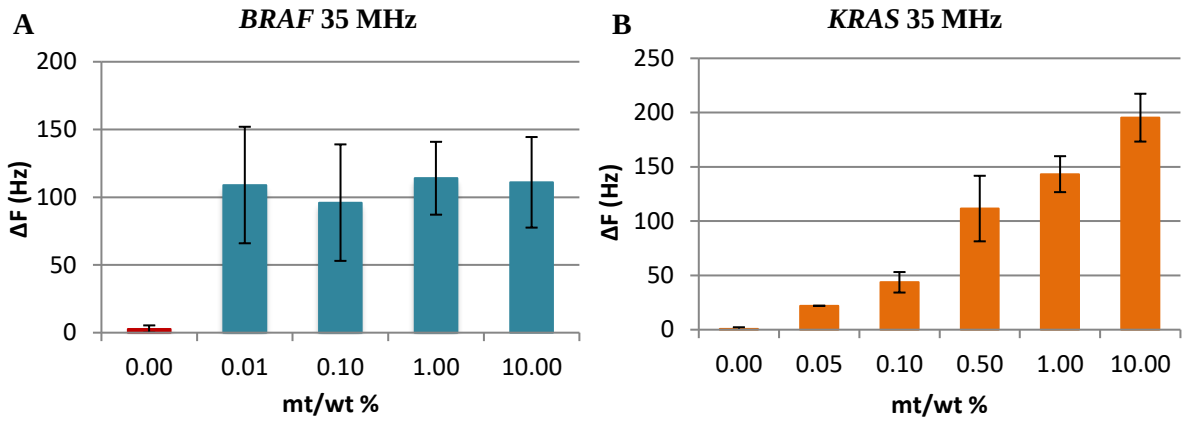

Figure 15: *(A) Comparison of frequency changes observed after loading of the BRAF V600E AS-PCR (0.01%, 0.1%, 1%, 10% and 0% mt:wt ratios) on b-BSA/NAv modified sensors followed by the addition of 200 nm POPC liposomes at 35 MHz. (B) As in (A) but for the KRAS G12D AS-PCR reactions (0.05%, 0.1%, 0.5%, 1%, 10% and 0% mt:wt ratios). 0.00% 0.00% corresponds to AS-PCR containing 0 mt and 10^4 wt molecules (control).*

Having a closer look at the real-time graphs obtained with the two platforms for both targets, *BRAF* and *KRAS*, we noticed that the relative liposome to NAv binding step at 35 MHz gave a much higher response, compared to the same steps obtained with the 150 MHz (Fig. 16). Taking into account the fact that frequency change was not sensitive enough in the case of the 150 MHz, we hypothesized that a lower surface coverage was achieved with the new array biochip due to differences in the geometry of the device and the flow cell. Overall, no significant differences were found between the 35 and 150 MHz QCM biosensors in terms of sensitivity and detection limit.

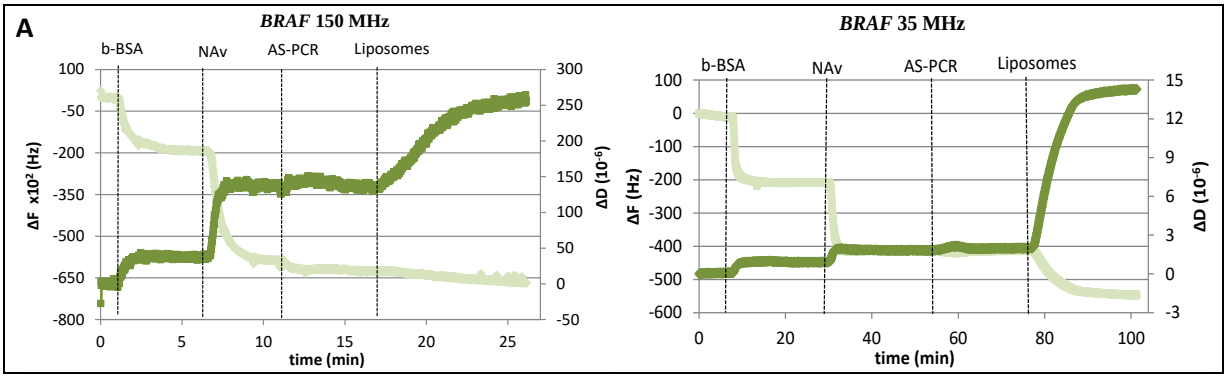

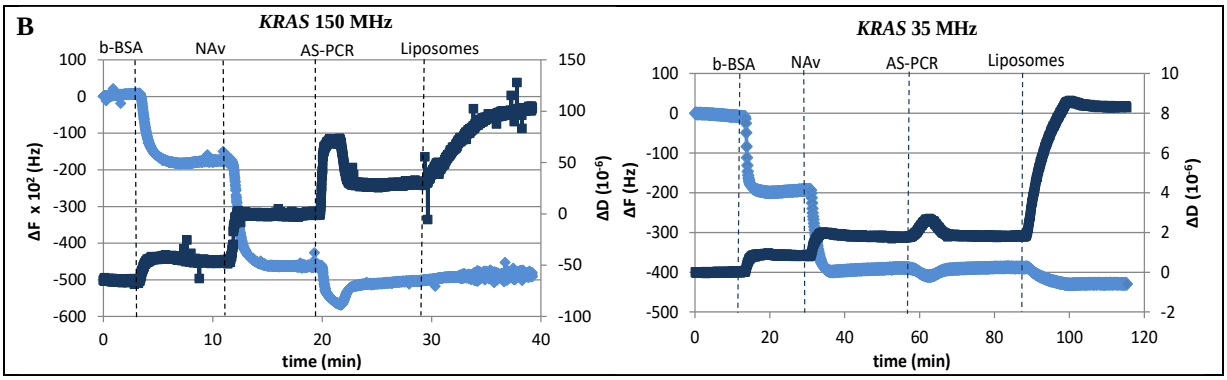

Figure 16. *(A) Comparison of the real-time graphs of the acoustic detection of BRAF V600E AS-PCR products using the 150 MHz acoustic array and the 35 MHz QCM device. Dashed lines represent the time of the addition of b-BSA on the sensor surface followed by the NAv, the AS-PCR reaction (here a reaction of 0.1% mt:wt ratio) and finally the injection of the 200 nm POPC liposomes. (B) Same as (A) for KRAS G12D.*

5. Comparison of the combined AS-PCR/acoustic method to current techniques for genomic and ct DNA detection

At this point we would like to note that due to the primer sets' design which resulted to PCR amplicons of less than 90 bp, the same protocols are suitable for the analysis of the highly fragmented cell-free DNA, too (see Chapter 5). Apart from that, advantages of the newly developed acoustic detection methodology are the (a) ability to work with crude (non-purified) AS-PCR samples, (b) complete elimination of a hybridization step and (c) excellent sensitivity. To our knowledge, the above performance is the best one reported so far among the traditional AS-PCR assay and its variants, e.g., the AS-NEPB-PCR[166], cAS-PCR, rcAS-PCR[71], CAST-PCR[167] and ARMS[66,70,74] which have the limited sensitivity of 0.1-2%, affecting their potential broad clinical use[57]. Moreover, in all the above assays, detection takes place in situ, i.e. during amplification, using fluorescent probes. Our AS-PCR/acoustic assay seems to be a promising alternative reaching a detection capability of 0.01% MAF without increasing the complexity of the assay.

Comparing to the gold-standard technique applied for tissue biopsy, i.e., the Sanger sequencing, our method is significantly improved in terms of sensitivity (15%-20% Vs 0.01%-0.05%, respectively). Furthermore, in contrast to the commercially available qPCR Cobas test, AS-PCR/acoustic detection is considerably improved in terms of both sensitivity (≥5% for COBAS vs 0.01%-0.05% for acoustic) and analysis time (8 hs for COBAS vs 5hs for acoustic, including sample treatment and DNA extraction). However, the COBAS test offers the advantages of multiple samples analysis and ability to detect a panel of mutations (4 BRAF, 19 KRAS) simultaneously. With the current acoustic biochip design, six samples can be detected per array (giving 4 readings per sample) as demonstrated during the detection of two point mutations. Employing a new flow-cell design with the current array, to test 8 (3 readings/sample) or 16 (2 readings/sample) mutations can improve multiple analysis. In addition, given the low cost of the biochip array (~1$ for large scale production), 2 or 3 array biochips could be used in parallel, without increasing substantially the complexity and size of

the instrumentation. Eventually, comparing to the ddPCR usually employed for the *BRAF* V600E/*KRAS* G12D analysis, our method is more cost-effective, since we employ a standard thermocycler (2.6K) and the acoustic platform (10K), both orders of magnitude less expensive than a ddPCR machine (110K). The development of a single platform integrating a thermocycling unit with acoustic detection is also a feasible future plan.

Conclusions

In this work, we report the successful application of the novel HFF-QCM 24-sensors array biochip for the acoustic detection of the *BRAF* V600E and *KRAS* G12D point-mutations in genomic DNA. We used AS-PCR for the specific amplification of the mutated target followed by acoustic detection in a two-step assay. The above, included the direct immobilization of the ds amplicons on the sensor surface and the detection through 200 nm liposomes which caused dissipation-signal amplification. We achieved the detection of a single DNA molecule carrying the *BRAF* V600E or 5 carrying the *KRAS* G12D point mutations in a 10^4 fold excess of the wt allele, i.e., with a sensitivity of 0.01% - 0.05% respectively and in total analysis time of 2 hours.

Regarding the two acoustic devices, although no significant differences were found between the 150 and 35 MHz QCM biosensors in terms of sensitivity and detection limit, the faster analysis time (30 min vs 100 min), the need for lower samples volumes (60 vs 200 μL) and the ability for multi-sample analysis, make the 24-acoustic array a promising diagnostic tool. Adding to the above the cost-effective nature of the acoustic technology, it is anticipated that the latter can become a promising tool for the high-throughput screening of cancerous mutations in tissue and plasma samples. The results concerning the performance of the AS-PCR combined with the acoustic array biochip for cancer mutation analysis in tissue and plasma samples are currently under submission[121].

Chapter 5

Application of the Allele-Specific PCR/acoustic array biochip technique for the detection of *BRAF* and *KRAS* point mutations in tissue and plasma samples; *comparison with Sanger Sequencing and ddPCR*

Introduction

In Chapter 4, a new technique consisted of AS-PCR combined with end-point acoustic detection was presented. For the acoustic detection, a novel HFF array biochip which permitted the fast and low-cost analysis of up to 6 AS-PCR samples was used. The assay was developed for the screening of the *BRAF* V600E and *KRAS* G12D mutant alleles in genomic DNA. It was characterized by remarkably high sensitivity (0.01% – 0.05% MAF) for an AS-PCR, quantitative analysis and ultralow detection limit (1 – 5 mutant copies). So far only genomic DNA samples were examined. Here the assay was evaluated for its performance in DNA derived from real patients FFPE tissue but also plasma samples. This means that our method was applied for mutational status analysis in the highly demanding circulating tumor DNA in the context of Liquid biopsy, too. Our results were compared with standard detection techniques applied for tissue and Liquid biopsy, i.e., Sanger sequencing and droplet digital PCR (Fig. 1).

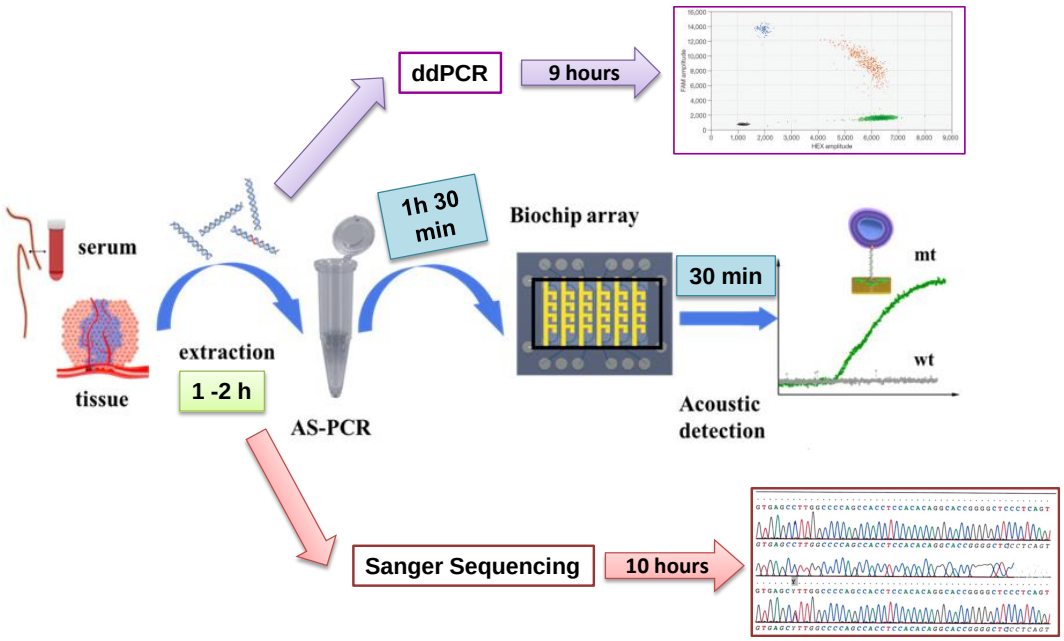

Figure 1. *Diagram of the acoustic protocol and the 2 additional detection techniques. In all cases genomic or cell-free DNA will be extracted using conventional methods. The extracted genomic DNA will then be subjected to analysis with all the 3 techniques while the cfDNA only with the acoustic and ddPCR methods. The total assay time is also indicated for each case.*

ddPCR

Digital PCR is a relatively new technology for the ultrasensitive detection of DNA targets in an absolute quantification manner. Nowadays, there are several commercial droplet-based digital PCR microfluidic platforms including RaindropTM digital PCR (Raindance Technologies, recently acquired by Bio-Rad) and the Bio-Rad QX200TM Droplet DigitalTM system (Bio-Rad Laboratories), with the latter being the most widely employed. Generally, in droplet digital PCR DNA samples are partitioned in aqueous droplets (ranging from nanoliter to few picoliter size) which act as independent micro-compartments where PCR is carried

out[72]. In the Bio-rad QX200TM Droplet DigitalTM system, the ddPCR mix plus the input DNA sample, Taqman probes with different fluorophores for the mt and the wt target genes (final volume of 20 µL) and the droplet generator oil are loaded into the wells of the droplet generator cartridge. Then, they pass through the microfluidic circuits via vacuum to form a dispersion of 1 nL droplets. In each well, the 20 µL mixture is divided into 20000 droplets which are stabilized by the use of surfactant chemistry[75]. The number of droplets has further been increased up to 10 million picoliter-sized droplets by the RainDrop dPCR System (RainDance Technologies)[61]. It is estimated that each droplet contains about 1 haploid genome[72]. Following sample division, the stabilized droplets are transferred to a 96-well PCR plate, and amplification is carried out in a thermal cycler. Following amplification, the plate is introduced into a droplet reader where droplets are aspirated from the wells and pass through a two-color detector. Depending on their fluorescence, droplets are classified as mt, wt or negative. Results are furthered analyzed to calculate target concentrations using a Poisson correction[75]. By counting the droplets with different fluorescent signals, the absolute quantification and identification of mutant sequences within wild-type ones can be achieved with a sensitivity of <0.001%[72]. Note that, a ddPCR sensitivity relies on the number of droplets that the applied system can generate[61] (Fig. 2).

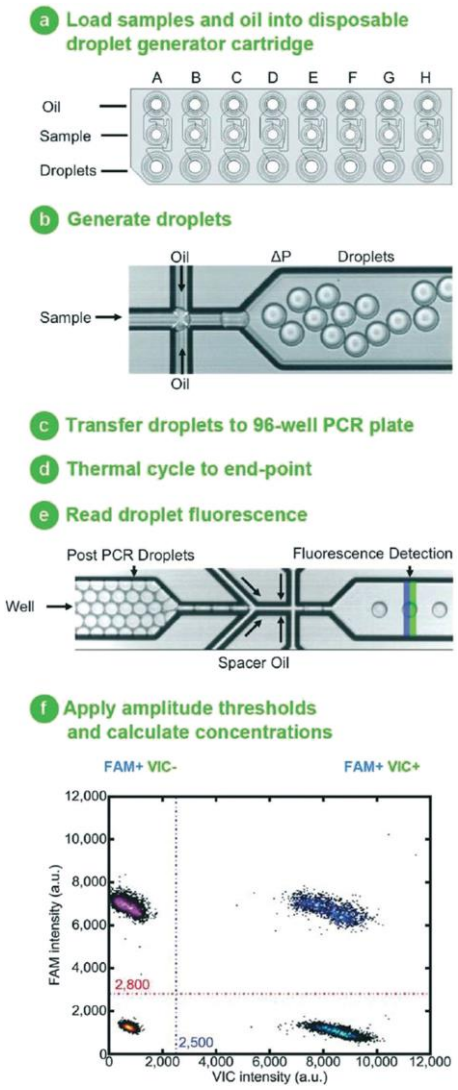

Figure 2. *Schematic representation of droplet digital PCR. (a) Samples and oil are loaded into a droplet generator cartridge. (b) Using a vacuum, droplets of 1 nL are produced. (c) Stabilized droplets are transferred to a 96-well PCR plate. (d) PCR amplification is carried out to a thermal cycler. (e) Then, fluorescence signals from each droplet are measured at the reader which aspirates the droplets from each well and passes them through a two-color detector (f) Results are appeared in a 2D scatter plot. Droplets are labelled as positive or negative based on their fluorescence signal. For example, purple dots correspond to mt targets, light blue to wt, dark blue to the presence of both mt and wt, and orange to negative droplets. Picture was obtained by* [61].

- Sanger Sequencing

During Sanger Sequencing the DNA sequence of interest is amplified through suitable oligonucleotide primers in the presence of the typical deoxynucleotide triphosphates (dNTPs) A, C, T, G and a small quantity of the chain-terminating dideoxynucleotide triphosphates (ddNTPs). Firstly, the DNA template is denaturated following by primer annealing and elongation. Elongation occurs until a ddNTP is incorporated, where due to the absence of 3-OH the growing DNA chain will be terminated. As the dNTPs and ddNTPs have an equal chance of attaching to the sequence, each sequence will terminate at varying lengths. Moreover, each ddNTP (ddATP, ddGTP, ddCTP, ddTTP) is labeled with a different fluorophore marker[168]. Thus, the final product of the reaction is a mixture of single-stranded

DNA fragments of various lengths, each labelled at the 3' end with a fluorophore. The reaction is then analyzed by capillary electrophoresis where the fluorescence intensity by the fragments is continuously recorded and finally presented as an electropherogram that can be interpreted by base-calling software, such as Mutation Surveyor[169]. In the electropherogram usually, A is indicated by green fluorescence, T by red, G by black, and C by blue. In the presence of heterozygosity within the examined sequence, the different variant will be labelled by 2 fluorescent dyes of equal intensity[168] (Fig. 3).

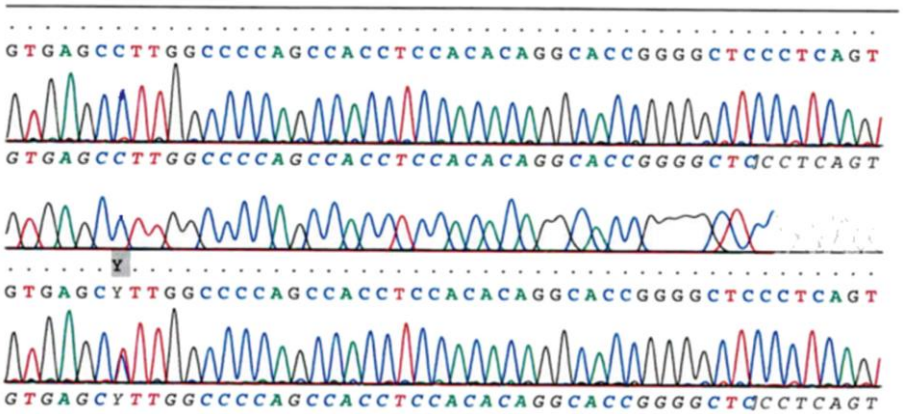

Figure 3. *Electropherogram from Sanger sequencing. The presence of a heterozygous single nucleotide variant from C to T (shown as Y) compared to sequencing of normal control samples is presented. Schematic was obtained by* [168].

In clinical application like the detection of mutations in genomic DNA, the sequence of interest is usually pre-amplified with conventional PCR. Moreover, for the performance of clinical Sanger sequencing the fluorescent dye-terminator method is used combined with the commercially available kits like the BigDye V3.1 (Applied Biosystems).

Materials & Methods

Materials	
High-performance liquid chromatography (HPLC)-grade oligonucleotides	Metabion International AG, Germany
Extracted DNA from Formalin Fixed paraffin-embedded (FFPE) tissue samples	Department of Medical Oncology, University Hospital of Heraklion
Extracted DNA from plasma samples	Department of Medical Oncology, University Hospital of Heraklion
***BRAF* wt reference standard**	Horizon Discovery Ltd, UK
KAPA2G Fast HotStart ReadyMix	Kapa Biosystems, Inc., US
SYBR® Green I Nucleic Acid Stain 10000X	Lonza, Switzerland
Platinum Taq DNA polymerase and 10X Reaction buffer	Invitrogen, US
ddPCR BRAF V600 Screening Multiplex Kit (Bio-Rad)	Bio-Rad Laboratories Inc., US
***KRAS* G12/G13 Screening Multiplex Kit**	Bio-Rad Laboratories Inc., US
NucleoSpin® Gel and PCR Clean-up	Macherey Nagel, GmbH & Co. KG

QIAamp DNA Micro Kit	Qiagen, Hilden, Germany
QIAamp Circulating Nucleic Acid kit	Qiagen, Hilden, Germany
Phosphate buffer Saline (PBS) tablet	Sigma-Aldrich, Miss., US
NeutrAvidiv Protein	Thermo Fischer Scientific, Mass., USA
BSA lyophilized powder, crystallized, ≥98.0% (GE)	Sigma-Aldrich, Miss., US
Biotin-$(AC_5)_2$-Sulfo-Osu	Dojindo, Japan
Microcon-30kDa Centrifugal Filter Unit with Ultracel-30 membrane	Merck KGaA, Darmstadt, Germany
1-palmitoyl-2-oleoyl-glycero-3-phosphocholine (POPC)	Avanti Polar Lipids, Inc., Alabaster, AL, USA
Nuclepore polycarbonate hydrophilic membranes 0.2 μm	Whatman plc, UK

DNA Sequences of primers (5' -> 3')		**Product size (bp)**
***BRAF*-V600EF**	**chol**-ACTACACCTCAGATATATTTCTTCATG	89
***BRAF*-V600ER**	**biotin**-CCCACTCCATCGAGATTGCT	
***KRAS*-G12DF**	**biotin**-CTTGTGGTAGTTGAAGCGGA	85
***KRAS*-G12DR**	**chol**-CATATTCGTCCACAAAATGATTCTG	
***KRAS*_Ex2F**	TAAGGCCTGCTGAAAATGAC	165
***KRAS*_Ex2R**	GTCCTGCACCAGTAATATGC	
***BRAF*_Ex15F**	TGTTTTCCTTTACTTACTACACCTCA	163
***BRAF*_Ex15R**	GCCTCAATTCTTACCATCCA	

Sample collection. A total of 21 FFPE tumor and 20 plasma samples were obtained from patients with various cancer types (NSCLC, melanoma, colorectal cancer), at the Department of Medical Oncology, University Hospital of Heraklion. The research protocol was approved by the Institutional Ethics Committee of the University Hospital of Heraklion and all patients provided written informed consent to participate in the study. FFPE tumor sections from all patients, underwent histopathologic evaluation to confirm the diagnosis and to define tumor-enriched areas. For samples with lower than 80% of malignant cells in the examined section, tumor areas were micro-dissected to enrich the analyzed specimen with cancer cells.

DNA extraction. Genomic DNA (gDNA) was extracted from manually micro-dissected tumor cells from FFPE specimens, using the QIAamp DNA Micro Kit according to the manufacturer's centrifuge-based protocol. Circulating cell-free DNA (cfDNA) was isolated from 2 mL of plasma for each sample *via* the QIAamp Circulating Nucleic Acid kit. cfDNA was eluted in 60 μL of nuclease-free water and concentration was measured using Qubit dsDNA HS Assay kit on a Qubit 2.0 Fluorometer (Thermo Fisher Scientific, Mass., USA), according to the manufacturer's instructions.

Tissue-based *KRAS* and *BRAF* Mutation analysis using Sanger Sequencing. Genomic DNA from FFPE tissues, was amplified by PCR using specific primer pairs for *KRAS* exon 2

[*KRAS*_Ex2F & *KRAS*_Ex2R (PCR amplicon of bp)] and *BRAF* exon 15 [*BRAF*_Ex15F & *BRAF*_Ex15R (PCR amplicon of 160 bp)] which include the mutation hotspot that encodes the *KRAS* G12D and *BRAF* V600E variant, respectively. PCR reactions were carried out and PCR products were purified with the Nucleospin PCR clean-up kit. Sequencing reactions were performed using the Big Dye terminator V3.1 cycle sequencing kit (Applied Biosystems, USA) according to the manufacturer's protocol. After purification by ethanol precipitation the products were assessed by capillary electrophoresis on an ABI3130 System and results were analyzed using Sequencing Analysis software v5.4 (Applied Biosystems, USA).

Droplet digital PCR (ddPCR)-based analysis for *BRAF* and *KRAS* quantification in gDNA and cfDNA. Droplet digital PCR (ddPCR) was performed using the QX200 Droplet Digital PCR System (Bio-Rad Laboratories Inc., US) and the ddPCR *BRAF* V600 or the *KRAS* G12/G13 Screening Multiplex Kits, according to the manufacturer's instructions. As template 50 ng genomic DNA were used extracted from FFPE tissue or 3.5 µL - 4 µL with cell-free DNA extracted from plasma samples were used. Each DNA sample was tested in two technical replicates and every ddPCR run included negative template controls (NTCs) and positive controls (mutant homozygous and heterozygous cancer cell lines, as well as WT samples for *KRAS* G12/13 and *BRAF* V600). After sample partition into up to 20 000 droplets using the Bio-Rad QX-200 droplet generator, 40 µL of emulsion for each sample was transferred to 96-well plates and PCR was done on C1000 Touch thermal cycler (Bio-Rad Laboratories Inc., US). The QX200 droplet reader and the QuantaSoft Analysis Pro Software (Version 1.0.596) were used to assign positive/negative droplets, to convert counts to target copies/µL of reaction and to calculate the mutant allele frequency (MAF). Threshold was manually set for each sample, based on positive control samples (mutant and WT for each channel-FAM and HEX, respectively). Wells with less than 10000 accepted droplets were excluded from further analyses. A minimum of three positive droplets was used to call a sample positive for the *BRAF* V600E mutation, which is the minimum acceptable value for the ddPCR Poisson precision calculation.

Amplification of the *BRAF* V600E via AS-PCR in real samples. 5 µL KAPA2G Fast HotStart ReadyMix 2X was mixed with 5 pmol of the allele-specific biotinylated reverse primer *BRAF*-V600ER and with 5 pmol of the cholesterol modified forward primer *BRAF*-V600EF in a total volume of 10 uL. These primers are optimized for the *BRAF* V600E mutation detection by Z. Yang et al.[71]. For tissue biopsy, as template, 50 ng genomic DNA extracted from FFPE tissue samples was used. For Liquid biopsy as template 2 - 3.5 uL extracted cell-free DNA were used in the presence of 2 ng background wt genomic DNA. The cycling protocol consisted of 50 (liquid biopsy) – 55 (tissue biopsy) cycles of 10 sec at 94 ^{o}C, 10 sec at 60 ^{o}C and 10 sec at 72 ^{o}C. As-PCR products were then subjected to acoustic analysis. A no template control (NTC) as well as positive (A375 homozygous cell line) and wt control (HCT-116 cell line) was included in every run.

Amplification of the *KRAS* G12D via real-time AS-PCR in real samples. For the *KRAS* G12D mutation analysis 10 pmol of the mutation-specific biotinylated forward primer (*KRAS*-

G12DF), 10 pmol of the cholesterol-modified reverse primer (*KRAS*-G12DR) and 1µL 20X SYBR® Green I Nucleic Acid Stain were mixed with 10 µL KAPA2G Fast HotStart ReadyMix 2X in a total volume of 20 µL. As template, 50 ng genomic DNA extracted from FFPE tissue samples or 3.5 µL extracted cell-free DNA were used. PCR reactions mixtures were carried out at CFX Real-Time PCR Detection Systems (Bio-Rad Laboratories Inc., US). The cycling protocol consisted of an initial denaturation step for 5 min at 95 ^{o}C followed by 45 cycles of 10 sec at 94 ^{o}C, 10 sec at 62 ^{o}C and 2 sec at 72 ^{o}C). A NTC reaction was included in every run.

Quartz crystal microbalance (QCM) with dissipation monitoring acoustic devices. For the experiments two QCM devices were used; the High Fundamental Frequency – QCM (HFF-QCM) (AWS S.L., Paterna, Spain) operating at 150 MHz and the commercial QSense Analyzer E4 instrument (QSense, Sweden). The HFF-QCM platform monitored a HFF-QCM array (AWS, S.L. Paterna, Spain) mounted on a custom Printed Circuit Board (PCB). Cleaning of the PCB and array included treatment with Hellmanex 2% for 30 min, rinsing with mili-Q water and 70 % EtOH and drying under N_2. Then, the array was cleaned by 30 min UV/Ozone (Ossila Ltd, Sheffield) followed by treatment with absolute EtOH for 30 min. The flow cell employed a PMMA gasket and a PDMS cell (AWS, S.L. Paterna, Spain), both cleaned with Hellmanex 2 % for 30 min, incubated with mili-Q water in a sonicator for 15 min and dried at 65 ^{o}C. The flow-cell was connected to a syringe pump of 50 µL or 250 µL installed in the platform. About the QSense Analyzer, the operating frequency for the results reported here is the 35 MHz (7 th overtone); ΔF was not normalized by the overtone number. Before use, the Au-coated 5 MHz sensors were cleaned with Hellmanex 2 % for 15 min, rinsed with mili-Q water, dried under N2 and treated for 30 min with UV/Ozone (Ossila Ltd, Sheffield). Acoustic experiments were carried out under a continuous flow of 20 µL/min for the AWS device and at 50 µL/min for the QSense at 25 ^{o}C. All samples were diluted in PBS pH=7.4, which was the running buffer. Following each sample addition, buffer rinsing was taken place and then frequency and dissipation changes were obtained.

Liposome preparation. Lyophilized 1-palmitoyl-2-oleoyl-glycero-3-phosphocholine (POPC) lipids were dissolved in chloroform at final concentration of 10 mg/mL. 100 – 200 µL of the 10 mg/mL lipids were added in round bottom glass flask and dried homogenously under N_2 flow. The lipid film was then left for 30 min under N_2 gas followed by resuspension in PBS at a final concentration of 2 mg/mL by gentle vortexing. The resulting suspension was passed through polycarbonate membranes with a nominal pore diameter of 200 nm, using the Avanti Mini-Extruder. Stock solutions were stored at 4 °C for up to 6 days.

Acoustic analysis of AS-PCR. Prior to the analysis of the AS-PCR reaction the gold sensor surface was modified with b-BSA injected at a concentration of 0.2 mg/mL followed by the addition 0.05 mg/mL of NAv. In all cases the working volumes were V_{150MHz}=60 µL and V_{35MHz}=200 µL. b-BSA was prepared after incubation of BSA lyophilized powder (Sigma-Aldrich) with biotin-$(AC_5)_2$-Sulfo-Osu linker in PBS, in a molar ratio of 1:10, for 1 h and 30 min at RT; after incubation, BSA was purified using the Microcon-30kDa Centrifugal Filter Unit

with Ultracel-30 membrane following manufacturer instructions. Following the creation of the substrate, a sample of 2.5 µL or 8 µL of the BRAF or KRAS AS-PCR reactions respectively, diluted in a total volume of 20 µL, was loaded on the 150 MHz sensors (flow rate: 14 µL/min). Similarly, 2.5 µL or 10 uL of the BRAF or KRAS AS-PCR, diluted in a total volume of 125 µL, was applied to the 35 MHz QCM device surface at a flow rate of 25 µL/min. In both cases, a suspension of 0.2 mg/mL of 200 nm POPC liposomes was added at a volume of 100 µL (150 MHz) or 500 µL (35 MHz).

Results & discussion

AS-PCR followed by acoustic analysis employing the HFF biochip array was evaluated for the detection of *BRAF* V600E and *KRAS* G12D mutant alleles in real samples obtained from melanoma, colorectal and lung cancer patients. Although the assay was initially developed and validated for the detection of point mutations in genomic DNA, here both FFPE tissue and plasma samples were tested. The primers were designed in such way in order to result to PCR amplicons of less than 90 bp. As a result, the same protocols were applicable for the analysis of the highly fragmented cell-free DNA, too. In both FFPE and plasma samples, DNA was extracted using standard procedures. Following extraction, DNA samples were analyzed by our method as well as conventional techniques used for tissue and liquid biopsy i.e., Sanger sequencing and droplet digital PCR.

1. Validation of the method with real FFPE tissue samples and comparison with Sanger sequencing and ddPCR

Regarding the *BRAF* mutation analysis, a total of 11 samples collected from lung (L), melanoma (MEL) and colorectal cancer (CRC) patients' tissues as well as healthy individuals were tested. Of the above samples, 6 were positive and 5 negative, as identified by Sanger sequencing and ddPCR. For the KRAS mutation, 10 samples in total were tested, 6 mt and 4 wt, also derived from patients and healthy donors and again identified as before. Results are summarized in Table 1 where, in addition to Sanger sequencing, ddPCR and AS-PCR/acoustic results, the calculated mutant allele frequency (MAF) is provided; the latter is defined as the % of mt/(mt+wt) for each sample, based on ddPCR-measurement of the absolute No of mt and wt copies in each sample. In addition to the acoustic detection, all samples were also analyzed by gel electrophoresis. Interestingly, two of the samples (1906 and 168096) were only detected through the acoustic analysis, confirming that the acoustic detection of AS-PCR products coupled with 200 nm liposomes was a more sensitive method than gel electrophoresis. Note that while for the KRAS we would expect quantitative results, due to the high MAF% (>37.5%) and the high number of mutated DNA copies (222-1752) the results were only qualitative since the reactions were at the early plateau phase at the 45 cycles.

Based on table 1, the obtained acoustic results were in full agreement with the Sanger sequencing and ddPCR. Overall, no false positives or false negatives were recorded, indicating 100% sensitivity and specificity for both targets. Moreover, all wt samples gave a

zero response, indicating the power of the proposed acoustic methodology to discriminate at least qualitatively (positive/negative result) between malignant and healthy tissues.

Finally, the analysis of the samples shown in Table 1 based on the frequency measurement failed to discriminate malignant from healthy tissue samples.

Table 1. *Description of the results obtained from patients' FFPE samples with all the three techniques (AS-PCR/acoustic detection, Sanger sequencing, ddPCR). Abbreviations: L-Lung; MEL-Melanoma; CRC-Colorectal; MAF-Mutant Allele Frequency.*

Tissue sample	Acoustic ΔD (x10^{-6})	Sanger	ddPCR Mt copies	ddPCR Wt copies	MAF%
BRAF V600E					
1906 (MEL)	**44 ± 10**	**mt**	**960**	**914**	**51.2**
1947(L)	0	wt	0	3040	0
2786 (CRC)	**120 ± 17**	**mt**	**262**	**560**	**31.8**
2840 (L)	0	wt	0	2600	0
4458 (L)	0	wt	0	3100	0
6316 (L)	0	wt	0	4480	0
7874 (L)	0	wt	0	410	0
10014 (MEL)	**110 ± 31**	**mt**	**448**	**666**	**40.2**
142648 (MEL)	**138 ± 25**	**mt**	**1994**	**2880**	**40.9**
168078 (L)	**224 ± 51**	**mt**	**1052**	**1706**	**38.1**
168906 (CRC)	**47 ± 3.9**	**mt**	**544**	**800**	**40.4**
KRAS G12D					
K534 (CRC)	0	wt	0	3860	0
10434 (CRC)	0	wt	0	1606	0
6229-10 (L)	**125 ± 9**	**mt**	**834**	**1384**	**37.6**
7102 (CRC)	**119 ± 11**	**mt**	**222**	**244**	**47.6**
7874 (L)	0	wt	0	592	0
10272 (L)	0	wt	0	1540	0
10732 (CRC)	**122 ± 15**	**mt**	**640**	**704**	**47.6**
12784 (CRC)	**135 ± 21**	**mt**	**390**	**592**	**39.7**
164665 (CRC)	**137 ± 16**	**mt**	**1752**	**1774**	**49.6**
159216 (CRC)	**104 ± 24**	**mt**	**774**	**1396**	**35.7**

*Mt, Wt copies referred to the number of the mt or wt molecules per 50 ng input DNA, respectively.

2. Application of the method to real plasma samples and comparison to ddPCR

While the assay was initially developed and validated for the detection of point mutations in tissue DNA, the method was further assessed in ctDNA derived from real plasma samples carrying the *BRAF* V600E or *KRAS* G12D mutation.

From previous results using synthetic dsDNA target of 140 bp mimicking the "cell-free" *BRAF* gene, we noticed that the AS-PCR of 55 cycles was prone to contamination and by-products formation (data not shown). For this reason, the protocol was further optimized by adding (a) 2 ng of background wt genomic DNA to each reaction and (b) reducing the number of cycles from 55 to 50. In practice, 10 plasma samples identified as *BRAF* V600E or *BRAF* wt by ddPCR were subjected to AS-PCR followed by acoustic detection. In contrast to results obtained with tissue samples, in the case of plasma a ΔD was detected for the wt specimens, although significantly lower to that obtained for positive samples. We first tried to identify the source of the background signal; gel electrophoresis of all tested wt samples indicated a high degree of by-products even after 50 PCR cycles (Fig. 1). We attributed this response to the presence of cholesterol-primers aggregation, possibly due to the specific batch used in these experiments. To define the cut off value above which ΔD change would be considered as an indication of a positive sample, we calculated the mean ΔD value from all wt samples (healthy) plus three standard deviations[87]; this cut off value was set at a $\Delta D > 80x10^{-6}$ (99% CI). Based on the above criterion and results presented in Table 2, we concluded that all samples carrying the *BRAF* V600E point mutation were correctly identified with our method as positive and discriminated from samples coming from healthy individuals. Statistical analysis verified that the mt:wt populations were significantly different ($p<0.001$).

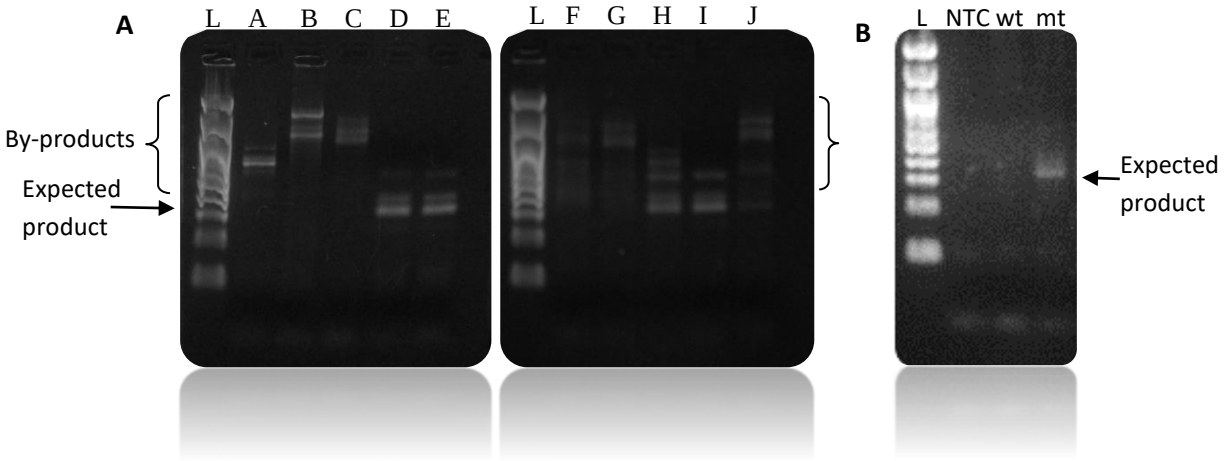

Figure 1. A) *Analysis of AS-PCR products from plasma samples by gel electrophoresis on 2% agarose gel. L:100 bp DNA Ladder. A, B, C, F, G corresponds to the wt samples 5MEL, 9MEL, 10MEL,3MEL, 14MEL and D, E, H, I, J to the mutant samples 2MEL, 1871L,1845L ,4MEL, 11MEL, respectively. The expected product is 89 bp, however due to the cholesterol the 89 bp band shifts between the 300-400 bp. As control a gel electrophoresis of AS-PCR derived from genomic DNA is presented (B).*

Regarding the *KRAS* G12D mutation analysis 10 plasma samples identified as *KRAS* G12D or *KRAS* wt by ddPCR were blindly tested by the AS-PCR/acoustic detection. For the reaction, the same protocol as for the genomic *KRAS* DNA presented in Chapter 3 was used. According to Table 2, the combined AS-PCR/acoustic method provided results in full agreement with the ddPCR. Note that, two samples, the 11MEL and 1797L ones, corresponding to 27 and 19 *BRAF* and *KRAS* mutant copies respectively, and a MAF value of <1% were clearly identified as positive by the acoustic method. Finally, as in genomic-based AS-PCR followed by acoustic detection at 150 MHz, frequency response was not as sensitive as the dissipation (Fig. 2).

Table 2. *Description of the results obtained from patients' plasma samples when analyzed by ddPCR and AS-PCR/acoustic detection. Abbreviations: L-Lung; CRC-Colorectal; MAF-Mutant Allele Frequency.*

Plasma sample	Acoustic ΔD (x10^{-6})	ddPCR Mt copies	ddPCR Wt copies	MAF%
BRAF V600E				
2 (MEL)	**166 ± 21**	**6110**	**4190**	**59.2**
3 (MEL)	40 ± 2	0	194	0
4 (MEL)	**230 ± 35**	**133**	**346**	**27.7**
5 (MEL)	35 ± 8	0	389	0
9 (MEL)	20	0	7050	0
10 (MEL)	9 ± 5	0	523	0
11 (MEL)	**97 ± 13**	**27**	**2680**	**0.99**
14 (MEL)	55	0	865	0
1845 (L)	**212 ± 53**	**67**	**1345**	**4.7**
1871 (L)	**199 ± 56**	**100**	**5490**	**1.78**
KRAS G12D				
1504 (CRC)	**123 ± 3**	**1432**	**8940**	**13.8**
1523 (CRC)	0	0	163	0
1574 (CRC)	0	0	698	0
1596 (CRC)	**118 ± 2.8**	**162**	**1198**	**11.91**
1597 (CRC)	**175 ± 35**	**1574**	**1838**	**46.13**
1602 (CRC)	0	0	2500	0
1604 (CRC)	3 ± 3.5	0	1594	0
1618 (CRC)	**113 ± 27**	**32.8**	**922**	**3.43**
1797 (L)	**21 ± 2**	**19**	**2080**	**0.91**
1827 (L)	**92 ± 5**	**70.6**	**910**	**7.19**

*Mt, Wt copies referred to the number of the mt or wt per AS-PCR reaction, as calculated by ddPCR.

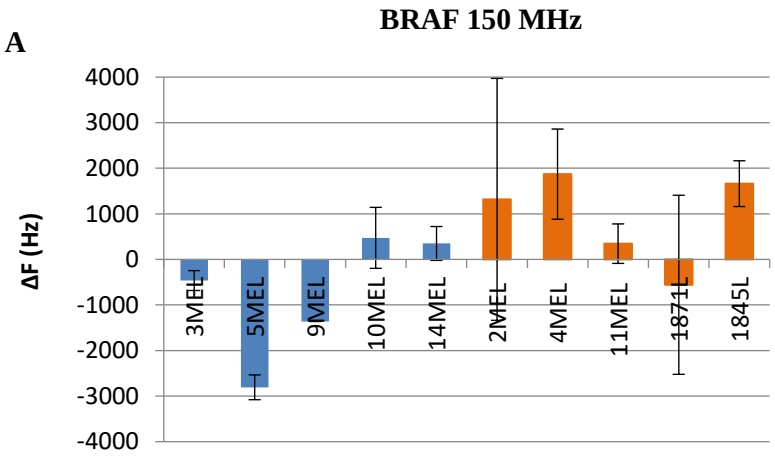

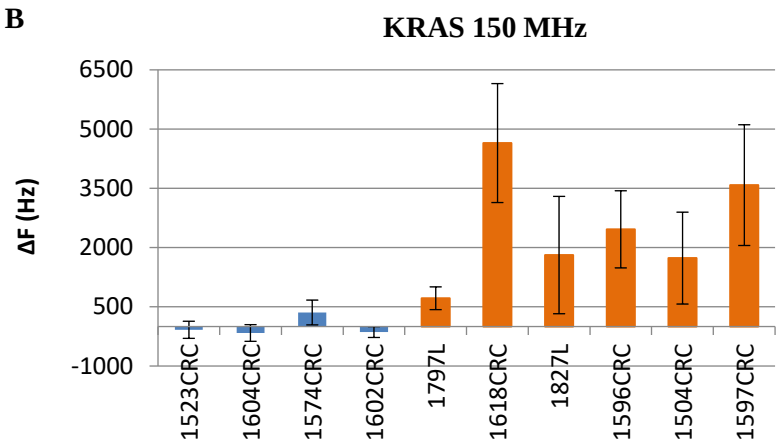

Figure 1. *Comparison of ΔF values obtained by the analysis of patients' (A) BRAF V600E and (B) KRAS G12D plasma samples by AS-PCR & acoustic detection at 150 MHz.*

Conclusions

Concluding, the newly developed acoustic method involving the use of the 24 HFF array biochip was successfully applied for the detection of the *BRAF* V600E and *KRAS* G12D mutations in real FFPE-tissue and plasma samples from colorectal, lung and melanoma cancer patients. The samples were previously analyzed by ddPCR and in the case of genomic DNA, by Sanger sequencing, as well. The obtained acoustic results were in good agreement with those of ddPCR and Sanger sequencing indicating the excellent performance of our assay.

The high technology readiness level of our method is demonstrated by the successful application to both circulating and genomic tumor DNA for both liquid and tissue biopsy, respectively. Tissue biopsy still remains the standard-of-care test for cancer diagnosis. However, is generally inappropriate for the monitoring of cancer patients during and following treatment; not only is hazardous, difficult to be obtained and time-consuming but also fails to reveal tumor heterogeneity[51–54] which leads to acquired treatment resistance[53,55]. The latter, actually reduces the reliability of solid biopsies for treatment selection, as well. Conversely, liquid biopsy is minimally invasive helps reveal tumor heterogeneity and is generally appropriate for monitoring of known tumors, treatment progress and minimal residual disease (MRD)[61]. Nevertheless, liquid biopsy is limited because its effectiveness can be affected by a variety of factors including the stage and location of tumor[51,170] as well as the extraction method and the sample type[161,171]. Finally, the combined analysis of tissue and liquid biopsy is of high clinical significance since in 86% of patients, solid and liquid biopsies provided different molecular information[51]. Our method will provide the possibility of complete characterization of tumor heterogeneity as well as the option for non-invasive monitoring.

The results regarding the evaluation of the AS-PCR combined with the acoustic array biochip for the detection of the *BRAF* V600E and *KRAS* G12D mutations in tissue and plasma samples are currently under submission by Naoumi N. et al.[121].

Overall Conclusions

1. Development of a b-BSA/NAv substrate for the capturing of double-labelled with biotin and cholesterol DNA targets in unpurified molecular amplification reactions through the biotin-NAv interaction. The above substrate was applied for the analysis of the LCR and AS-PCR products described below.

2. Detection of the immobilized DNA targets using POPC liposomes of 200nm after capturing to the targets through the cholesterol.

3. Successful application of the novel 24 sensors acoustic array and acoustic platform for the analysis of proteins, dsDNA and dsDNA through liposomes.

4. Enrichment of DNA targets carrying the *BRAF* V600E point mutation using LCR. During LCR, double-labelled with biotin and cholesterol products were created and detected through the 200nm POPC liposomes at 35 MHz. By this method, 3.3 $x10^3$ or 5.5 zmol or 220 aM of mt target were detected. However, this detection limit was far more than the required one (1-10 mt copies). We concluded that LCR was limited by the target-independent-ligated by-products which became predominant following several amplification cycles. Target-independent-ligation was finally the main reason affecting the overall detection limit of the assay. Note that, during the investigation of LCR's capability to selectively amplify the mt target vs the wt, only spiked-in samples were tested and no sensitivity assays were performed. Despite LCR's failure to reach the required detection limit, the above was close to the best reported and better than other LCR and LCR variants usually coupled with (q)PCR and (Hype-)RCA indicating a generally good performance of our method. Thus, LCR may be applicable to the detection of other targets like miRNAs and pathogens.

5. Although the microfluidic magnetic fluidized bed was successfully applied for the extraction of dsDNA target spiked-in human serum and plasma followed by detection through LCR and acoustic analysis, the detection of the dsDNA sequence of interest was possible only at the high concentrations of 100 fM (9 $x10^6$ copies) - 1 pM (9 $x10^7$ copies) and 1 pM (9 $x10^7$ copies) – 10 pM (9 $x10^8$ copies) in human serum and plasma samples, respectively. Moreover, while the main goal was to perform LCR directly on the beads with the captured target in order to reduce the overall assay steps, LCR worked only after releasing the target from the beads.

6. Since LCR failed to give the required detection limit and sensitivity, a very efficient AS-PCR was developed and combined with acoustic analysis this time at 150MHz. The new method showed a sensitivity of 0.01% MAF for the *BRAF* V600E detection providing qualitative results and of 0.05% for the *KRAS* G12D mutation giving quantitative results as well. Results

were compared with the 35 MHz sensors and were in good agreement. However, the 150MHz array provided a multi-sample, more cost-effective and faster analysis (overall assay time of just 2 hours). Our method exhibited a better sensitivity compared to a variety of AS-PCR techniques based on fluorescence detection such as the ARMS-PCR, PNA/LNA-PCR, COLD-PCR, AS-NEBP-PCR, cAS-PCR, CAST-PCR (0.1 – 2%). Moreover, we achieve a better sensitivity than the standard of care Sanger sequencing (15% -20%) and the FDA approved Cobas PCR test (5%). Our sensitivity was closer to the dPCRs in a faster and more affordable way but without providing absolute quantification.

7. The method was successfully validated in real *BRAF* V600E and *KRAS* G12D tissue and plasma samples. The above results confirmed the high technology-readiness level of the method and the suitability for clinical use in an oncology lab for both tissue and liquid biopsy.

Future Prospects

The current PhD thesis focused on the development of DNA acoustic biosensing assays for the analysis of point mutations in the context of liquid biopsy, tissue biopsy and precision medicine. Due to the required ultralow detection limits, acoustic assays were combined with molecular amplification techniques like Ligase Chain Reaction (LCR) and Allele-Specific PCR (AS-PCR). We observed that although ligation-based techniques are considered the best candidates for a highly specific assay, they suffered from limitations like low sensitivity. Exponential ligase-based amplification through LCR, significantly improved detection limit however, limitations due to decreased specificity were observed. On the other hand, traditional PCR-based techniques like AS-PCR, continue to hold the first place for these kinds of applications. In our approach, we firstly developed a proof-of-concept method combining acoustic biosensors with LCR reaction and liposome-based acoustic signal enhancers. Even though we didn't go down to the required detection limits, this assay is quite promising for application to other low abundance gene targets. Eventually, we developed a highly sensitive and specific AS-PCR coupled with acoustic detection utilizing a novel acoustic biochip consisted of 24 miniaturized sensors, thus, allowing multiple sample analysis in a more cost-effective way and with faster analysis time. For the detection, we employed 200nm liposomes to enhance the acoustic signal, as well. The overall assay was evaluated in real patients FFPE-tissue and plasma samples. The results were in concordance with those obtained by the standard techniques used for tissue and liquid biopsy, indicating the validity of our assay and its potential commercial exploitation in the Liquid and tissue biopsy market.

The past few years, the global market of Liquid biopsy for cancer has grown fast and is anticipated to increase from $1.7 billion to $13.6 billion for the period of 2020-2025 with a compound annual growth rate (CAGR) of 50.7%. This fast growth is attributed to the increased public and private funding for research in the corresponding field, the preference of oncologists for liquid biopsy, the continuous development of new products and the increased demand for personalized treatment (https://www.bccresearch.com/market-research/biotechnology/liquid-biopsy-research-tools-services-diagnostics.html). Currently, the market invests more in the analysis of circulating tumor cells in blood however, due to the advancements in ctDNA detection techniques (i.e., NGS, ddPCR and others) circulating tumor DNA is expected to be the fastest growing segment during the aforementioned period. Regarding products and services, the biggest part of the market focuses on kits & reagents, probably due to the large requirement of reagents to perform liquid biopsy tests and their applicability. Platforms & instruments segment is the 2nd largest part but is expected to rise significantly in the upcoming years (https://www.alliedmarketresearch.com/liquid-biopsy-market). A huge variety of biosensors has been developed or currently are under development to provide an efficient and reliable approach for Liquid biopsy. Biosensors are commonly characterized as "fast", "cost-effective", "sensitive" and "specific" tools for early detection with the potential of "mass production". However, still commercially available biosensors do not exist. We could also say that their absence during

the COVID-19 pandemic, actually proved that there are still many technological challenges to be addressed and bottlenecks to be overcome. Biosensors, still need improvement in terms of sensitivity and should be more automated, simplified and user-friendly. Regarding DNA biosensors for liquid biopsy, while there are some exceptions of sensitive and simplified biosensors where even a PCR-step is obviated[86], still none of them have entered the market. Recent advancements in nanomaterials applied a. on surfaces for enhanced sensitivity like the graphene oxide[172] and programmable nanostructured microelectrodes (NMEs)[173] and b. as signal enhancers through binding on the DNA target like the gold nanoparticles (AuNPs), quantum dots, liposomes and nanoamplicons[117] (many AuNPs per one target) keep biosensors as very promising tool for wide application in the field of diagnostics in the future. In any case, the above is clearly demonstrated by the huge market size of biosensors as well.

References

1. Karunakaran, C., Rajkumar, R. & Bhargava, K. *Introduction to Biosensors*. *Biosensors and Bioelectronics* (Elsevier Inc., 2015). doi:10.1016/B978-0-12-803100-1.00001-3.

2. Mehrotra, P. Biosensors and their applications - A review. *J. Oral Biol. Craniofacial Res.* **6**, 153–159 (2016).

3. Thvenot, D. R., Toth, K., Durst, R. A. & Wilson, G. S. Electrochemical biosensors: Recommended definitions and classification (Technical Report). *Pure Appl. Chem.* **71**, 2333–2348 (1999).

4. Thévenot, D. R., Toth, K., Durst, R. A. & Wilson, G. S. Electrochemical biosensors: Recommended definitions and classification. *Biosens. Bioelectron.* **16**, 121–131 (2001).

5. Mohankumar, P., Ajayan, J., Mohanraj, T. & Yasodharan, R. Recent developments in biosensors for healthcare and biomedical applications: A review. *Meas. J. Int. Meas. Confed.* **167**, 108293 (2021).

6. Griesche, C. & Baeumner, A. J. Biosensors to support sustainable agriculture and food safety. *TrAC - Trends Anal. Chem.* **128**, 115906 (2020).

7. Arora, P., Sindhu, A., Dilbaghi, N. & Chaudhury, A. Biosensors as innovative tools for the detection of food borne pathogens. *Biosens. Bioelectron.* **28**, 1–12 (2011).

8. Metkar, S. K. & Girigoswami, K. Diagnostic biosensors in medicine – A review. *Biocatal. Agric. Biotechnol.* **17**, 271–283 (2019).

9. Bhalla, N., Jolly, P., Formisano, N. & Estrela, P. Introduction to biosensors. *Essays Biochem.* **60**, 1–8 (2016).

10. Turner, A. P. F. Biosensors: Sense and sensibility. *Chem. Soc. Rev.* **42**, 3184–3196 (2013).

11. Heineman, W. R. & Jensen, W. B. Leland C. Clark Jr. (1918–2005). *Biosens. Bioelectron.* **21**, 1403–1404 (2006).

12. Alhadrami, H. A. Biosensors: Classifications, medical applications, and future prospective. *Biotechnol. Appl. Biochem.* **65**, 497–508 (2018).

13. Nikoleli, G. P., Nikolelis, D. P., Evtugyn, G. & Hianik, T. Advances in lipid film based biosensors. *Trends Anal. Chem.* **79**, 210–221 (2016).

14. Martín-Gracia, B., Martín-Barreiro, A., Cuestas-Ayllón, C., Grazú, V., Line, A., Llorente, A., De La Fuente, J. M. & Moros, M. Nanoparticle-based biosensors for detection of extracellular vesicles in liquid biopsies. *J. Mater. Chem. B* **8**, 6710–6738 (2020).

15. Damborský, P., Švitel, J. & Katrlík, J. Optical biosensors. *Essays Biochem.* **60**, 91–100 (2016).

16. Fogel, R., Limson, J. & Seshia, A. A. Acoustic biosensors. *Essays Biochem.* **60**, 101–110 (2016).

17. Hammond, J. L., Formisano, N., Estrela, P., Carrara, S. & Tkac, J. Electrochemical biosensors and nanobiosensors. *Essays Biochem.* **60**, 69–80 (2016).

18. Durmu, N. G., Lin, R. L., Kozberg, M., Dermici, D., Khademhosseini, A. & Demirci, U. *Acoustic - based sensors*. *Encyclopedia of Microfluidics and Nanofluidics* (2013). doi:10.1007/978-3-642-27758-0.

19. Drafts, B. Acoustic wave technology sensors. *IEEE Trans. Microw. Theory Tech.* **49**, 795–802 (2001).

20. Gizeli, E., Goddard, N. J., Lowe, C. R. & Stevenson, A. C. A Love plate biosensor utilising a polymer layer. *Sensors Actuators B. Chem.* **6**, 131–137 (1992).

21. Länge, K., Rapp, B. E. & Rapp, M. Surface acoustic wave biosensors: A review. *Anal. Bioanal. Chem.* **391**, 1509–1519 (2008).

22. Gronewold, T. M. A. Surface acoustic wave sensors in the bioanalytical field: Recent trends and challenges. *Anal. Chim. Acta* **603**, 119–128 (2007).

23. Hoummady, M., Campitelli, A. & Wlodarski, W. Acoustic wave sensors: Design, sensing mechanisms and applications. *Smart Mater. Struct.* **6**, 647–657 (1997).

24. Rasmusson, A. & Gizeli, E. Comparison of Poly(methylmethacrylate) and Novolak waveguide coatings for an acoustic biosensor. *J. Appl. Phys.* **90**, 5911–5914 (2001).

25. Gizeli, E. Design considerations for the acoustic waveguide biosensor. *Smart Mater. Struct.* **6**, 700–706 (1997).

26. Ferreira, G. N. M., Da-Silva, A. C. & Tomé, B. Acoustic wave biosensors: physical models and biological applications of quartz crystal microbalance. *Trends Biotechnol.* **27**, 689–697 (2009).

27. Reviakine, I., Johannsmann, D. & Richter, R. P. Hearing what you cannot see and visualizing what you hear: Interpreting quartz crystal microbalance data from solvated interfaces. *Anal. Chem.* **83**, 8838–8848 (2011).

28. Sauerbrey, G. Verwendung von Schwingquarzen zur Wägung dünner Schichten und zur Mikrowägung. *Zeitschrift für Phys.* **155**, 206–222 (1959).

29. Fernández, R., García, P., García, M., García, J. V., Jiménez, Y. & Arnau, A. Design and validation of a 150 MHz HFFQCM sensor for bio-sensing applications. *Sensors (Switzerland)* **17**, 1–13 (2017).

30. MUJAHID, A., AFZAL, A. & DICKERT, F. L. An Overview of High Frequency Acoustic. *Sensors* **19**, 4395 (2019).

31. García, J. V., Rocha, M. I., March, C., García, P., Francis, L. A., Montoya, A., Arnau, A. & Jimenez, Y. Love Mode surface acoustic wave and high fundamental frequency quartz crystal microbalance immunosensors for the detection of carbaryl pesticide. in *Procedia Engineering* vol. 87 759–762 (Elsevier B.V., 2014).

32. Cervera-Chiner, L., Juan-Borrás, M., March, C., Arnau, A., Escriche, I., Montoya, Á. &

Jiménez, Y. High Fundamental Frequency Quartz Crystal Microbalance (HFF-QCM) immunosensor for pesticide detection in honey. *Food Control* **92**, 1–6 (2018).

33. March, C., García, J. V., Sánchez, Á., Arnau, A., Jiménez, Y., García, P., Manclús, J. J. & Montoya, Á. High-frequency phase shift measurement greatly enhances the sensitivity of QCM immunosensors. *Biosens. Bioelectron.* **65**, 1–8 (2015).

34. Dixon, M. C. Quartz crystal microbalance with dissipation monitoring: Enabling real-time characterization of biological materials and their interactions. *J. Biomol. Tech.* **19**, 151–158 (2008).

35. Teramura, Y. & Takai, M. Quartz Crystal Microbalance. in *Compendium of Surface and Interface Analysis* (ed. of Japan, T. S. S. S.) 509–520 (Springer Singapore, 2018). doi:10.1007/978-981-10-6156-1_83.

36. Voinova, M. V, Rodahl, M., Jonson, M. & Kasemo, B. Viscoelastic Acoustic Response of Layered Polymer Films at Fluid-Solid Interfaces: Continuum Mechanics Approach. *Phys. Scr.* **59**, 391–396 (1999).

37. Qiao, X., Zhang, X., Tian, Y. & Meng, Y. Progresses on the theory and application of quartz crystal microbalance. *Appl. Phys. Rev.* **3**, (2016).

38. Tsortos, A., Papadakis, G. & Gizeli, E. Shear acoustic wave biosensor for detecting DNA intrinsic viscosity and conformation: A study with QCM-D. *Biosens. Bioelectron.* **24**, 836–841 (2008).

39. Papadakis, G., Tsortos, A., Bender, F., Ferapontova, E. E. & Gizeli, E. Direct detection of DNA conformation in hybridization processes. *Anal. Chem.* **84**, 1854–1861 (2012).

40. Tsortos, A., Papadakis, G. & Gizeli, E. On the Hydrodynamic Nature of DNA Acoustic Sensing. *Anal. Chem.* **88**, 6472–6478 (2016).

41. Milioni, D., Tsortos, A., Velez, M. & Gizeli, E. Extracting the Shape and Size of Biomolecules Attached to a Surface as Suspended Discrete Nanoparticles. *Anal. Chem.* **89**, 4198–4203 (2017).

42. Papadakis, G., Tsortos, A. & Gizeli, E. Acoustic characterization of nanoswitch structures: Application to the DNA holliday junction. *Nano Lett.* **10**, 5093–5097 (2010).

43. Tsortos, A., Papadakis, G., Mitsakakis, K., Melzak, K. A. & Gizeli, E. Quantitative determination of size and shape of surface-bound DNA using an acoustic wave sensor. *Biophys. J.* **94**, 2706–2715 (2008).

44. Papadakis, G., Tsortos, A., Kordas, A., Tiniakou, I., Morou, E., Vontas, J., Kardassis, D. & Gizeli, E. Acoustic detection of DNA conformation in genetic assays combined with PCR. *Sci. Rep.* **3**, 1–8 (2013).

45. Papadakis, G. & Gizeli, E. Screening for mutations in BRCA1 and BRCA2 genes by measuring the acoustic ratio with QCM. **6**, (2014).

46. Blass, B. E. Editorial for Cancer Virtual Issue. *ACS Med. Chem. Lett.* **8**, 1205–1207 (2017).

47. Han, X., Wang, J. & Sun, Y. Circulating Tumor DNA as Biomarkers for Cancer Detection. *Genomics, Proteomics and Bioinformatics* vol. 15 59–72 (2017).

48. Heitzer, E., Haque, I. S., Roberts, C. E. S. & Speicher, M. R. Current and future perspectives of liquid biopsies in genomics-driven oncology. *Nat. Rev. Genet.* **20**, 71–88 (2019).

49. Tanda, E. T., Vanni, I., Boutros, A., Andreotti, V., Bruno, W., Ghiorzo, P. & Spagnolo, F. Current State of Target Treatment in BRAF Mutated Melanoma. *Front. Mol. Biosci.* **7**, (2020).

50. Battaglin, F., Puccini, A., Naseem, M., Schirripa, M., Berger, M. D., Tokunaga, R., McSkane, M., Khoukaz, T., Soni, S., Zhang, W., *et al.* Pharmacogenomics in colorectal cancer: current role in clinical practice and future perspectives. *J. Cancer Metastasis Treat.* **4**, 12 (2018).

51. Finzel, A., Sadik, H., Ghitti, G. & Laes, J. The combined analysis of solid and liquid biopsies provides additional clinical information to improve patient care. *J. Cancer Metastasis Treat.* **4**, 21 (2018).

52. Chae, Y. K., Davis, A. A., Carneiro, B. A., Chandra, S., Mohindra, N., Kalyan, A., Kaplan, J., Matsangou, M., Pai, S., Costa, R., *et al.* Concordance between genomic alterations assessed by next-generation sequencing in tumor tissue or circulating cell-free DNA. *Oncotarget* **7**, 65364–65373 (2016).

53. Parikh, A. R., Leshchiner, I., Elagina, L., Goyal, L., Levovitz, C., Siravegna, G., Livitz, D., Rhrissorrakrai, K., Martin, E. E., Van Seventer, E. E., *et al.* Liquid versus tissue biopsy for detecting acquired resistance and tumor heterogeneity in gastrointestinal cancers. *Nat. Med.* **25**, 1415–1421 (2019).

54. Grzywa, T. M., Paskal, W. & Włodarski, P. K. Intratumor and Intertumor Heterogeneity in Melanoma. *Transl. Oncol.* **10**, 956–975 (2017).

55. Zahreddine, H. & Borden, K. L. B. Mechanisms and insights into drug resistance in cancer. *Front. Pharmacol.* **4 MAR**, 1–8 (2013).

56. Soda, N., Rehm, B. H. A., Sonar, P., Nguyen, N. T. & Shiddiky, M. J. A. Advanced liquid biopsy technologies for circulating biomarker detection. *J. Mater. Chem. B* **7**, 6670–6704 (2019).

57. Siravegna, G., Marsoni, S., Siena, S. & Bardelli, A. Integrating liquid biopsies into the management of cancer. *Nature Reviews Clinical Oncology* vol. 14 531–548 (2017).

58. Wan, J. C. M., Massie, C., Garcia-Corbacho, J., Mouliere, F., Brenton, J. D., Caldas, C., Pacey, S., Baird, R. & Rosenfeld, N. Liquid biopsies come of age: towards implementation of circulating tumour DNA. *Nature Reviews Cancer* vol. 17 223–238 (2017).

59. Mouliere, F., Chandrananda, D., Piskorz, A. M., Moore, E. K., Morris, J., Ahlborn, L. B., Mair, R., Goranova, T., Marass, F., Heider, K., *et al.* Enhanced detection of circulating tumor DNA by fragment size analysis. *Sci. Transl. Med.* **10**, (2018).

60. Underhill, H. R., Kitzman, J. O., Hellwig, S., Welker, N. C., Daza, R., Baker, D. N., Gligorich, K. M., Rostomily, R. C., Bronner, M. P. & Shendure, J. Fragment Length of Circulating Tumor DNA. *PLoS Genet.* **12**, 1–24 (2016).

61. Gorgannezhad, L., Umer, M., Islam, M. N., Nguyen, N. T. & Shiddiky, M. J. A. Circulating tumor DNA and liquid biopsy: Opportunities, challenges, and recent advances in detection technologies. *Lab on a Chip* vol. 18 1174–1196 (2018).

62. Gormally, E., Vineis, P., Matullo, G., Veglia, F., Caboux, E., Le Roux, E., Peluso, M., Garte, S., Guarrera, S., Munnia, A., *et al.* TP53 and KRAS2 mutations in plasma DNA of healthy subjects and subsequent cancer occurrence: A prospective study. *Cancer Res.* **66**, 6871–6876 (2006).

63. Fiala, C. & Diamandis, E. P. Utility of circulating tumor DNA in cancer diagnostics with emphasis on early detection. *BMC Medicine* vol. 16 1–10 (2018).

64. Corcoran, R. B. Circulating tumor DNA: Clinical monitoring and early detection. *Annu. Rev. Cancer Biol.* **3**, 187–201 (2019).

65. Tsiatis, A. C., Norris-Kirby, A., Rich, R. G., Hafez, M. J., Gocke, C. D., Eshleman, J. R. & Murphy, K. M. Comparison of Sanger sequencing, pyrosequencing, and melting curve analysis for the detection of KRAS mutations: Diagnostic and clinical implications. *J. Mol. Diagnostics* **12**, 425–432 (2010).

66. Lade-Keller, J., Rømer, K. M., Guldberg, P., Riber-Hansen, R., Hansen, L. L., Steiniche, T., Hager, H. & Kristensen, L. S. Evaluation of BRAF mutation testing methodologies in formalin-fixed, paraffin-embedded cutaneous melanomas. *J. Mol. Diagnostics* **15**, 70–80 (2013).

67. De Leng, W. W. J., Gadellaa-Van Hooijdonk, C. G., Barendregt-Smouter, F. A. S., Koudijs, M. J., Nijman, I., Hinrichs, J. W. J., Cuppen, E., Van Lieshout, S., Loberg, R. D., De Jonge, M., *et al.* Targeted next generation sequencing as a reliable diagnostic assay for the detection of somatic mutations in tumours using minimal DNA amounts from formalin fixed paraffin embedded material. *PLoS One* **11**, 1–18 (2016).

68. Ivanov, M., Laktionov, K., Breder, V., Chernenko, P., Novikova, E., Telysheva, E., Musienko, S., Baranova, A. & Mileyko, V. Towards standardization of next-generation sequencing of FFPE samples for clinical oncology: Intrinsic obstacles and possible solutions. *J. Transl. Med.* **15**, 1–13 (2017).

69. Gao, J., Wu, H., Wang, L., Zhang, H., Duan, H., Lu, J. & Liang, Z. Validation of targeted next-generation sequencing for RAS mutation detection in FFPE colorectal cancer tissues: Comparison with Sanger sequencing and ARMS-Scorpion real-time PCR. *BMJ Open* **6**, 1–10 (2016).

70. Lang, A. H., Drexel, H., Geller-Rhomberg, S., Stark, N., Winder, T., Geiger, K. & Muendlein, A. Optimized allele-specific real-time PCR assays for the detection of common mutations in KRAS and BRAF. *J. Mol. Diagnostics* **13**, 23–28 (2011).

71. Yang, Z., Zhao, N., Chen, D., Wei, K., Su, N., Huang, J. F., Xu, H. Q., Duan, G. J., Fu, W. L. & Huang, Q. Improved detection of BRAF V600E using allele-specific PCR coupled with

external and internal controllers. *Sci. Rep.* **7**, 1–12 (2017).

72. Postel, M., Roosen, A., Laurent-Puig, P., Taly, V. & Wang-Renault, S. F. Droplet-based digital PCR and next generation sequencing for monitoring circulating tumor DNA: a cancer diagnostic perspective. *Expert Rev. Mol. Diagn.* **18**, 7–17 (2018).

73. Elazezy, M. & Joosse, S. A. Techniques of using circulating tumor DNA as a liquid biopsy component in cancer management. *Comput. Struct. Biotechnol. J.* **16**, 370–378 (2018).

74. Aung, K. L., Donald, E., Ellison, G., Bujac, S., Fletcher, L., Cantarini, M., Brady, G., Orr, M., Clack, G., Ranson, M., *et al.* Analytical validation of BRAF mutation testing from circulating free DNA using the amplification refractory mutation testing system. *J. Mol. Diagnostics* **16**, 343–349 (2014).

75. Olmedillas-López, S., García-Arranz, M. & García-Olmo, D. Current and Emerging Applications of Droplet Digital PCR in Oncology. *Molecular Diagnosis and Therapy* vol. 21 493–510 (2017).

76. Nur, S., Kosova, B. & Ozsoz, M. Detection of Janus Kinase 2 gene single point mutation in real samples with electrochemical DNA biosensor. *Clin. Chim. Acta* **429**, 134–139 (2014).

77. Wang, D., Chen, G., Wang, H., Tang, W., Pan, W., Li, N. & Liu, F. A reusable quartz crystal microbalance biosensor for highly specific detection of single-base DNA mutation. *Biosens. Bioelectron.* **48**, 276–280 (2013).

78. Zeng, N. & Xiang, J. Detection of KRAS G12D point mutation level by anchor-like DNA electrochemical biosensor. *Talanta* **198**, 111–117 (2019).

79. Chang, K., Deng, S. & Chen, M. Novel biosensing methodologies for improving the detection of single nucleotide polymorphism. *Biosens. Bioelectron.* **66**, 297–307 (2015).

80. Lapitan, L. D. S., Guo, Y. & Zhou, D. Nano-enabled bioanalytical approaches to ultrasensitive detection of low abundance single nucleotide polymorphisms. *Analyst* vol. 140 3872–3887 (2015).

81. Xu, Q., Chang, K., Lu, W., Chen, W., Ding, Y., Jia, S., Zhang, K., Li, F., Shi, J., Cao, L., *et al.* Detection of single-nucleotide polymorphisms with novel leaky surface acoustic wave biosensors , DNA ligation and enzymatic signal amplification. *Biosens. Bioelectron.* **33**, 274–278 (2012).

82. Feng, K., Li, J., Jiang, J. H., Shen, G. L. & Yu, R. Q. QCM detection of DNA targets with single-base mutation based on DNA ligase reaction and biocatalyzed deposition amplification. *Biosens. Bioelectron.* **22**, 1651–1657 (2007).

83. Wang, Q., Yang, L., Yang, X., Wang, K., He, L. & Zhu, J. Electrochemical biosensors for detection of point mutation based on surface ligation reaction and oligonucleotides modified gold nanoparticles. *Anal. Chim. Acta* **688**, 163–167 (2011).

84. Weizmann, Y., Patolsky, F. & Willner, I. Amplified detection of DNA and analysis of single-base mismatches by the catalyzed deposition of gold on Au-nanoparticles. *Analyst* **25**, 1502–1504 (2001).

85. Willner, I., Patolsky, F., Weizmann, Y. & Willner, B. Amplified detection of single-base mismatches in DNA using microgravimetric quartz-crystal-microbalance transduction. *Talanta* **56**, 847–856 (2002).

86. Bellassai, N. & Spoto, G. Biosensors for liquid biopsy: circulating nucleic acids to diagnose and treat cancer. *Analytical and Bioanalytical Chemistry* vol. 408 7255–7264 (2016).

87. Das, J., Ivanov, I., Sargent, E. H. & Kelley, S. O. DNA Clutch Probes for Circulating Tumor DNA Analysis. *J. Am. Chem. Soc.* **138**, 11009–11016 (2016).

88. D'Agata, R., Bellassai, N., Allegretti, M., Rozzi, A., Korom, S., Manicardi, A., Melucci, E., Pescarmona, E., Corradini, R., Giacomini, P., *et al.* Direct plasmonic detection of circulating RAS mutated DNA in colorectal cancer patients. *Biosens. Bioelectron.* **170**, (2020).

89. Kirimli, C., Lin, S., Su, Y., Shih, W. & Shih, W. Y. In situ , amplification-free double-stranded mutation detection at 60 copies / ml with thousand-fold wild type in urine. *Biosens. Bioelectron.* **119**, 221–229 (2018).

90. Timar, J. & Kashofer, K. Molecular epidemiology and diagnostics of KRAS mutations in human cancer. *Cancer Metastasis Rev.* **39**, 1029–1038 (2020).

91. Falini, B., Martelli, M. P. & Tiacci, E. BRAF V600E mutation in hairy cell leukemia: From bench to bedside. *Blood* **128**, 1918–1927 (2016).

92. Halilovic, E. & Solit, D. B. Therapeutic strategies for inhibiting oncogenic BRAF signaling. *Current Opinion in Pharmacology* vol. 8 419–426 (2008).

93. Zaman, A., Wu, W. & Bivona, T. G. Targeting oncogenic braf: Past, present, and future. *Cancers (Basel).* **11**, (2019).

94. Merz, V., Gaule, M., Zecchetto, C., Cavaliere, A., Casalino, S., Pesoni, C., Contarelli, S., Sabbadini, F., Bertolini, M., Mangiameli, D., *et al.* Targeting KRAS: The Elephant in the Room of Epithelial Cancers. *Front. Oncol.* **11**, 1–16 (2021).

95. Adjei, A. A. Blocking oncogenic Ras signaling for cancer therapy. *J. Natl. Cancer Inst.* **93**, 1062–1074 (2001).

96. Prior, I. A., Lewis, P. D. & Mattos, C. A comprehensive survey of ras mutations in cancer. *Cancer Res.* **72**, 2457–2467 (2012).

97. Solit, C. A. P. and D. B. Therapeutic Strategies for Targeting BRAF in Human Cancer. 121–134 (2007) doi:doi.org/10.2174/157488707780599393.

98. Anguera, G. & Majem, M. BRAF inhibitors in metastatic non-small cell lung cancer. *Journal of Thoracic Disease* vol. 10 589–592 (2018).

99. Mazieres, J., Cropet, C., Montané, L., Barlesi, F., Souquet, P. J., Quantin, X., Otto, J. & Favier, L. Vemurafenib in non-small-cell lung cancer patients with BRAF V600 and BRAF nonV600 mutations. *Ann. Oncol.* **31**, 289–294 (2020).

100. Kennedy, C. J., Wain, G. V, Patch, A., Pearson, J. V & Grimmond, S. M. BRAF Mutations in Low-Grade Serous Ovarian Cancer and Response to BRAF Inhibition. 1–14 (2019).

101. Holmes, A., Ph, D., Kern, W., Martelli, M. P., Pucciarini, A., Ph, D., Bigerna, B., Sc, B., Pacini, R., Sc, B., *et al.* Mutations in Hairy-Cell Leukemia. (2011).

102. Davies, H., Bignell, G. R., Cox, C., Stephens, P., Edkins, S., Clegg, S., Teague, J., Woffendin, H., Garnett, M. J., Bottomley, W., *et al.* Mutations of the BRAF gene in human cancer. *Nature* 949–954 (2002).

103. Davies, H., Bignell, G. R., Cox, C., Stephens, P., Edkins, S., Clegg, S., Teague, J., Woffendin, H., Garnett, M. J., Bottomley, W., *et al.* Mutations of the BRAF gene in human cancer. *Nature* **417**, 949–954 (2002).

104. Chapman, P. B., Hauschild, A., Robert, C., Haanen, J. B., Ascierto, P., Larkin, J., Dummer, R., Garbe, C., Testori, A., Maio, M., *et al.* Improved Survival with Vemurafenib in Melanoma with BRAF V600E Mutation. *N. Engl. J. Med.* **364**, 2507–2516 (2011).

105. Mazieres, J., Cropet, C., Montané, L., Barlesi, F., Souquet, P. J., Quantin, X., Dubos-Arvis, C., Otto, J., Favier, L., Avrillon, V., *et al.* Vemurafenib in non-small-cell lung cancer patients with BRAFV600 and BRAFnonV600 mutations. *Ann. Oncol.* **31**, 289–294 (2020).

106. Di Nicolantonio, F., Martini, M., Molinari, F., Sartore-Bianchi, A., Arena, S., Saletti, P., De Dosso, S., Mazzucchelli, L., Frattini, M., Siena, S., *et al.* Wild-type BRAF is required for response to panitumumab or cetuximab in metastatic colorectal cancer. *J. Clin. Oncol.* **26**, 5705–5712 (2008).

107. Orlandi, A., Calegari, M. A., Inno, A., Berenato, R., Caporale, M., Niger, M., Bossi, I., Bartolomeo, M. Di, Braud, F. De & Pietrantonio, F. BRAF in metastatic colorectal cancer: The future starts now. *Pharmacogenomics* **16**, 2069–2081 (2015).

108. López-Cortés, A., Paz-y-Miño, C., Guerrero, S., Jaramillo-Koupermann, G., León Cáceres, Á., Intriago-Baldeón, D. P., García-Cárdenas, J. M., Guevara-Ramírez, P., Armendáriz-Castillo, I., Leone, P. E., *et al.* Pharmacogenomics, biomarker network, and allele frequencies in colorectal cancer. *Pharmacogenomics J.* **20**, 136–158 (2020).

109. Pereiro, I., Tabnaoui, S., Fermigier, M., Du Roure, O., Descroix, S., Viovy, J. L. & Malaquin, L. Magnetic fluidized bed for solid phase extraction in microfluidic systems. *Lab Chip* **17**, 1603–1615 (2017).

110. Hernández-Neuta, I., Pereiro, I., Ahlford, A., Ferraro, D., Zhang, Q., Viovy, J. L., Descroix, S. & Nilsson, M. Microfluidic magnetic fluidized bed for DNA analysis in continuous flow mode. *Biosens. Bioelectron.* **102**, 531–539 (2018).

111. Milioni, D., Mateos-Gil, P., Papadakis, G., Tsortos, A., Sarlidou, O. & Gizeli, E. Acoustic

Methodology for Selecting Highly Dissipative Probes for Ultrasensitive DNA Detection. *Anal. Chem.* **92**, 8186–8193 (2020).

112. Liu, T., Tang, J. & Jiang, L. Sensitivity enhancement of DNA sensors by nanogold surface modification. *Biochem. Biophys. Res. Commun.* **295**, 14–16 (2002).

113. Zhao, H. Q., Lin, L., Li, J. R., Tang, J. A., Duan, M. X. & Jiang, L. DNA biosensor with high sensitivity amplified by gold nanoparticles. *J. Nanoparticle Res.* **3**, 321–323 (2001).

114. Gunnarsson, A., Jo, P., Marie, R. & Tegenfeldt, J. O. Single-Molecule Detection and Mismatch Discrimination of Unlabeled DNA Targets. (2008) doi:10.1021/nl072401j.

115. Patolsky, F., Lichtenstein, A., Willner, I. & October, R. V. Electronic Transduction of DNA Sensing Processes on Surfaces : Amplification of DNA Detection and Analysis of Single-Base Mismatches by Tagged Liposomes. *Am. Chem. Soc.* **123**, 5194–5205 (2001).

116. Patolsky, F., Lichtenstein, A. & Willner, I. Amplified microgravimetric quartz-crystal-microbalance assay of DNA using oligonucleotide-functionalized liposomes or biotinylated liposomes. *J. Am. Chem. Soc.* **122**, 418–419 (2000).

117. Mo, Z. H. & Wei, X. L. Toward hybridization assays without PCR using universal nanoamplicons. *Anal. Bioanal. Chem.* **386**, 2219–2223 (2006).

118. Grammoustianou, A., Papadakis, G. & Gizeli, E. Solid-Phase Isothermal DNA Amplification and Detection on Quartz Crystal Microbalance Using Liposomes and Dissipation Monitoring. *IEEE Sensors Lett.* **1**, 1–4 (2017).

119. Patolsky, F., Lichtenstein, A., Willner, I. & August, R. V. Amplified Microgravimetric Quartz-Crystal-Microbalance Assay of DNA Using Oligonucleotide-Functionalized Liposomes or Biotinylated Liposomes. 418–419 (2000) doi:10.1021/ja992834r.

120. Fernandez, R., Calero, M., Reiviakine, I., Garcia, J. V., Rocha-Gaso, M. I., Arnau, A. & Jimenez, Y. High Fundamental Frequency (HFF) Monolithic Resonator Arrays for Biosensing Applications: Design, Simulations, Experimental Characterization. *IEEE Sens. J.* **XX**, 1–1 (2020).

121. Naoumi, N., Michaelidou, K., Papadakis, G., Simaiaki, A. E., Calero, M., Arnau, A., Tsortos, A. & Agelaki, S. Acoustic array biochip combined with allele-specific PCR for multiple cancer mutation analysis in tissue and liquid biopsy. 1–12 (2021).

122. Mitsakakis, K. & Gizeli, E. Multi-sample acoustic biosensing microsystem for protein interaction analysis. *Biosens. Bioelectron.* **26**, 4579–4584 (2011).

123. Gibriel, A. A. & Adel, O. Advances in ligase chain reaction and ligation-based amplifications for genotyping assays: Detection and applications. *Mutation Research - Reviews in Mutation Research* vol. 773 66–90 (2017).

124. Rothschild, C. B., Brewer, C. S., Loggie, B., Beard, G. A. & Triscott, M. X. Detection of colorectal cancer k-ras mutations using a simplified oligonucleotide ligation assay. *J. Immunol. Methods* **206**, 11–19 (1997).

125. Davis, J. D., Riley, P. K., Peters, C. W. & Rand, K. H. A comparison of ligase chain reaction to polymerase chain reaction in the detection of Chlamydia trachomatis endocervical infections. *Infect. Dis. Obstet. Gynecol.* **6**, 57–60 (1998).

126. Kanagawa, T. Bias and artifacts in multitemplate polymerase chain reactions (PCR). *J. Biosci. Bioeng.* **96**, 317–323 (2003).

127. Polz, M. F. & Cavanaugh, C. M. Bias in template-to-product ratios in multitemplate PCR. *Appl. Environ. Microbiol.* **64**, 3724–3730 (1998).

128. Acinas, S. G., Sarma-Rupavtarm, R., Klepac-Ceraj, V. & Polz, M. F. PCR-induced sequence artifacts and bias: Insights from comparison of two 16s rRNA clone libraries constructed from the same sample. *Appl. Environ. Microbiol.* **71**, 8966–8969 (2005).

129. Kapala, J., Copes, D., Sproston, A., Patel, J., Jang, D., Petrich, A., Mahony, J., Biers, K. & Chernesky, M. Pooling cervical swabs and testing by ligase chain reaction are accurate and cost-saving strategies for diagnosis of Chlamydia trachomatis. *J. Clin. Microbiol.* **38**, 2480–2483 (2000).

130. Wang, S. X. & Tay, L. Early identification of Mycobacterium tuberculosis complex in BACTEC cultures by ligase chain reaction. *J. Med. Microbiol.* **51**, 710–712 (2002).

131. Wiedmann, M., Czajka, J., Barany, F. & Batt, C. A. Discrimination of Listeria monocytogenes from other Listeria species by ligase chain reaction. *Appl. Environ. Microbiol.* **58**, 3443–3447 (1992).

132. Kacena, K. A., Quinn, S. B., Hartman, S. C., Quinn, T. C. & Gaydos, C. A. Pooling of urine samples for screening for Neisseria gonorrhoeae by ligase chain reaction: Accuracy and application. *J. Clin. Microbiol.* **36**, 3624–3628 (1998).

133. Moore, D. F. & Curry, J. I. Detection and identification of Mycobacterium tuberculosis directly from sputum sediments by ligase chain reaction. *J. Clin. Microbiol.* **36**, 1028–1031 (1998).

134. Osiowy, C. Sensitive detection of HBsAG mutants by a gap ligase chain reaction assay. *J. Clin. Microbiol.* **40**, 2566–2571 (2002).

135. Minamitani, S., Nishiguchi, S., Kuroki, T., Otani, S. & Monna, T. Detection by ligase chain reaction of precore mutant of hepatitis B virus. *Hepatology* **25**, 216–222 (1997).

136. Reyes, A. A., Carrera, P., Cardillo, E., Ugozzoli, L., Lowery, J. D., Lin, C. I. P., Go, M., Ferrari, M. & Wallace, R. B. Ligase chain reaction assay for human mutations: The sickle cell by LCR assay. *Clin. Chem.* **43**, 40–44 (1997).

137. Liu, Z. J., Yang, L. Y., Wei, Q. X., Ye, C. L., Xu, X. W., Zhong, G. X., Zheng, Y. J., Chen, J. Y., Lin, X. H. & Liu, A. L. A novel ligase chain reaction-based electrochemical biosensing strategy for highly sensitive point mutation detection from human whole blood. *Talanta* **216**, 120966 (2020).

138. Yi, P., Jiang, H., Li, L., Dai, F., Zheng, Y., Han, J., Chen, Z. & Guo, J. A New Genotyping Method for Detecting Low Abundance Single Nucleotide Mutations Based on Gap

Ligase Chain Reaction and Quantitative PCR Assay. *Cell Biochem. Biophys.* **62**, 161–167 (2012).

139. Jenner, S. & Techel, D. Development of a gLCR-based KRAS mutation detection approach and its comparison with other screening methods. *Tumor Biol.* **36**, 6361–6368 (2015).

140. Hamada, M., Shimase, K., Tsukagoshi, K. & Hashimoto, M. Discriminative detection of low-abundance point mutations using a PCR/ligase detection reaction/capillary gel electrophoresis method and fluorescence dual-channel monitoring. *Electrophoresis* **35**, 1204–1210 (2014).

141. Wu, Z.-S., Jiang, J.-H., Shen, G.-L. & Yu, R.-Q. Highly Sensitive DNA Detection and Point Mutation Identification : An Electrochemical Approach Based on the Combined Use of Ligase and Reverse Molecular Beacon. *Hum. Mutat.* **28**, 630–637 (2006).

142. Zhang, P., Chu, X., Xu, X., Shen, G. & Yu, R. Electrochemical detection of point mutation based on surface ligation reaction and biometallization. *Biosens. Bioelectron.* **23**, 1435–1441 (2008).

143. Hu, F., Zhang, W., Meng, W., Ma, Y., Zhang, X., Xu, Y., Wang, P. & Gu, Y. Ferrocene-labeled and purification-free electrochemical biosensor based on ligase chain reaction for ultrasensitive single nucleotide polymorphism detection. *Anal. Chim. Acta* **1109**, 9–18 (2020).

144. Zhang, W., Hu, F., Zhang, X., Meng, W., Zhang, Y., Song, Y., Wang, H., Wang, P. & Gu, Y. Ligase chain reaction-based electrochemical biosensor for the ultrasensitive and specific detection of single nucleotide polymorphisms. *New J. Chem.* **43**, 14327–14335 (2019).

145. Abravaya, K., Carrino, J. J., Muldoon, S. & Lee, H. H. Detection of point mutations with a modified ligase chain reaction (gap-LCR). *Nucleic Acids Res.* **23**, 675–682 (1995).

146. Kälin, I., Shephard, S. & Candrian, U. Evaluation of the ligase chain reaction (LCR) for the detection of points mutation. *Mutat. Res. Lett.* **283**, 119–123 (1992).

147. Cheng, Y., Zhao, J., Jia, H., Yuan, Z. & Li, Z. Ligase chain reaction coupled with rolling circle amplification for high sensitivity detection of single nucleotide polymorphisms. *Analyst* **138**, 2958–2963 (2013).

148. Barany, F. The ligase chain reaction in a PCR world. *Genome Res.* **1**, 5–16 (1991).

149. Song, Y., Zhang, Y. & Wang, T.-H. Single Quantum Dot Analysis Enables Multiplexed Point Mutation Detection by Gap Ligase Chain Reaction. *Small* **9**, 1096–1105 (2013).

150. Zhou, H., Xing, D., Zhu, D. & Zhou, X. Rapid and sensitive detection of point mutation by DNA ligase-based electrochemiluminescence assay. *Talanta* **78**, 1253–1258 (2009).

151. Wang, Q., Yang, L., Yang, X., Wang, K., He, L. & Zhu, J. Electrochemical biosensors for detection of point mutation based on surface ligation reaction and oligonucleotides modified gold nanoparticles. *Anal. Chim. Acta* **688**, 163–167 (2011).

152. Meng, X., Yang, X., Wang, K., Guo, Q., Tan, Y., Mo, Q. & Xu, X. Direct fluorescence detection of point mutations in human genomic DNA using microbead-based ligase chain reaction. *Talanta* **80**, 1725–1729 (2010).

153. Shen, W., Deng, H. & Gao, Z. Gold nanoparticle-enabled real-time ligation chain reaction for ultrasensitive detectionof DNA. *J. Am. Chem. Soc.* **134**, 14678–14681 (2012).

154. Sun, Y., Lu, X., Su, F., Wang, L., Liu, C., Duan, X. & Li, Z. Real-time fluorescence ligase chain reaction for sensitive detection of single nucleotide polymorphism based on fluorescence resonance energy transfer. *Biosens. Bioelectron.* **74**, 705–710 (2015).

155. Zhang, L., Zhang, Y., Huang, L., Zhang, Y., Li, Y., Ding, S. & Cheng, W. Ultrasensitive biosensing of low abundance BRAF V600E mutation in real samples by coupling dual padlock-gap-ligase chain reaction with hyperbranched rolling circle amplification. *Sensors Actuators, B Chem.* **287**, 111–117 (2019).

156. Yi, P., Lu, W., Guo, J., Liu, Q., Chen, Z., Han, J. & Li, L. Development of a PCR/Ligase Detection Reaction/Nanogold-Based Universal Array Approach for the Detection of Low-Abundant DNA Point Mutations. *Cell Biochem. Biophys.* **61**, 629–636 (2011).

157. Wabuyele, M. B., Farquar, H., Stryjewski, W., Hammer, R. P., Soper, S. A., Cheng, Y. W. & Barany, F. Approaching real-time molecular diagnostics: Single-pair fluorescence resonance energy transfer (spFRET) detection for the analysis of low abundant point mutations in K-ras oncogenes. *J. Am. Chem. Soc.* **125**, 6937–6945 (2003).

158. Choi, W., Shin, G. W., Hwang, H. S., Pack, S. P., Jung, G. Y. & Jung, G. Y. A multiplex single nucleotide polymorphism genotyping method using ligase-based mismatch discrimination and CE-SSCP. *Electrophoresis* **35**, 1196–1203 (2014).

159. Bui, M. H., Stone, G. G., Nilius, A. M., Almer, L. & Flamm, R. K. PCR-oligonucleotide ligation assay for detection of point mutations associated with quinolone resistance in Streptococcus pneumoniae. *Antimicrob. Agents Chemother.* **47**, 1456–1459 (2003).

160. van der Leest, P., Boonstra, P. A., Elst, A. Ter, van Kempen, L. C., Tibbesma, M., Koopmans, J., Miedema, A., Tamminga, M., Groen, H. J. M., Reyners, A. K. L., *et al.* Comparison of circulating cell-free dna extraction methods for downstream analysis in cancer patients. *Cancers (Basel).* **12**, (2020).

161. Pérez-Barrios, C., Nieto-Alcolado, I., Torrente, M., Jiménez-Sánchez, C., Calvo, V., Gutierrez-Sanz, L., Palka, M., Donoso-Navarro, E., Provencio, M. & Romero, A. Comparison of methods for circulating cell-free DNA isolation using blood from cancer patients: Impact on biomarker testing. *Transl. Lung Cancer Res.* **5**, 665–672 (2016).

162. Lee, H., Park, C., Na, W., Park, K. H. & Shin, S. Precision cell-free DNA extraction for liquid biopsy by integrated microfluidics. *npj Precis. Oncol.* **4**, (2020).

163. Franczak, C., Filhine-Tresarrieu, P., Gilson, P., Merlin, J. L., Au, L. & Harlé, A. Technical considerations for circulating tumor DNA detection in oncology. *Expert Rev. Mol. Diagn.* **19**, 121–135 (2019).

164. Campuzano, S., Serafín, V., Gamella, M., Pedrero, M., Yáñez-sedeño, P. & Pingarrón, J. M. Opportunities, challenges, and prospects in electrochemical biosensing of circulating tumor dna and its specific features. *Sensors (Switzerland)* vol. 19 (2019).

165. Wangkumhang, P., Chaichoompu, K., Ngamphiw, C., Ruangrit, U., Chanprasert, J., Assawamakin, A. & Tongsima, S. WASP: A Web-based Allele-Specific PCR assay designing tool for detecting SNPs and mutations. *BMC Genomics* **8**, 1–9 (2007).

166. Wang, H., Jiang, J., Mostert, B., Sieuwerts, A., Martens, J. W. M., Sleijfer, S., Foekens, J. A. & Wang, Y. Allele-specific, non-extendable primer blocker PCR (AS-NEPB-PCR) for DNA mutation detection in cancer. *J. Mol. Diagnostics* **15**, 62–69 (2013).

167. Barbano, R., Pascull, B., Coco, M., Fontana, A., Copetti, M., Rendina, M., Valori, V. M., Graziano, P., Maiello, E., Fazio, V. M., *et al.* Competitive allele-specific TaqMan PCR (Cast-PCR) is a sensitive , specific and fast method for BRAF V600 mutation detection in Melanoma patients. 1–11 (2015) doi:10.1038/srep18592.

168. Gomes, A. & Korf, B. R. *Genetic Testing Techniques*. *Pediatric Cancer Genetics* (Elsevier Inc., 2018). doi:10.1016/B978-0-323-48555-5.00005-3.

169. Hagemann, I. S. *Overview of Technical Aspects and Chemistries of Next-Generation Sequencing*. *Clinical Genomics* (Elsevier Inc., 2015). doi:10.1016/B978-0-12-404748-8.00001-0.

170. Yang, N., Li, Y., Liu, Z., Qin, H., Du, D., Cao, X., Cao, X., Li, J., Li, D., Jiang, B., *et al.* The characteristics of ctDNA reveal the high complexity in matching the corresponding tumor tissues. *BMC Cancer* **18**, 1–12 (2018).

171. Sorber, L., Zwaenepoel, K., Deschoolmeester, V., Roeyen, G. & Filip, Q. Q. A Comparison of Cell-Free DNA Isolation Kits Isolation and Quantification of Cell-Free DNA in Plasma. *J. Mol. Diagnostics* 1–7 (2016) doi:10.1016/j.jmoldx.2016.09.009.

172. Chen, S. L., Chen, C. Y., Hsieh, J. C. H., Yu, Z. Y., Cheng, S. J., Hsieh, K. Y., Yang, J. W., Kumar, P. V., Lin, S. F. & Chen, G. Y. Graphene oxide-based biosensors for liquid biopsies in cancer diagnosis. *Nanomaterials* **9**, 1–17 (2019).

173. Soleymani, L., Fang, Z., Sargent, E. H. & Kelley, S. O. Programming the detection limits of biosensors through controlled nanostructuring. *Nat. Nanotechnol.* **4**, 844–848 (2009).

Publications

1. Nikoletta Naoumi, Kleita Michaelidou, George Papadakis, Agapi E. Simaiaki, Román Fernández, Maria Calero, Antonio Arnau, Achilleas Tsortos, Sofia Agelaki, Electra Gizeli. Acoustic array biochip combined with allele-specific PCR for multiple cancer mutation analysis in tissue and liquid biopsy. 2021, 460590, bioRxiv, https://www.biorxiv.org/content/10.1101/2021.09.16.460590v1 (December 7, 2021)

2. Alexandre, L.; Araya-Farias, M.; Nguyen M-L.; Naoumi, N.; Gropplero , G.; Gizeli, E.; Descroix, S.: Circulating tumor DNA extraction from biological samples on magnetic microfluidic fluidized bed at high throughput. 2021 (manuscript under preparation)

NIKOLETTA NAOUMI

A dynamic and self-motivated molecular biologist. I Love to work on the development of simplified techniques for molecular diagnosis & instrument-free methods for point-of-care testing. I always have new ideas, creative thinking and good problem-solving abilities. I really enjoy taking responsibilities, challenge myself and try new things. I am passionate about science, loving multidisciplinarity, collaborations, mentoring and supervising.

@ nikoletta.naoumi@gmail.com
linkedin.com/in/nikoletta-naoumi-8b76a4178

EDUCATION

Ph.D. in Molecular Biology & Biotechnology

Biosensors Lab, University of Crete, IMBB-FORTH

Nov 2017 – Nov 2021 Crete, Greece

- Thesis title: "Acoustic-based technologies combined with enzymatic amplification for the analysis of point mutations in tissue and liquid biopsy"
- Deliverables' writing & presentations for the CATCH-U-DNA project
- Mentoring & Supervising of 6 (undergraduate & graduate) students
- Internship @ MMBM Lab, Institut Curie, Paris, France: "Combining the microfluidic magnetic fluidized bed with the LCR amplification assay"
- Internship @ AWS S.L., Paterna, Spain: "Validation of a novel miniaturized high fundamental frequency QCM 24-sensors array"
- Continuous expansion of my knowledge through collaborations & the multidisciplinary nature of the project

M.Sc. in in Molecular Biology and Biomedicine

University of Crete - IMBB

Oct 2015 – Oct 2017 Crete, Greece

- Grade: Excellent 9.56/10
- 1-year thesis titled as "Detection of Circulating Nucleic Acids associated with cancer using an acoustic device combined with RCA isothermal DNA amplification method" @ Biosensors Lab (IMBB - FORTH)
- Rotations @ Minotech Biotechnology (IMBB – FORTH), Computational Genomics Lab (University of Crete), Chromatin and Gene expression Lab (IMBB - FORTH)

B.Sc. in Biology

University of Crete

Sep 2011 – July 2015 Crete, Greece

- Grade: Excellent 8.72/10
- Diploma thesis @ Genome (In)stability and Mammalian physiology Lab (IMBB-FORTH)

A DAY OF MY LIFE

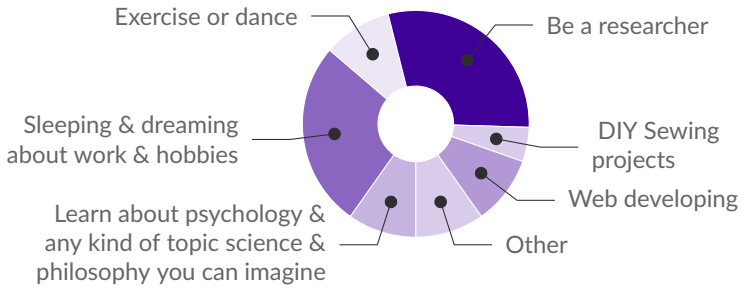

PUBLICATIONS

N. Naoumi, et al. Acoustic array biochip combined with AS-PCR for multiple cancer mutation-analysis in tissue & liquid biopsy. BIORXIV/2021/460590

STRENGTHS & SKILLS

Hard-working | Fast - learner | Flexible | Mentoring | Creativity | Problem-solving | Responsible

Molecular amplification assays | Acoustic biosensors | Molecular Cloning | Recombinant protein expression | Affinity Chromatography | Immunocytochemistry | Western blot | Mammalian & Bacterial cell culture

Familiar with R | HTML | CSS

LANGUAGES

English ●●●●◐

HONORS & AWARDS

Invited speaker at the 8th Annual Diagnostics Innovation Summit, Developing Rapid Tests and Liquid Biopsies, 19-21 May 2020, Lisbon, Portugal

Cambridge Healthtech Institute

May 2020

MS.c. & Ph.D. Scholarship Award

Bodossaki Foundation

Sept 2016 – Aug 2020